

AD-766 639

**STOL TACTICAL AIRCRAFT INVESTIGATION.  
VOLUME II. PART I. AERODYNAMIC TECH-  
NOLOGY: MECHANICAL FLAPS**

**William J. Runciman, et al**

**Boeing Aerospace Company**

**Prepared for:**

**Air Force Flight Dynamics Laboratory**

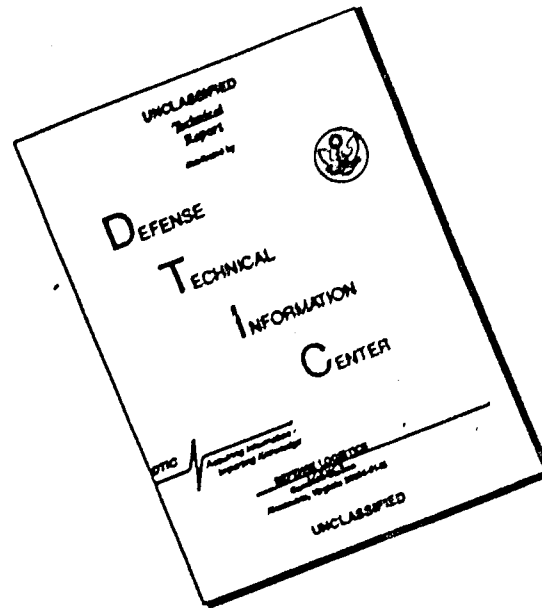
**May 1973**

**DISTRIBUTED BY:**

**NTIS**

**National Technical Information Service  
U. S. DEPARTMENT OF COMMERCE  
5285 Port Royal Road, Springfield Va. 22151**

# DISCLAIMER NOTICE



THIS DOCUMENT IS BEST QUALITY AVAILABLE. THE COPY FURNISHED TO DTIC CONTAINED A SIGNIFICANT NUMBER OF PAGES WHICH DO NOT REPRODUCE LEGIBLY.

**AFFDL-TR-73-19**  
**Volume II, Part I**

**AD 766639**

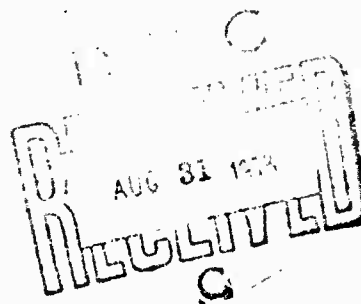
# **STOL TACTICAL AIRCRAFT INVESTIGATION**

**Volume II, Part I**

## **Aerodynamic Technology: Design Compendium, Vectored Thrust/Mechanical Flaps**

*William J. Runciman  
Gary R. Letsinger  
Bernard F. Ray  
Fred W. May*

THE BOEING COMPANY



**Technical Report AFFDL-TR-73-19 -- Volume II, Part I**

**May, 1973**

**Approved for public release; distribution unlimited**

Reproduced by  
**NATIONAL TECHNICAL  
INFORMATION SERVICE**  
US Department of Commerce  
Springfield, VA. 22151

**Air Force Flight Dynamics Laboratory  
Air Force Systems Command  
Wright-Patterson Air Force Base, Ohio 45433**

# Notice

When Government drawings, specifications, or other data are used for any purpose other than in connection with a definitely related Government procurement operation, the United States Government thereby incurs no responsibility nor any obligation whatsoever; and the fact that the Government may have formulated, furnished, or in any way supplied the said drawings, specifications, or other data, is not to be regarded by implication or otherwise as in any manner licensing the holder or any other person or corporation, or conveying any rights or permission to manufacture, use or sell any patented invention that may in any way be related thereto.

ACCESSION for		
NTIS	White Section	<input checked="" type="checkbox"/>
D O	Blue Section	<input type="checkbox"/>
EXAM. OFFICER		<input type="checkbox"/>
JUL 11 1973		
BY		
DISTRIBUTION/AVAILABILITY CODES		
Dist.	AVAIL. AND OF SERIAL	
A		

Copies of this report should not be returned unless return is required by security considerations, contractual obligations, or notice on a specific document.



Unclassified

Security Classification

DOCUMENT CONTROL DATA - R & D		
(Security classification of title, body of abstract and indexing annotation must be entered when the overall report is classified)		
1. ORIGINATING ACTIVITY (Corporate author) The Boeing Aerospace Company P.O. Box 3999 Seattle, Washington 98124		2a. REPORT SECURITY CLASSIFICATION  Unclassified
		2b. GROUP ---
3. REPORT TITLE STOL Tactical Aircraft Investigation - Aerodynamic Technology: Design Compendium, Vectored Thrust/Mechanical Flaps		
4. DESCRIPTIVE NOTES (Type of report and inclusive dates) Final Technical Report 8 June 1971 to 8 December 1972		
5. AUTHOR(S) (First name, middle initial, last name) William J. Runciman Bernard F. Ray Gary R. Letsinger Fred W. May		
6. REPORT DATE May 1973	7a. TOTAL NO. OF PAGES 217	7b. NO. OF REFS 12
8a. CONTRACT OR GRANT NO. F33615-71-C-1757	8b. ORIGINATOR'S REPORT NUMBER(S)  AFFDL-TR-73-19	
8c. PROJECT NO.  643A	9b. OTHER REPORT NO(S) (Any other numbers that may be assigned this report) D-180-14409-1, Volume II, Part I	
10. DISTRIBUTION STATEMENT  Approved for public release; distribution unlimited.		
11. SUPPLEMENTARY NOTES  None	12. SPONSORING MILITARY ACTIVITY Air Force Flight Dynamics Laboratory Wright-Patterson AFB, Ohio 45433	
13. ABSTRACT  This report presents methods for predicting the performance determining aerodynamic characteristics and the stability derivatives of transport-type configurations employing the vectored-thrust mechanical-flap high-lift concept. These methods are suitable for preliminary design. They have been automated in a FORTRAN IV computer program, for which a users' manual and listing are included in this document.		

DD FORM 1 NOV 65 1473

ia

Unclassified

Security Classification

~~Unclassified~~  
Security Classification

14. KEY WORDS	LINK A		LINK B		LINK C	
	ROLE	WT	ROLE	WT	ROLE	WT
Aerodynamic characteristics						
Vectored thrust						
High-lift systems						
Stability and control						
STOL						
Powered lift						

1h

# **STOL TACTICAL AIRCRAFT INVESTIGATION**

**Volume II, Part 1**

## **Aerodynamic Technology: Design Compendium, Vectored Thrust/Mechanical Flaps**

*William J. Runciman  
Gary R. Letsinger  
Bernard F. Ray  
Fred W. May*

**Approved for public release; distribution unlimited**

## FOREWORD

This report was prepared for the United States Air Force by The Boeing Company, Seattle, Washington in partial fulfillment of Contract F33615-71-C-1757, Project No. 643A. It is one of eight related documents covering the results of investigations of vectored-thrust and jet-flap powered lift technology, under the STOL Tactical Aircraft Investigation (STAI) Program sponsored by the Air Force Flight Dynamics Laboratory, Air Force Systems Command, Wright-Patterson Air Force Base, Ohio. The relation of this report to the others of this series is indicated below:

AFFDL-TR-73-19      STOL TACTICAL AIRCRAFT INVESTIGATION

Vol I                      Configuration Definition:  
Medium STOL Transport with  
Vectored Thrust/Mechanical Flaps

Vol II Part I	Aerodynamic Technology: Design Compendium, Vectored Thrust/Mechanical Flaps
------------------	-----------------------------------------------------------------------------------

THIS  
REPORT

Vol II  
Part II                      A Lifting Line Analysis Method  
for Jet-Flapped Wings

Vol III                      Takeoff and Landing Performance  
Ground Rules for Powered Lift  
STOL Transport Aircraft

Vol IV                      Analysis of Wind Tunnel Data:  
Vectored Thrust/Mechanical  
Flaps and Internally Blown  
Jet Flaps

Vol V  
Part I                      Flight Control Technology: System  
Analysis and Trade Studies for a  
Medium STOL Transport with Vectored  
Thrust and Mechanical Flaps

Vol V  
Part II                      Flight Control Technology: Piloted  
Simulation of a Medium STOL Transport  
with Vectored Thrust/Mechanical Flaps

Vol VI                      Air Cushion Landing System Study

The work reported here was performed in the period June 1971 through December 1972 by the Aero/Propulsion Staff of the Research and Engineering Division, Aerospace Group, The Boeing Company. Mr. Franklyn J. Davenport served as Program Manager.

The Air Force Project Engineer for this investigation was Mr. Garland S. Oates, Air Force Flight Dynamics Laboratory, PIA, Wright-Patterson Air Force Base, Ohio.

This report was released within The Boeing Company as Document D180-14409-1, and submitted to the Air Force in December 1972.

This technical report has been reviewed and is approved.



E. J. Cross Jr., Lt. Col., USAF  
Chief, Prototype Division  
Air Force Flight Dynamics Laboratory

## ABSTRACT

This report presents methods for predicting the performance-determining aerodynamic characteristics and the stability derivatives of transport-type configurations employing the vectored-thrust/mechanical-flap high-lift concept. These methods are suitable for preliminary design. They have been automated in a FORTRAN IV computer program, for which a users' manual is included in the appendix of this document.

## TABLE OF CONTENTS

<u>Section</u>	<u>Page</u>
I        INTRODUCTION	1
II       LONGITUDINAL CHARACTERISTICS	3
2.1    Unpowered Aerodynamic Characteristics, Free Air	3
2.1.1    Lift	3
2.1.2    Maximum Lift	21
2.1.3    Drag	30
2.1.4    Pitching Moment	38
2.2    Ground Effect	56
2.2.1    Lift	56
2.2.2    Drag	57
2.2.3    Pitching Moment	59
2.2.4    Downwash	59
2.3    Vectored Thrust, Free Air	63
2.3.1    Lift Interference	63
2.3.2    Drag Interference	65
2.3.3    Pitching Moment Interference	71
2.3.4    Downwash Interference	71
2.4    Vectored Thrust, Ground Effect	77
2.4.1    Lift Interference	77
2.4.2    Drag Interference	77
2.4.3    Pitching Moment Interference	80
2.4.4    Downwash Interference	80
2.5    Trim	81
III      STABILITY AND CONTROL DERIVATIVE PREDICTION METHODS	83
3.1    Stability Derivative Sensitivity Study	83
3.1.1    Longitudinal	87
3.1.2    Lateral-Directional	93
3.2    Stability and Control	96
3.2.1    Longitudinal Stability and Control	101
3.2.2    Lateral-Directional Stability Derivatives	116
3.3    Engine Out	136
APPENDIX    Users Manual for Computer Program	139
References	219

## LIST OF ILLUSTRATIONS

<u>Figure No.</u>		<u>Page</u>
1	Lift Curve Slope, Test-Estimate Comparison	4
2	2-D Flap Effectiveness, Single Slotted Flap	8
3	2-D Flap Effectiveness, Double Slotted Flap	9
4	3-D Effect on Flap Effectiveness	10
5	Span Loading Factor	11
6	Multi-Element Flap Nomenclature	12
7	Body Lift Carryover	14
8	Flap Lift Increment, Test-Estimate Comparison	15
9	Leading-Edge Flap Effectiveness	19
10	Effect of Leading Edge Device on Maximum Lift	22
11	2-D Maximum Lift Increment	24
12	Trailing-Edge Flap Maximum Lift	26
13	Leading Edge Blowing Boundary Layer Control Effectiveness	29
14	Parasite Drag of Trailing-Edge Flaps	31
15	Part Span Induced Drag Factors (Continuous Flaps with Central Cutout)	33
16	Profile Drag Variation with Lift	34
17	Comparison of Measured and Predicted Power-off Drag Polars	36
18	Nomenclature for $\alpha_c$ Location with Inboard Leading-Edge Devices	40
19	Local Aerodynamic Centers Near Middle of Wing	41
20	Load Effectiveness of Part Span Chord Extensions	42



# LIST OF ILLUSTRATIONS (Continued)

<u>Figure No.</u>		<u>Page</u>
21	Nomenclature for ac Location with Outboard Leading-Edge Devices	44
22	Chordwise Center of Load Due to Flaps	49
23	Spanwise Center of Load Due to Flaps	51
24	Change in Downwash at Horizontal Tail	53
25	Comparison of Measured and Predicted Power-Off Pitching Moment	55
26	Wing-in-Ground Effect	58
27	Ground Effect, Power Off, Test-Estimate Comparison	60
28	Ground Effect, Power Off, Test-Estimate Comparison	61
29	Vectored Thrust, Test-Estimate Comparison	64
30	Vectored Thrust, Lift Interference	66
31	Vectored Thrust, Lift Interference Effect of Nozzle Location	67
32	Vectored Thrust, Drag Interference - Vector Angle $30^\circ$	68
33	Vectored Thrust, Drag Interference - Vector Angle $60^\circ$	69
34	Vectored Thrust, Drag Interference - Vector Angle $90^\circ$	70
35	Vectored Thrust, Pitching Moment Interference - Vector Angle $30^\circ$	72
36	Vectored Thrust, Pitching Moment Interference - Vector Angle $60^\circ$	73
37	Vectored Thrust, Pitching Moment Interference - Vector Angle $90^\circ$	74
38	Vectored Thrust, Downwash Change at Horizontal Tail	75

# LIST OF ILLUSTRATIONS (Continued)

<u>Figure No.</u>		<u>Page</u>
39	Vectored Thrust in Ground Effect, Test-Estimate Comparison	78
40	Change in Thrust Interference Effects Due to Ground Effect	79
41	General Arrangement STOL Tactical Transport Model 953-801	84
42	Effect of Angle of Attack Derivative, $C_{m_{\alpha}}$ on Longitudinal Dynamic Stability	89
43	Effect of Angle of Attack Derivatives, $C_{x_{\alpha}}$ and $C_{L_{\alpha}}$ on Longitudinal Dynamic Stability	89
44	Effect of Speed Derivatives on Longitudinal Dynamic Stability	90
45	Effect of Aerodynamic Lag Derivatives on Longitudinal Dynamic Stability	91
46	Effect of Pitch Damping Derivatives on Longitudinal Dynamic Stability	92
47	Effect of Sideslip Derivatives on Dutch Roll Characteristics	94
48	Effect of Sideslip Derivatives on Spiral Mode Stability	95
49	Effect of Roll Rate Derivatives on Dutch Roll Characteristics	97
50	Effect of Roll Rate Derivatives on Spiral Mode Stability	98
51	Effect of Yaw Rate Derivatives on Dutch Roll Characteristics	99
52	Effect of Yaw Rate Derivatives on Spiral Mode Stability	100
53	Effect of Vectored Thrust on Lift Curve Slope	103
54	Effect of Vectored Thrust on Aerodynamic Center	104

# LIST OF ILLUSTRATIONS (Continued)

<u>Figure No.</u>		<u>Page</u>
55	Effect of Nacelle Spanwise Location on Aerodynamic Center	105
56	Lift Curve Slope Error	108
57	Aerodynamic Center Error	109
58	Effect of Vectored Thrust on Downwash	111
59	Effect of Vectored Thrust on Horizontal Tail Dynamic Pressure	112
60	Vectored Thrust Effect Factors for Sideslip Derivatives, Tail-Off	118
61	Vectored Thrust Effect Factors for Sideslip Derivatives in Ground Effect, Tail-Off	119
62	Sidewash at the Vertical Tail	121
63	Powered Sideslip Derivatives Error	122
64	Thrust Effect on Rudder Power	130
65	Effect of Sideslip on Aileron Power	131
66	Effect of Thrust on Aileron Effectiveness in Free Air and in Ground Effect	132
67	Effect of Aileron Blowing and Engine Thrust on Aileron Effectiveness	133
68	Effect of Thrust on Spoiler Effectiveness	134
69	Spoiler Effectiveness	135
70	Rolling Moment Due to Thrust Loss	137
71	Yawing Moment Due to Thrust Loss	138
72	Nomenclature for Leading Edge Flap	146
73	Nomenclature for Trailing Edge Flap	149
74	Program Deck Stacking	153

## LIST OF TABLES

<u>Table Number</u>	<u>Title</u>	<u>Page</u>
I	Stability Derivatives, Mass Properties, and Reference Dimensions of Example Airplane	85
II	Stability Derivatives with Important Influence on Airplane Stability	86
III	Test-Prediction Comparison, Angle of Attack Derivatives	106
IV	Test-Prediction Comparison, Sideslip Derivatives	123
V	Input Data Format	155

# LIST OF ABBREVIATIONS AND SYMBOLS

A	Aspect ratio, $\frac{b^2}{S}$
$A_G$	Gross aspect ratio, $\frac{b^2}{S_G}$
ac	Aerodynamic center
$a_v$	Vertical tail lift curve slope, per radian
b	Wing span, ft
$b_v$	Vortex span, ft
$V_e$	Equivalent jet velocity ratio
c	Chord length, ft
$c'$	Extended chord length, ft
$\bar{c}$ or $c_{REF}$	Mean aerodynamic chord, ft
$C_D$	Drag coefficient
$\Delta C_{DBLC}$	Drag coefficient due to leading edge boundary layer control
$C_{Di}$	Induced drag coefficient
$C_{Dp}$	Parasite drag coefficient
$C_{DRAM}$	Ram drag coefficient
$c_f$	Flap chord length, ft
$c'_f$	Extended flap chord length, ft
cg	Center of gravity
$C_J$	Thrust coefficient
$C_L$	Lift coefficient
$C_\ell$	Section lift coefficient, or rolling moment coefficient (depends on context)

# LIST OF ABBREVIATIONS AND SYMBOLS (Continued)

$C_{L_\alpha}$	Lift curve slope, per degree
$C_{\ell_\alpha}$	Section lift curve slope, per degree
$C_n$	Yawing moment coefficient
$C_m$	Pitching moment coefficient
cp	Center of pressure
$C_x$	Longitudinal force coefficient, stability axis
$C_y$	Sidelforce coefficient, stability axis
$C_z$	Vertical force coefficient, stability axis
$C_\mu$	Boundary layer control momentum coefficient
h	Height of wing quarter mac above ground plane, ft
$I_{xx}$	Moment of inertia about the x body reference axis, slug-ft <sup>2</sup>
$I_{yy}$	Moment of inertia about the y body reference axis, slug-ft <sup>2</sup>
$I_{zz}$	Moment of inertia about the z body reference axis, slug-ft <sup>2</sup>
$I_{xz}$	Product of inertia about the x and z body reference axis, slug-ft <sup>2</sup>
$\mathcal{I}$	Imaginary part of a complex number
L	Lift force, lb
$\ell_H$	Distance from c.g. to horizontal tail ac, ft
$\ell_V$	Distance from c.g. to vertical tail ac, ft
M	Pitching moment, ft-lb
mac	Mean aerodynamic chord, ft
p	Roll rate, radians/sec

# LIST OF ABBREVIATIONS AND SYMBOLS (Continued)

p	Wing semi-perimeter, or wing tip helix angle, $\frac{Pb}{2V}$ , rad (depends on context)
q	Pitch rate angle, $\frac{Qc}{2V}$ , rads or dynamic pressure, $\text{lbs/ft}^2$ (depends on context)
Q	Pitch rate, rad/sec
R	Real part of complex number
R	Yaw rate, rad/sec
r	Yaw rate angle, $\frac{Rb}{2V}$ , rad
S	Wing area, sq ft
S <sub>G</sub>	Wing gross area, sq ft
S <sub>H</sub>	Horizontal tail area, sq ft
S <sub>REF</sub>	Wing reference area, sq ft
S <sub>V</sub>	Vertical tail area, sq ft
T <sub>i/2</sub>	Time to half amplitude, sec
T <sub>2</sub>	Time to double amplitude, sec
u	Perturbation speed normalized by initial speed, $\frac{\Delta U}{V}$
v <sub>i</sub>	Induced longitudinal velocity due to image vortex system, ft/sec
v <sub>r</sub>	Induced longitudinal velocity due to real vortex system, ft/sec
V	Free stream velocity, ft/sec
W	Weight, lb
w <sub>i</sub>	Induced vertical velocity due to image vortex system, ft/sec
w <sub>r</sub>	Induced vertical velocity due to real vortex system, ft/sec
x	Longitudinal coordinate, f from reference station
X <sub>E</sub>	Longitudinal distance from nozzle centerline to cg, ft
X <sub>R</sub>	Longitudinal distance from centerline of inlet face to cg, ft

# LIST OF ABBREVIATIONS AND SYMBOLS (Continued)

$X_T$	Distance from cg to thrust vector in fraction of MAC
$Z_T$	Distance from c.g. to thrust vector in fraction of MAC, positive down
$Z_E$	Vertical distance from nozzle centerline to cg, ft
$Z_R$	Vertical distance from centerline of inlet face to cg, ft
$Z_V$	Distance from cg down to vertical tail ac, ft
$\alpha$	Angle of attack, deg
$\epsilon_f$	Flap effectiveness
$\beta$	Angle of sideslip, deg
$\Gamma$	Wing circulation, ft <sup>2</sup> /sec
$\gamma$	Climb angle, deg
$\Delta$	Incremental value
$\delta_{AIL}$	Aileron deflection, deg
$\delta_E$	Elevator deflection, deg
$\delta_e$	Effective flap deflection angle, deg
$\delta_F$	Flap deflection angle, deg
$\epsilon$	Downwash angle, deg
$\epsilon_e$	Effective downwash angle at horizontal tail, deg
$\eta$	Ratio of dynamic pressure at the tail to free-stream dynamic pressure, or dimensionless wing semi span (depends on context)
$\Lambda$	Sweep angle, deg
$\lambda$	Wing loading factor
$\mu_s$	Part span load effectiveness
$\sigma$	Thrust deflection angle, side wash angle, deg (depends on context)



## LIST OF ABBREVIATIONS AND SYMBOLS (Continued)

### Subscripts

AIL	Aileron
avg	Average
B	Body
c/4	1/4 chord
c/2	1/2 chord
c'/2	1/2 extended chord
FA	Free air
GE	Ground effects
H	Horizontal tail
HL	Hinge line
IB	Inboard
INT	Interference
LE	Leading edge
max	Maximum
NET	Indicates data (power on) that has the engine thrust removed
min	Minimum
OB	Outboard
OL	Zero lift
REF	Reference
TE	Trailing edge
TO	Tail-off
trap	Trapezoidal
V	Vertical tail

## SECTION I

### INTRODUCTION

#### 1.1 Background

The U. S. Air Force's need for modernization of its Tactical Airlift capability led to establishment of the Tactical Airlift Technology Advanced Development Program (TAT-ADP). This program was designed to contribute to the technology base for development of an Advanced Medium STOL Transport (AMST).

The AMST must be capable of handling substantial payloads and using airfields considerably shorter than those required by large tactical transports now in the Air Force inventory. If this short field requirement is to be met without unduly compromising aircraft speed, economy, and ride quality, an advanced-technology powered-lift concept will be required.

The STOL Tactical Aircraft Investigation (STAI) is a major part of the TAT-ADP, and comprises studies of the aerodynamics and flight control technology of powered-lift systems under consideration for use on the AMST. Under the STOL-TAI, The Boeing Company was awarded Contract No. F33615-71-C-1757 by the USAF Flight Dynamics Laboratory to conduct investigations of the technology of the vectored-thrust and internally blown jet flap powered-lift concepts. These investigations included:

- o Aerodynamic analysis and wind tunnel testing
- o Configuration studies
- o Control system design, analysis, and simulation

#### 1.2 Objective

The objective of the work reported here was to develop convenient and rapid methods for predicting the performance-determining aerodynamic characteristics and the stability derivatives of configurations using the vectored thrust/mechanical flap powered lift concept. The methods are intended for preliminary design purposes and ease of application has been emphasized.

#### 1.3 State of the Art Prior to the STAI

Early in the STAI, the available literature and test data on vectored thrust was surveyed. It was found that the data base for vectored thrust interference effects on transport-type configurations was almost nonexistent. Consequently, the "State of the Art Design Compendium" compiled from the information then available consisted only of procedures for estimating power-off characteristics and the recommendation to correct for power simply by direct vector addition of the propulsive forces. That is, interference effects were assumed to be zero.

To fill the gap in the data base, an extensive program of testing was then carried out in the Boeing V/STOL Wind Tunnel. The results of that program are reported in Volume IV of the present series of documents, and are the basis for the methods presented here.

#### 1.4 Technical Approach

Power effects are described in this report as the sum of forces and moments computed by direct vector addition, plus interference increments. The interference increments were usually found to be best described graphically. That is, no improvement in convenience or understanding was apparent in attempting to reduce the curves to analytical formulae, except for a general dependence of the interference forces on the square root of the thrust coefficient.

#### 1.5 Scope

The scope of this investigation covers vectored thrust/mechanical flap high-lift systems installed on configurations suitable for a STOL tactical transport. These methods are intended to be used in conjunction with the USAF Stability and Control DATCOM (Reference 1).

#### 1.6 Document Organization

Section II presents methods for predicting performance determining aerodynamic characteristics with power off, and for estimating interference effects due to vectored thrust.

Section III presents procedures for computing stability and control derivative corrections due to vectored thrust.

The appendices provide a users' manual and a listing of a FORTRAN IV computer program which automates the procedures given in Section II.

## SECTION II

### LONGITUDINAL CHARACTERISTICS

Aerodynamic estimation techniques are presented which provide increments of lift, drag, and pitching moment for leading and trailing edge devices. These increments are to be added to the clean airplane values which may be estimated from Datcom or other alternate source.

#### 2.1 Unpowered Aerodynamic Characteristics, Free Air

##### 2.1.1 Lift

Lift estimation below maximum lift has been divided into lift curve slope and flap lift increments. The effects of flap extension (chord extension) which increases the wing area, and flap deflection, which changes the wing camber, are treated separately.

##### 2.1.1.1 Lift Curve Slope

There are a number of theoretical or semi-theoretical formulae which give good agreement between the estimated and experimental lift curve slopes of three-dimensional wings (Refs. 1, 2, 3, 4). One easy-to-use method is that from Jones and Cohen (Ref. 4). See sample problem for additional definition of  $S_G$  and  $p$ , Page 5.

$$C_{L_\alpha} = \frac{2\pi A}{(p/b)(A)+2} \frac{S_G}{S_R} \frac{1}{\text{rad}} \quad (2.1-1)$$

The modern high lift system usually has trailing edge flaps with rearward displacement (chord extension) and may also include a leading edge device with forward displacement. The areas added by these displacements of the leading and trailing edges must be added to the basic planform when estimating flaps down  $C_{L_\alpha}$ . If the inboard edge of the flap is at the side of the body, the added area for flap extension will be based on the assumption that the flap extends to the body centerline.

A comparison of estimated and test  $C_{L_\alpha}$  are shown in Fig. 1.

$\Lambda c/4$	AR	LE	TE	$C_{L\alpha\text{Test}}$	$C_{L\alpha\text{Est}}$	$\frac{C_{L\alpha\text{Est}} - C_{L\alpha\text{Test}}}{C_{L\alpha\text{Est}}}$
15	6.5	Up	Up	0.0710	0.0713	0.0042
✓	8.0	✓	✓	0.0811	0.0790	-0.0267
✓	10.0	✓	✓	0.0870	0.0860	-0.0116
30	5.36	✓	✓	0.0700	0.0673	-0.0401
✓	6.61	✓	✓	0.0717	0.0735	0.0245
✓	8.26	✓	✓	0.0765	0.0761	-0.0053
0	8.3	✓	✓	0.0790	0.0840	0.0595
30	6.61	Ext	✓	0.0790	0.0779	-0.0141
15	8.0	✓	✓	0.0860	0.0880	0.0227
0	8.3	✓	✓	0.0940	0.0905	-0.0387
15	8.0	Up	Ext	0.0933	0.0970	0.0381
✓	✓	✓	✓	0.0926	0.0970	0.0454
30	6.61	✓	✓	0.0850	0.0800	-0.0625
15	8.0	Ext	✓	0.0940	0.0988	0.0485
30	6.61	✓	✓	0.0920	0.0846	-0.0875
0	8.3	✓	✓	0.0990	0.1016	0.0256

Data from BVWT 097 (Ref 5)

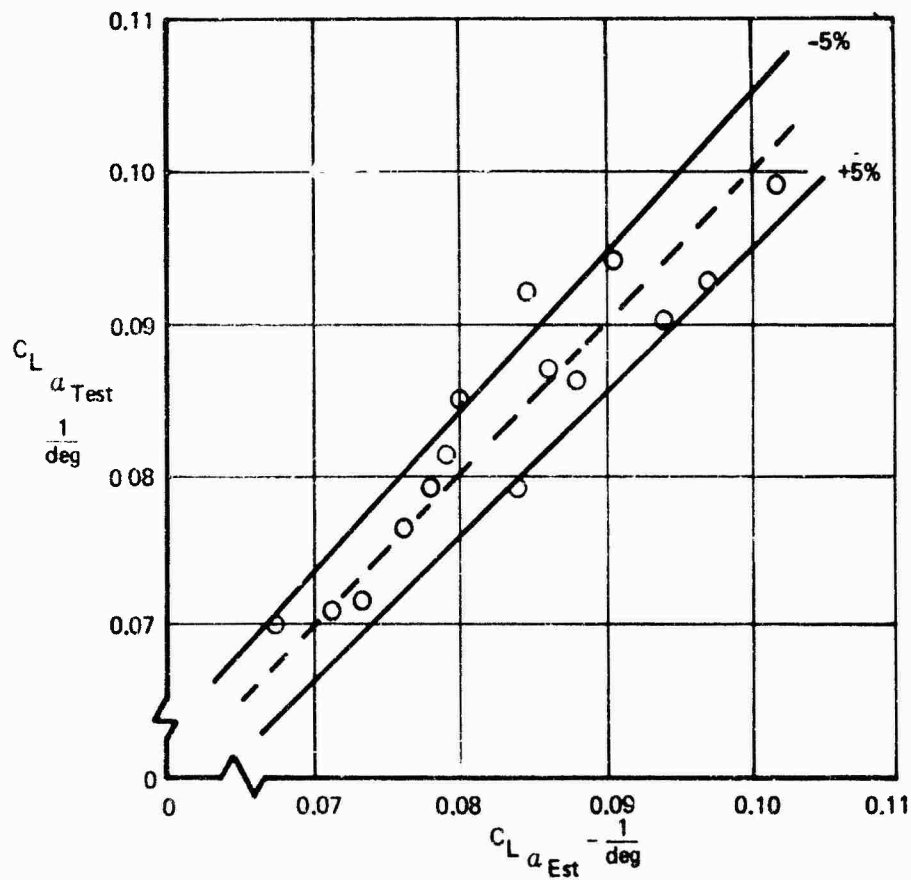
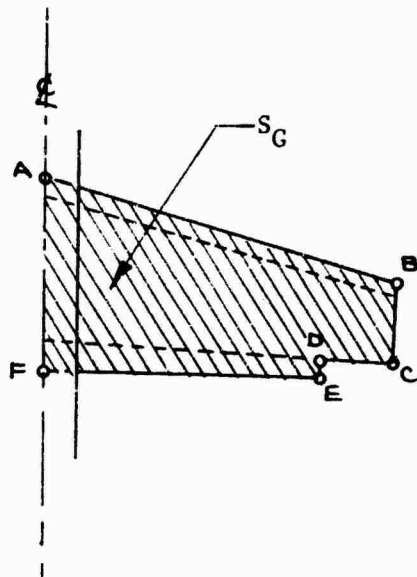


Figure 1: Lift Curve Slope, Test – Estimate Comparison

# SAMPLE PROBLEM - LIFT CURVE SLOPE

STAI wind tunnel model LE & TE devices deployed, 15° sweep.



$$S_G = \text{Area ABCDEF} = 8.592 \text{ SF}$$

$$S_{\text{Ref}} = 6.164 \text{ SF}$$

$$b = 34.274 \text{ in.}$$

$$A_{\text{Gross}} = b^2 / S_G = 5.74 \text{ SF}$$

$$P = \text{ABCDEF} = 100.952 \text{ in.}$$

Calculate  $C_{L\alpha}$  from Equation 2.1-1.

$$C_{L\alpha} = \frac{\left[ \frac{(2\pi)(5.74)}{(100.952)(5.74) + 2} \right] \left( \frac{8.592}{6.164} \right) \frac{1}{57.3}}$$

$$C_{L\alpha} = .0988 \text{ deg.}$$

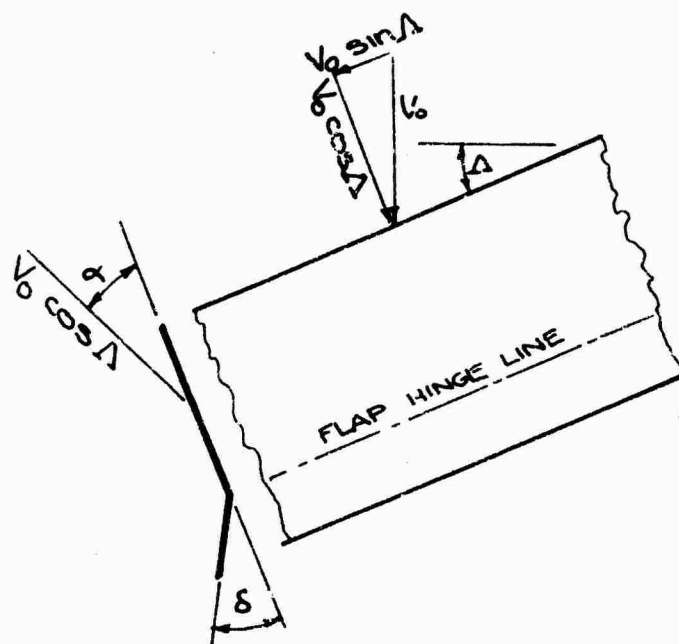
FROM TEST BWWT 097, REF 5

$$C_{L\alpha} = .0940$$

## 2.1.1.2 Effect of Trailing Edge Flap Deflection

The effect of pure (i.e., no area increase) trailing edge flap deflection is to change the zero-lift angle ( $\alpha_{0L}$ ) without changing the wing lift curve slope. The approach chosen here to estimate trailing edge zero-lift angle shift is due to Eldridge (Ref. 6 and 7).

Consider an infinite yawed constant-chord wing with trailing edge flap deflection.



It can be shown that, referenced to the free stream velocity,

$$C_{l\alpha} = 2\pi \cos \Delta \quad (2.1-2)$$

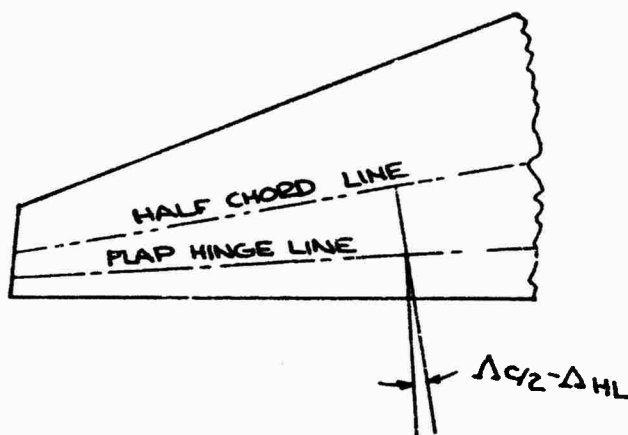
$$C_{l\delta} = 2\pi \alpha_{\delta, \Lambda=0} \cos^2 \Delta \quad (2.1-3)$$

Therefore:

$$\frac{C_{l\delta}}{C_{l\alpha}} = \alpha_{\delta, \Lambda=0} \cos \Delta$$

For flaps on tapered wings, the significant sweep angle is that of the locus of sectional aerodynamic centers for the wing, approximately the quarter chord (used for  $C_{l\alpha}$ ), and the locus of sectional flap centers of pressure, approximately the half chord (used for  $C_{l\delta}$ ). If the flap angle,  $\delta_f$ , is measured normal to the hingeline, then the effective angle along a chordline normal to the half chordline is

$$\delta_e = \tan^{-1} [\tan \delta_f \cos(\Lambda_{c/2} - \Lambda_{HL})] \quad (2.1-4)$$



$$\Delta \alpha_{OL_{2D}} = [\alpha_{\delta_{2D}}]_{\Lambda=0} \left[ \frac{\cos^2 \Lambda c/2}{\cos \Lambda c/4} \right] \tan^{-1} [\tan \delta_f \cos(\Lambda c/2 - \Delta_{HL})] \quad (2.1-6)$$

For a finite aspect ratio wing, lifting surface theory shows that the effective  $\alpha_\delta$  is increased above the two-dimensional value. Therefore, for wings

$$\Delta \alpha_{OL} = [\alpha_{\delta_{2D}}]_{\Lambda=0} \left[ \frac{\alpha_{\delta_{3D}}}{\alpha_{\delta_{2D}}} \right] \left[ \frac{\cos^2 \Lambda c/2}{\cos \Lambda c/4} \right] \tan^{-1} [\tan \delta_f \cos(\Lambda c/2 - \Delta_{HL})] \Lambda_{TE} \quad (2.1-7)$$

Empirical two-dimensional data has been correlated for single and vane-type double-slotted flaps, Figs. 2 and 3. Lifting surface theory shows that flap effectiveness is affected by aspect ratio. The two-dimensional test value of  $\alpha_\delta$  can be corrected to three-dimensional using the theoretical results of Ref. 8, Fig. 4.

The part span load factor used in Equation 2.1-7 may be found in Figure 5.

For multi-element clamps, contributions of individual elements add algebraically (Fig. 6), so

$$(\Delta \alpha_{OL})_{TE} = (\Delta \alpha_{OL})_1 + (\Delta \alpha_{OL})_2 \quad (2.1-8)$$



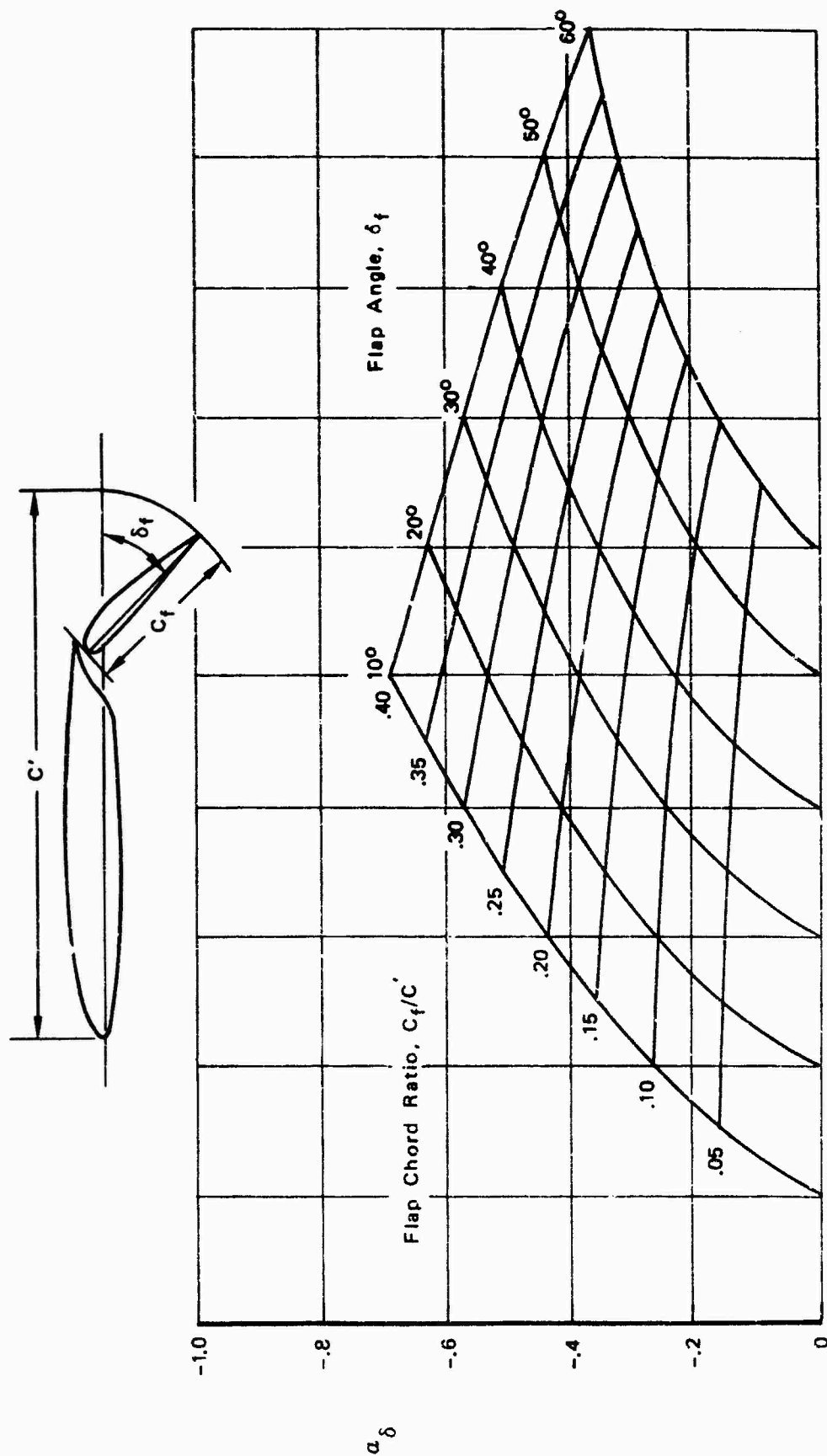


Figure 2: 2-D Flap Effectiveness, Single-Slotted Flap

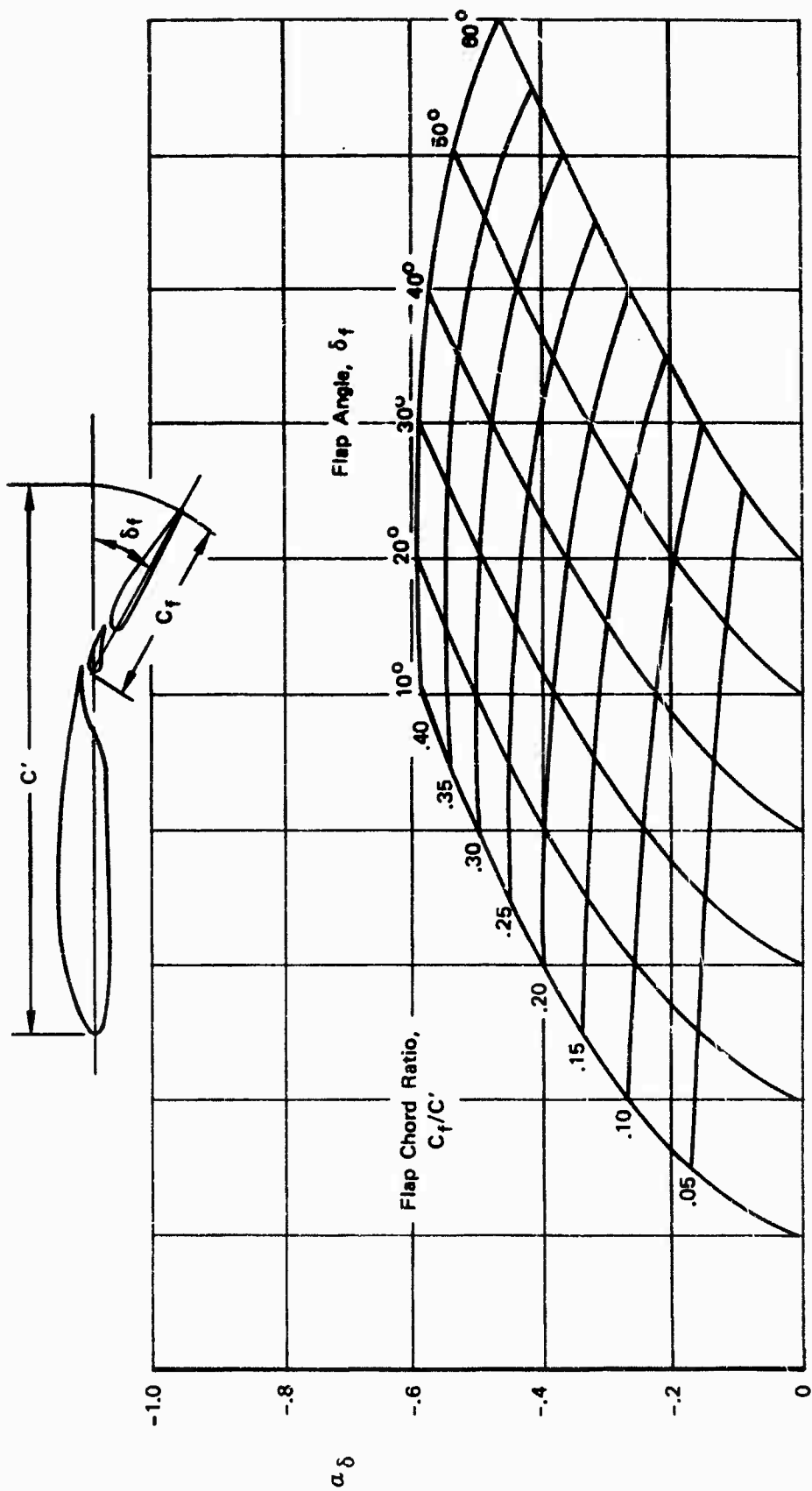


Figure 3: 2-D Flap Effectiveness, Double-Slotted Flap

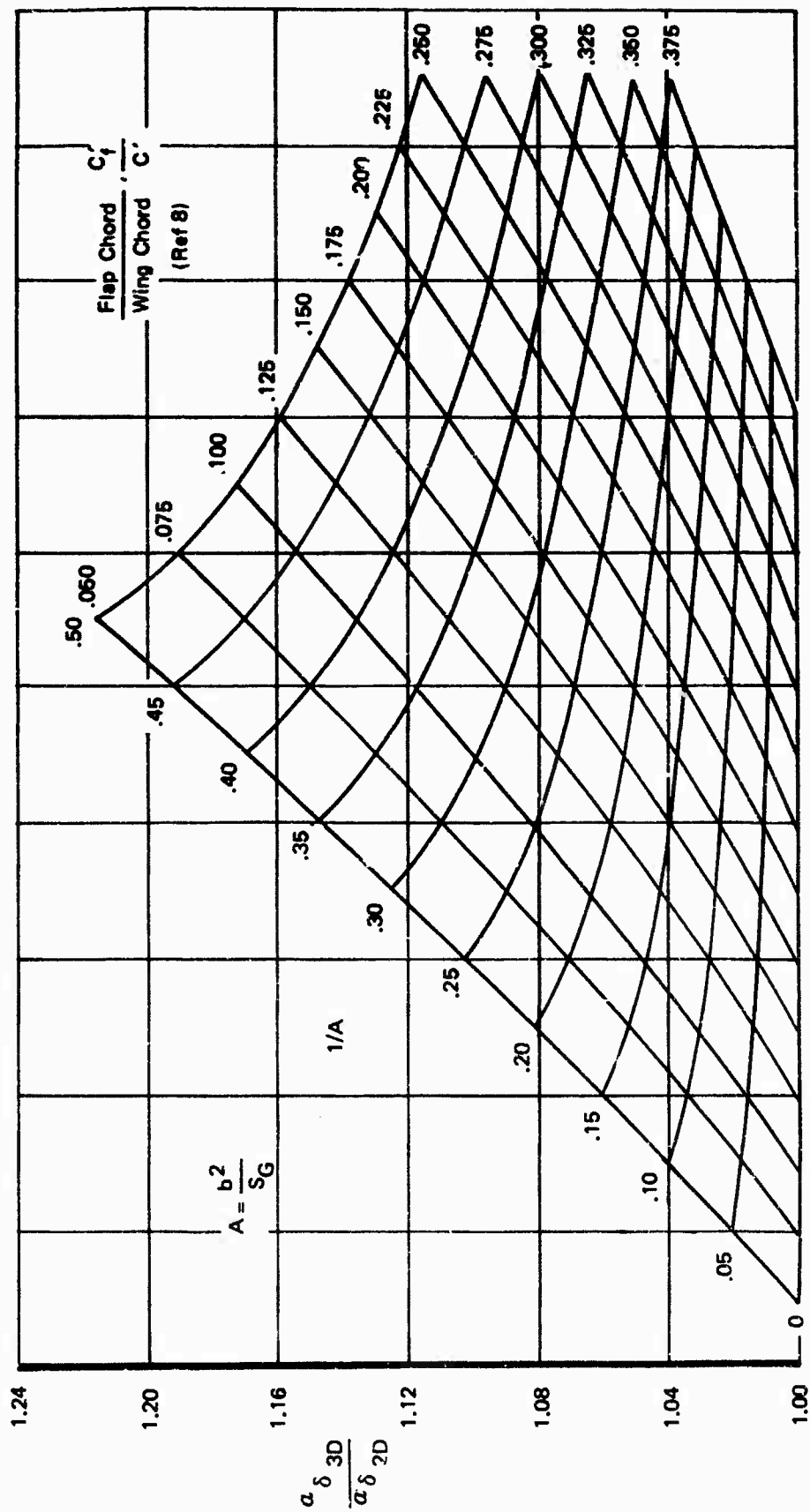


Figure 4: 3-D Effect on Flap Effectiveness

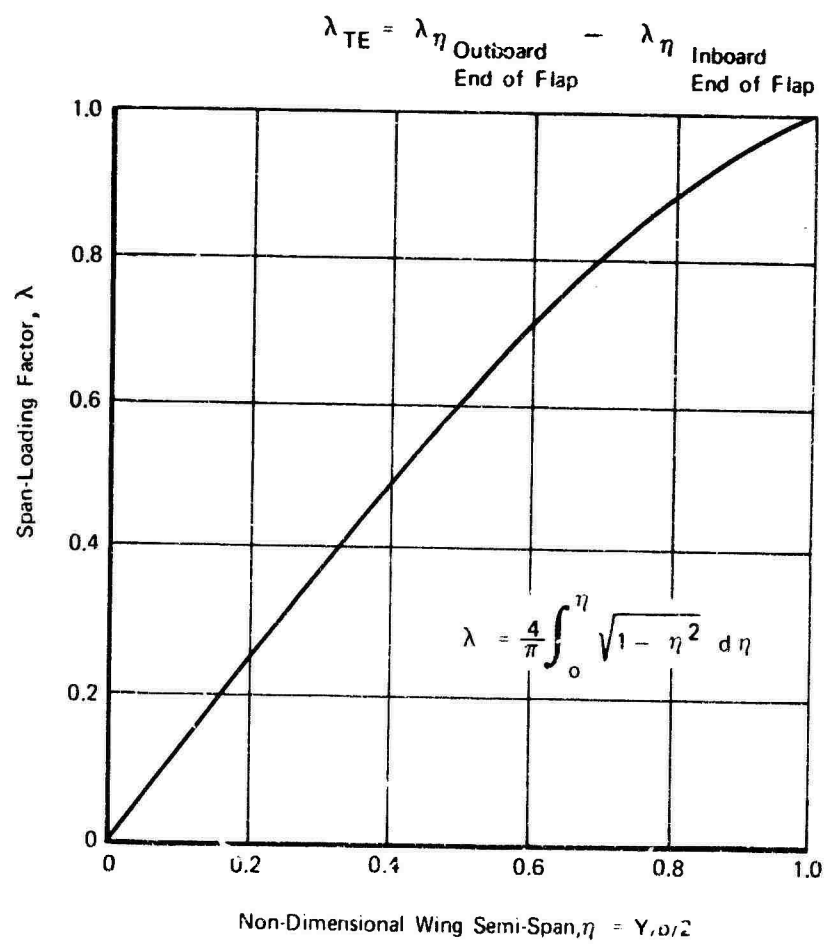
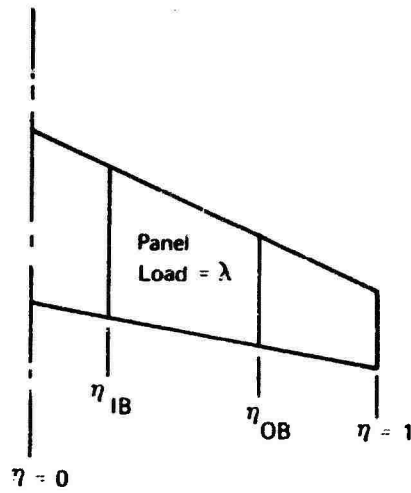


Figure 5: Span-Loading Factor

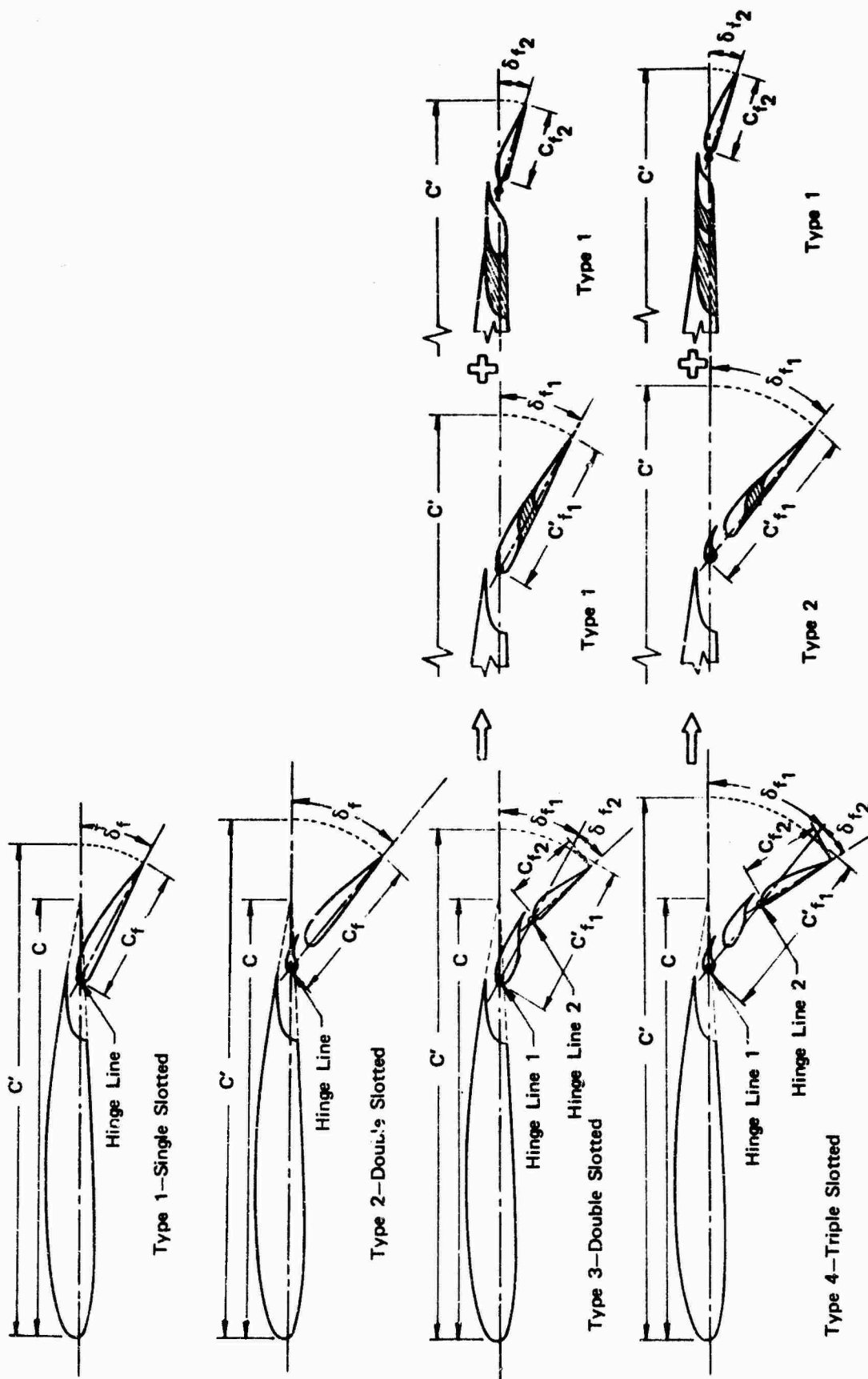


Figure 6: Multi-Element Flap Nomenclature

The flap lift increment, measured at the angle for zero lift of the flaps-up wing is

$$\Delta C_{L TE flap} = (C_{L \alpha}) (-\Delta \alpha_{OL TE flap}) \quad (2.1-9)$$

Some flap lift will be carried over onto the body. The amount of carry-over will depend on the wing position on the body, the body span to wing span ratio, and the flap lift increment. A limited amount of data for high wing configurations have been correlated as shown in Fig. 7. If it is desired to make the correction for body carry-over, flap lift increments should be calculated assuming the flap ends at the body side and that it extends to the centerline. The difference between these values is then multiplied by the body carry-over factor (k) from Fig. 7 trailing edge flap lift increment with body carry-over is

$$\Delta C_{L TE} = \Delta C_{L TE flap} + (\Delta C_{L TE flap}) \left( \frac{\lambda_{IB}}{\lambda_{OB} - \lambda_{IB}} \right) k \quad (2.1-10)$$

The body carry-over lift increment also results in shifting the angle for zero lift by

$$\Delta \alpha_{OL B} = - \frac{\Delta C_{LB}}{C_{L \alpha_{flaps \text{ down}}}} \quad (2.1-11)$$

$$\Delta \alpha_{OL TE} = \Delta \alpha_{OL flap} + \Delta \alpha_{OL B} \quad (2.1-12)$$

A comparison between test data obtained from STAI wind tunnel testing and calculated data are presented in Fig. 8.

#### SAMPLE PROBLEM, TRAILING EDGE FLAP LIFT INCREMENT

STAI Wind Tunnel Model LE & LE Devices deployed, T.E. deflection 45°/60°,  $\Lambda_{c/4} = 15^\circ$ .

$$S_G = 8.952 \text{ SF}$$

$$S_R = 6.164 \text{ SF}$$

$$b = 84.274 \text{ in.}$$

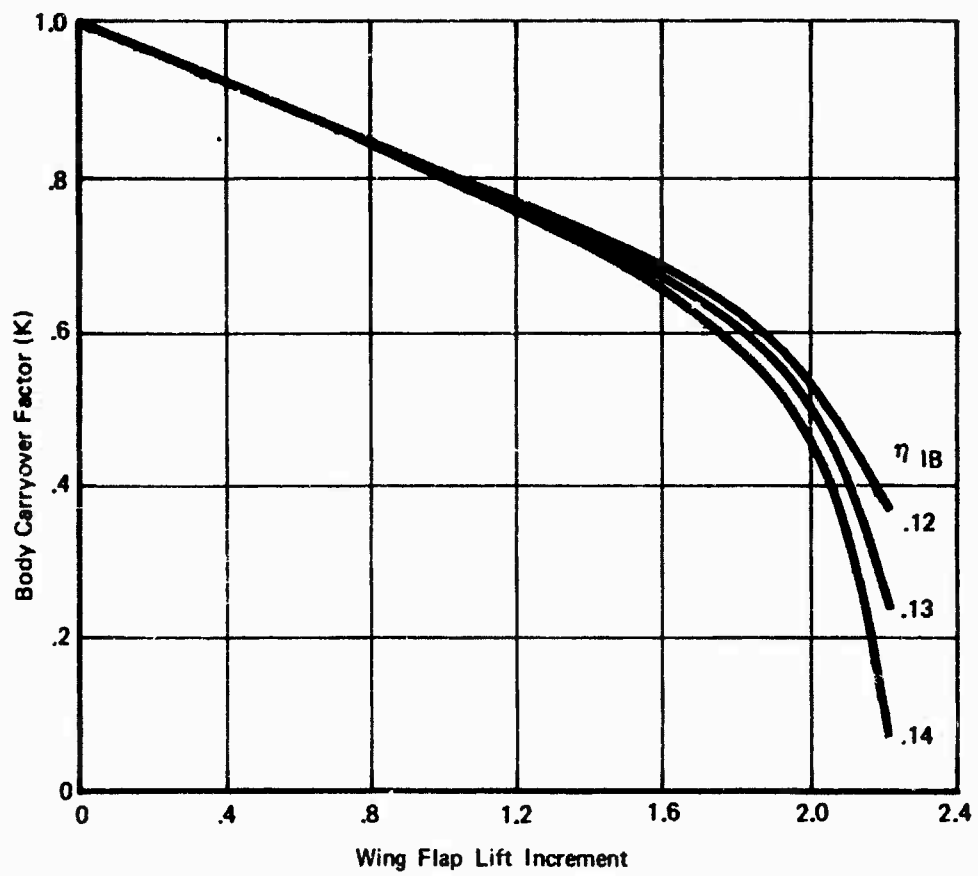


Figure 7: Body Lift Carryover

$\Lambda C/4$	AR	Flap Span	$\delta_F$ Actual	$\Delta C_{L_f \text{ test}}$	$\Delta C_{L_f \text{ Est.}}$	$\frac{\Delta C_{L_f \text{ test}} - \Delta C_{L_f \text{ Est.}}}{\Delta C_{L_f \text{ Est.}}}$
30	6.61	0.716	30/30	1.03	0.98	-0.051
✓	✓	✓	40/40	1.29	1.26	-0.024
✓	✓	✓	58/40	1.56	1.56	0.090
✓	✓	✓	45/60	1.58	1.59	0.006
✓	✓	0.570	✓	1.26	1.34	0.060
✓	✓	0.848	✓	1.80	1.78	-0.011
✓	✓	1.000	✓	2.01	1.92	-0.047
15	8	0.75	30/30	1.2	1.20	0.0
✓	✓	✓	40/40	1.61	1.55	-0.039
✓	✓	✓	58/60	1.94	1.89	-0.026
✓	✓	✓	45/60	1.91	1.92	0.005
✓	✓	1.0	✓	2.29	2.25	-0.018
✓	6.5	✓	✓	2.15	2.12	-0.014
✓	10.0	✓	✓	2.45	2.31	-0.016
30	5.36	✓	✓	1.65	1.68	0.018
✓	8.26	✓	✓	1.95	2.02	0.035
0	8.30	0.776	30/30	1.36	1.36	0
✓	✓	✓	40/40	1.78	1.72	-0.035
✓	✓	✓	58/60	2.10	2.07	-0.014
✓	✓	✓	45/60	2.17	2.14	-0.014

Data from BVWT 097 (Ref. 5)

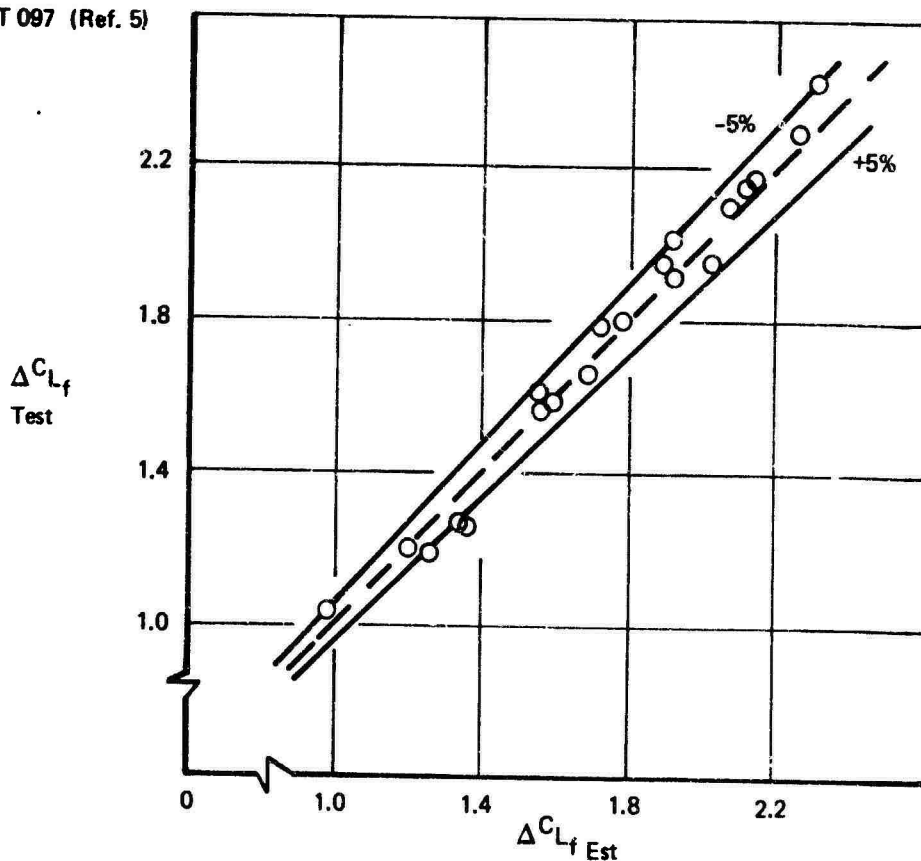


Figure 8: Flap Lift Increment, Test-Estimate Comparison



$$A_{\text{Gross}} = 5.74$$

$$p = 100.952 \text{ in.}$$

Flap Type 4, Triple Slotted, see Fig. 6.

$$C'/C = 1.283$$

$$\frac{C_{f1}}{C'} = .323$$

$$C_{f2}/C' = .091$$

$$\delta_{f1} = 45.14$$

$$\delta_{f2} = 15.13$$

$$\eta_{OB} = .145$$

$$\eta_{OB} = .75 \quad \text{Trailing Edge}$$

$$AC'/4 = 15.401$$

$$AC'/2 = 11.625^\circ$$

$$\angle HL_1 = 7.295^\circ$$

$$\angle HL_2 = 3.525^\circ$$

$$C_{L\alpha} = .0988 \quad (\text{calculated by method in Section 2.1.1.1})$$

Calculate flap angles normal to half chord line, Equation 2.1-4.

$$\delta_{e1} = \tan^{-1} [\tan 43.14 \cos (11.625 - 7.295)] = 45.06^\circ$$

$$\delta_{e2} = \tan^{-1} [\tan 15.13 \cos (11.625 - 3.525)] = 14.98^\circ$$

For forward flap section using Figure 3,  $C'_f/C'$  and  $\delta_{e1}$  read

$$(\alpha_\delta)_1 = -.485$$

For aft flap section using Fig. 2,  $C'_{f2}/C'$  and  $\delta_{e2}$

$$(\alpha_\delta)_2 = -.25$$

From Fig. 4,  $C'_f/C'$  and A determine

$$\frac{(\alpha_\delta)_{3D}}{(\alpha_\delta)_{2D}} = 1.03$$

From Fig. 4,  $C_{f2}/C'$  and A determine

$$\left(\frac{\alpha_{\delta 3D}}{\alpha_{\delta 2D}}\right)_2 = 1.057$$

From Fig. 5,  $\eta_{1B}$  and  $\eta_{0B}$

$$\lambda_{TE} = .849 - .183 = .666$$

Since the flap is the sum of its parts,

$$(\Delta\alpha_{OL})_{TE} = \Delta\alpha_{OL1} + \Delta\alpha_{OL2}$$

and  $\alpha_{OL}$  from Equation 2.1-7

$$(\Delta\alpha_{OL})_1 = (-.485)(1.03) \left(\frac{\cos^2 11.62}{\cos 15.40}\right) (45.06)(.666) = -14.92$$

$$(\Delta\alpha_{OL})_2 = (-.25)(1.056) \left(\frac{\cos^2 11.62}{\cos 15.40}\right) (14.98)(.666) = -2.62$$

$$\Delta\alpha_{OLTE} = -17.54$$

Then from Equation 2.1-9

$$\Delta C_{L_{TEFLAP}} = -(-17.54)(.0988) = 1.73$$

body carry over factor from Fig. 7,  $\Delta C_{L_{TE}}$  and  $\eta_{1B}$  (flaps end at side of body)

$$K = .58$$

with equation 2.1-10

$$\Delta C_{L_{TE}} = 1.73 + (1.73) \left(\frac{.183}{.666}\right) (.58)$$

$$= 1.73 + .28$$

$$\Delta C_{L_{TE}} = 2.01$$

from test

$$C_{L_{TE}} = 1.91$$

### 2.1.1.3 Effect of Leading Edge Flap Deflection

There has been little work done to correlate test data on the effect of leading edge flap deflection on lift below  $C_{L_{max}}$ . Since this effect is relatively small compared to trailing edge flap deflection, leading edge flap effectiveness is taken to be the potential flow value given in Figure 9.

On a three-dimensional swept wing with a part span leading edge device,

$$\Delta \alpha_{OLE} = \alpha_{\delta_{LE}} \delta_{LE} \cos \Lambda_{c/4} \lambda_{LE} \quad (2.1-13)$$

$$\Delta C_{L_{LE}} = (C_{L_{\alpha}})(-\Delta \alpha_{LE}) \quad (2.1-14)$$

#### SAMPLE PROBLEM, LEADING EDGE LIFT INCREMENT

$$C_{LE}/C = .166$$

$$\delta_{LE} = 70^\circ$$

$$\Lambda_{c/4} = 15^\circ$$

$$\eta_{1B} = .145$$

$$\eta_{0B} = 1.0$$

$$C_{L_{\alpha}} = .0988$$

From Fig. 9 and  $C_{LE}/C$  read

$$\alpha_{\delta_{LE}} = .028$$

From Fig. 5 and  $\eta_{1B}$  and  $\eta_{0B}$

$$\lambda_{LE} = 1 - .183 = .817$$

using Equation 2.1-13 and 2.1-16

$$\Delta \alpha_{OL} = (.028)(70)(.966)(.817) = 1.55$$

$$\Delta C_{L_{LE}} = -(.0988)(1.55) = -.15$$

from test

$$\Delta C_{L_{LE}} = -.18$$

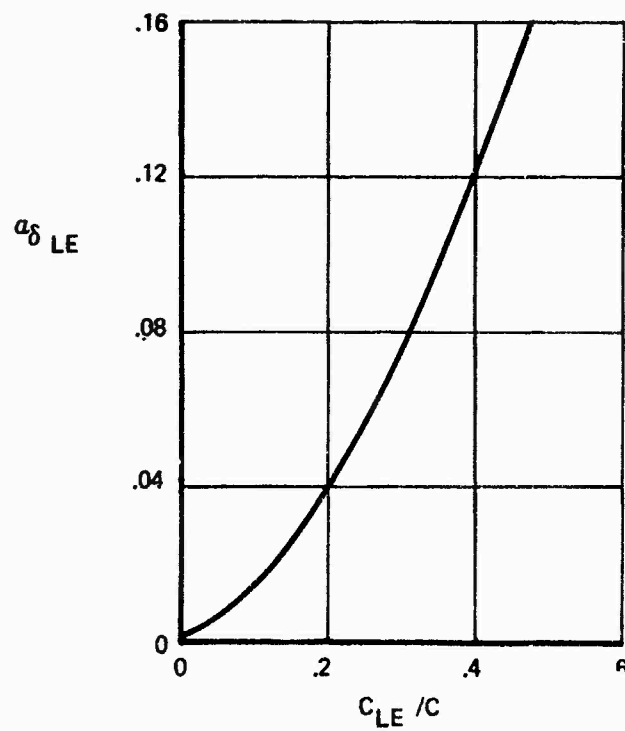
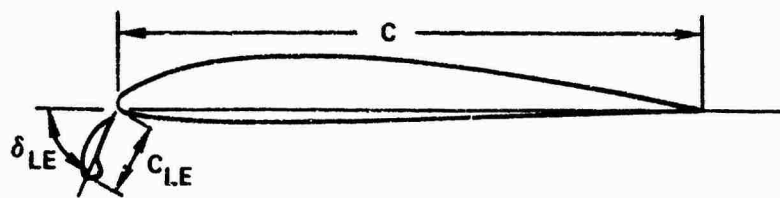
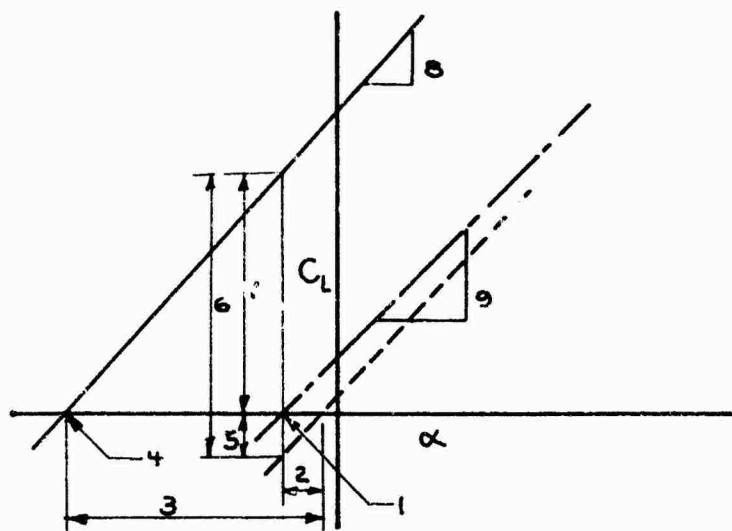


Figure 9: Leading Edge Flap Effectiveness

#### 2.1.1.4 Total Free Air Lift

The increments obtained,  $\Delta\alpha_{OL}$  and  $\Delta C_L$ , and the slope of the flaps down lift curve may be combined with flaps up estimates from Datcom or other sources.



- (1)  $\alpha_{OL}$  flaps up from Datcom or other source
- (2)  $\Delta\alpha_{OLLE}$
- (3)  $\Delta\alpha_{OLTE}$
- (4)  $\alpha_{OL}$  flaps down = (1) + (2) + (3)
- (5)  $\Delta C_{LLE}$
- (6)  $\Delta C_{LTE}$
- (7)  $\Delta C_{Lf} = (5) + (6)$
- (8)  $C_{L\alpha}$  flaps down
- (9)  $C_{L\alpha}$  flaps up Datcom

### 2.1.2 Maximum Lift

Many attempts have been made to develop methods for estimating the maximum lift of an airplane with a high lift system. No method has given consistently reliable results. The method given here should apply to the type of configuration likely to be considered for a STOL transport. Unfortunately,  $C_{L_{max}}$  may vary widely from the values calculated by this method for particular configurations with unusual arrangements.

The approach taken divides the problem into the  $C_{L_{max}}$  of the clean wing plus increments due to leading edge and trailing edge devices.

For the clean wing, the methods of Datcom may be used to estimate  $C_{L_{max}}$ . Next the increment in maximum lift due to leading edge devices will be added to the clean wing, then the trailing edge increment added. This technique has been chosen because of the availability of data in this form. It would be more satisfying to add a leading edge increment to the flaps-down maximum lift, since the shape and optimum deflection of the leading edge device is a function of the trailing edge lift increment. However, insufficient data is available to use this approach.

#### 2.1.2.1 Leading Edge Devices

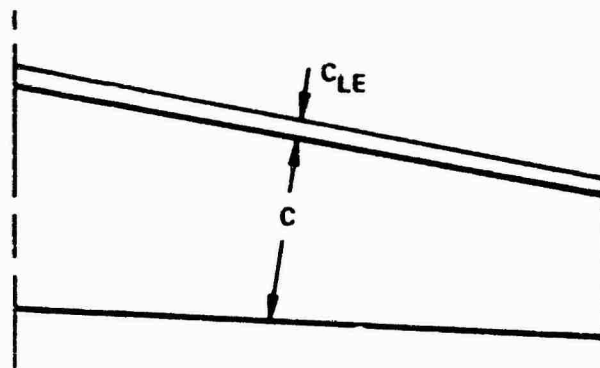
The maximum lift increment due to leading edge devices is a function of wing sweep, device chord, shape, deflection, and span. It is assumed that care will be taken in tailoring and fairing areas such as intersections of nacelle struts and wings, etc., where relatively large penalties may result from local flow separation and interference effects.

Correlations of  $\Delta C_{L_{max}} / \cos^2 \Lambda_{c/4}$  versus leading edge device chord ratio are shown in Fig. 10 for conventional leading edge slats and for shaped leading edge devices representative of current state-of-the-art variable-camber Krueger flaps.

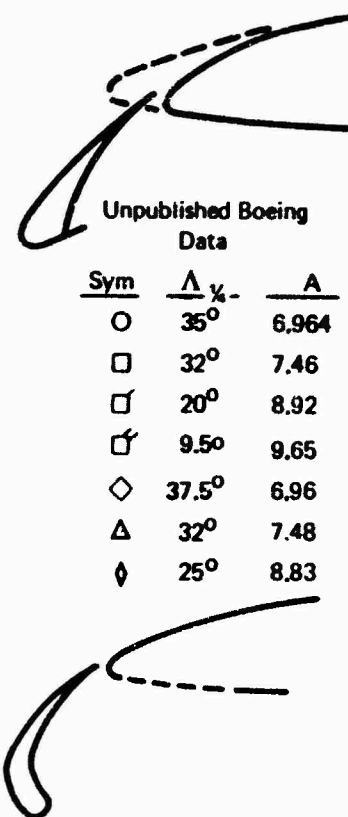
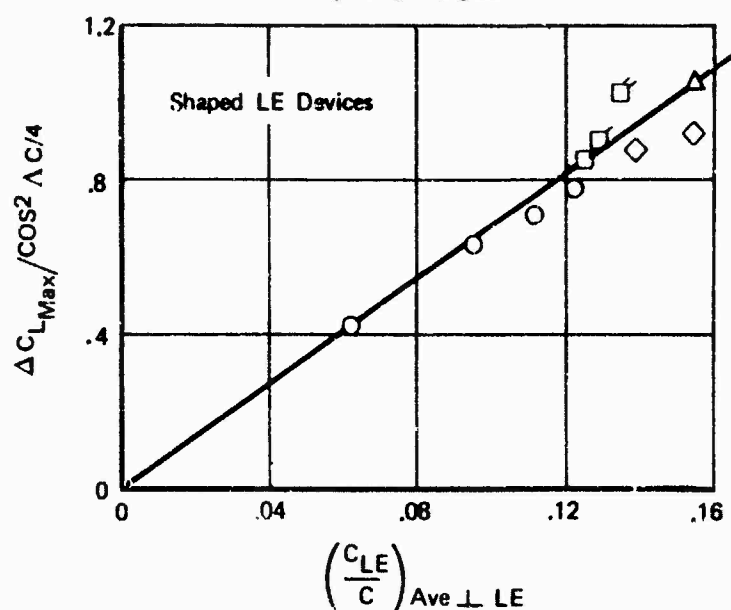
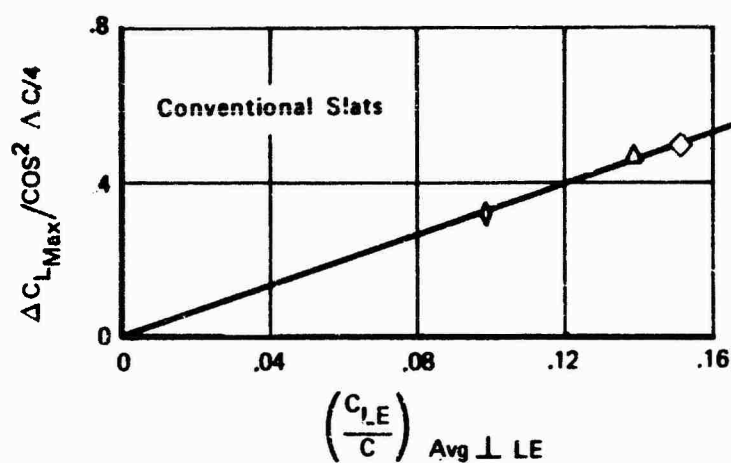
The maximum lift increment due to the leading edge device is then:

$$\Delta C_{L_{max}LE} = \left( \frac{\Delta C_{L_{max}}}{\cos^2 \Lambda_{c/4}} \right) \cos^2 \Lambda_{c/4} \quad (2.1-15)$$

It should be noted that for this estimate the chord lengths are measured normal to the basic wing leading edge and that the gross area is the area of the basic wing extended to the body centerline.



Chords Normal to Leading Edge



Sym	$\Lambda$ °	A
○	35°	6.964
□	32°	7.46
◻	20°	8.92
◻	9.5°	9.65
◇	37.5°	6.96
△	32°	7.48
◊	25°	8.83

Figure 10: Effect of Leading Edge Device on Maximum Lift

# SAMPLE PROBLEM, LEADING EDGE MAXIMUM LIFT

STAI Wind Tunnel Model, L.E. deployed, 15° sweep.

$$\frac{C_{LE}}{C} = .166$$

$$\Lambda_c/4 = 15^\circ$$

from Fig. 10 and  $C_{LE}/C$  read

$$\frac{\Delta C_{L_{max}}}{\cos^2 \Lambda_c/4} = 1.14 \text{ (shaped leading edge)}$$

with Equation 2.1-15

$$\begin{aligned} \Delta C_{L_{maxLE}} &= (1.14) \cos^2 15.0 \\ &= 1.06 \end{aligned}$$

from test data

$$\Delta C_{L_{maxLE}} = .57$$

The calculated value is too high because the leading edge device tested was a compromise designed for several nacelle strut locations and leading edge sweep angles. A larger  $\Delta C_{L_{max}}$  for a given configuration could normally be achieved by tailoring the leading edge.

## 2.1.2.2 Trailing Edge Devices

The increment in  $C_{L_{max}}$  due to deploying trailing edge flaps is caused by two effects; increased area due to chord extension, if any, and increased camber. Assuming that the airfoil stalls when leading edge pressure distributions are similar for the flaps-up and -down cases, the theoretical maximum lift increment is related trailing edge flap lift increment by:

$$\Delta C_{L_{max}} = \left[ \frac{\Delta C_{l_{max}}}{\Delta C_{l_{f\alpha=0}}} \right] \left( \frac{A+2}{A} \right) \Delta C_{L_{TE}} \quad (2.1-16)$$

camber

where  $\left[ \frac{\Delta C_{l_{max}}}{\Delta C_{l_{f\alpha=0}}} \right]$ , taken from Ref. 9, is given in Fig. 11.



$$\frac{\Delta C_{l_{\max}}}{\Delta C_{l_{\alpha=0}}}$$

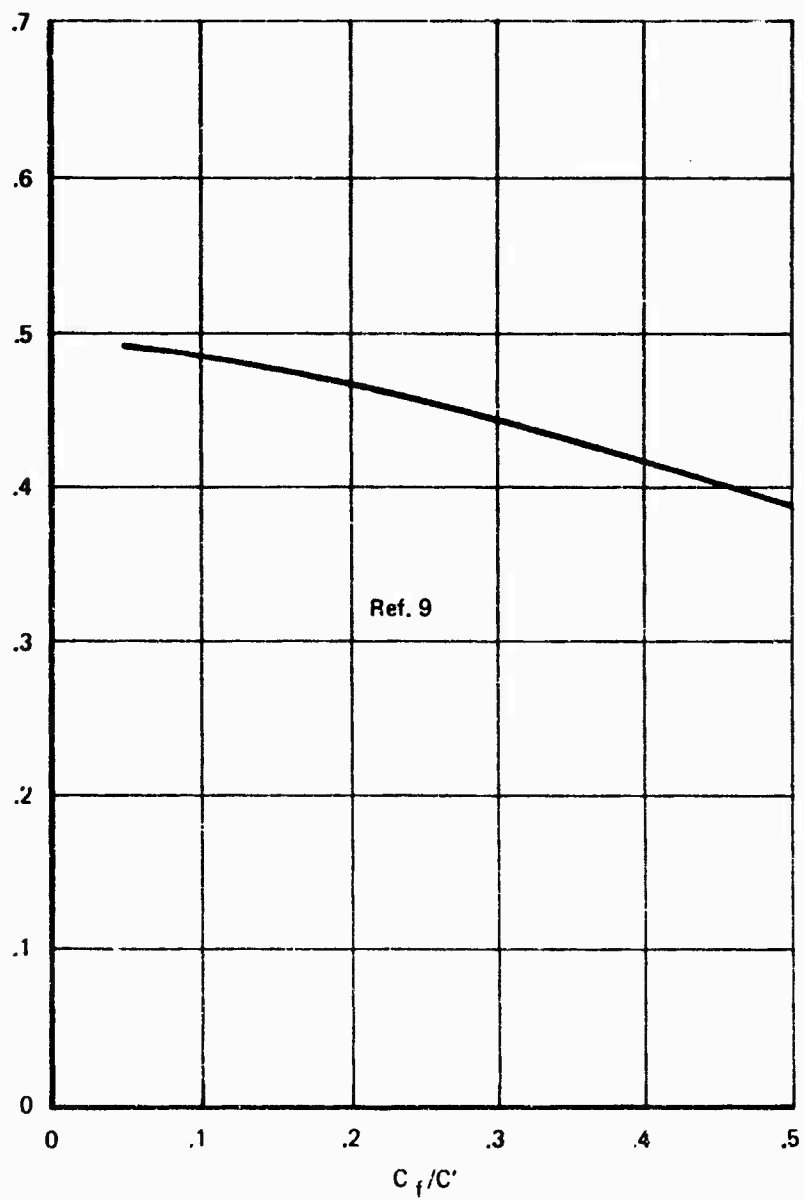


Figure 11: 2-D Maximum Lift Increment

The maximum lift of a wing section based on the extended chord would be almost unchanged if the trailing edge flaps were translated aft without deflection. When a leading edge flap is used, however, increase in wing chord would result in a reduction in the ratio of the leading edge flap chord to the wing chord. This reduction in the leading edge chord ratio reduces the increment in maximum lift due to the leading edge flap since this increment is based on the wing chord without extension.

The increase in maximum lift from a trailing edge chord extension is:

$$\Delta C_{L\max} = \left( \underset{\substack{\text{chord} \\ \text{extension}}}{C_{L\max}} + \underset{\substack{\text{flaps up} \\ \text{leading} \\ \text{edge}}}{\Delta C_{L\max}} \right) \left( \frac{\Delta S_{TE}}{S_{GROSS} + \Delta S'_{LE}} \right) (\lambda_{TE}) \quad (2.1-17)$$

The reduction in maximum lift from the reduction in leading edge chord to wing chord ratio is:

$$\Delta C_{L\max} = \frac{d \left( \frac{\Delta C_{L\max}}{\cos \Lambda/4} \right)}{d \left( \frac{C_{LE}}{C} \right)} \cos^2 \Lambda/4 \left( \frac{C_{LE}}{C'} - \frac{C_{LE}}{C} \right) \left( \frac{S'_{GROSS} + \Delta S'_{TE}}{S_{REF}} \right) (\lambda_{TE}) \quad (2.1-18)$$

In the foregoing equations the gross area is that area of the basic wing between the outboard edge of the trailing flaps and the body centerline. The trailing edge area is the increase in the wing planform area due to chord extension with the flap rotated into the plane of the wing. The leading edge area is the increase in wing planform area from leading edge chord extension counting only the area between the outboard edge of the trailing edge flap and the side of the body. See sample problem Page 27 for sketch defining areas.

The total increase in maximum lift from the trailing edge flap is

$$\Delta C_{L\max} = \underset{\substack{\text{trailing} \\ \text{edge}}}{\Delta C_{L\max}} + \underset{\substack{\text{camber}}}{\Delta C_{L\max}} + \underset{\substack{\text{chord} \\ \text{extension}}}{\Delta C_{L\max}} + \underset{\substack{\text{LE chord} \\ \text{ratio}}}{\Delta C_{L\max}} \quad (2.1-19)$$

Figure 12 shows the estimated maximum lift coefficient increment correlates with test data within  $\pm 1$ .

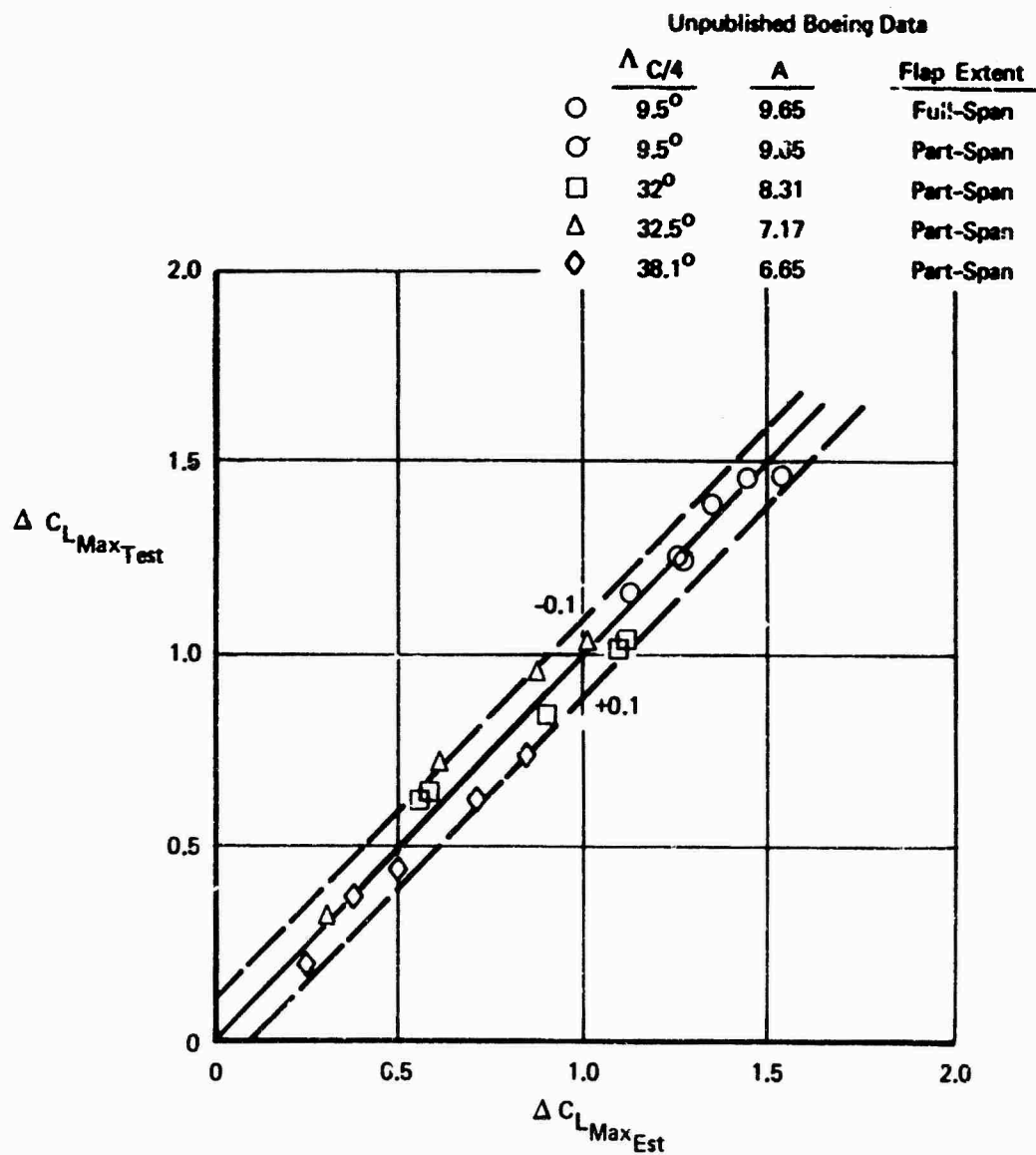


Figure 12: Trailing Edge Flap, Maximum Lift Increment

# SAMPLE PROBLEM, TRAILING EDGE MAXIMUM LIFT

STAI wind tunnel model L.E. and T.E. devices deployed, 15° sweep.

$$\lambda_{TE} = .666 \text{ (from Section 2.1.1.2)}$$

$$C'_f/C' = .323$$

$$A_G = 5.74$$

$$\Delta C_{L_{TE}} = .201 \text{ from Section 2.1.1.2}$$

$$\Delta S_{TE} = 1.104 \text{ SF}$$

$$S'_{Gross} = 5.119 \text{ SF}$$

$$\Delta S'_{LE} = .624 \text{ SF}$$

$$C_{LE}/C = .167$$

$$C_{LE}/C' = .130$$

$$\Lambda_{c/4} = 15.4^\circ$$

$$S_{REF} = 6.164 \text{ SF}$$

$$C_{L_{MaxFU}} = .98 \text{ flaps up (rest data)}$$

$$\Delta C_{L_{mLE}} = 1.06 \text{ from Section 2.1.2.1}$$

from Fig. 11 and  $C'_f/C'$

$$\frac{\Delta C_{L_{Max}}}{\Delta C_{L_{\alpha=0}}} = .438$$

maximum lift increment from camber, Equation 2.1-16

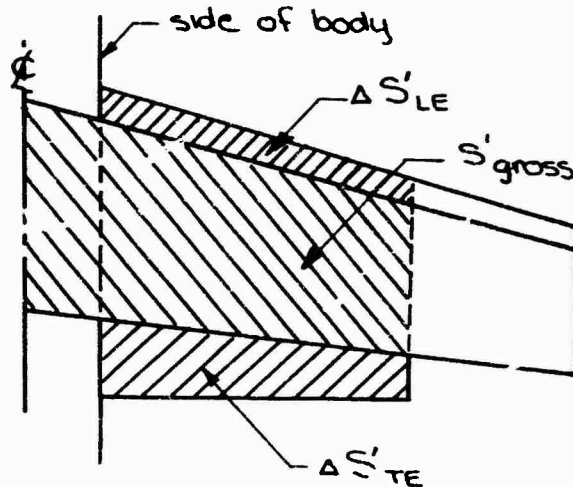
$$\Delta C_{L_{Max}} = (.438) \left( \frac{5.74 + 2}{5.74} \right) (2.01) = 1.19$$

maximum lift increment from chord extension, Equation 2.1-17.

$$\Delta C_{L_{Max}} = (.98 + 1.06) \left( \frac{1.104}{5.119 + .624} \right) (.666) = .27$$

From Fig. 10 at  $C_{LE}/C$  read slope of curve

$$\frac{d \left( \frac{\Delta C_{L_{Max}}}{\cos^2 \Lambda_{c/4}} \right)}{d \left( \frac{C_{LE}}{C} \right)} = 6.9$$



Change in maximum lift increment for reduction in leading edge chord ratio, Equation 2.1-18

$$\Delta C_{L_{Max}} = (6.9)(\cos^2 15.)(.130 - .167)\left(\frac{5.119 + 1.104}{6.164}\right)(.666) = -.16$$

The total increase in maximum lift from the trailing edge flap

$$\begin{aligned}\Delta C_{L_{Max}} &= 1.19 + .26 - .16 \\ &= 1.29\end{aligned}$$

from test data

$$\Delta C_{L_{Max}} = 1.57$$

Total Estimated, leading edge and trailing edge flap

$$\begin{aligned}C_{L_{Max}} &= .98 + 1.29 + 1.06 \\ &= 3.33\end{aligned}$$

from test data

$$C_{L_{Max}} = 3.12$$

The comparison between the estimate and test data show a fortunate combination in the estimated data. The increment from the leading edge was low and the trailing edge increment high resulting in a better comparison with the total from test data.

### 2.1.2.3 Leading Edge Boundary Layer Control

The effectiveness of leading edge blowing boundary layer control is very configuration dependent. For example, a wing with large regions of separated flow near the leading edge would show large improvement in maximum lift with small amounts of blowing momentum. The correlation to be shown in this section does not include the effect of BLC as a cure for problem areas; e.g., separated flow in the wing/nacelle strut intersection region.

A correlation based on unpublished Boeing data is shown in Fig. 13 for leading edge devices designed specifically for blowing applications. The upper curve is based on configurations with uninterrupted leading edges; i.e., no wing mounted nacelles, and represents a design goal for a well-tailored configuration with wing mounted nacelles. The lower curve represents the level achieved with wing mounted nacelles with no additional system tailoring. An optimized leading edge device may achieve the lift levels indicated only to fall below this level when operated at off design conditions. The curves should yield reasonable, achievable, levels but no generalized information is available regarding best device shape or deflection or in what manner the blowing should be distributed on the wing.

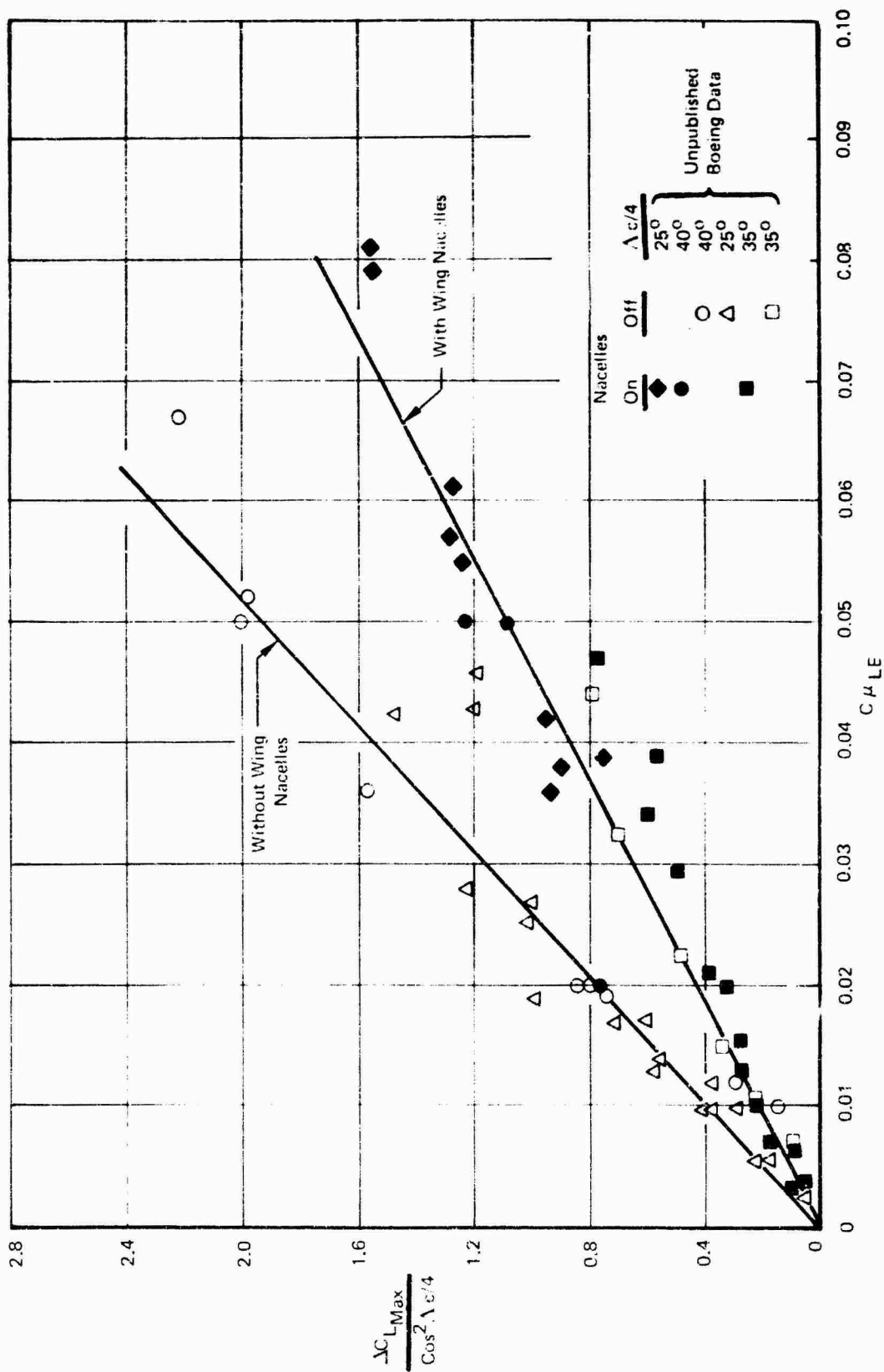


Figure 13: Leading Edge Blowing Boundary Layer Control Effectiveness

Leading edge blowing boundary layer control may also result in some increase in trailing edge effectiveness. This is a result of the thinner boundary layer that then exists ahead of the trailing edge flaps. Insufficient data exists to allow a rational correlation of this effect to be developed.

#### SAMPLE PROBLEM, MAXIMUM LIFT WITH L.E. BOUNDARY LAYER CONTROL

STAI Wind Tunnel Model, Nacelles On

$$C_{\mu_{LE}} = .06$$

$$\Lambda_c/4 = 15.40$$

from Fig. 13 and  $C_{\mu_{LE}}$

$$\frac{\Delta C_{L_{Max}}}{\cos^2 \Lambda_c/4} = 1.3$$

Maximum lift increment for leading edge blowing

$$\begin{aligned} \Delta C_{L_{Max}} &= (1.3)(\cos^2 15.4) \\ &= 1.21 \end{aligned}$$

from test data

$$C_{L_{Max}} = .29$$

This increment from test data is much too low, which may be the result of off-design operation of the leading edge devices, i.e. 15° rather than 30° sweep. Also, the model had not been tailored, and there were grounds to believe that there was trailing edge separation adjacent to the body. It would be expected with proper refinement of the model configuration the maximum lift increment from leading edge blowing would approach the predicted levels.

#### 2.1.3 Drag

The approach will be to divide the drag into the clean airplane drag, the profile drag of the leading and trailing edge devices, the induced drag, and the pressure drag of the wing. Clean airplane drag can be found by conventional methods.

##### 2.1.3.1 Trailing Edge Flap Parasite Drag

The parasite drag of trailing edge flaps is a function of flap type, area, and deflection. An empirical correlation for slotted flaps is given in Figure 14.

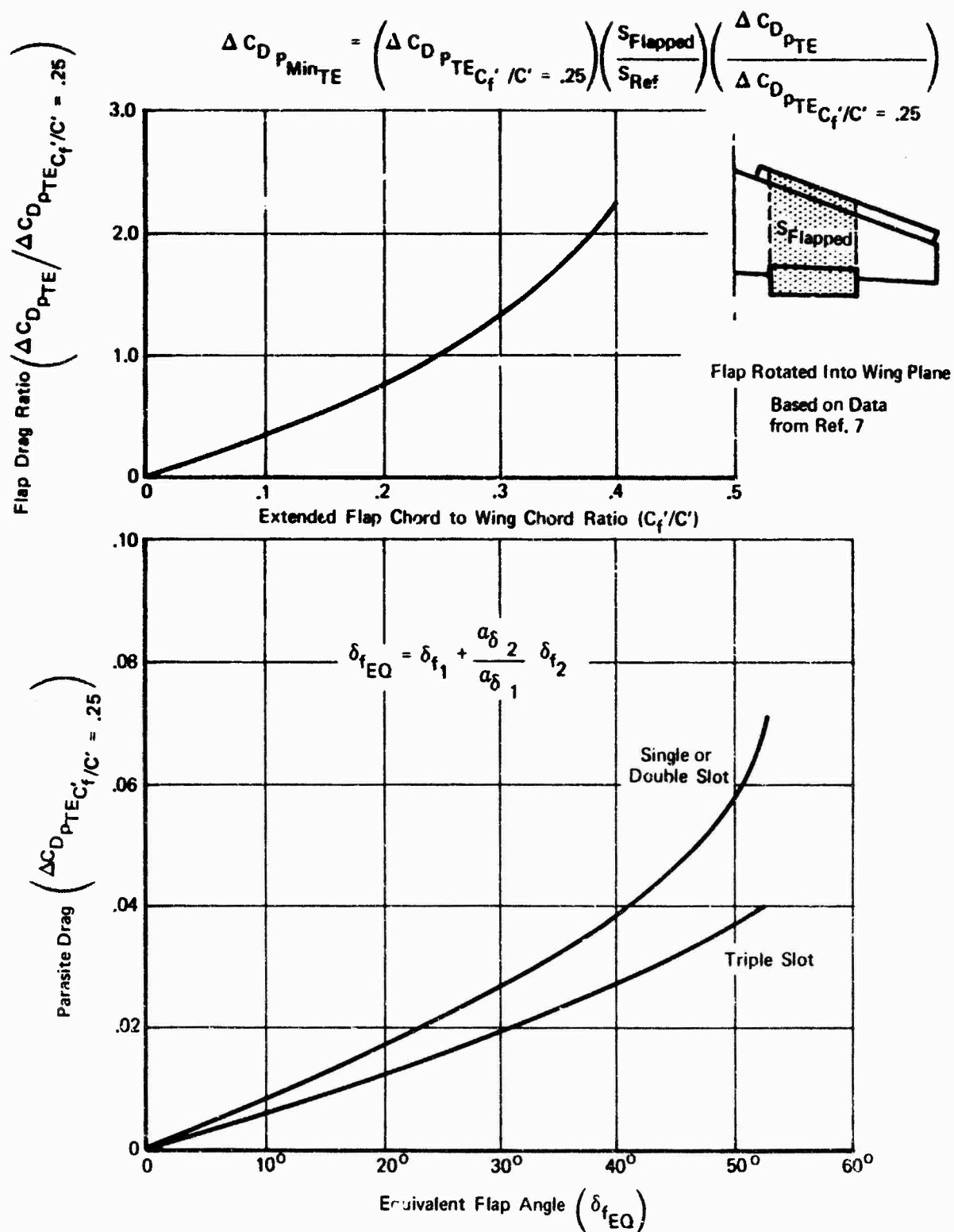


Figure 14: Parasite Drag of Trailing Edge Flaps



$$C_{DP_{min}} = \left( \Delta C_{DP_{TE}} \right) \frac{C'_f}{C} = .25 \left( \frac{S_{flapped}}{S_{REF}} \right) \left( \frac{\Delta C_{DP_{TE}}}{\left[ \Delta C_{DP_{TE}} \right] \frac{C'_f}{C} = .25} \right) \quad (2.1-20)$$

In this correlation the flapped area is the area forward (streamwise) of the trailing edge flap with the flaps, leading and trailing edge, extended and rotated into the plane of the wing.

### 2.1.3.2 Leading Edge Flap Parasite Drag

The parasite drag of leading edge devices is a function of device area and deflection. Insufficient data is available to establish an optimum leading edge deflection angle. However, unpublished Boeing data indicates that at the optimum angle

$$\Delta C_{DP_{min}} = .154 \frac{S_{LE}}{S_{REF}} \quad (2.1-21)$$

where the leading edge area is the planform area of the leading edge device measured parallel to the device chord plane.

### 2.1.3.3 Change in Induced Drag from Trailing Edge Flaps

Deflecting trailing edge flaps results in a change in load distribution from that of the clean wing. Since the clean wing is normally designed to have a load distribution close to elliptic, the loading due to flaps will normally cause the load distribution to depart from elliptic, resulting in an additional induced drag. A. D. Young (Ref. 10) gives this drag for part-span flaps proportional to the square of the flap lift increment

$$\Delta C_{Di} = K \left( \frac{C_{L_f}^2}{\pi A} \right) \quad (2.1-22)$$

where K is determined from Figure 15.

More accurate estimate of the polar shape may be determined by methods such as that in Ref. 1. However, these methods require the span loading to be determined.

### 2.1.3.4 Parasite Drag Variation with Lift

Both the friction and pressure drag vary with lift. It is impossible to estimate these variations precisely, yet some allowance should be made for them. The data from a number of wind tunnel tests of transport configurations with highly developed mechanical high lift systems have been correlated to obtain the curve shown in Figure 16. This curve is intended to give a reasonable preliminary design estimate of the parasite drag variation with lift with both leading and trailing edge devices deployed.

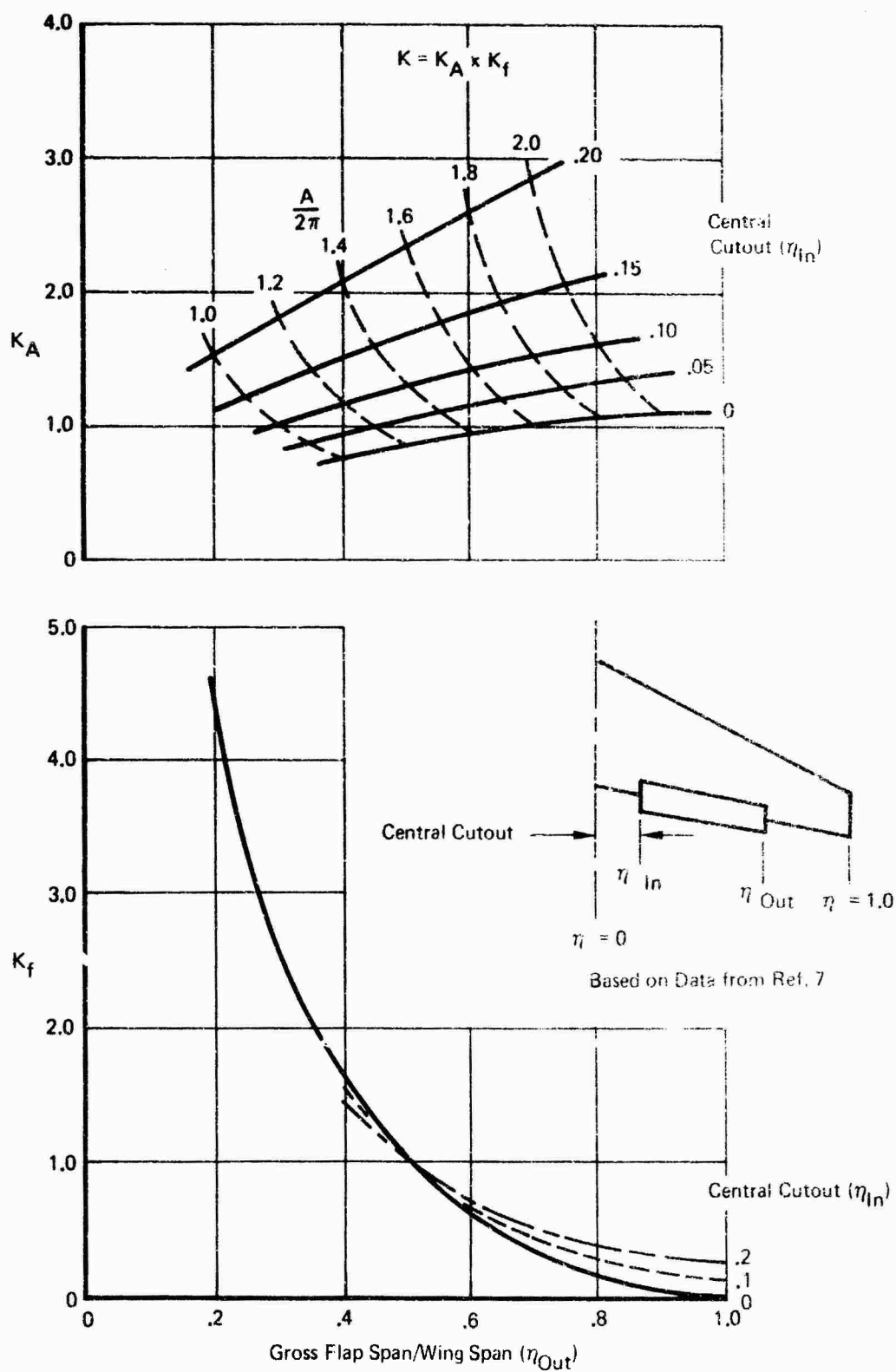


Figure 15: Part-Span Induced Drag Factors (Continuous Flaps with Central Cutout)

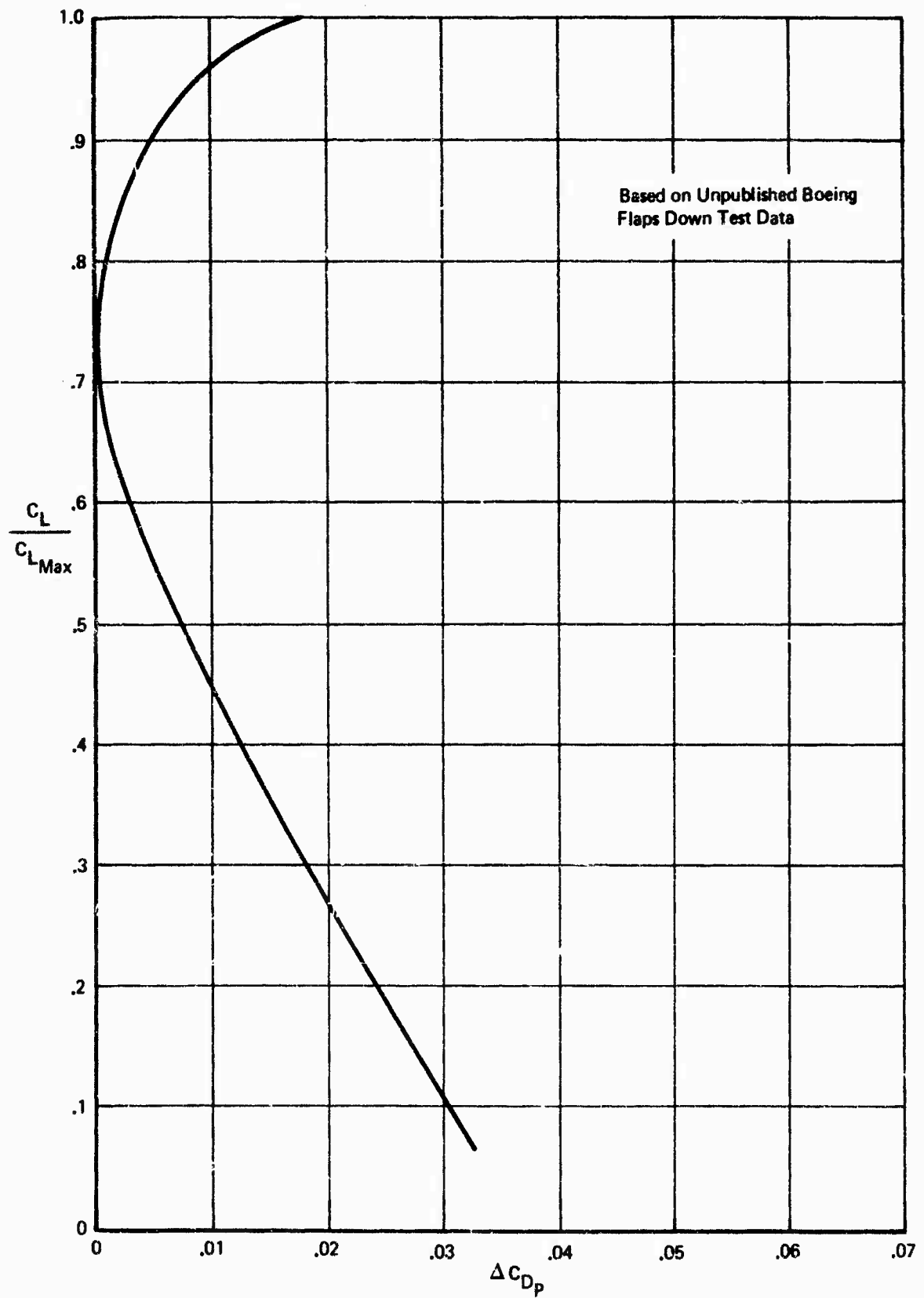


Figure 16: Profile Drag Variation with Lift

### 2.1.3.5 Induced Drag

The drag due to lift is estimated assuming elliptic load distribution.

$$C_{Di} = \frac{C_L^2}{\pi A} \quad (2.1-23)$$

This is used since the drag increments estimated in the previous sections are designed to account for the departure from an elliptic load.

A comparison between drag estimated by the methods described and drag obtained from the STAI wind tunnel test program is shown in Figure 17.

### 2.1.3.6 Leading Edge Boundary Layer Control

The effects of leading edge blowing boundary layer control on drag were obtained from the STAI wind tunnel test data. These data indicate that

$$\Delta C_{D_{BLC}} = -.5 C_{\mu_{LE}} \quad (2.1-24)$$

#### SAMPLE PROBLEM, FREE AIR DRAG

$$S_{\text{flapped}} = 5.577 \text{ SF}$$

$$S_{\text{Ref}} = 6.164 \text{ SF}$$

$$\delta_{f1} = 44.9^\circ$$

$$\delta_{f2} = 15.1^\circ$$

$$(\alpha_\delta)_1 = -.50$$

$$(\alpha_\delta)_2 = -.25$$

$$C'_{f1}/C' = .289 \text{ (includes leading edge extension)}$$

$$S_{LE} = .882 \text{ SF}$$

$$C_{L_{TEF}} = 1.73$$

$$A_G = 5.74$$

$$A = 8.00$$

$$\eta_{1B} = .145$$

$$\eta_{OB} = .75$$

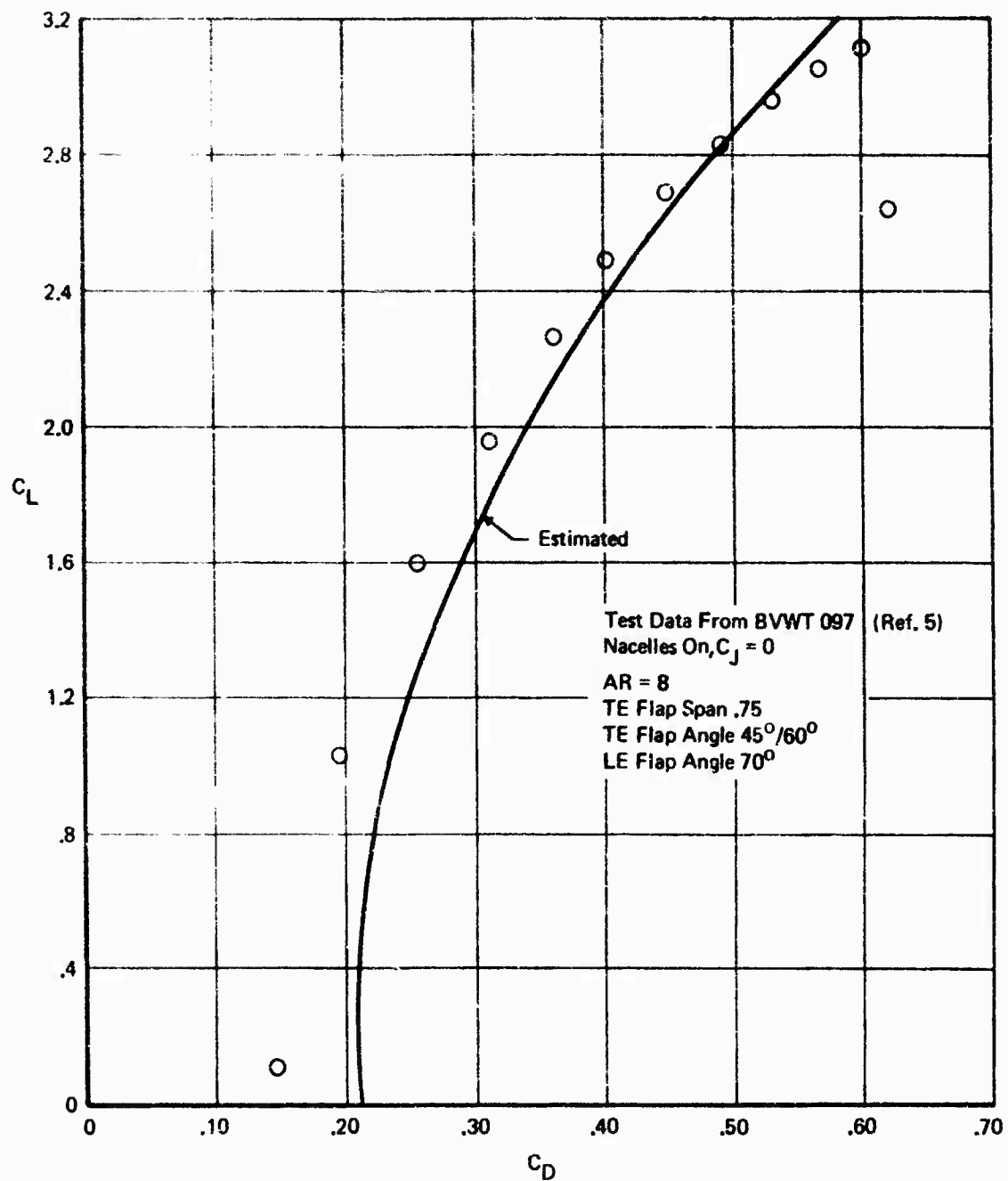


Figure 17: Comparison of Measured and Predicted Power-Off Drag Polars

$$C_{L_{Max}} = 3.33 \text{ from Section 2.1.2.1 and 2.1.2.2}$$

$$C_{L_{Max}} = .98 \text{ test data flaps retracted}$$

$$C_{D_0} = .0600 \text{ test data, flaps retracted}$$

$$C_{u_{LE}} = 0$$

Calculate equivalent flap angle, Figure 14.

$$\delta_{f_e} = 45.14 + \left(\frac{.25}{.485}\right) (15.13) = 52.94$$

Read from Figure 14 and  $C'_f/C'$  and  $\delta_{f_e}$

$$\left(\frac{\Delta C_{DP_{TE}}}{C'}\right) \frac{C'_f}{C} = .25$$

$$\left(\frac{\Delta C_{DP_{TE}}}{C'}\right) \frac{C'_f}{C} = .25$$

Trailing Edge parasite drag, Equation 2.1-20

$$\Delta C_{D_{P_{MIN}}} = (.0395) \left(\frac{5.577}{6.164}\right) (1.0) = .0447$$

Leading edge parasite drag, Equation 2.1-21

$$\Delta C_{D_{P_{MIN}}} = (.154) \left(\frac{.882}{6.164}\right) = .0220$$

From Figure 15 and  $A_G \eta_{1B}$  and  $\eta_{0B}$  read

$$K_a = 1.05$$

$$K_f = .4$$

$$K = (1.05) (.4) = .42$$

Change in induced drag from trailing edge flaps, Equation 2.1-22

$$\Delta C_{D_i} = (.42) \left(\frac{(1.73)^2}{(8)}\right) = .0500$$

at a  $C_L = 2.4$  parasite drag variation with lift, with  $C_{L_{Max}} = 3.33$

$$\Delta C_{D_P} = .0005$$

Induced drag

$$C_{Di} = \frac{(2.4)^2}{(\pi)(8)} = .2290$$

Total Drag

$$C_D = .0600 + .0447 + .0220 + .0500 + .0005 + .2290 \\ = .4062$$

From Test Data at  $C_L = 2.4$

$$C_D = .3880$$

#### 2.1.4 Pitching Moment

Deflection of leading and trailing edge devices affects the tail-off airplane pitching moment characteristics by:

- (1) Moving the aerodynamic center location if chord extension is involved.
- (2) Changing the pitching moment at zero lift because of a change in camber.

An additional effect which influences the tail-on pitching moment is the change in the downwash field behind the wing. In the following sections these effects are examined. The methods for estimating the change in aerodynamic center location and pitching moment at zero lift are taken from Ref. 7. Methods for predicting the effects of high lift devices on the downwash field behind the wing are from Ref. 1 and 11.

##### 2.1.4.1 Aerodynamic Center Shift Due to Leading Edge Devices

Leading edge devices without chord extension do not move the aerodynamic center as long as the flow remains attached. When chord extension is present, the a.c. shift may be calculated by considering the leading edge planform extension. The estimate of the aerodynamic center shift is made relative to the a.c. location of the basic trapezoidal wing.

An elliptical additional span load is assumed for the trapezoidal wing. The part span load of the wing panel where the chord is extended is  $\lambda$ . Using the Schrenk-Thorpe span load approximation, this panel load increases by half the fractional area increase upon addition of the chord extension covering a small fraction of the wing span. As the chord extension tends to full span, the panel load increment approaches the fractional chord extension.

The inner wing panel loads are assumed to be centered at 50 percent of the panel span on the local aerodynamic center both for the original trapezoidal wing and the modified wing. The part of the wing planform contained within the body plan view is treated in a similar manner, letting the local load move forward (or aft for trailing edge devices) as dictated by the chord extension, but the load on the body is held constant.

Two different equations have been derived, for the leading edge devices extending to the side of the body, and for outboard devices which do not extend to the body.

In the following analysis it is assumed that the basic trapezoidal wing aerodynamic center position  $(x_{ac})_{trap}$  is known (see Ref. 1 or 2) and the value of the load is unity, i.e.

$$L = 1.0 \quad (2.1-25)$$

Using Figures 5 and 18 and taking moments about A - A gives

$$M = \lambda_1 x_1 - \lambda_2 x_2 + M \Big|_{\eta=2}^{\eta=1} \quad (2.1-26)$$

In Equation 2.1-25  $x_1$  is the moment arm to the local aerodynamic center of the trapezoid where it intersects the body (use Figure 19 for correction to quarter chord location) and  $x_2$  is the moment arm to the midspan of the wing panel with leading edge devices.

Assuming that  $M$  is a linear function of  $L$  and  $M = 0$  at  $L = 0$  leads to

$$\frac{\partial M}{\partial L} = \frac{M}{L} \quad (2.1-27)$$

Since

$$(x_{ac})_{trap} = - \frac{\partial M}{\partial L} = - \frac{M}{L} \quad (2.1-28)$$

it follows from Equation 2.1-25, 2.1-26, and 2.1-28 that

$$(x_{ac})_{trap} = \lambda_1 x_1 + \lambda_2 x_2 - M \Big|_{\eta=2}^{\eta=1} \quad (2.1-29)$$

and

$$-M \Big|_{\eta=2}^{\eta=1} = (x_{ac})_{trap} - \lambda_1 x_1 - \lambda_2 x_2 \quad (2.1-30)$$

The load of the wing with leading edge devices extended is

$$L = 1 + \mu_s \frac{\Delta S}{S_2} \lambda_2 \quad (2.1-31)$$

where  $\mu_s \frac{\Delta S}{S_2} \lambda_2$  is the load increase based upon the Schrenk-Thorp span load assumption. The area increase  $\Delta S$  is shown in Figure 18 and the load factor is obtained from Figure 20.



Note: Primed Quantities Are For Wing With Chord Extension

Area  $\Delta S$

$(x_{ac})_{Trap}$

Local Aerodynamic Centers

Local A.C. With Chord Extens.

$x_2$ ,  $x_1$ ,  $x_2'$ ,  $x_1'$

$x$

$\eta_1$

$\eta = \frac{\eta_1 + \eta_2}{2}$

$\eta_2$

$\eta = 1.0$

$\eta = 0$

Assumed Loading of Trapezoid Wing (Elliptical)

Load  $\lambda_1$

Load  $\lambda_2$

Load  $1 - \lambda_1 - \lambda_2$

40

For High Wing Locations

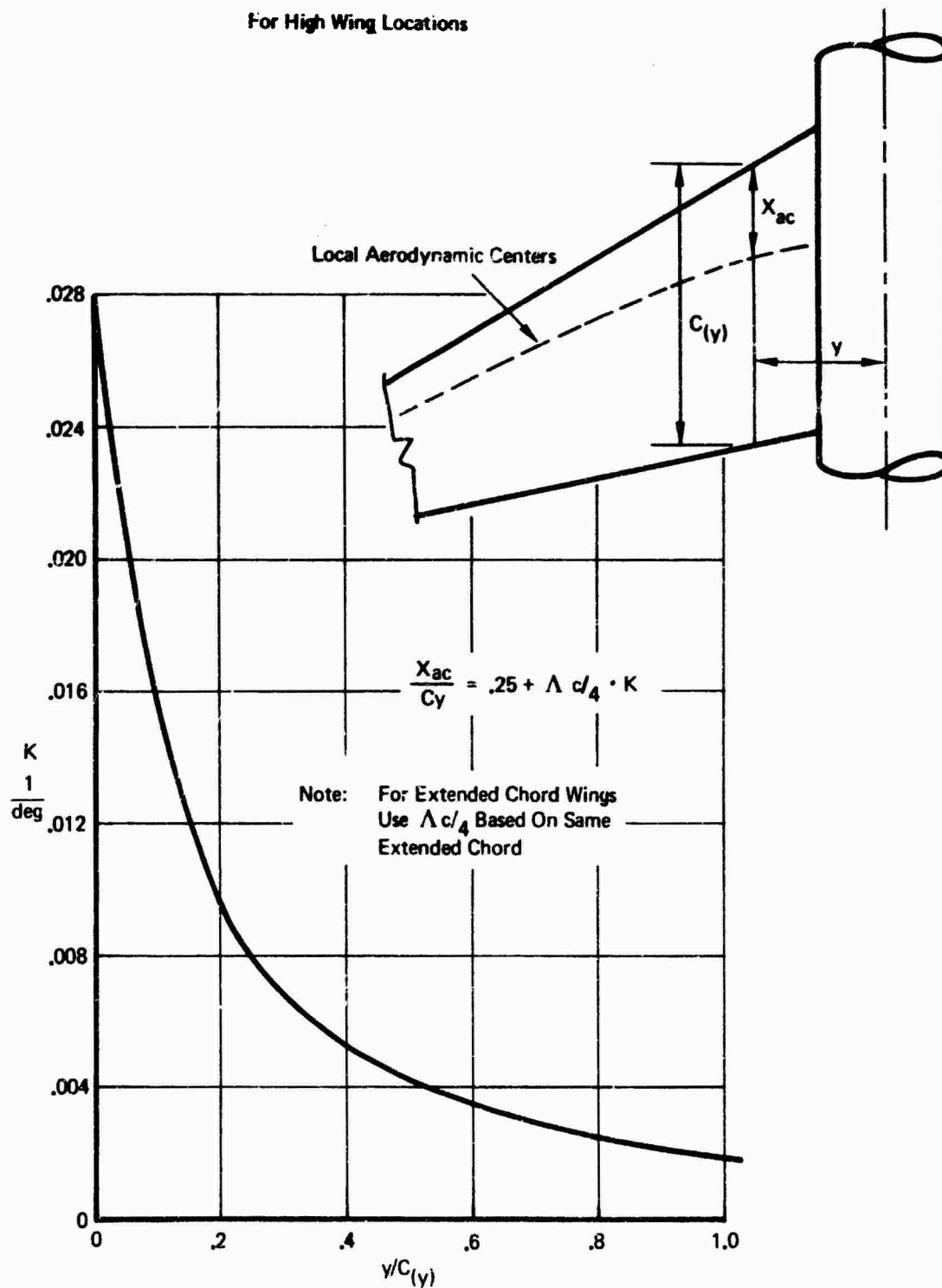


Figure 19: Local Aerodynamic Centers Near Middle Of Wing

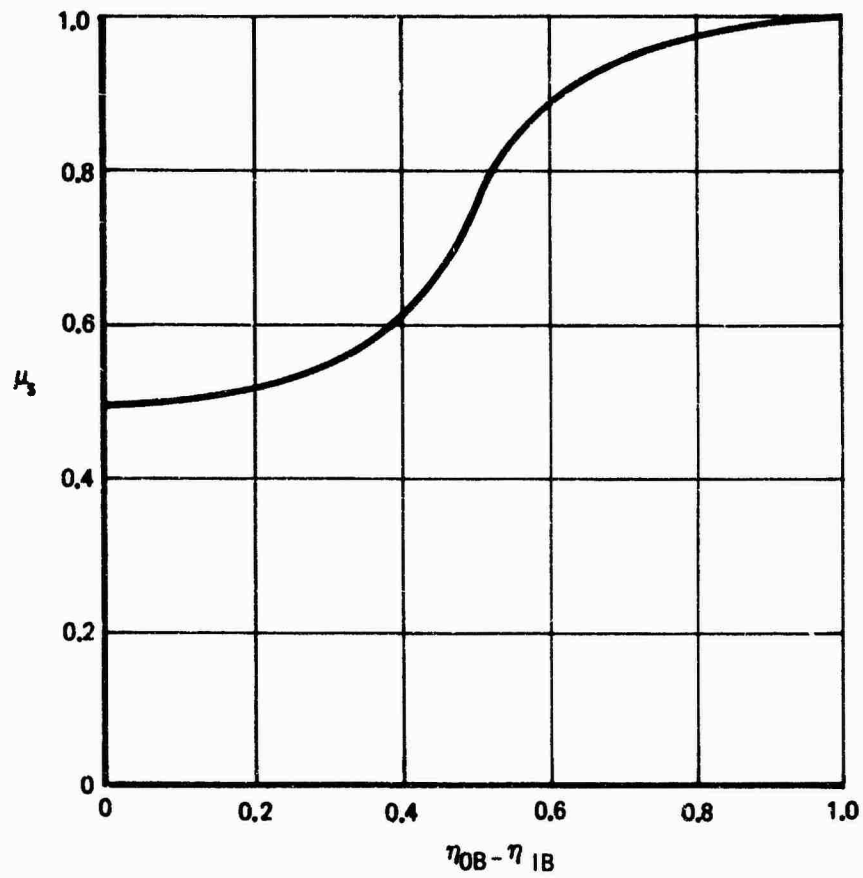
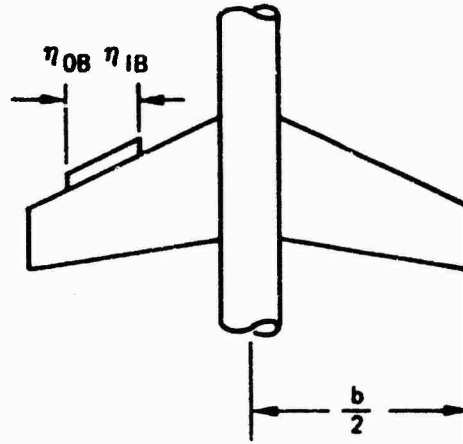


Figure 20: Load Effectiveness of Part Span Chord Extensions

Again taking moments about A - A gives:

$$M = -\lambda_1 x'_1 - \lambda_2 x'_2 - \mu_3 \frac{\Delta S}{S_2} \lambda_2 x'_2 + M \Big|_{\eta=2}^{\eta=1} \quad (2.1-32)$$

In Equation 2.1-32  $x'_1$  is the moment arm to the local aerodynamic center of the wing panel with the extended chord at the body side and  $x'_2$  is measured to the extended chord wing local aerodynamic center at  $\eta = \frac{\eta_1 + \eta_2}{2}$

The aerodynamic center for the wing with the leading edge devices extended follows from

$$\frac{\partial M}{\partial L} = (x_{ac})_{LE} = \frac{\lambda_1 x'_1 + \lambda_2 x'_2 \left(1 + \mu_3 \frac{\Delta S}{S_2}\right) x'_2 - M \Big|_{\eta=2}^{\eta=1}}{1 + \mu_3 \frac{\Delta S}{S_2} \lambda_2} \quad (2.1-33)$$

Substituting Equation 2.1-30 into 2.1-33 gives:

$$(x_{ac})_{LE} = \frac{\lambda_1 (x'_1 - x_1) + \lambda_2 \left[1 + \mu_3 \frac{\Delta S}{S_2}\right] x'_2 - x_2}{1 + \mu_3 \frac{\Delta S}{S_2} \lambda_2} + (x_{ac})_{trap} \quad (2.1-34)$$

The analysis for the outboard leading edge devices is very similar to the one employed above. A simplification here is that the load on the body region does not require separate identification.

Assuming again a unity load

$$L = 1.0 \quad (2.1-35)$$

and taking moments about A-A (see Figure 21) leads to

$$M = M \Big|_{\eta=0}^{\eta=1} - \lambda_2 x_2 + M \Big|_{\eta=2}^{\eta=1} \quad (2.1-36)$$

Hence,

$$(x_{ac})_{trap} = \frac{\partial M}{\partial L} = \lambda_2 x_2 - M \Big|_{\eta=0}^{\eta=1} - M \Big|_{\eta=2}^{\eta=1} \quad (2.1-37)$$

and

$$-M \Big|_{\eta=0}^{\eta=1} - M \Big|_{\eta=2}^{\eta=1} = (x_{ac})_{trap} - \lambda_2 x_2 \quad (2.1-38)$$

Note: Applies To Either Leading Edge Or  
Trailing Edge Chord Extensions

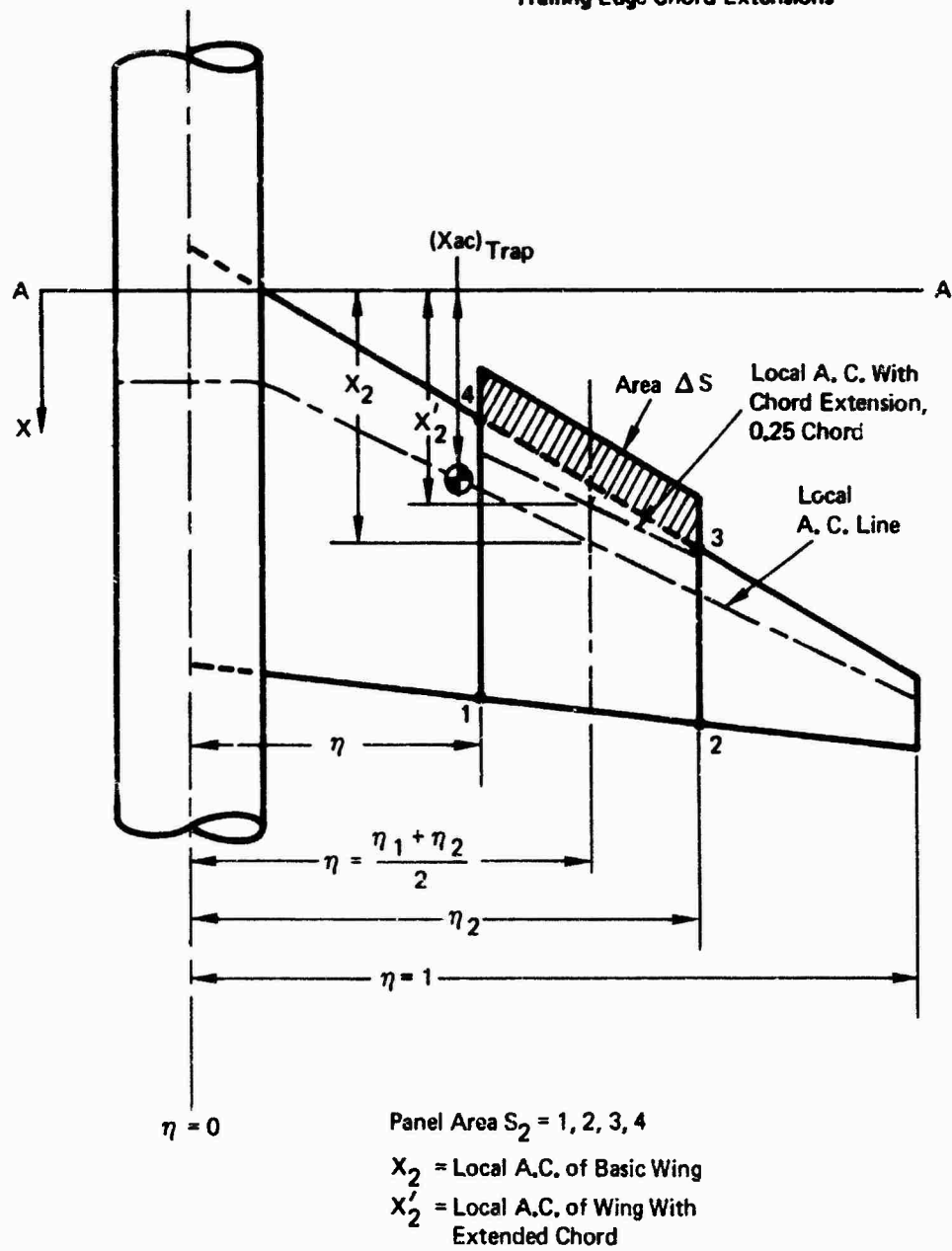


Figure 221: Nomenclature for  $ac$  Location with Outboard L.E. Devices

$$L = 1 + \mu_s \frac{\Delta S}{S_2} \lambda_2 \quad (2.1-39)$$

The moment is

$$M = M|_{\eta=0}^{\eta=1} + \lambda_2 \left( 1 + \mu_s \frac{\Delta S}{S_2} \right) x_2' + M|_{\eta=2}^{\eta=1} \quad (2.1-40)$$

Using the Equation 2.1-28 and 2.1-40 gives the a.c. location

$$(x_{ac})_{LE} = -\frac{\partial M}{\partial L} = \frac{-M|_{\eta=0}^{\eta=1} - M|_{\eta=2}^{\eta=1} + \lambda_2 \left( 1 + \mu_s \frac{\Delta S}{S_2} \right) \lambda_2'}{1 + \mu_s \frac{\Delta S}{S_2}} \quad (2.1-41)$$

Substituting Equation 2.1-38 and 2.1-41 gives

$$(x_{ac})_{LE} = \frac{\lambda_1(x_1' - x_1) + \lambda_2 \left[ \left( 1 + \mu_s \frac{\Delta S}{S_2} \right) x_2' - x_2 \right] + (x_{ac})_{trap}}{1 + \mu_s \frac{\Delta S}{S_2} \lambda_2} \quad (2.1-42)$$

and the a.c. shift due to the leading edge devices becomes for the two cases:

(a) Leading edge devices extending to the side of the body:

$$(\Delta x_{ac})_{LE} = \frac{\lambda_1(x_1' - x_1) + \lambda_2 \left[ \left( 1 + \mu_s \frac{\Delta S}{S_2} \right) x_2' - x_2 \right] + (x_{ac})_{trap} - (x_{ac})_{trap}}{1 + \mu_s \frac{\Delta S}{S_2} \lambda_2} \quad (2.1-43)$$

(b) Outboard leading edge devices:

$$(\Delta x_{ac})_{LE} = \frac{\lambda_2 \left[ \left( 1 + \mu_s \frac{\Delta S}{S_2} \right) x_2' - x_2 \right] + (x_{ac})_{trap} - (x_{ac})_{trap}}{1 + \mu_s \frac{\Delta S}{S_2} \lambda_2} \quad (2.1-44)$$

# SAMPLE PROBLEM, LEADING EDGE EXTENSION ac SHIFT

$$\eta_1 = .145$$

$$\eta_2 = 1.0$$

$$X_1 = 35.82 \text{ in.}$$

$$X_1' = 34.76 \text{ in.}$$

$$X_2 = 39.63 \text{ in.}$$

$$X_2' = 38.38 \text{ in.}$$

$$\Delta S = .882 \text{ SF}$$

$$S_2 = 4.945 \text{ SF}$$

$$(X_{ac})_{\text{Trap}} = 37.98 \text{ in.}$$

from chart Figure 20

$$\mu_S = .985$$

from Figure 5 read

$$\lambda_1 = .183$$

$$\lambda_2 = .817$$

with Equation 2.1-43 calculate shift on ac with leading edge extension

$$(X_{ac})_{LE} =$$

$$\begin{aligned} & \frac{(.183)(34.76 - 35.82) + .817 \left\{ \left[ 1 + (.985) \left( \frac{.882}{4.945} \right) \right] (38.38) - 39.63 \right\} + 37.98}{1 + (.985) \left( \frac{.882}{4.945} \right) (.817)} \\ & = \frac{-.194 + 4.488 + 37.98}{1.143} = 36.98 \text{ in.} \end{aligned}$$

For the change in aerodynamic center, Equation 2.1-43

$$(\Delta X_{ac})_{LE} = 36.98 - 37.98 = 1.00 \text{ in.}$$

## 2.1.4.2 Aerodynamic Center Shift Due to Trailing Edge Flaps

Simple hinged flaps do not affect the aerodynamic center substantially so long as the air flow remains attached. Flaps with chord extension move the aerodynamic center back. Their effects may be determined by the methods developed for the leading edge devices in the preceding section. By using the appropriate values from Figures 19

and 21. with  $\mu_S$  from Figure 20 and  $\lambda$  from Figure 5 in Equation 2.1-43 and 2.1-44 the a.c. shift due to trailing edge flaps extending to the side of the body and outboard trailing edge flaps may be computed, respectively.

#### SAMPLE PROBLEM, TRAILING EDGE EXTENSION ac SHIFT

$$\eta_1 = .145$$

$$\eta_2 = .75$$

$$X_1 = 35.82 \text{ in.}$$

$$X_1' = 37.38 \text{ in.}$$

$$X_2 = 38.22 \text{ in.}$$

$$X_2' = 39.00 \text{ in.}$$

$$\Delta S = 1.104 \text{ SF}$$

$$S_2 = 3.881 \text{ SF}$$

$$(\lambda_{ac})_{\text{Trap}} = 37.98 \text{ in.}$$

$$\lambda_1 = .183$$

$$\lambda_2 = .666$$

from Fig. 20 read

$$\mu_S = .89$$

The aerodynamic center with trailing edge extended equation, Equation 2.1-34

$$(X_{ac})_{TE} =$$

$$\frac{(.183)(37.38 - 35.82) + (.666) \left\{ [(1 + (.89) \frac{(1.104)}{(3.881)})] (39.00) - 38.22 \right\} + 37.98}{1 + (.89) \left( \frac{1.104}{3.881} \right) (.666)}$$

$$= \frac{.285 + 7.095 + 37.98}{1.169} = \frac{45.36}{1.169} = 38.80$$

For the change in aerodynamic center (2.1-43)

$$(\Delta X_{ac})_{TE} = 38.80 - 37.98 = .820$$

#### 2.1.4.3 Pitching Moment at Zero Lift Due to Trailing Edge Flap

$\Delta C_{mOL}$  is calculated by estimating the spanwise and chordwise position of the center of loading induced by the flap.  $\Delta C_{mOL}$  is then equal to the estimated flap lift increment times the arm from the estimated flap load center to the flaps extended aerodynamic center.



The flap load center is estimated as follows:

- (a) As a first approximation, assume the flap load center is along the wing half-chord line.
- (b) Along chordwise cuts normal to the half-chord line evaluate the flap chord ratio  $c'_f/c$ .
- (c) Determine the locus of chordwise flap load center positions using Figure 22.
- (d) Iterate if the new flap center of pressure line differs greatly from the initial approximation.
- (e) Locate the flap load center.

Finally,

$$(\Delta C_m)_{OL TE} = \frac{-(\Delta C_L)_{TE}}{C_{REF}} \left[ x_{CPTe} - (x_{ac})_{\text{flaps extended}} \right] \quad (2.1-45)$$

SAMPLE PROBLEM, PITCHING MOMENT AT ZERO LIFT DUE TO TRAILING EDGE FLAP

$$c'_f/c = .323 \text{ (constant \% chord flap)}$$

$$\bar{c} = 11.179 \text{ in.}$$

$$A = 6.786$$

$$P = 98.831 \text{ in.}$$

$$\eta_{LB} = .145$$

$$\eta_{OB} = .75$$

$$\Delta C_{LTE} = 2.01$$

Calculate

$$\frac{C_{L\alpha}}{C_{L\alpha}} \sim \frac{6.786}{\left( \frac{98831}{84274} \right) (6.786) + 2} = .681$$

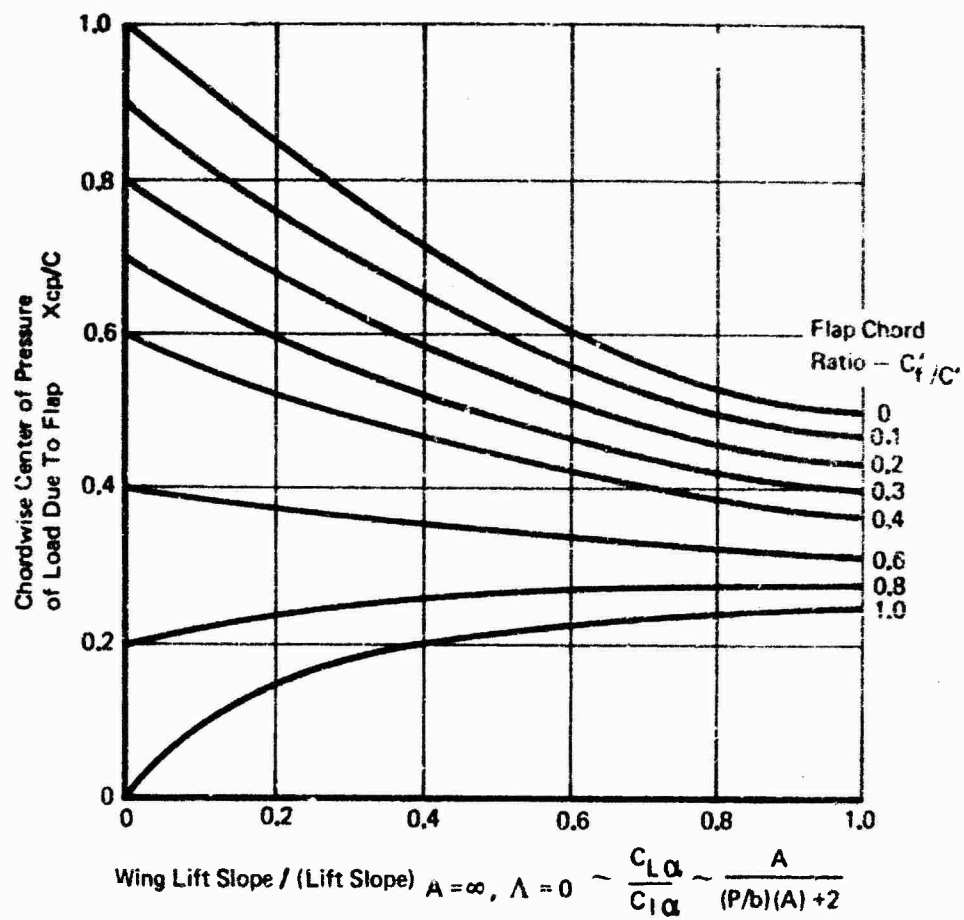


Figure 22: Chordwise Center of Load Due To Flaps

From Figure 22 obtain chordwise center of pressure

$$\frac{x_{cp}}{c} = .44, \text{ this is near enough to the original assumption of } x_{cp}/c = .50$$

that iteration will not result in a significant change. From Figure 23 determine spanwise center of pressure

$$\eta_{cp} = .422$$

The center of pressure is then located at the intersection of the .44 chord line and  $\eta_{cp} = .422$ . In the model longitudinal reference system

$$x_{cp \text{ TE}} = 41.47$$

The  $(C_{m_{OL}})_{TE}$  is then calculated from equation 2.1-45

$$\begin{aligned} (C_{m_{OL}})_{TE} &= - \frac{2.01}{11.179} (41.47 - 38.88) \\ &= -.4637 \end{aligned}$$

#### 2.1.4.4 Pitching Moment at Zero Lift Due to Leading Edge Devices

The pitching moment at zero lift increment due to leading edge flaps is much smaller than that due to trailing edge flaps so that a simpler approach can be adopted

$$(\Delta C_{m_{OL}})_{LE} = \frac{+(\Delta C_L)_{LE}}{C_{REF}} \left[ x'_{c/4} - (x_{ac})_{LE \text{ extended}} \right] \quad (2.1-46)$$

Where  $x'_{c/4}$  is the quarter chord of the mean aerodynamic chord determined with the leading edge extended in the plane of the wing.

#### SAMPLE PROBLEM, PITCHING MOMENT AT ZERO LIFT DUE TO LEADING EDGE

$$\begin{aligned} C_{L_{LE}} &= -.15 \\ C_{REF} &= 11.179 \text{ in.} \\ x'_{c/4} &= 36.867 \text{ in} \end{aligned}$$

$$x_{ac_{LE}} = 36.98 \text{ in.}$$

calculate  $(\Delta C_{m_{OL}})_{LE}$  with equation 2.1-46

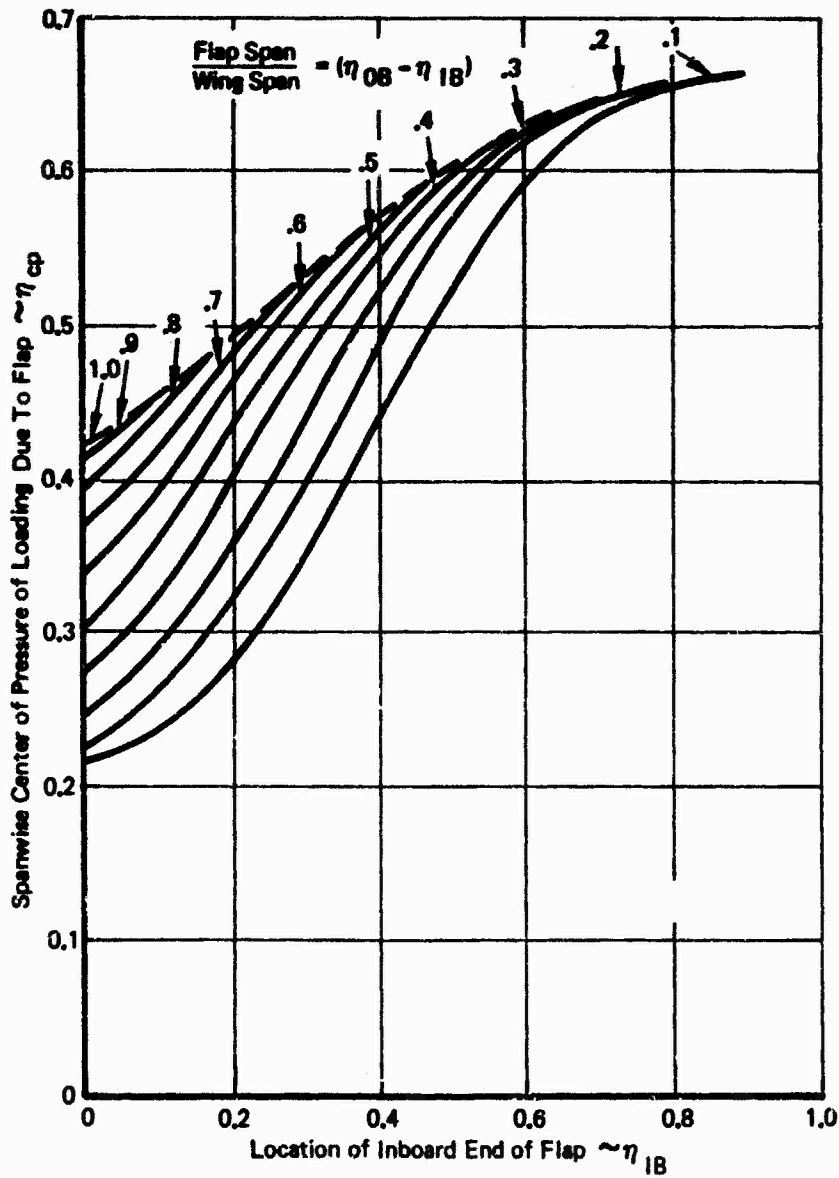
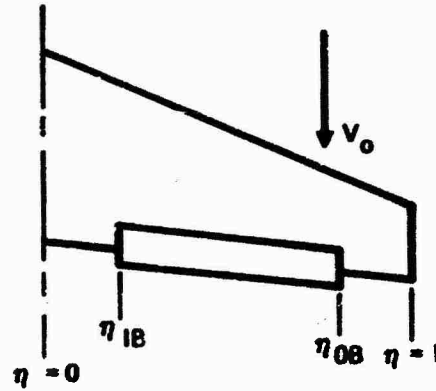


Figure 23: Spanwise Center of Load Due To Flaps

$$(\Delta C_{m_{ol LE}}) = - \frac{.15}{11.179} (36.867 - 36.980)$$

$$= + .0015$$

#### 2.1.4.5 Change in Downwash Due to Leading Edge and Trailing Edge High-Lift Devices

Generally accepted methods for predicting the downwash variation behind the wing due to leading and trailing edge high lift devices are at present not available. However, qualitative design guidelines based on the analysis of large amount of experimental data are summarized in Ref. 11. Quantitative data for estimating the increment of downwash due to trailing edge flap deflection have also been obtained. All of the following discussion is based on Ref. 10.

Analysis of the air flow characteristics behind sweptback wings shows that before separation occurs the downwash remains unaffected by leading edge flaps. The increments of down wash due to deflecting trailing-edge flaps on wing-body combinations are summarized in Figure 24. The ratio of measured effective downwash increment to the factor  $\Delta C_{LE}$  was

found to give satisfactory correlation of the flap span effect and is shown in Figure 24 as a function of height of the horizontal tail. Only the lift increment due to trailing edge flap deflection is used in Ref. 10 indicates that leading edge devices have negligible effect on downwash.

The correlation of  $\frac{\Delta \epsilon}{\Delta C_{LE} A(\eta_{OB} - \eta_{IB})}$  indicated in Figure 24 was found satisfactory as long as  $\Delta \epsilon$  was smaller than  $10^\circ$ . When  $\Delta \epsilon$  was larger than  $10^\circ$ , at low tail positions (close to the wing wake), the correlation was not as good.

#### SAMPLE PROBLEM, CHANGE IN DOWNWASH FROM TRAILING EDGE FLAPS

$$Z_t = 17.566 \text{ in.}$$

$$b = 84.27 \text{ in.}$$

$$\eta_{IB} = .145$$

$$\eta_{OB} = .75$$

$$\Delta C_{L_{TE}} = 2.01$$

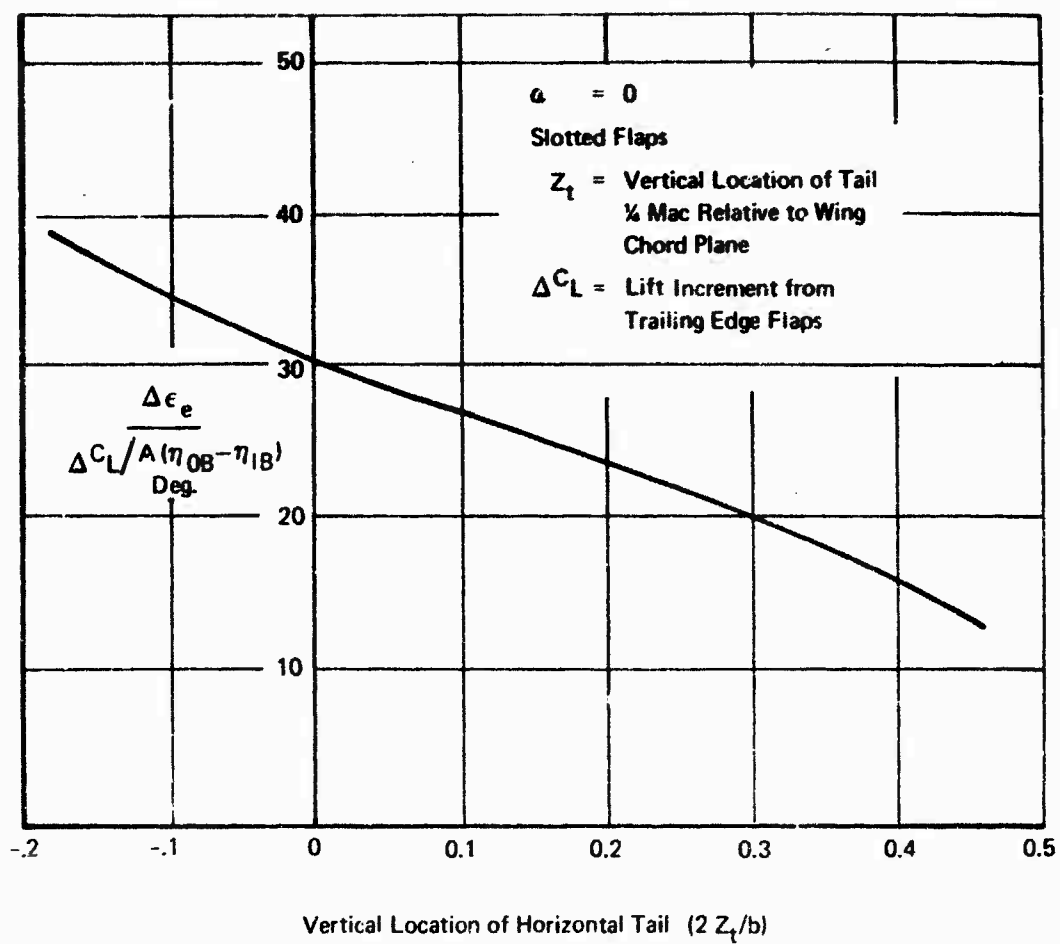


Figure 24: Change in Downwash at Horizontal Tail

from Figure 24 read @  $2h/b = .417$

$$\frac{\Delta \epsilon_e}{\Delta C_{L/A}(\eta_{OB} - \eta_{1B})} = 15.2$$

$$\Delta \epsilon_e = \frac{(15.2)(2.01)}{(8)(.75 - .145)} = 6.21$$

#### 2.1.4.6 Total Free Air Pitching Moment

The increments in zero lift pitching moment and aerodynamic center from extension are combined with the flaps up data and provide pitching moment as a function of lift coefficient.

$$C_{m_{OL}} = C_{m_{OL}}^{\text{flaps up}} + \Delta C_{m_{OL}}^{\text{leading edge}} + \Delta C_{m_{OL}}^{\text{trailing edge}} \quad (2.1-47)$$

$$x_{ac} = x_{ac}^{\text{flaps up}} + \Delta x_{ac}^{\text{leading edge}} + \Delta x_{ac}^{\text{trailing edge}} \quad (2.1-48)$$

$$C_m = C_{m_{OL}}^{\text{flaps down}} + \left[ \frac{x_{cg}}{C_{REF}} - \frac{x_{ac}}{C_{REF}^{\text{flaps down}}} \right] C_L \quad (2.1-49)$$

Figure 25 compares pitching moment estimated with the test data.

#### SAMPLE PROBLEM, PITCHING MOMENT

$$(C_{mo})_{\text{flaps up}} = -.11$$

$$(\Delta C_{mo})_{LE} = +.0015$$

$$(\Delta C_{mo})_{TE} = -.4657$$

$$(x_{ac})_{\text{flap up}} = 37.98 \text{ in.}$$

$$(\Delta x_{ac})_{LE} = -1.00 \text{ in.}$$

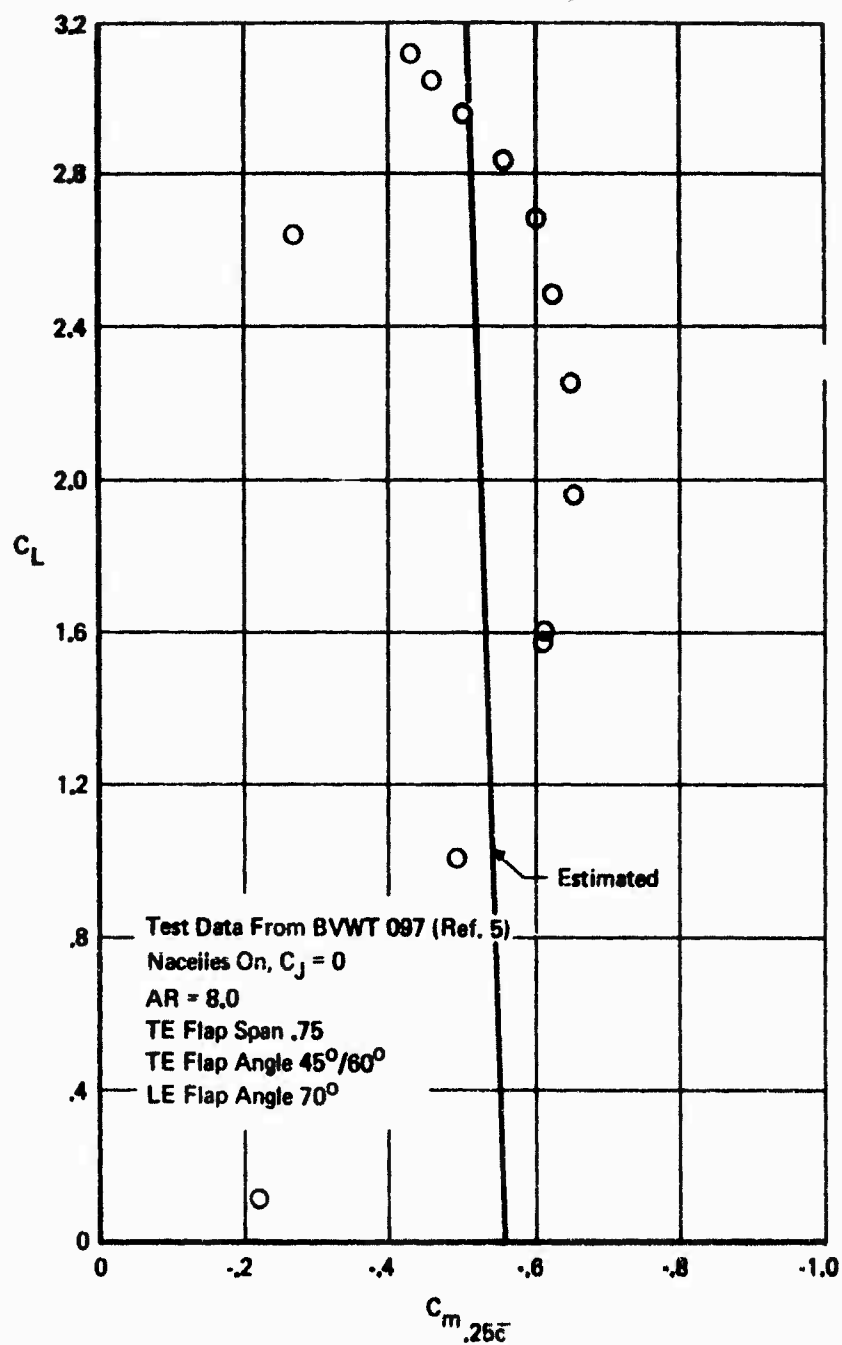


Figure 25: Comparison of Measured and Predicted Power-Off Pitching Moment



$$(X_{ac})_{TE} = + .820 \text{ in.}$$

$$X_{cg} = 37.98 \text{ in. } (.25 \text{ mac})$$

from equation 2.1-47

$$\begin{aligned} (C_{mo})_{\text{flap down}} &= -.11 + .0015 - .4657 \\ &= -.5742 \end{aligned}$$

from equation 2.1-48

$$\begin{aligned} (X_{ac})_{\text{flap down}} &= 37.98 - 1.00 + .820 \\ &= 37.80 \end{aligned}$$

Pitching moment from equation 2.1-49 @ a lift coefficient = 2.4

$$\begin{aligned} C_m &= -.5742 + \left( \frac{37.98}{11.179} - \frac{37.80}{11.179} \right) (2.4) \\ &= -.5742 + .0386 = -.5356 \end{aligned}$$

From Test Data

$$C_m = -.630$$

## 2.2 Ground Effect

Proximity to the ground affects the wing aerodynamic characteristics in three ways. There is a reduction in dynamic pressure at the wing, a reduction in induced angle of attack, and an induced camber.

The assumption is usually made (Ref. 1) that the effects of reduced  $q$  and induced camber are small and, since they are of opposite sign, can be ignored. While this assumption was reasonable prior to the advent of modern high lift systems, it is certainly not valid with today's very high lift STOL systems.

A very simple analysis has been performed using a single horseshoe vortex and its image in the ground plane. This will give a theoretical estimate of the induced change in angle of attack and the reduced dynamic pressure. The camber effect is assumed to be small compared to those effects for STOL configurations with high mounted wings.

### 2.2.1 Lift

To approximate an elliptically loaded wing by a single rectangular vortex, the vortex span should be  $\pi b/4$ . In this analysis a single horseshoe vortex with span  $\pi b/4$  is used with the induced velocities

averaged over the span. Consider the longitudinal velocity (see Figure 26) induced at any point along the wing span by the image bound vortex:

$$v(x) = \frac{\Gamma}{8\pi h} (\cos\theta_1 + \cos\theta_2) \quad (2.2-1)$$

It may be shown with the assumption of the same lift coefficient based on the local dynamic pressure in free air and in ground effect that the velocity ratio is

$$\frac{V_{FA}}{V_{FA} - v_{avg}} = 1 + \frac{2C_{LFA}}{\pi^3 A} \left\{ \left[ 1 + \left( \frac{\pi}{8h/b} \right)^2 \right]^{-1} \right\} \quad (2.2-2)$$

The ratio of lift coefficients must then be

$$\frac{C_{LGE}}{C_{LFA}} = \left[ \frac{1}{1 + \frac{2C_{LFA}}{\pi^3 A} \left\{ \left[ 1 + \left( \frac{\pi}{8h/b} \right)^2 \right]^{-1} \right\}} \right] \quad (2.2-3)$$

This lift ratio is achieved at a reduced angle of attack due to the induced velocities from the image trailing vortices. The change in angle of attack is

$$\Delta\alpha = \frac{\omega_r}{V_{FA}} - \frac{\omega_r + \omega_i}{V_{FA} - v_{avg}} \quad (2.2-4)$$

and it may be shown that

$$\Delta\alpha = \frac{2C_{LFA}}{\pi^3 A} \ln \left[ 1 + \left( \frac{\pi}{8h/b} \right)^2 \right] \quad (\text{RAD}) \quad (2.2-5)$$

### 2.2.2 Drag

The ratio of drag in ground effect to that in free air is

$$\frac{C_{DGE}}{C_{DFA}} = \frac{[C_{DP} + C_{LFA} \left( \frac{\omega_r + \omega_i}{V_{FA} - v_{avg}} \right)] \frac{q}{8FA}}{C_{DP} + C_{LFA} \frac{\omega_i}{\omega_r}} \quad (2.2-6)$$

or

$$\frac{C_{DGE}}{C_{DFA}} = \left\{ 1 - \left( \frac{2}{\pi^3 A} \right) \left( \frac{C_{LFA}^2}{C_{DFA}} \right) \ln \left[ 1 + \left( \frac{\pi}{8h/b} \right)^2 \right] \right\} \frac{C_{LGE}}{C_{LFA}} \quad (2.2-7)$$

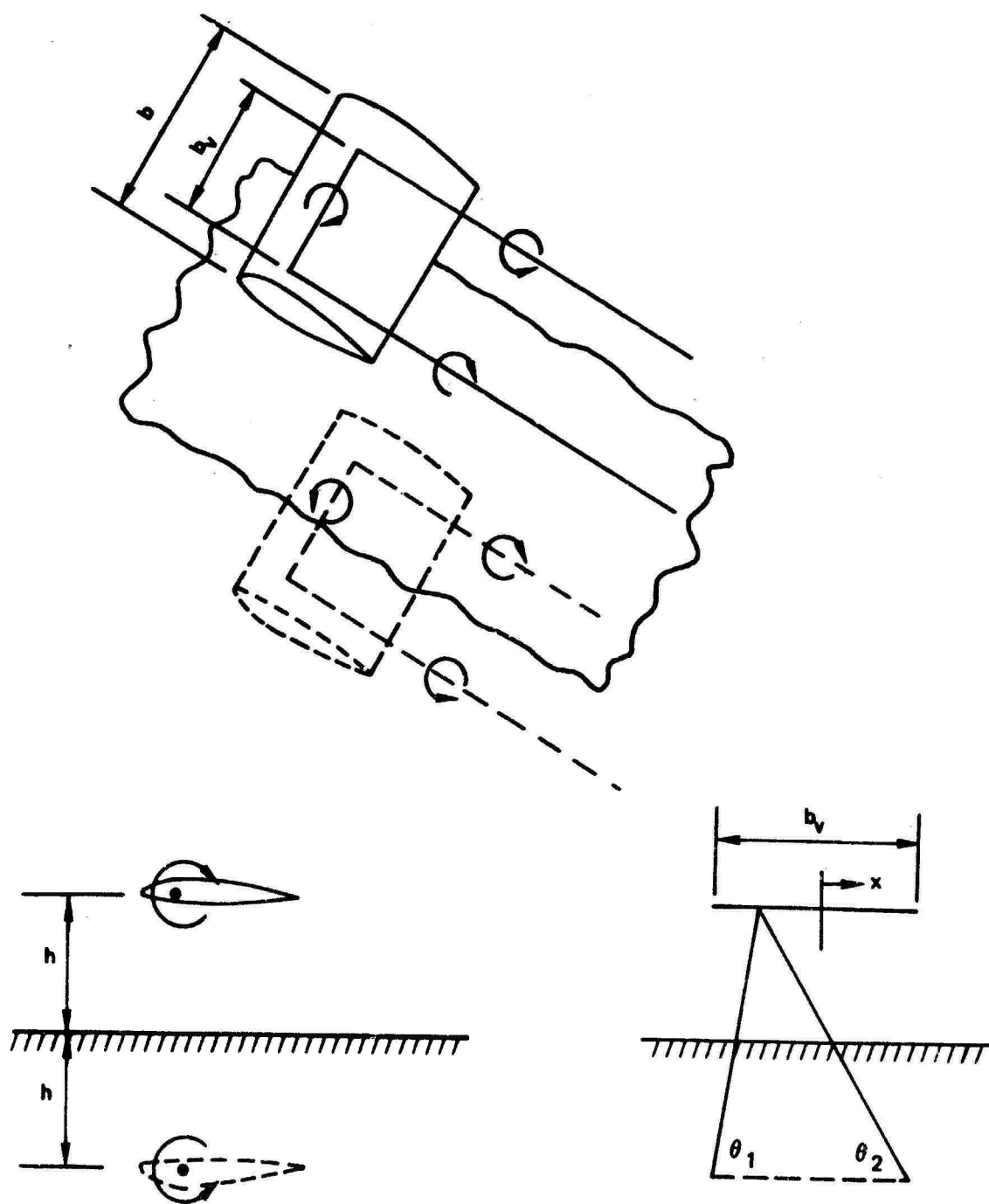


Figure 26: Wing in Ground Effect

### 2.2.3 Pitching Moment

The simple horseshoe vortex approximation cannot be used to find how the center of pressure of the wing changes from free air to ground effect. This would require a more sophisticated lifting surface analysis. As a first approximation we will assume that the location of the center of pressure does not change in ground effect. Therefore,

$$\frac{C_{m_{GE}}}{C_{m_{FA}}} = \frac{C_{L_{GE}}}{C_{L_{FA}}} \quad (2.2-8)$$

while this approach does not have any theoretical justification, it does correlate well with the test data, see Figures 27 and 28.

### 2.2.4 Downwash

Using a similar analysis to that for  $C_L$ ,  $\alpha$  and  $C_D$  it may be shown that the change in downwash at the horizontal tail in ground effect is

$$\Delta \epsilon_{GE} = -\frac{C_L b^2}{8\pi A} \left\{ \left( \frac{\ell_t}{\ell_t^2 + (2h - z_t)^2} \right) \left( \frac{1}{\left[ \ell_t^2 + (2h - z_t)^2 + \frac{\pi^2 b^2}{64} \right]^{1/2}} \right) \right. \\ \left. + \left( \frac{1}{(2h - z_t)^2 + \frac{\pi^2 b^2}{64}} \right) \left( 1 + \frac{\ell_t}{\left[ \ell_t^2 + (2h - z_t)^2 + \frac{\pi^2 b^2}{64} \right]^{1/2}} \right) \right\} \quad (\text{RAD}) \quad (2.2-9)$$

A comparison of free air test data corrected for ground effects, and test data in ground effect is shown in Figures 27 and 28.

#### SAMPLE PROBLEM, LONGITUDINAL CHARACTERISTICS IN GROUND EFFECT

$$C_L = 2.0$$

$$h/b = .209$$

$$b = 84.274 \text{ in.}$$

$$A = 8.0$$

$$\alpha = 2.33^\circ$$

$$C_D = .3410$$

$$C_m = -.5273$$

$$z_t = 17.566 \text{ in.}$$

$$\ell_t = 49.171 \text{ in.}$$

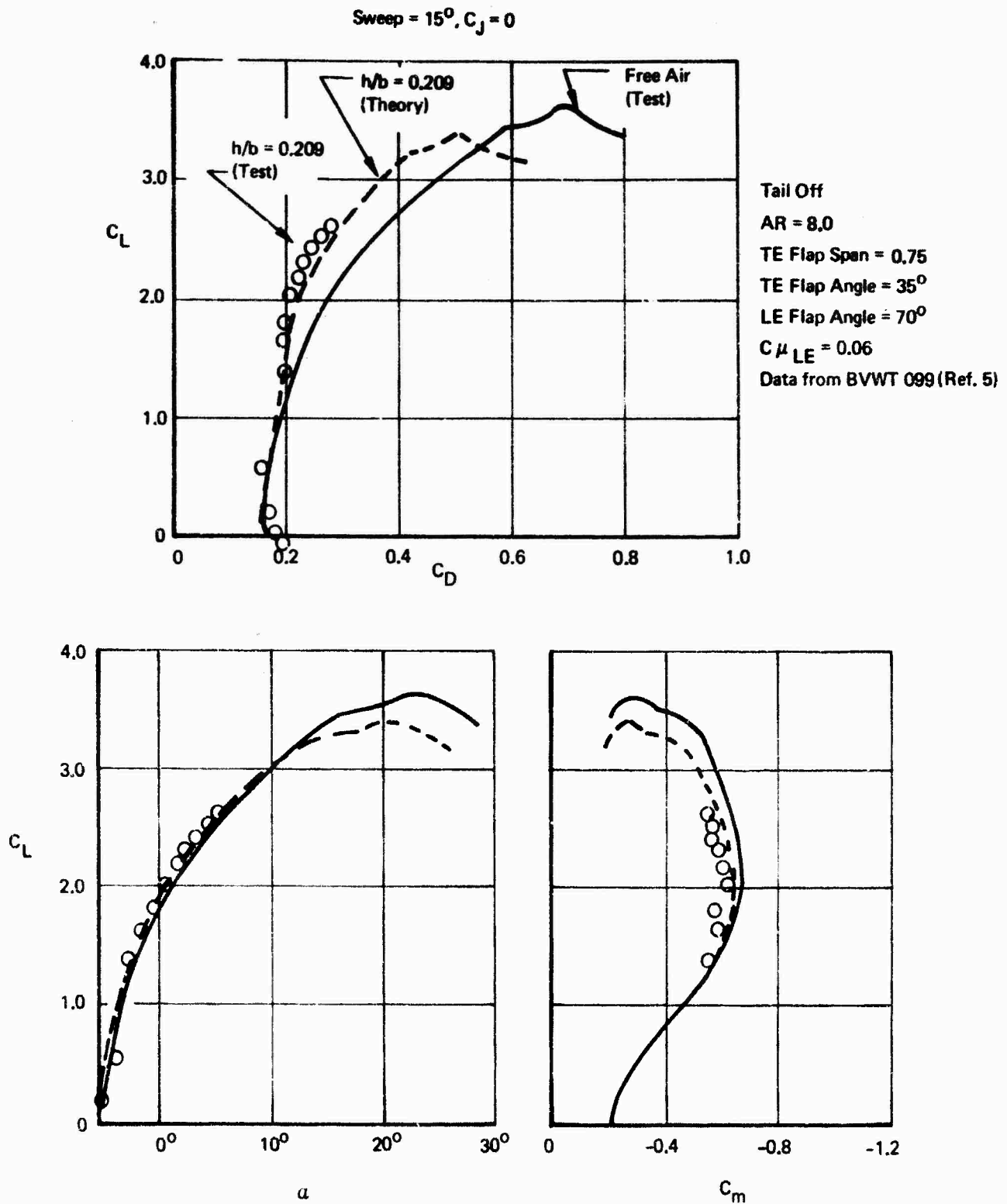


Figure 27: Ground Effect, Power Off, Test – Estimate Comparison

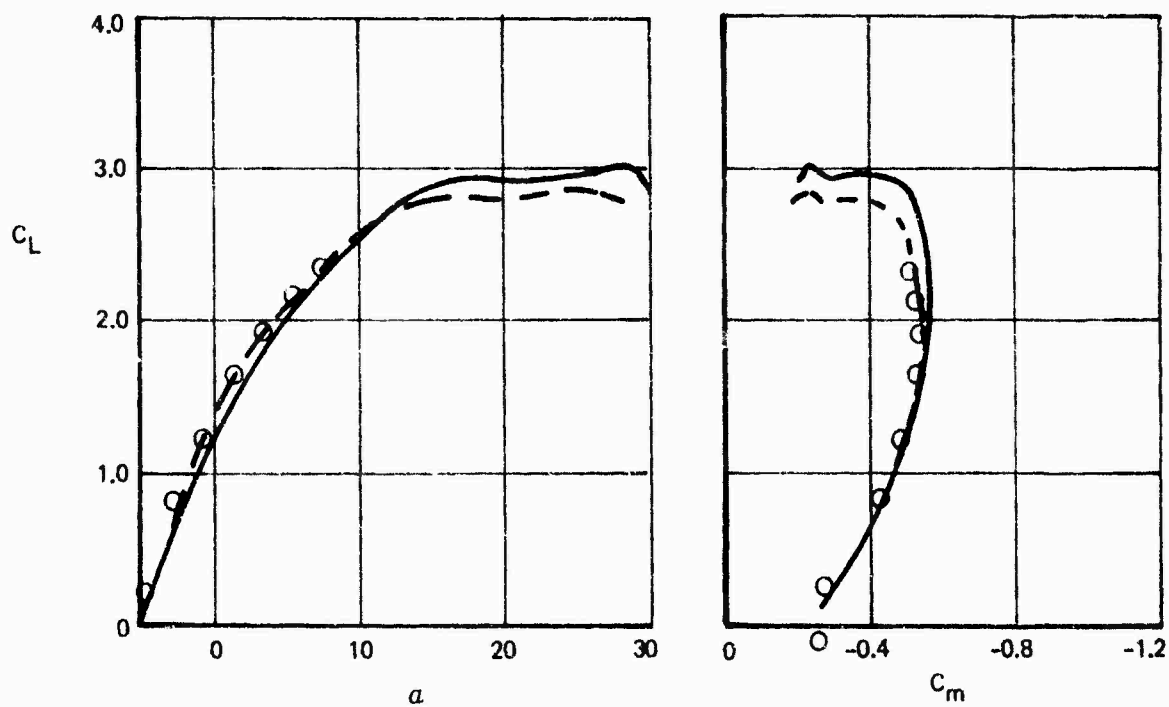
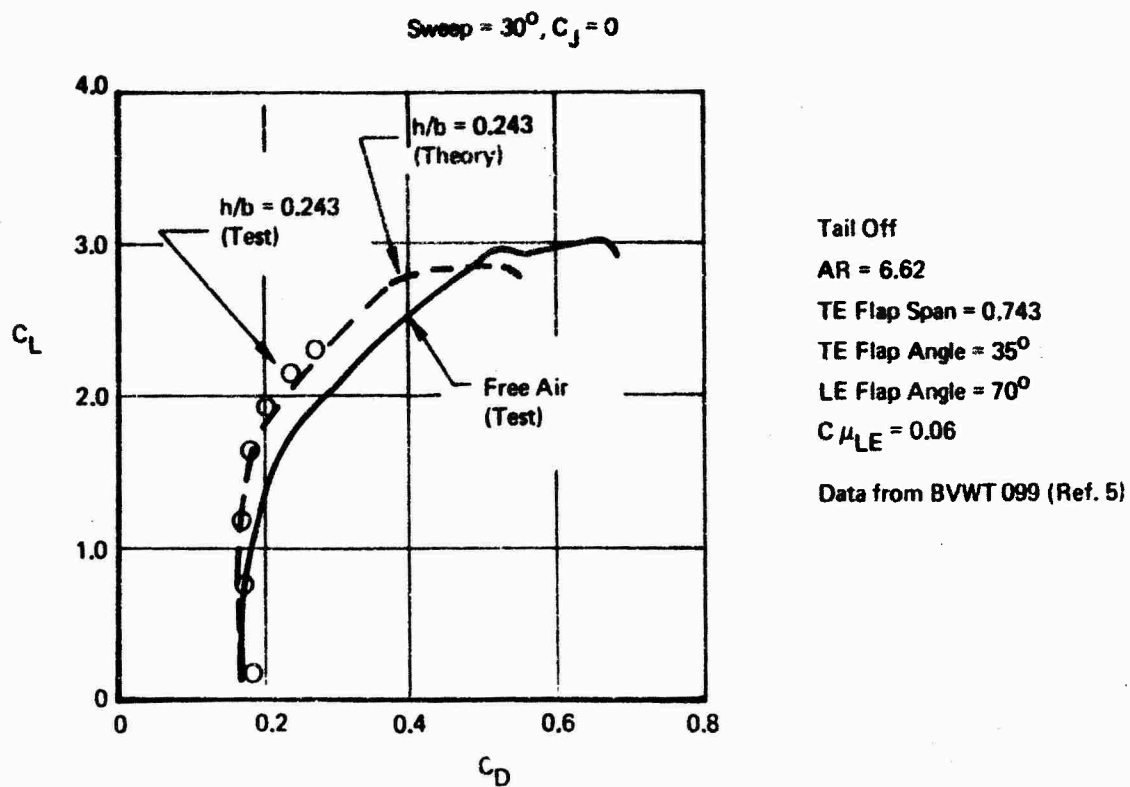


Figure 28: Ground Effect, Power Off, Test – Estimate Comparison

For lift in ground effect, equation 2.2-3

$$C_{L_{GE}} = 2 \left[ \frac{1}{1 + \frac{(2 \times 2)}{\pi^2 \times 8} \left[ \left( \frac{\pi}{(8 \times 200)} \right)^2 + 1 \right]^{1/2} - 1} \right]^2$$

$$= 1.93$$

For angle of attack in ground effect 2.2-5

$$\alpha_{GE} = 2.33 - \left\{ \frac{(2 \times 2)}{\pi^2 \times 8} \ln \left[ 1 + \left( \frac{\pi}{(8 \times 200)} \right)^2 \right] \right\} 57.3$$

$$= 2.33 - 1.40$$

$$= .93$$

For drag in ground effect, equation 2.2-6

$$C_{D_{GE}} = .341 \left\{ 1 - \left( \frac{2}{\pi^2 \times 8} \right) \left( \frac{20^2}{.341} \right) \ln \left[ 1 + \left( \frac{\pi}{(8 \times 200)} \right)^2 \right] \right\} \frac{1.93}{2.0}$$

$$= .282$$

Pitching moment in ground effect, equation 2.2-8

$$C_{m_{GE}} = (-.5273) \frac{1.93}{2.00}$$

$$= -.5088$$

Change in downwash in ground effect, equation 2.2-9

$$\Delta \epsilon_{GE} = - \frac{(20 \times 84.27)^2}{(8 \times \pi \times 8)} \left( \frac{49.17}{(49.17)^2 + [(2 \times 17.4) - 17.57]^2} - \frac{1}{(49.17)^2 + [(2 \times 17.4) - 17.57]^2 + \frac{\pi^2 (84.27)^2}{64}} \right)^{1/2}$$

$$+ \left( \frac{1}{[(2 \times 17.4) - 17.57]^2 + \frac{\pi^2 (84.27)^2}{64}} \right) \left( 1 + \frac{49.17}{(49.17)^2 + [(2 \times 17.4) - 17.57]^2 + \frac{\pi^2 (84.27)^2}{64}} \right)^{1/2}$$

$$= -.1107 \text{ RAD}$$

$$= -6.34^\circ$$

## 2.3 Vectored Thrust

This section contains formulae for longitudinal force and moment coefficients incorporating thrust effects and a discussion of thrust interference effects on these coefficients. The longitudinal force and moment coefficients are presented below.

$$C_L = C_{L_{\text{POWER OFF}}} + C_{L_{\text{INT}}} + C_J \sin(\alpha + \delta) \quad (2.3-1)$$

$$C_D = C_{D_{\text{POWER OFF}}} + C_{D_{\text{INT}}} - C_J \cos(\alpha + \delta) + C_{D_{\text{RAM}}} \quad (2.3-2)$$

$$C_m = C_{m_{\text{POWER OFF}}} + C_{m_{\text{INT}}} + C_J \left( \frac{x_F}{c} \sin \delta + \frac{z_F}{c} \cos \delta \right) + C_{D_{\text{RAM}}} \left( \frac{x_R}{c} \sin \alpha - \frac{z_R}{c} \cos \alpha \right) \quad (2.3-3)$$

The interference effects presented were obtained from the STAI wind tunnel test BVWT 099. These effects are the differences between the power-on and power-off test data with the appropriate thrust component removed from the power-on data. The interference corrections are shown as functions of thrust vector angle, angle of attack, nozzle longitudinal location and nozzle gross thrust coefficient.

The vertical and spanwise location effects are apparently negligible, although the available data was limited. Spanwise locations tested were from 27% to 60% of wing semi-span. The nacelle centerline heights tested were  $h/\bar{c} = .371$  and  $.453$  below chord plane. These variables are not included in the estimating procedure.

The vectored thrust interference data were analyzed to generalize the data with sufficient accuracy for preliminary design purposes. The methods will provide good results for configurations having reasonably high aspect ratios and engines located under the wing, since the data base for their derivation was so restricted. Application to other arrangements is subject to considerable uncertainty. Figure 29 shows the satisfactory agreement between measured forces and those predicted by the present methods which can be expected when this restriction is observed.

### 2.3.1 Lift Interference

Since the chordwise position of the exit centerline of the nozzle varies with vector angle, the data had to be crossplotted to obtain all of the vector angles at the same chordwise position. The limited data on spanwise location effects indicated that these were minimal.



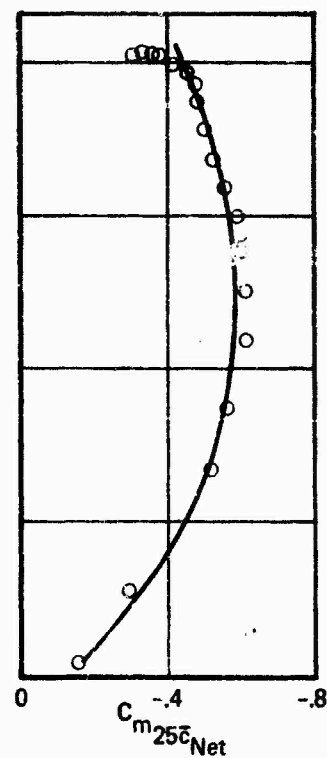
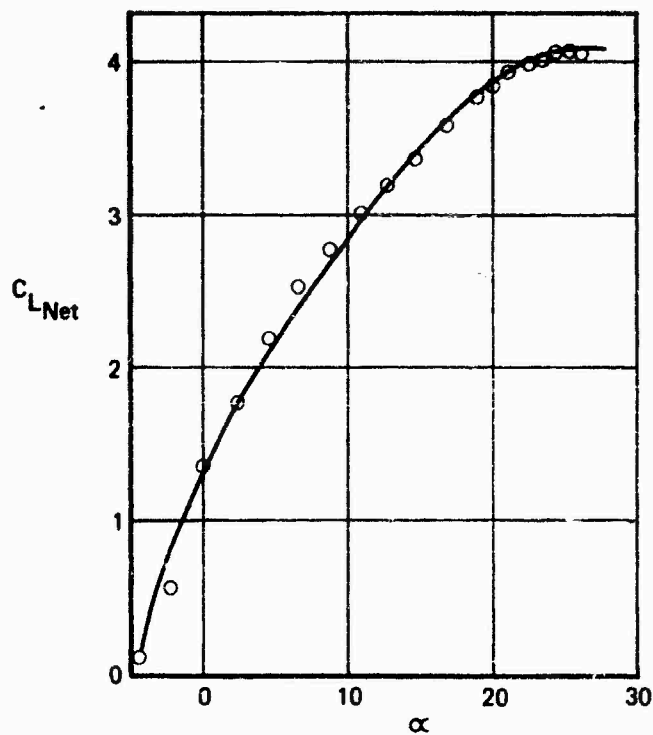
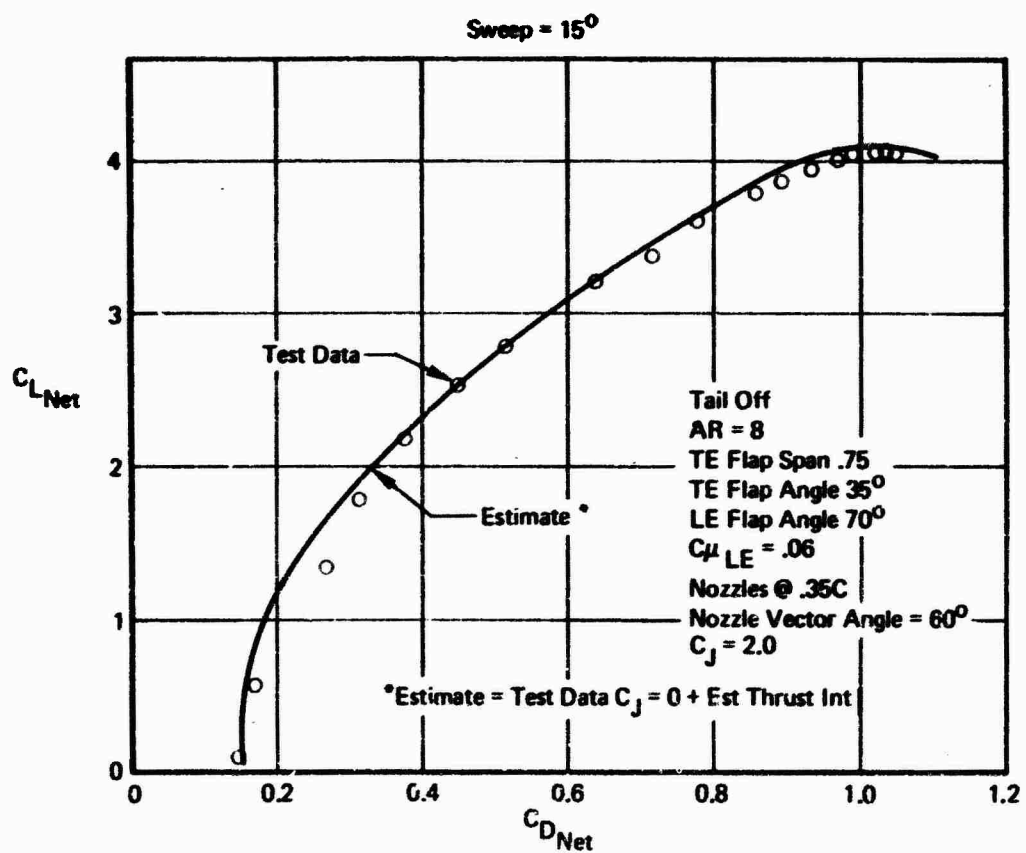


Figure29: Vectored Thrust , Test – Estimate Comparison

Free air lift interference due to vectored thrust may be found for  $x/c = .35$  and  $C_J = 2.0$  from Figure 30. An increment for other nozzle locations may be found from Figure 31. A parameter which has proved of some use in correlating vectored thrust and V/STOL aerodynamic interference effects is the equivalent jet velocity ratio,

$V_e = \left( \frac{q_\infty}{q_{jet}} \right)^{1/2}$ .  $V_e$  is directly proportional to  $(1/C_J)^{1/2}$ . It was found that the lift interference correlated directly with  $C_J^{1/2}$  with sufficient accuracy for preliminary design purposes, though it begins to break down at high thrust coefficients or angles of attack.

The lift interference for any  $C_J$  and chordwise nacelle location is then

$$C_{LINT} = \left[ C_{LINT} \begin{matrix} \text{(FIG 30)} \\ \text{(FIG 31)} \end{matrix} + \Delta C_{LINT} \begin{matrix} \text{(FIG 31)} \end{matrix} \right] \left[ \frac{C_J}{2} \right]^{1/2} \quad (2.3-4)$$

For this analysis the nacelle longitudinal location is measured from the leading edge of the local wing chord at the engine centerline location, to the center of nozzle exit plane.

Symmetric thrust conditions have been assumed for the lift interference design charts developed. For nonsymmetric thrust conditions, the charts developed may be used assuming that each wing operates independently of the other. If one wing has  $C_J = X$  and the other  $C_J = Y$ , the configuration will then have a lift interference given by

$$C_{LINT} = \frac{1}{2} [C_{LINT} @ C_J = 2X] + \frac{1}{2} [C_{LINT} @ C_J = 2Y] \quad (2.3-5)$$

### 2.3.2 Drag Interference

At a given nacelle location and nozzle vector angle, the free air drag interference could be correlated directly with the free air lift interference. This permitted a relatively simple procedure to be used. Free air drag interference is given in Figures 32 through 34.

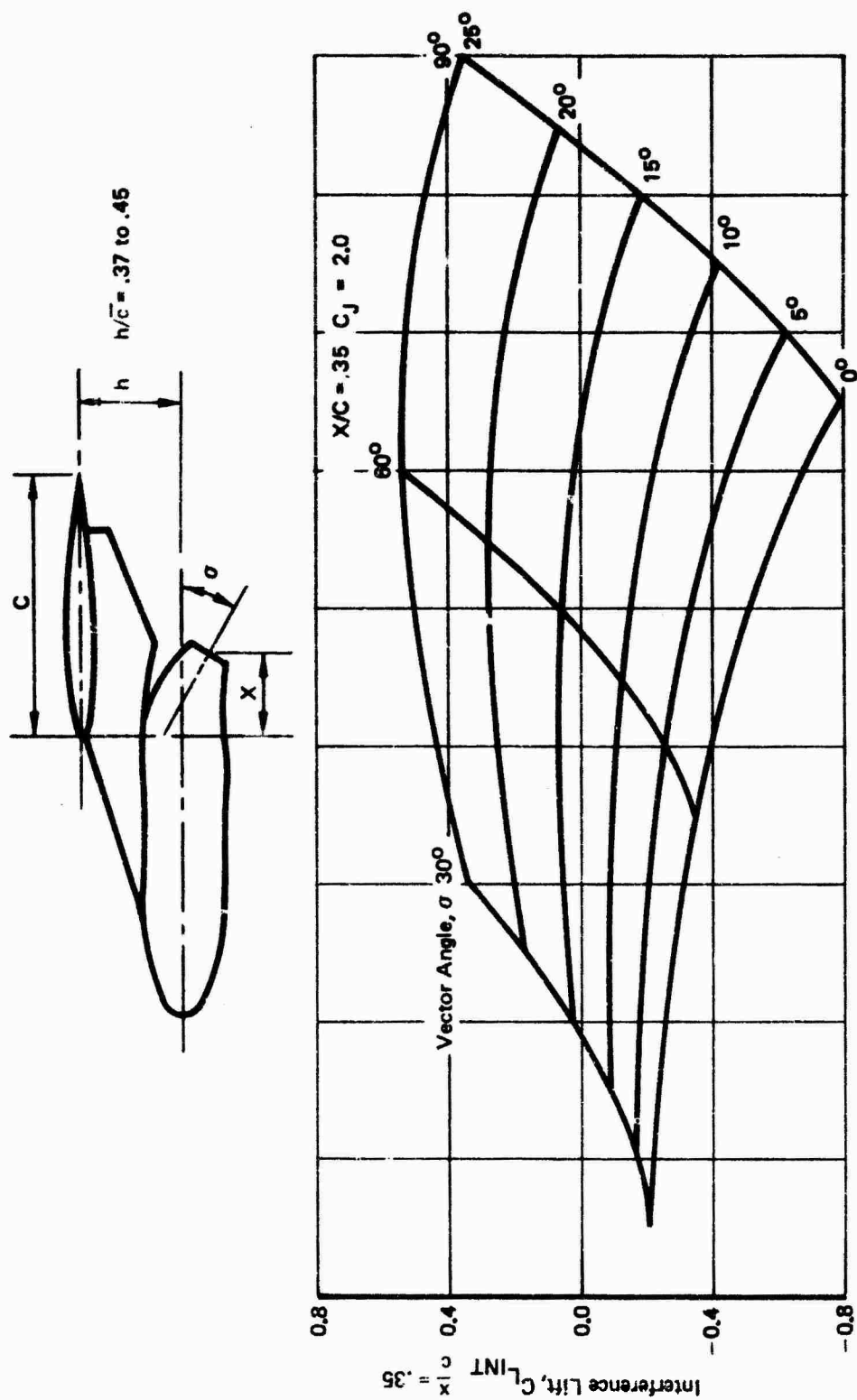


Figure 30: Vectored Thrust Lift Interference

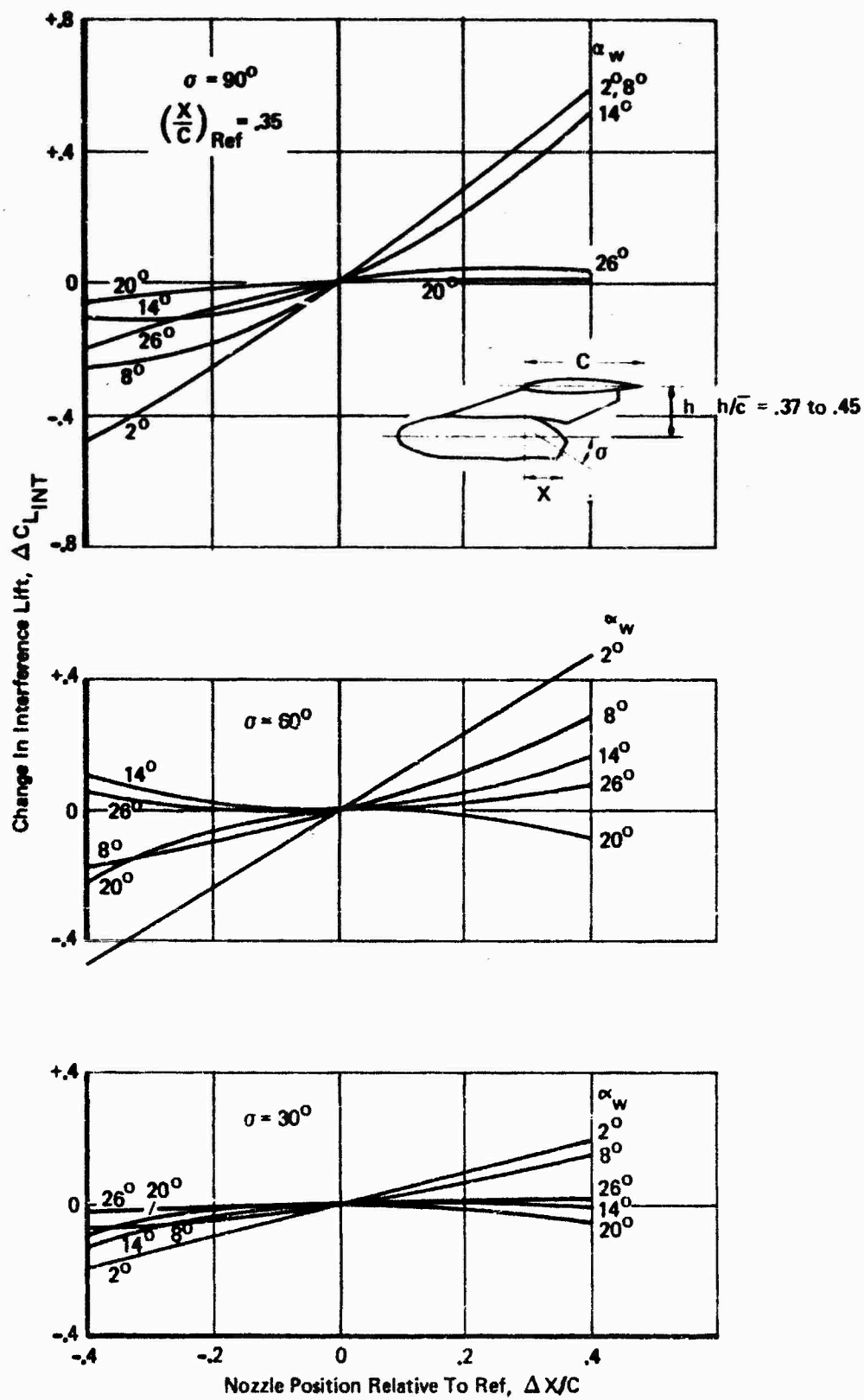
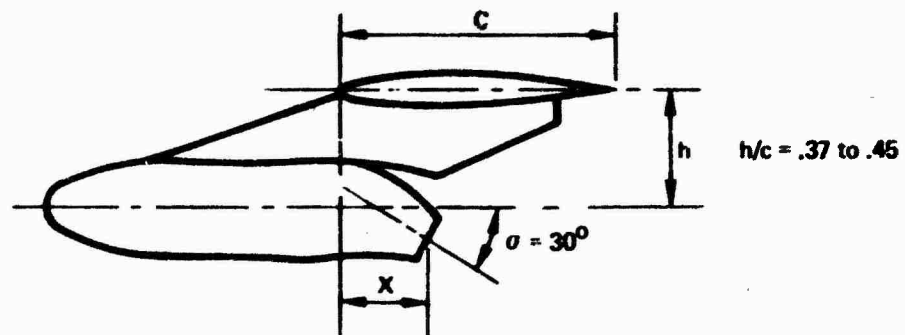


Figure 31: Vectored Thrust, Lift Interference, Effect of Nozzle Location



$\sigma = 30^\circ$   
All  $C_J$

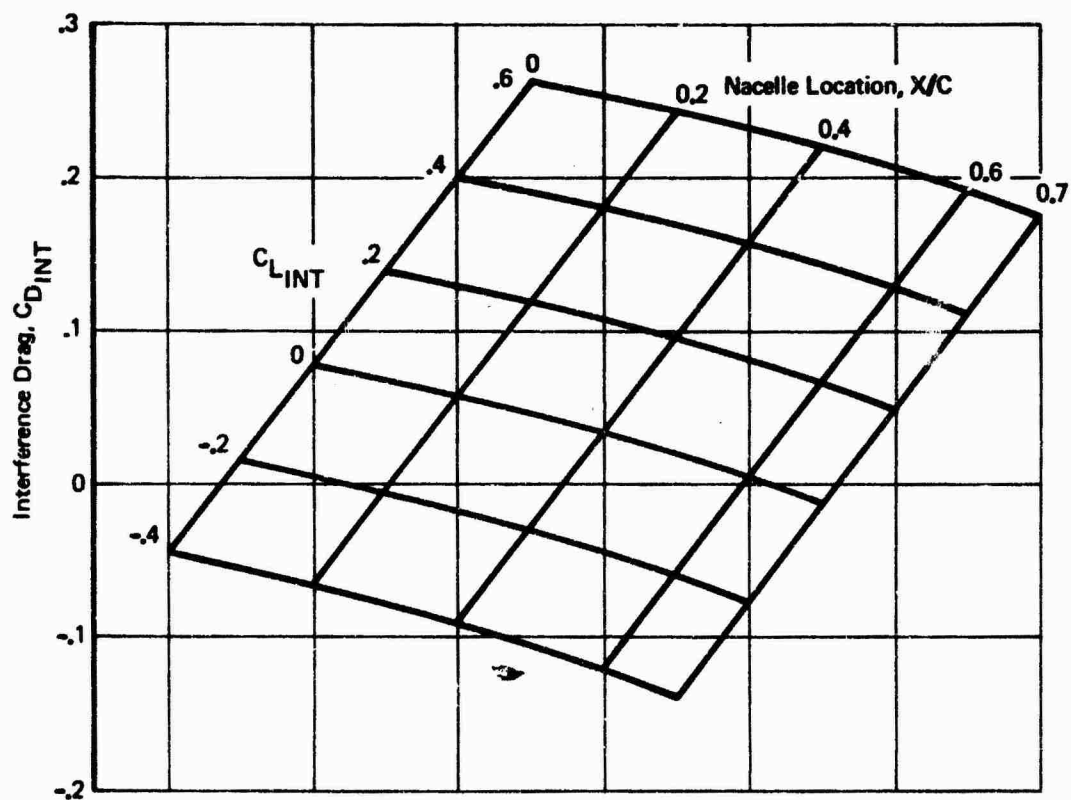


Figure 32: Vectored Thrust, Drag Interference, Vector Angle  $30^\circ$

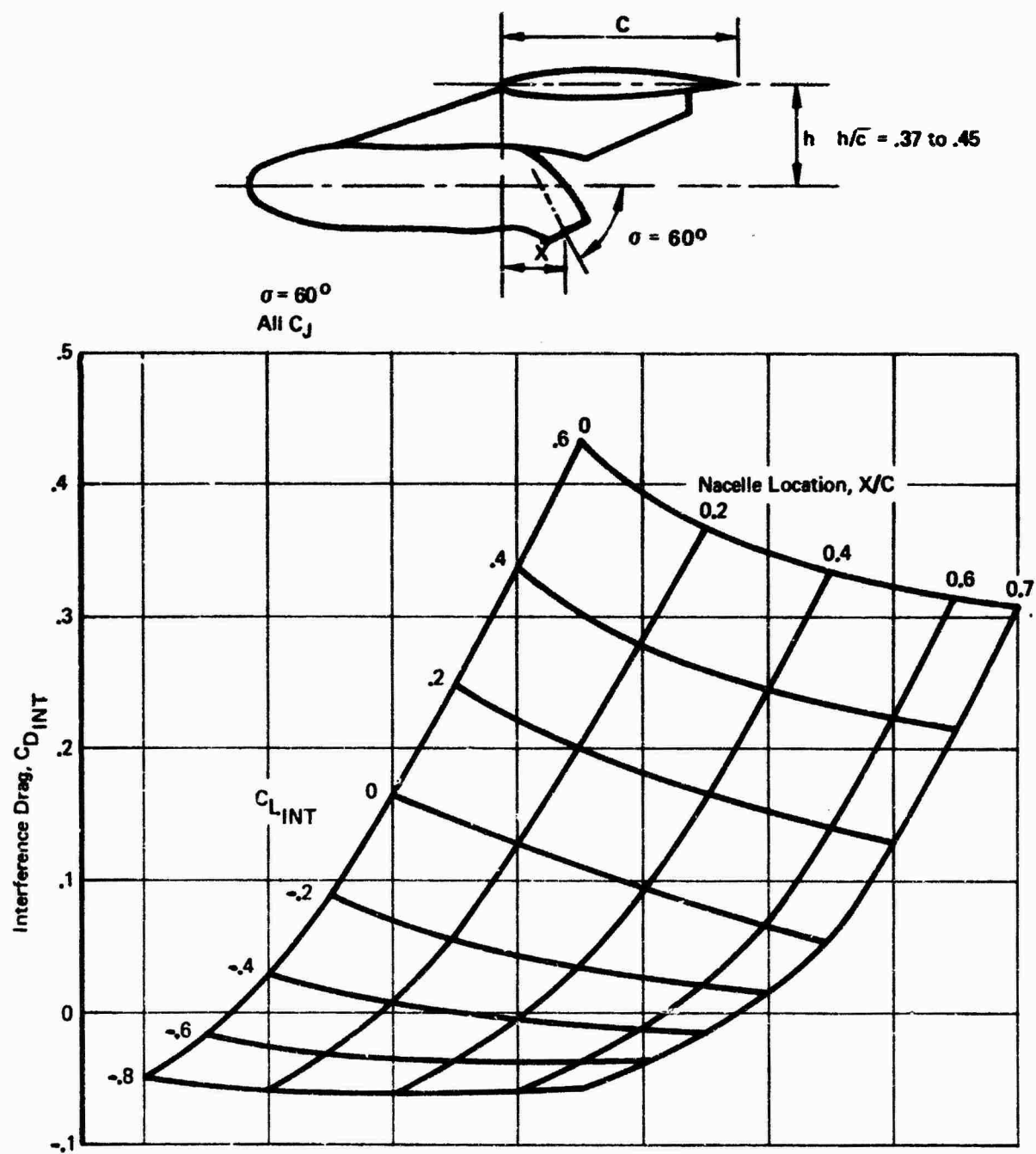
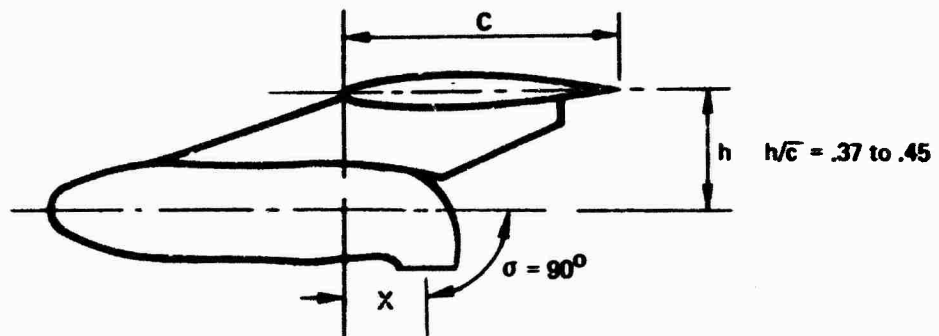


Figure 33: Vectored Thrust, Drag Interference, Vector Angle  $60^\circ$



$\sigma = 90^\circ$   
All  $C_j$

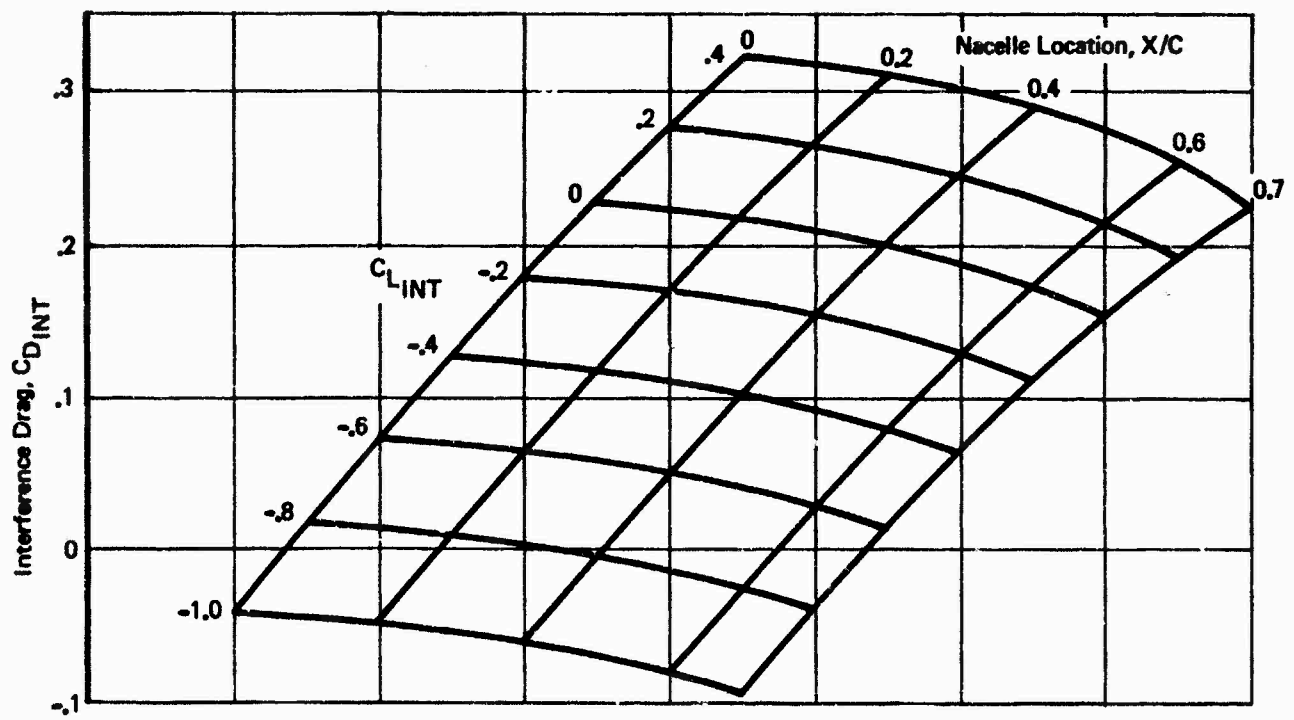


Figure 34: Vectored Thrust, Drag Interference, Vector Angle  $90^\circ$

### 2.3.3 Pitching Moment Interference

Free air pitching moment interference also correlated well with the free air lift interference at a given nacelle location and nozzle vector angle. This indicates that the center of pressure of the induced lift remains constant with angle of attack for a given nacelle configuration. For pitching moments, the important length parameter is the distance from the center of pressure of the induced lift to the moment center. Therefore, for the pitching moment interference in free air, Figures 35 through 37, the nozzle location has been given as the distance from the center of the nozzle exit to the moment center. For a swept wing, the average nozzle location is used.

### 2.3.4 Downwash Interference

The effect of vectored thrust on downwash is shown in Figure 38.

#### SAMPLE PROBLEM - VECTORED THRUST, FREE AIR

$$\alpha = 5.46^\circ \text{ (estimated power-off aerodynamic characteristics)}$$

$$\sigma = 30^\circ$$

$$C_L = 2.4$$

$$C_D = .4062$$

$$C_{RAM} = 0 \text{ (model with blowing nozzles)}$$

$$C_J = 2.0$$

$$C_m = -.5356$$

$$\bar{c} = 11.179 \text{ in.}$$

$$X_E = -.066 \text{ in.}$$

$$Z_E = + 2.787 \text{ in.}$$

$$x/c = .35$$

Lift

from chart Figure 30 read  $C_{L_{INT}}$

$$C_{L_{INT}} = -.15$$

from Figure 31  $C_{L_{INT}} = 0$

Total lift interference

$$C_{L_{INT}} = (-.15+0) \left(\frac{2.0}{2}\right)^{1/2} = -.15$$



$$\sigma = 30^\circ$$

All  $C_J$

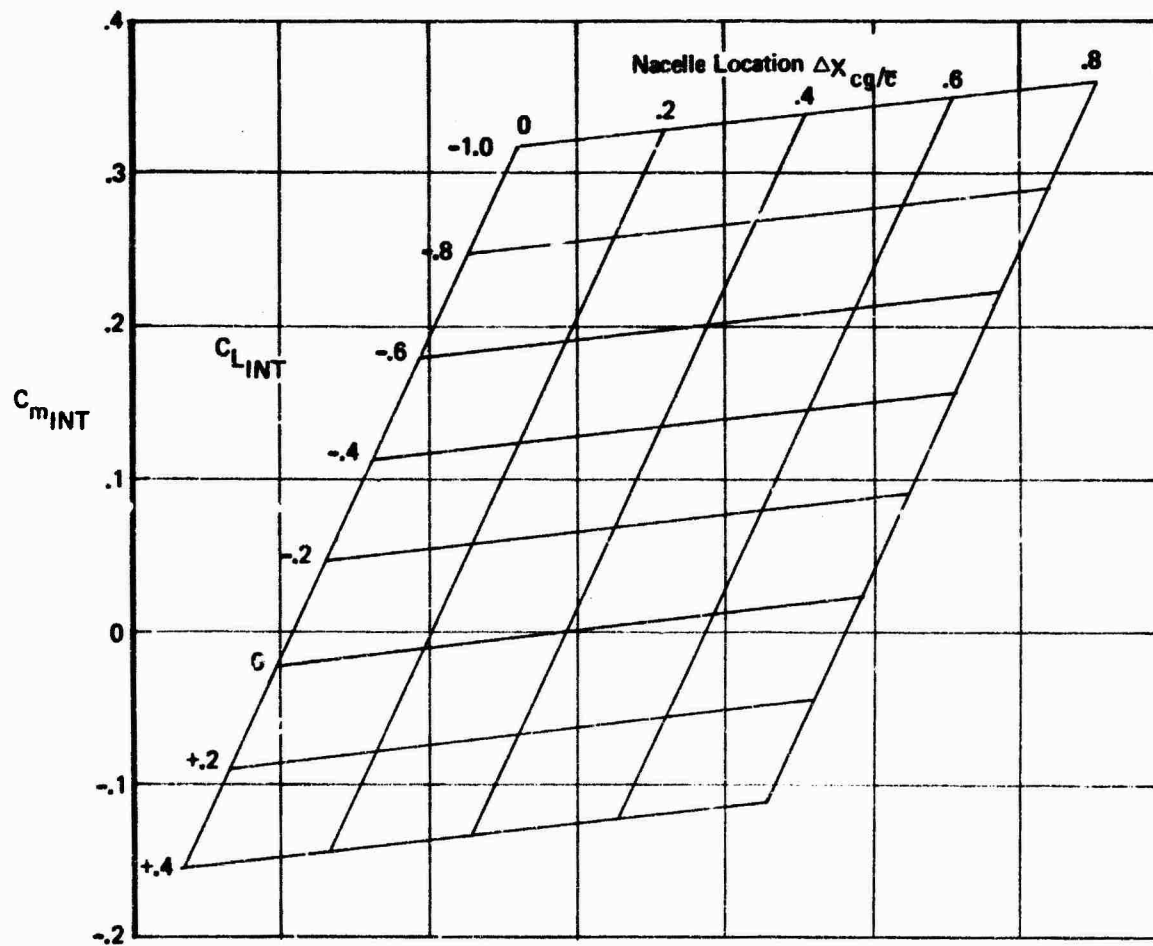
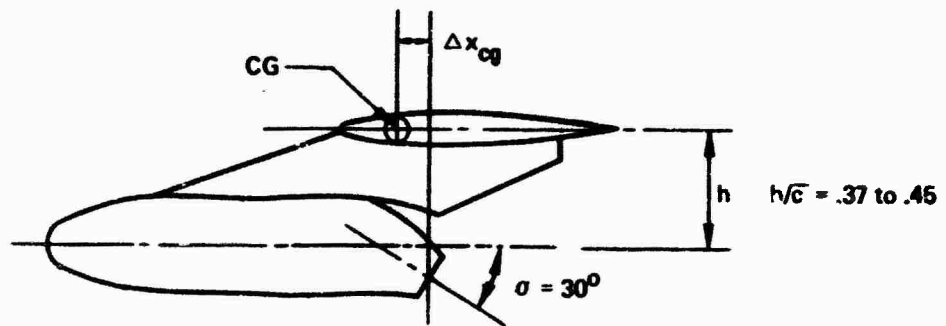


Figure 35: Vectored Thrust Pitching Moment Interference, Vector Angle  $30^\circ$

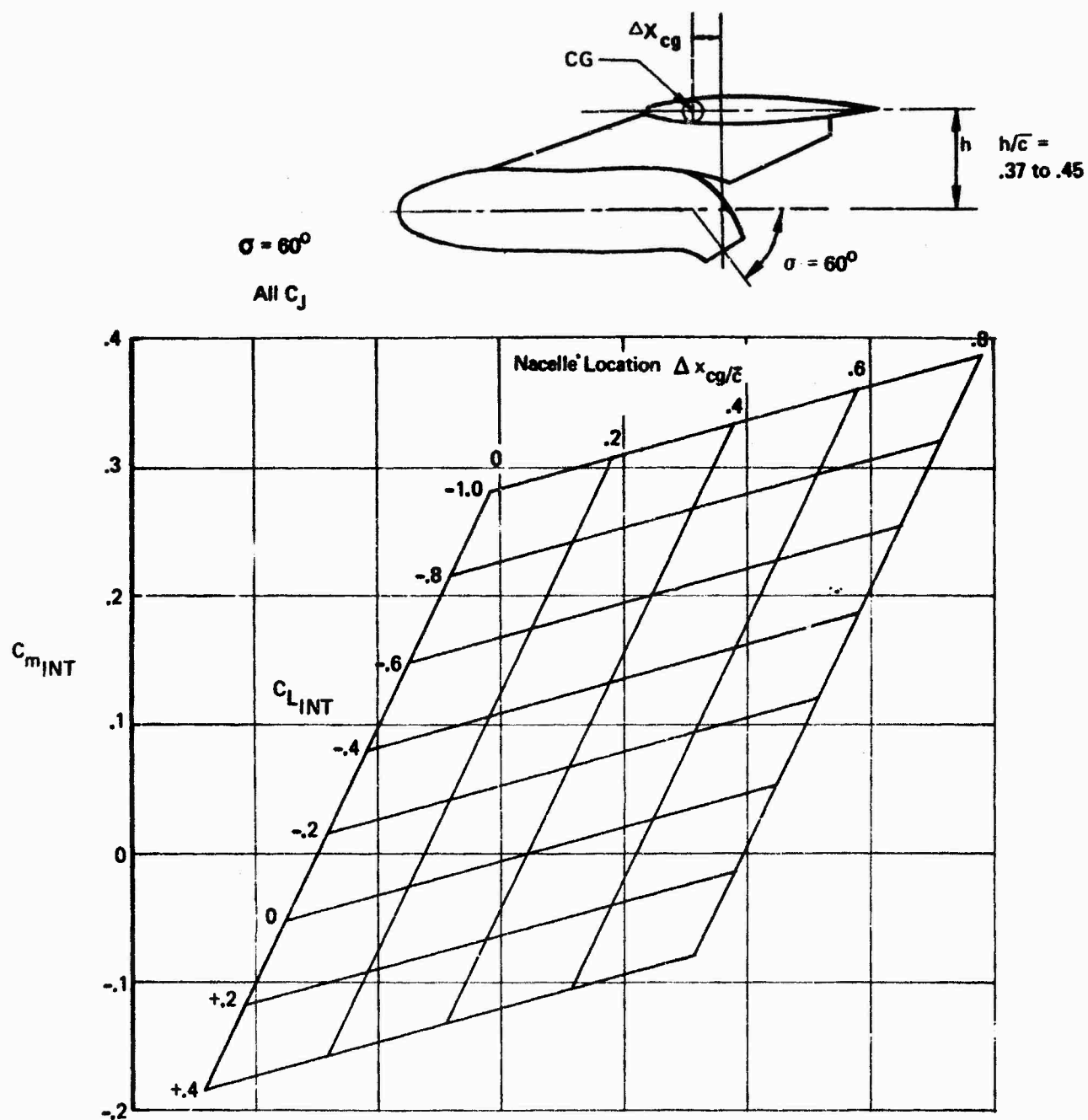


Figure 36: Vectored Thrust Pitching Moment Interference, Vector Angle  $60^\circ$

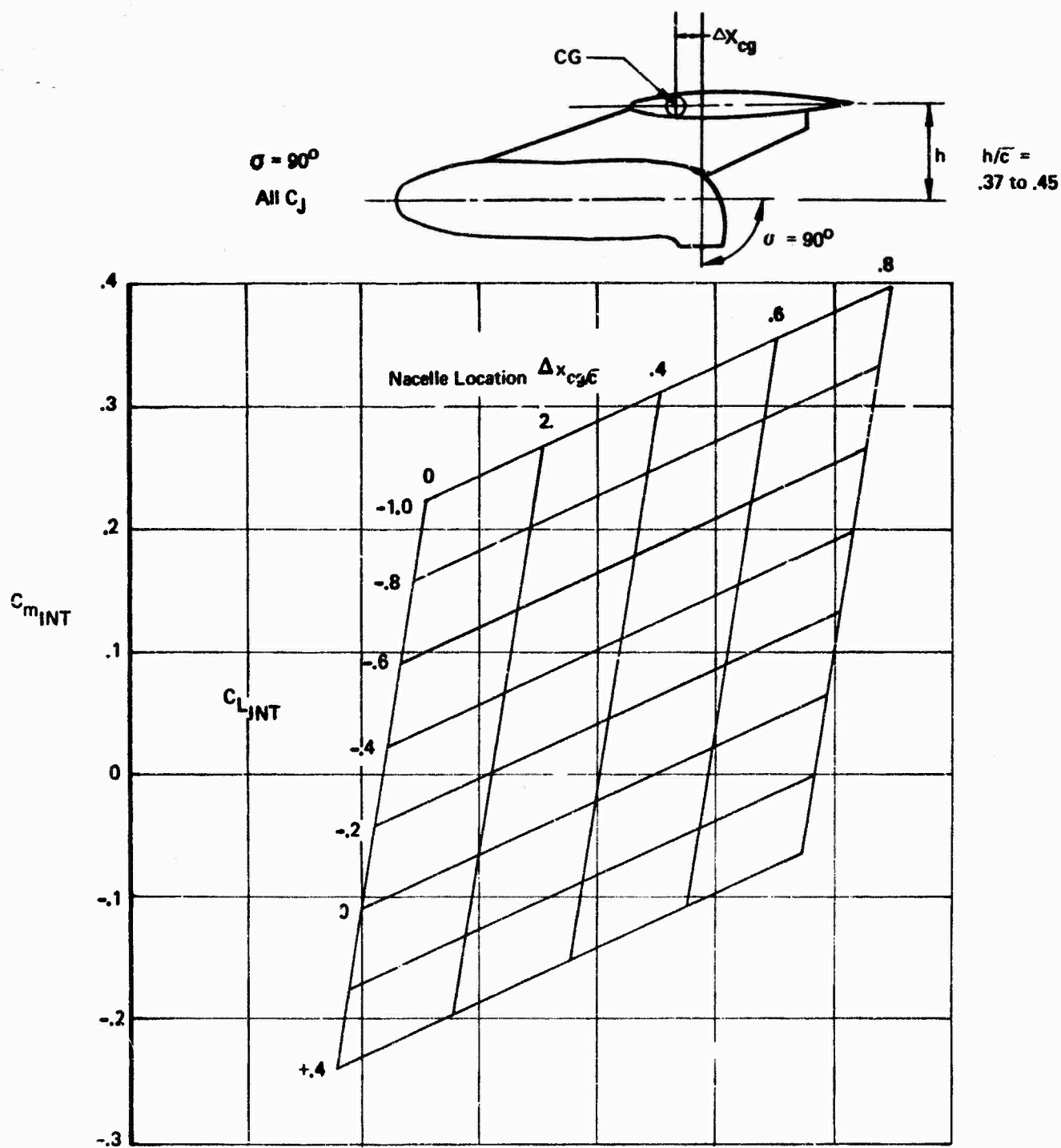


Figure 37: Vectored Thrust Pitching Moment Interference, Vector Angle  $90^\circ$

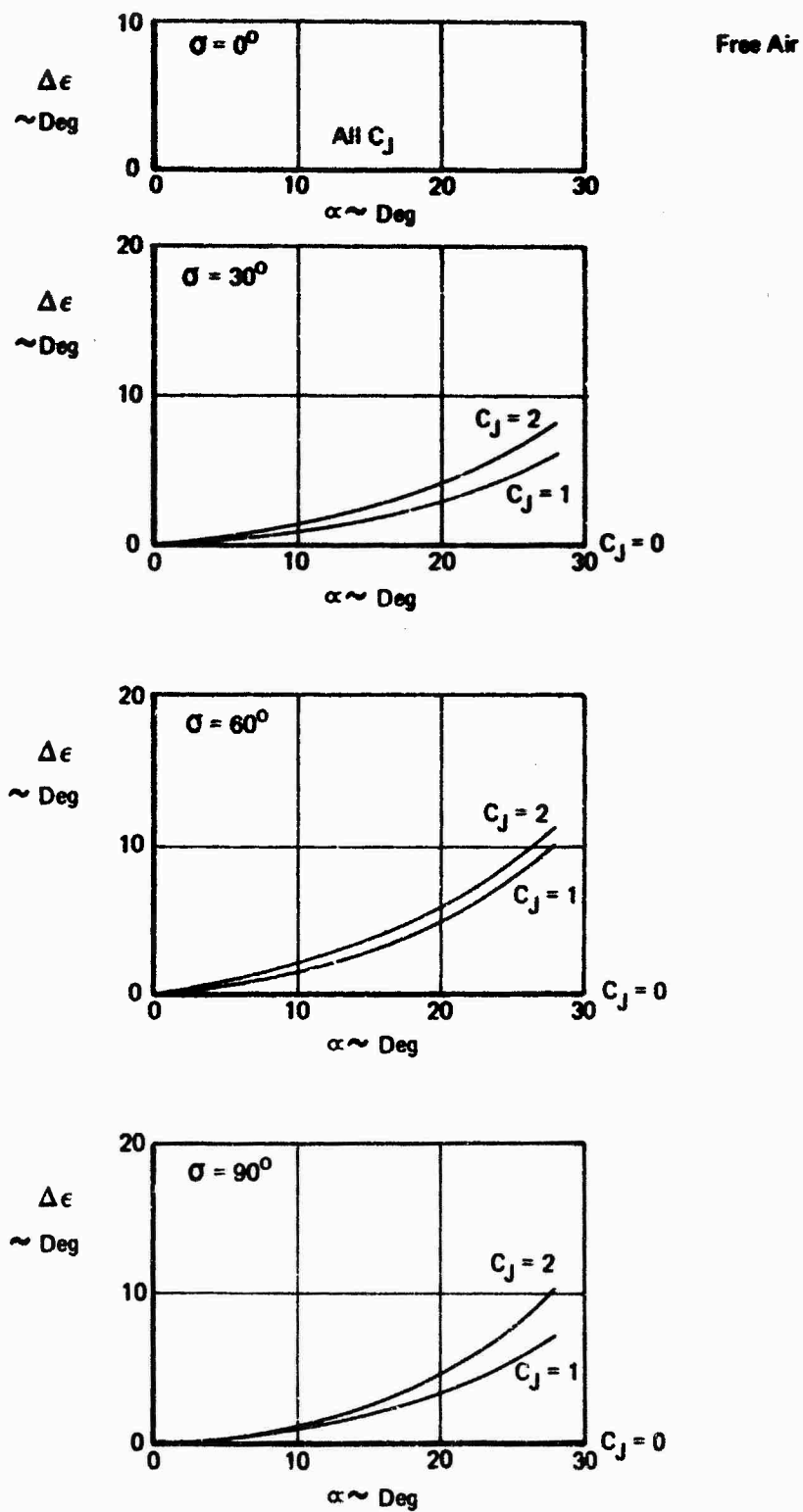


Figure 38: Vectored Thrust Downwash Change at Horizontal Tail

With equation 2.3-1

$$\begin{aligned}C_L &= 2.4 - .15 + 2.0 \sin (30 + 5.46) \\&= 3.43\end{aligned}$$

from wind tunnel test data

$$C_L = 3.63 @ \alpha = 5.46$$

Drag

from chart Figure 32 at  $C_{L_{INT}}$  read

$$C_{D_{INT}} = -.010$$

calculate with equation 2.3.2

$$C_D = .4062 - .010 - (2.0) \cos (30 + 5.46) + 0$$

$$C_D = -1.2852$$

observed from TAI test data at  $C_L = 3.43$

$$C_D = -1.28$$

Pitching Moment

from Figure 35 at  $C_{L_{INT}}$  read

$$C_{m_{INT}} = +.0450$$

calculate  $C_m$  power on with equation 2.3-3

$$\begin{aligned}C_m &= -.5356 + .0450 + 2.0 \left[ \frac{-.066}{11.179} \sin 30^\circ + \frac{2.787}{11.179} \cos 30^\circ \right] \\&= -.074\end{aligned}$$

$C_m$  observed at  $C_L = 3.43$  wind tunnel test

$$C_m = -.190$$

Downwash

from Figure 38 read

$$\Delta \epsilon = +.09^\circ$$

## 2.4 Vectored Thrust in Ground Effect

Vectored thrust interference effects in the presence of the ground were also obtained from STAI wind tunnel test BVWT 099. Figure 39 presents a comparison of free air test data, free air test data corrected for ground influence and test data in ground effect. These show a good correlation between the corrected data and the test data in ground effect.

### 2.4.1 Lift Interference

As in the case of the power-off ground effect procedure, the  $C_L$  vs  $\alpha$  curve in ground effect is determined from the free air curve by adjusting both  $C_L$  and  $\alpha$ . Lift interference due to vectored thrust in ground effect is the sum of the lift interference due to vectored thrust in free air and an additional increment for the effect of ground proximity. This additional increment is presented in Figure 40. The angle of attack adjustment is the same as for the power off case (Eq. 2.2-5), but must be based on  $C_{L_{NET}}$ .

Lift in ground effect with vectored thrust is

$$C_L = C_{L_{GE}} + C_{L_{INT}} + \Delta C_{L_{INT}} + C_J \sin(\alpha + \sigma) \quad (2.4-1)$$

Poweroff   free air   ground effect increment

### 2.4.2 Drag Interference

Drag interference due to vectored thrust in ground effect is the sum of the drag interference due to vectored thrust in free air and an additional increment for the effect of ground proximity. The additional increment is presented in Figure 40.

Drag in ground effect with vectored thrust is

$$C_D = C_{D_{GE}} + C_{D_{INT}} + \Delta C_{D_{INT}} + C_J(\cos \alpha + \sigma) + C_{D_{RAM}} \quad (2.4-2)$$

Poweroff   free air   ground effect increment

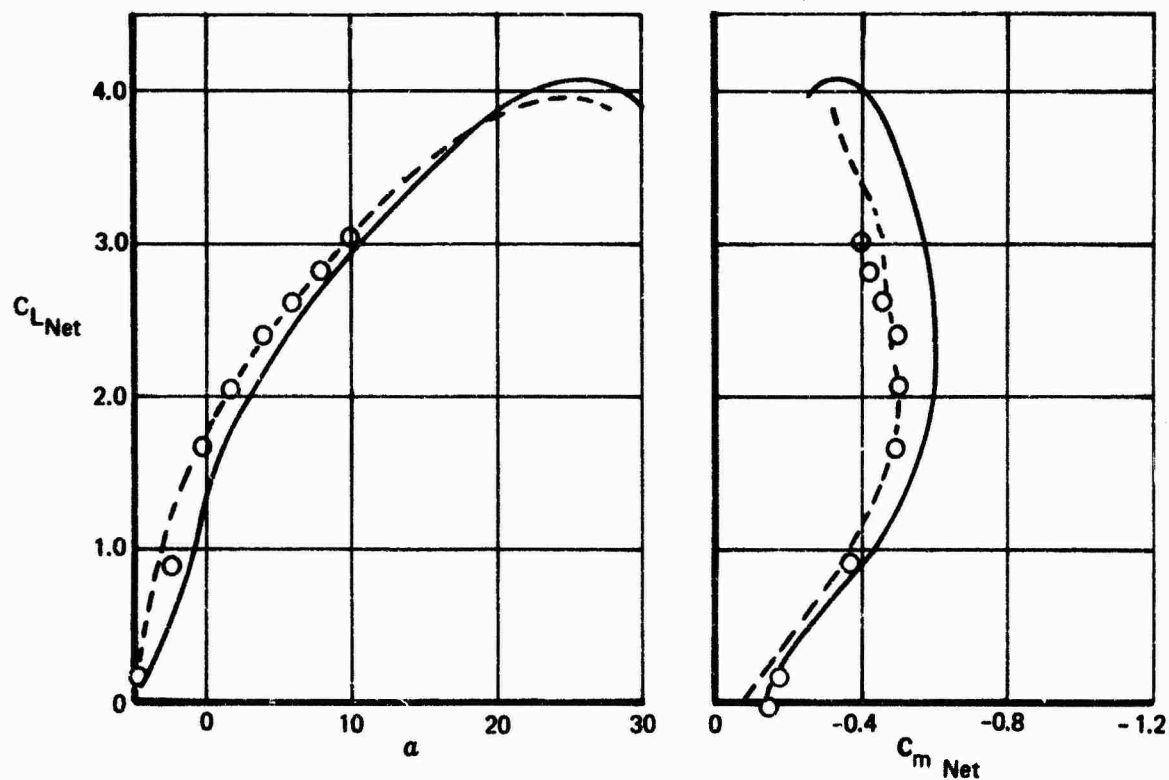
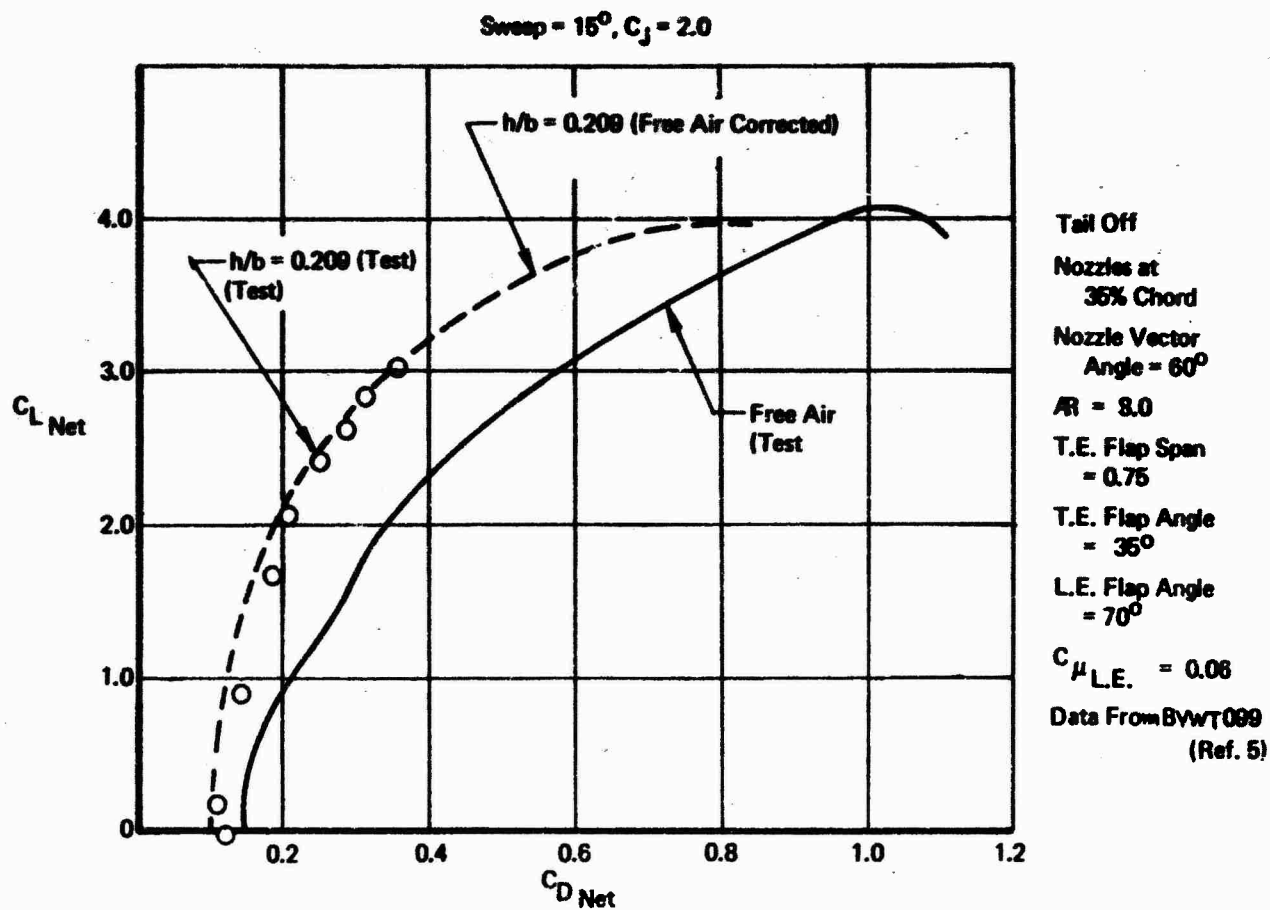
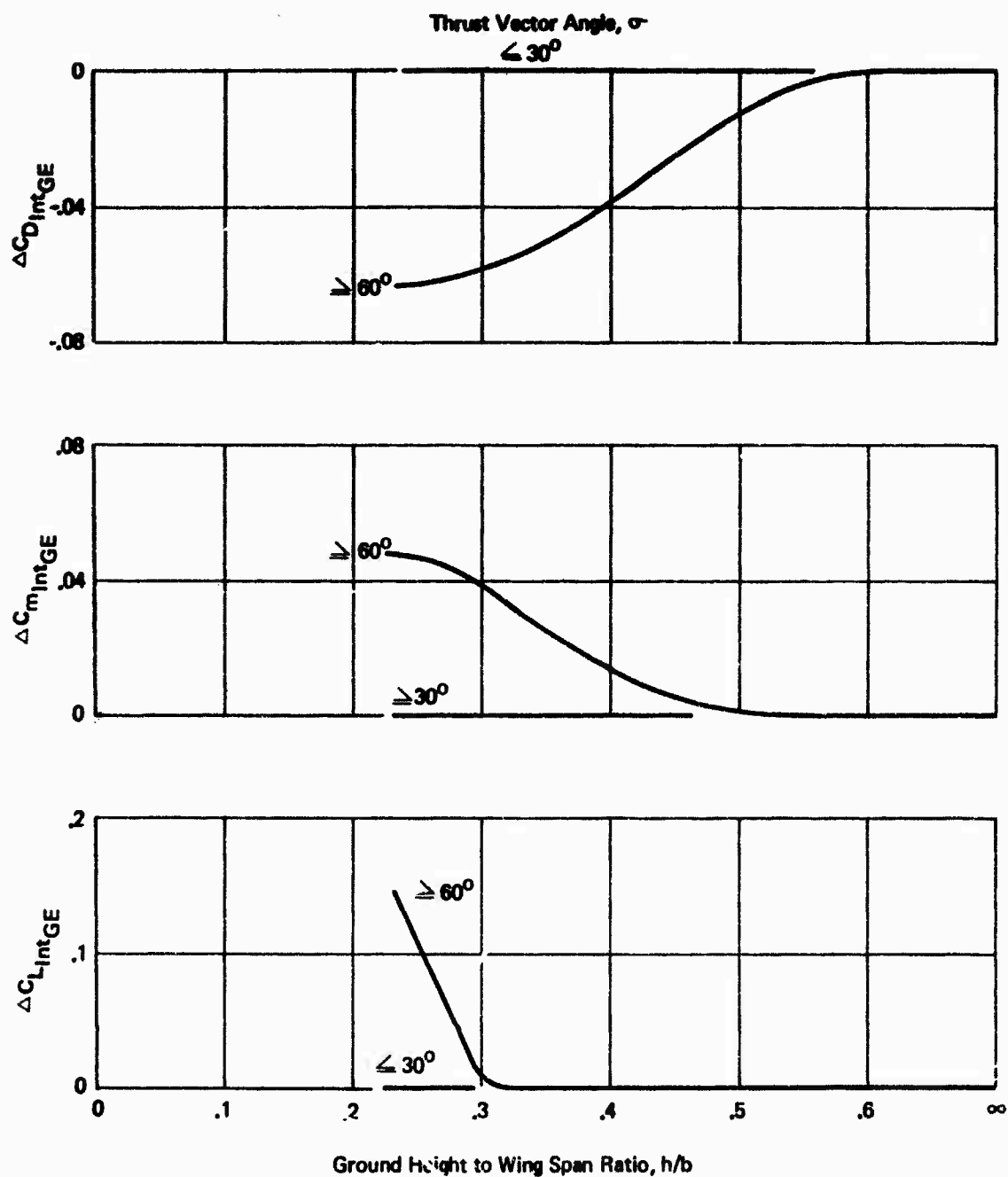


Figure 39: Vectored Thrust in Ground Effect Test—Estimate Comparison



Obtained from Test Data  $C_L = 0$  to 3.0 (BVWT 099, Ref. 5)

**Figure 40: Change in Thrust Interference Effects Due to Ground Effect**



### 2.4.3 Pitching Moment Interference

Pitching moment interference due to vectored thrust in ground effect is the sum of the pitching moment interference due to vectored thrust in free air and an additional increment for the effect of ground proximity. This additional increment is presented in Figure 40.

Pitching moment in ground effect with vectored thrust is

$$C_m = C_{m_{GE}} + C_{m_{INT}} + \Delta C_{m_{INT}} + C_J \left( \frac{x_E}{c} \sin \sigma + \frac{z_E}{c} \cos \sigma \right) + C_{DEAM} \left( \frac{x_E}{c} \sin \alpha + \frac{z_E}{c} \cos \alpha \right) \quad (2.4-3)$$

power off    free air    ground effect increment

### 2.4.4 Downwash Interference

Analysis of the test data did not show significant changes in downwash angle in ground effect with the addition of vectored thrust.

SAMPLE PROBLEM, THRUST INTERFERENCE IN GROUND EFFECT.

$$h/b = .208$$

$$\sigma = 30^\circ$$

From sample problem in Part 2.2 the test conditions in ground effect, power off

$$C_{L_{GE}} = 1.93$$

$$\alpha_{GE} = .93$$

$$C_{D_{GE}} = .282$$

$$C_{m_{GE}} = -.5088$$

The free air vectored thrust corrections at  $\sigma = 30^\circ$ ,  $C_J = 0$ , nacelle  $x/c = .35$ .

$$\begin{aligned}C_{L_{INT}} &= -.2 \\C_{D_{INT}} &= -.025 \\C_{m_{INT}} &= +.065\end{aligned}$$

For this example the thrust interference effects in ground effect are zero. Coefficients in ground effect are then, Lift equation 2.3-1

$$\begin{aligned}C_L &= 1.93 - .2 + 2.0 (\sin 30.93) \\&= 2.76\end{aligned}$$

Drag equation 2.3-2

$$\begin{aligned}C_D &= .282 - .025 - 2.0 (\cos 30.93) + 0 \\&= -1.458\end{aligned}$$

Pitching Moment equation 2.3-3

$$\begin{aligned}C_m &= -.5088 + .065 + .255 \\&= -.1888\end{aligned}$$

The comparable test values at this angle of attack

$$\begin{aligned}C_L &= 2.88 \\C_D &= -1.465 \\C_m &= -.143\end{aligned}$$

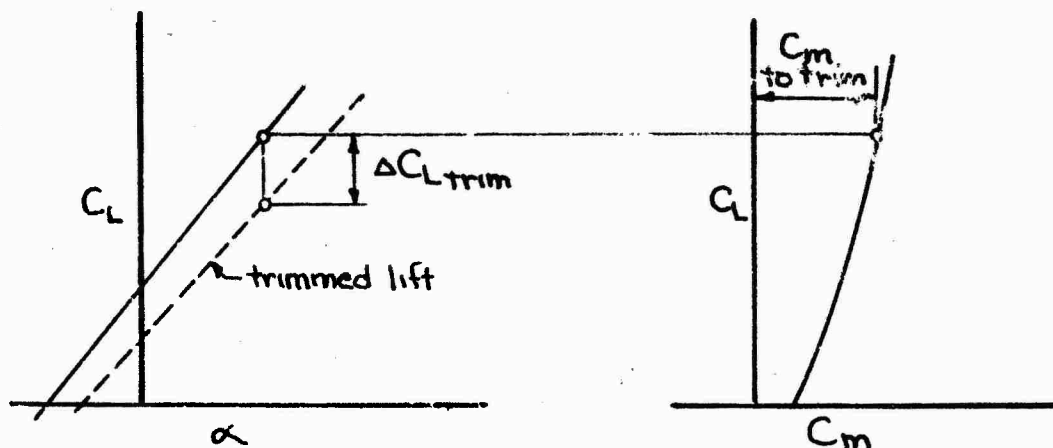
## 2.5 Trim

Any complete set of longitudinal data, lift, drag, pitching moment, and downwash at the tail may be reduced to trimmed lift and drag by the methods presented in this section. Note that these methods are valid for relating long tail arms; close coupled tails or canards would require a considerably more involved analysis.

### 2.5.1 Trimmed Lift

The lift increment required to trim is the increment required at the horizontal tail  $l/4$  mac to reduce the pitching about the center of gravity to zero.

$$\Delta C_{L_{trim}} = \frac{C_m}{l_{w/c}} \quad (2.5-1)$$

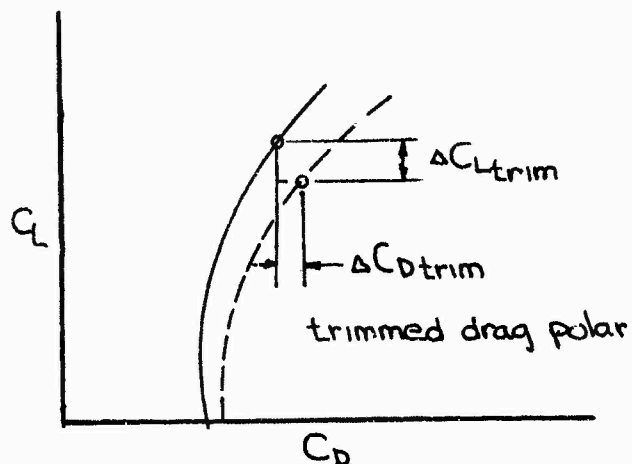


### 2.5.2 Trimmed Drag

The drag increment for trim is considered to be made up of two components. First, the inclination of the lift vector since it is in the downwash of the wing. Second, the tail drag both friction and the tail drag due to lift.

$$\Delta C_{Dtrim} = (\Delta C_{Ltrim}) (e) + \left[ (C_{Dmin})_{tail} + \left( \frac{\partial C_D}{\partial C_L^2} \right)_{tail} (C_L^2)_{tail} \right] \frac{S_{tail}}{S_{REF}}$$

(2.5-2)



## SECTION III

### STABILITY AND CONTROL DERIVATIVE PREDICTION METHODS

This section includes methods for predicting vectored thrust effects on stability derivatives, and a sensitivity study to determine the importance of each derivative. Methods are based on wind tunnel data from Reference 5. Accuracy adequate for preliminary design purposes is provided. This results in a simple, quick method.

Error charts and tables are included. These should be used in conjunction with the sensitivity study. The reader should guard against falling into the trap of thinking of errors only in terms of "percent error." Often it is the increment of error that is important. For instance, in predicting the tail-off  $C_{n\dot{\beta}}$ , an error of 200% would be insignificant if the actual value were only  $-.0001 \text{ deg}^{-1}$ . On the other hand, if the tail-on  $C_{n\dot{\beta}}$  is  $.008 \text{ deg}^{-1}$ , a 15% error might be quite noticeable.

#### 3.1 Stability Derivative Sensitivity Study

It is important in the study of an airplane's stability characteristics to understand the consequences of errors in estimating stability derivatives. When the sensitivity of the dynamic response to each parameter is known, effort to improve accuracy can be expended on the more important derivatives.

Such a sensitivity study was performed for the airplane shown in Figure 41.\* A nominal STOL approach condition of 75 knots was selected, and stability derivatives were estimated. The derivatives, together with mass properties and reference dimensions, are given in Table I. Derivatives found to be the more important ones are listed in Table II.

Angle of attack and sideslip derivatives are based on wind tunnel data from Reference 5. Rotary derivatives were predicted using DATCOM methods.

Three degree of freedom equations of motion for longitudinal and lateral-directional stability were solved, using the nominal derivatives. Then each derivative was varied over a range of  $\pm 150\%$ , except in a few cases where this would have resulted in an unreasonably large increment.

---

\*This airplane is the "Baseline Configuration" developed early in the STAI program and reported in detail in Appendix A of Volume I of the STAI Series (Ref. 12).

# REFERENCE GEOMETRY

$S = 1640 \text{ FT}^2$

$b = 114.5 \text{ FT}$

$\bar{c} = 15.7 \text{ FT}$

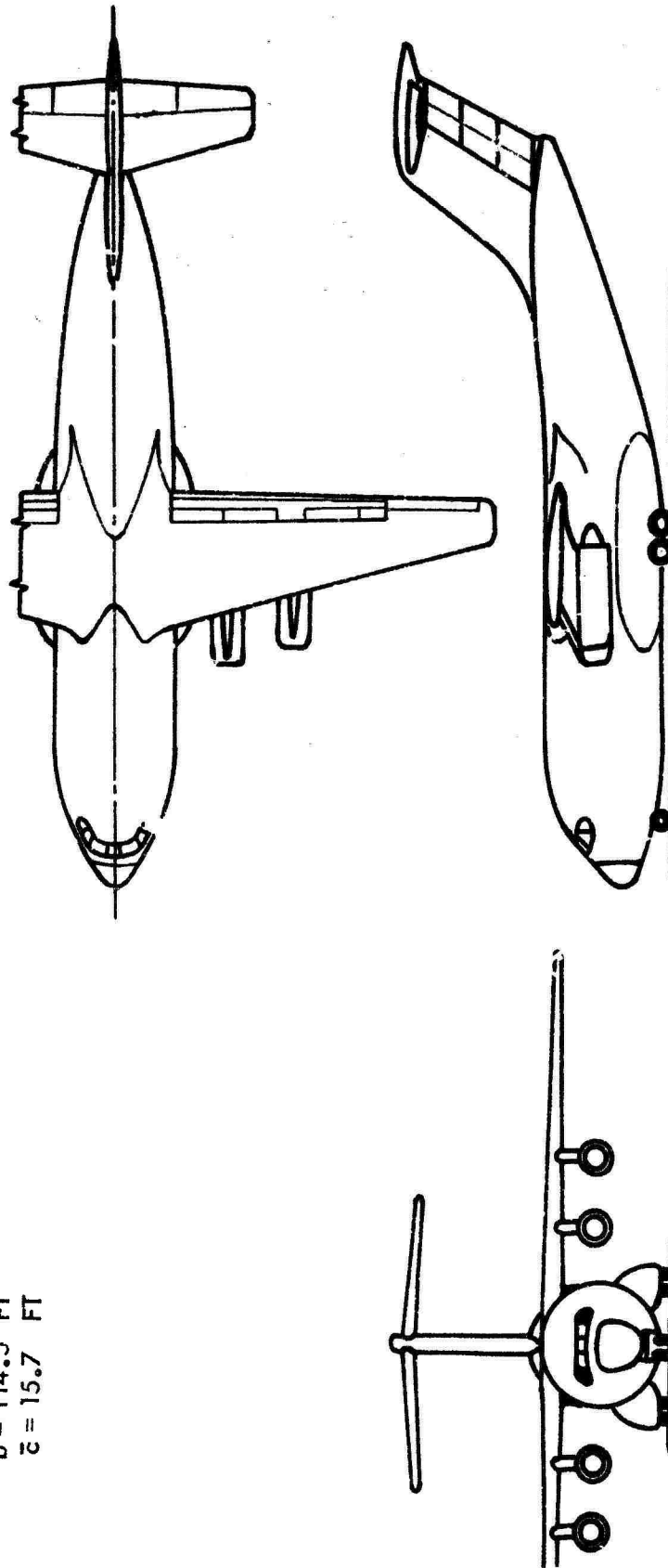


Figure 41: General Arrangement STOL Tactical Transport — Model 953-801

TABLE I

Stability Derivatives, Mass Properties, and  
Reference Dimensions of Example Airplane

All angles are in radians.

$C_{X_\alpha} = 1.297$	$C_{X_\alpha} = 0$	$C_{X_q} = 0$	$C_{X_u} = -1.77$
$C_{L_\alpha} = 7.84$	$C_{L_\alpha} = -8.18$	$C_{L_q} = 7.54$	$C_{L_u} = .0341$
$C_{m_\alpha} = -.496$	$C_{m_\alpha} = -6.06$	$C_{m_q} = -32.94$	$C_{m_u} = -.453$
$C_{Y_\beta} = -1.415$	$C_{Y_p} = .51$	$C_{Y_r} = .02$	
$C_{n_\beta} = .27$	$C_{n_p} = -.45$	$C_{n_r} = -.35$	
$C_{l_\beta} = -.191$	$C_{l_p} = -.59$	$C_{l_r} = 1.16$	

$S = 1640 \text{ ft}^2$	$W = 133,000 \text{ lbs.}$	$I_{ZZ} = 2.62 \times 10^6 \text{-slug-ft}^2$
$\bar{c} = 15.7 \text{ ft}$	$I_{xx} = 1.26 \times 10^6 \text{-slug-ft}^2$	$I_{xz} = 1.4 \times 10^5 \text{-slug-ft}^2$
$b = 114.5 \text{ ft.}$	$I_{yy} = 1.46 \times 10^6 \text{-slug-ft}^2$	

Angle of attack,  $\alpha = .182$ Thrust deflection,  $\sigma = 1.13$ Thrust coefficient,  $C_J = 1.72$

TABLE II

Stability Derivatives With Important Influence  
On Airplane Stability

	<u>Stability Derivative</u>	<u>Major Influence</u>
Longitudinal	$C_{L_\alpha}$	neutral point (Note: when $C_{L_\alpha}$ was varied, $C_{m_\alpha}$ was held constant so the a.c. was moving.)
	$C_{m_\alpha}$	neutral point, short period frequency and damping ratio, long period frequency and damping ratio
	$C_{m_\alpha}^{\cdot}$	short period damping ratio
	$C_{m_q}$	short period damping ratio
	$C_{m_u}$	neutral point, long period frequency and damping
Lateral-Directional	$C_{n_\beta}$	Dutch roll frequency, spiral stability
	$C_{l_\beta}$	Dutch roll damping ratio, spiral stability
	$C_{n_p}$	Dutch roll frequency, spiral stability
	$C_{l_p}$	Dutch roll damping ratio, spiral stability
	$C_{n_r}$	Dutch roll damping ratio, spiral stability
	$C_{l_r}$	Dutch roll frequency and damping ratio, spiral stability

Roots of the longitudinal characteristic equation were plotted on the s-plane. Dutch roll mode roots are also presented on the s-plane. Spiral mode time constants were plotted versus the derivative being varied. These plots are shown, and significant trends discussed in the next sections.

### 3.1.1 Longitudinal

The influence of angle of attack, aerodynamic lag, pitch damping, and speed derivatives is shown in Figures 42, 43, 44, 45 and 46. These charts show that the derivatives critical to an accurate determination of the longitudinal characteristics are:  $C_{L\alpha}$ ,  $C_{m\alpha}$ ,  $C_{m\dot{q}}$ , and  $C_{m\ddot{u}}$ .

Sensitivity of longitudinal characteristics to variations of the pitching moment due to angle of attack,  $C_{m\alpha}$ , are shown in Figure 42. Even though  $C_{m\alpha}$  is negative (the a.c. is more than 6%  $\bar{c}$  aft of the c.g.), the airplane is statically unstable. (There is a real root in the right half plane.) This is due to the large negative value of  $C_{m\ddot{u}}$ . As  $C_{m\alpha}$  is increased from its initial value, the unstable root moves to the left, toward the other real root, while the complex root moves upward. The short period frequency is increasing and the damping decreasing. At about 1.5 times the initial  $C_{m\alpha}$ , the previously unstable root goes to the origin and the airplane becomes neutrally stable. (The c.g. is at the neutral point.) When  $C_{m\alpha}$  is further increased, the two real roots couple and form a long period oscillatory mode, the phugoid. If  $C_{m\alpha}$  were further increased, the phugoid mode may go unstable but the airplane would still be statically stable (the neutral point would still be aft of the c.g.).

When  $C_{m\alpha}$  is decreased the short period frequency decreases and the damping ratio increases. The unstable root goes more unstable and the other real root moves to the left. At about .57 times the initial  $C_{m\alpha}$ , the short period mode becomes critically damped. (The short period mode is now described by real roots.) As  $C_{m\alpha}$  is increased more, one short period real root moves to the left while the other one moves toward the other stable real root. At about .53 times the initial  $C_{m\alpha}$  these latter two roots couple and form an oscillatory mode.

It is necessary to know  $C_{m\alpha}$  accurately for reasons other than longitudinal dynamics considerations. The aerodynamic center should be known within about  $\pm 1\%$  MAC in order to design the tail, locate the c.g. envelope, compute control surface deflections for trim and maneuver, etc. In this case, a  $\pm 1\%$  MAC error in the aerodynamic center location corresponds to about a  $\pm 15\%$  error in  $C_{m\alpha}$ . Figure 42 shows that a 15% error in  $C_{m\alpha}$  will only result in about a 5% error in natural undamped frequency and a .05 change in damping ratio.

Sensitivity to lift curve slope,  $C_{L\alpha}$ , and axial force due to angle of attack,  $C_{X\alpha}$ , is also shown in Figure 43. Varying  $C_{X\alpha}$  had no noticeable effect on the unstable root and only a small effect on the others. A large error,  $\pm 50\%$ , in  $C_{X\alpha}$ , should cause no serious inaccuracies. It is hard to conceive of a 30% error in  $C_{L\alpha}$  so this derivative



Approach Condition  
 $V = 74.6$  Knots  
 $W = 133,000$  Lbs  
 $\sigma = 64.6$  Deg  
 $\gamma = -6$  Deg  
 $C_J = 1.76$

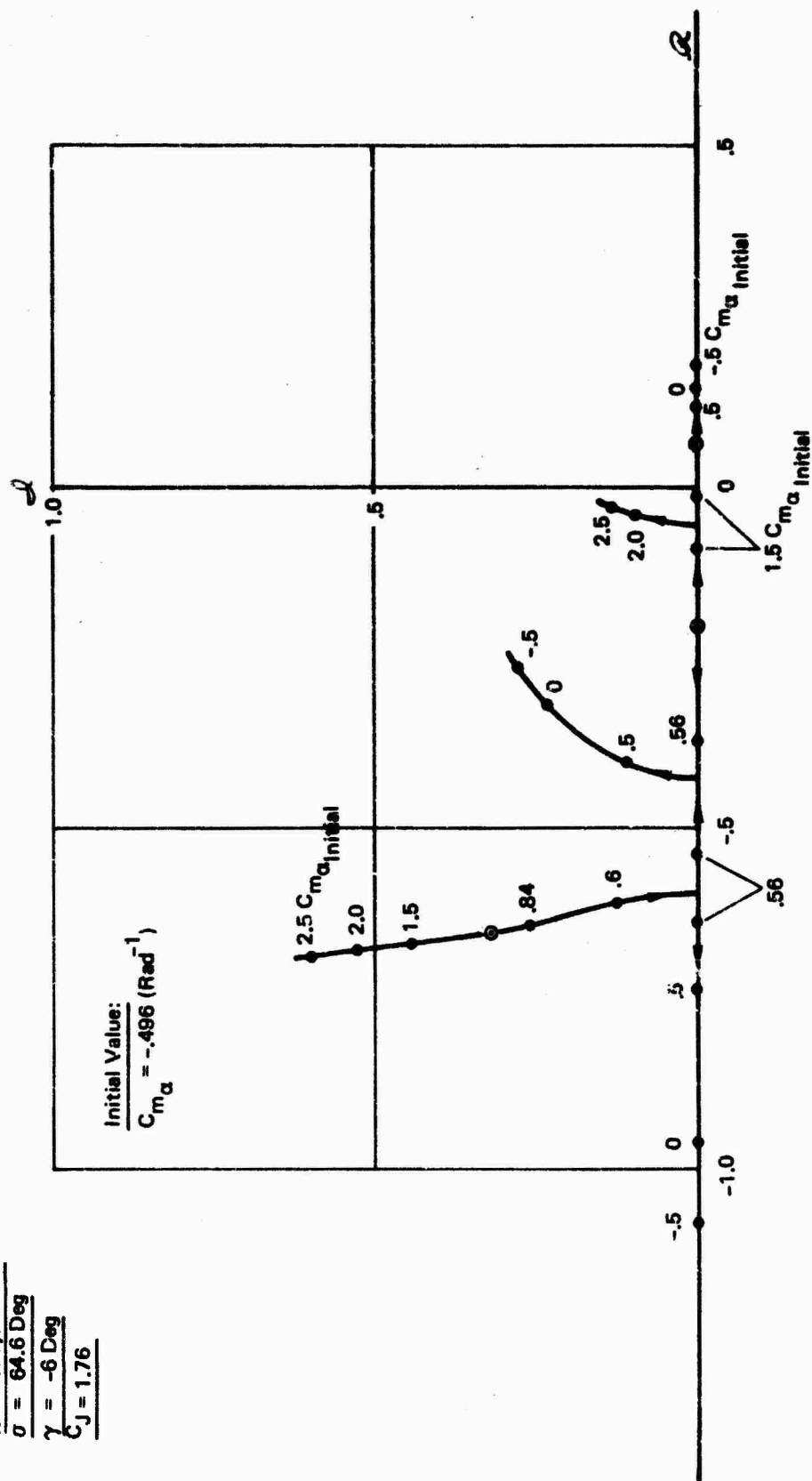


Figure 42 : Effect of Angle of Attack Derivative,  $C_{m_\alpha}$ , on Longitudinal Dynamic Stability

Approach Condition  
 $V = 74.6 \text{ Knots}$   
 $W = 133,000 \text{ Lbs}$   
 $\sigma = 64.6 \text{ Deg}$   
 $\gamma = -6 \text{ Deg}$   
 $C_J = 1.76$

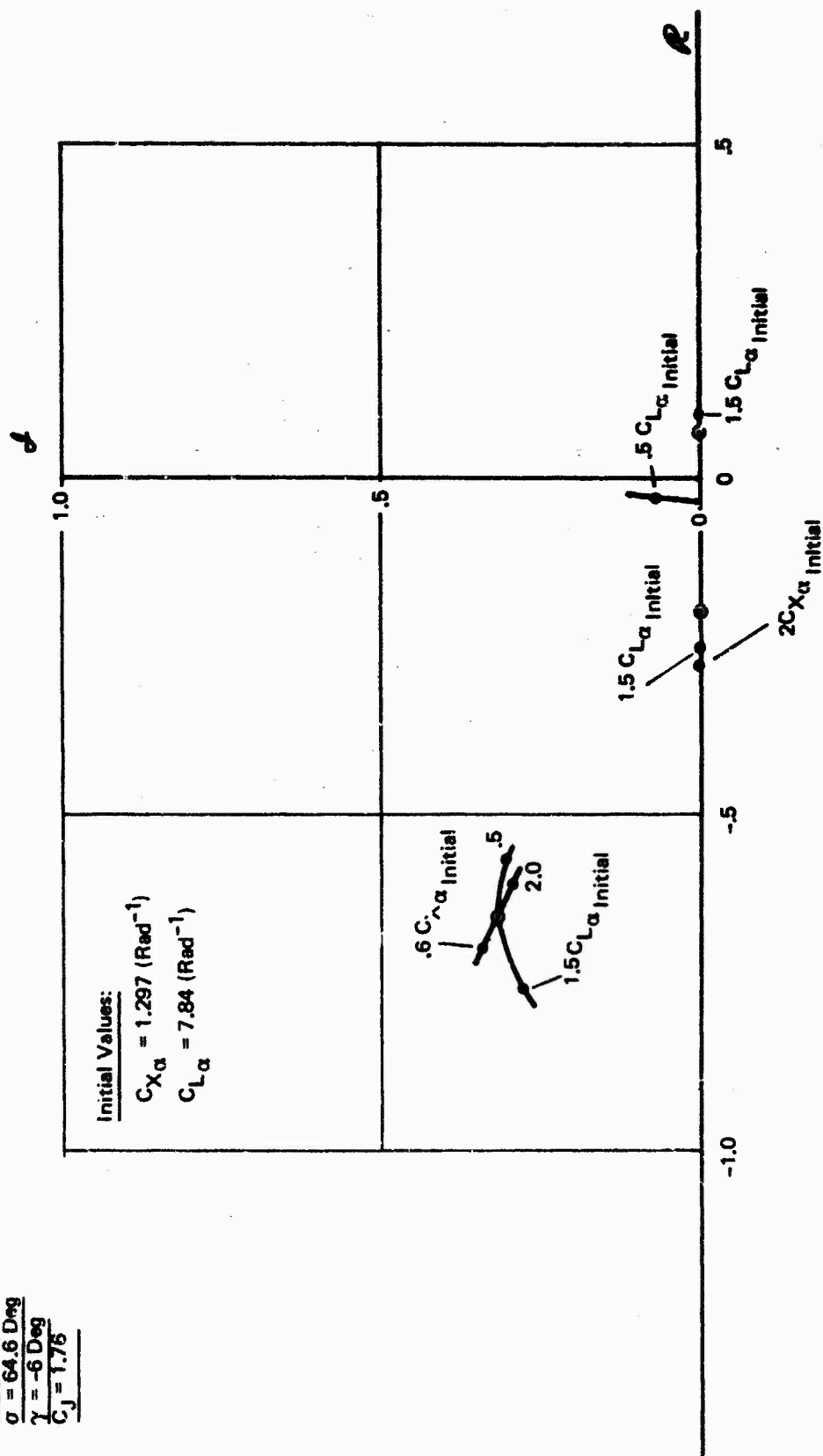
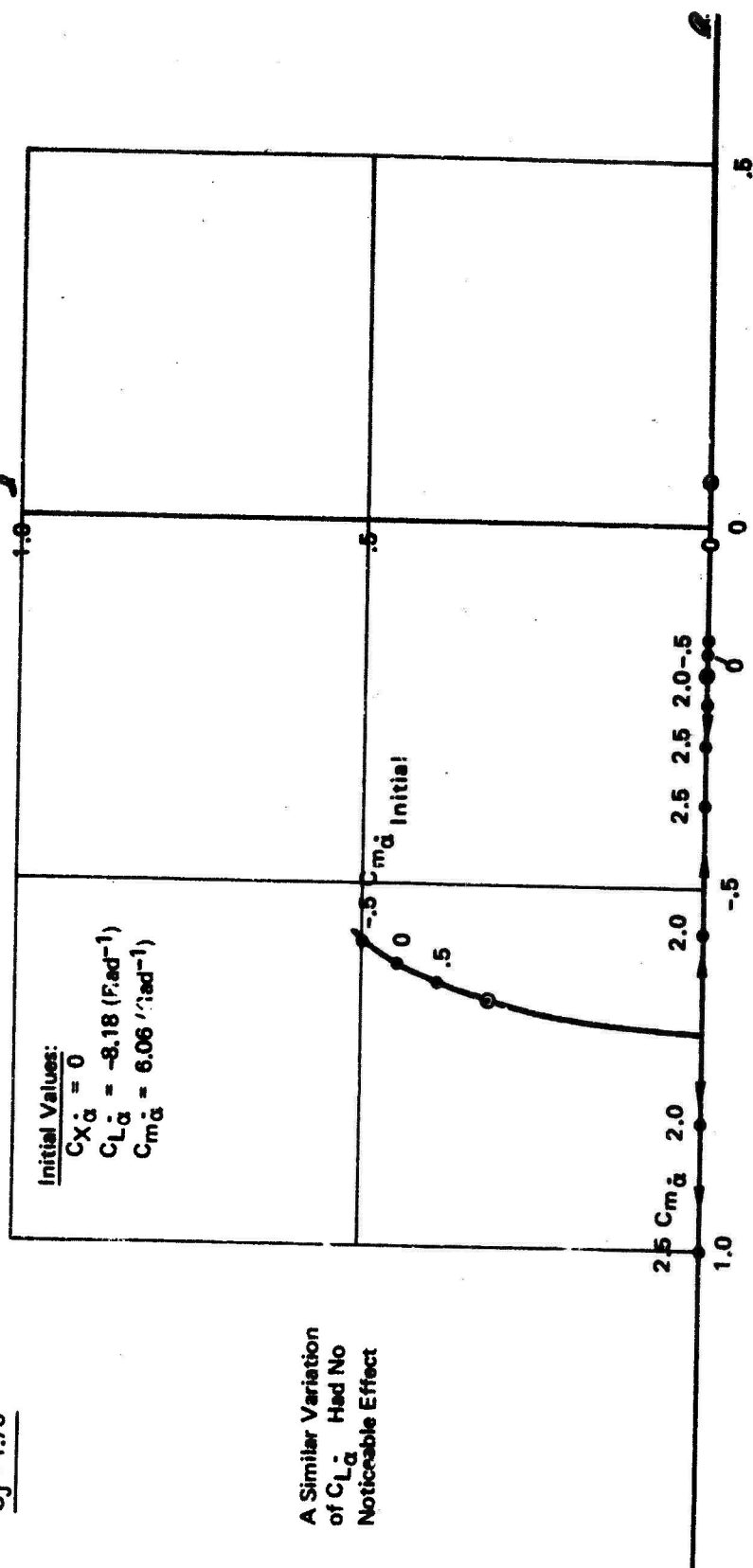


Figure 43 : Effect of Angle of Attack Derivatives,  $C_{X_\alpha}$  and  $C_{L_\alpha}$  on Longitudinal Dynamic Stability

### A Similar Variation of $C_{L_u}$ Had No Noticeable Effect



Approach Condition  
 $V = 74.6$  Knots  
 $W = 133,000$  Lbs  
 $\sigma = 64.6$  Deg  
 $\gamma = -6$  Deg  
 $C_J = 1.76$



A Similar Variation  
of  $C_{L\dot{\alpha}}$  Had No  
Noticeable Effect

Figure 45 : Effect of Aerodynamic Lag Derivatives on Longitudinal Dynamic Stability

Approach Condition  
 $V = 74.6$  Knots  
 $W = 133,000$  Lbs  
 $\eta = 64.6$  Deg  
 $\gamma = -6$  Deg  
 $C_J = 1.76$

A Similar Variation  
of  $C_{Lq}$  Had No  
Noticeable Effect

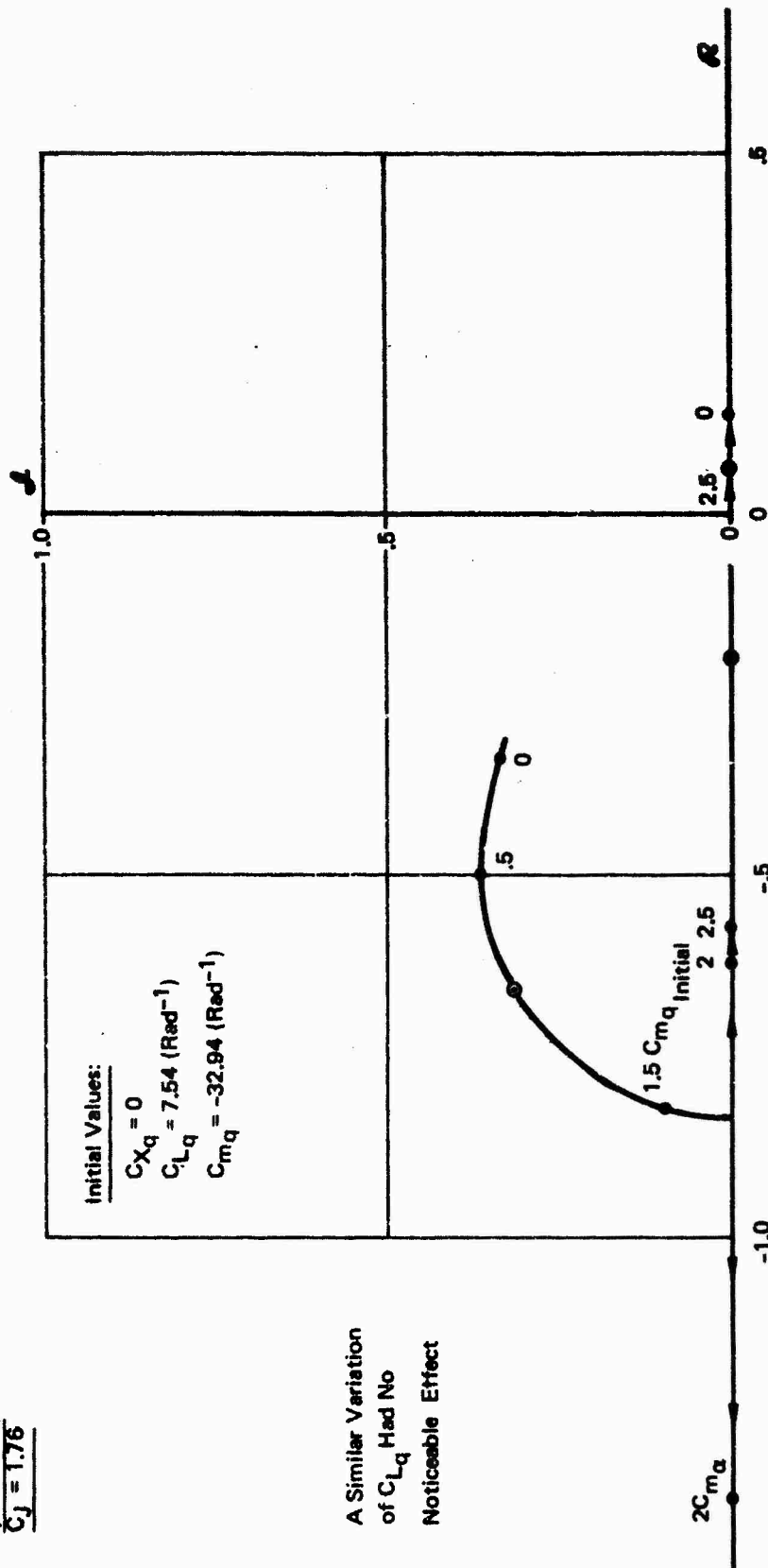


Figure 46 : Effect of Pitch Damping Derivatives on Longitudinal Dynamic Stability

was only varied  $\pm 50\%$ . A 30% error in lift curve slope would only affect the undamped natural frequency by about 6% and has a negligible effect on the damping ratio. Its greatest effect appears to be on the real roots. As  $C_{L\alpha}$  is reduced, the unstable root moves to the left, couples with the other real root, and forms the oscillatory phugoid mode. With a large unstable value for  $C_{m_u}$ , a 20% or 30% error in  $C_{L\alpha}$  could make the difference between whether or not the airplane was statically stable. Keep in mind that  $C_{m\dot{\alpha}}$  was held constant while  $C_{L\alpha}$  varied, so changing  $C_{L\alpha}$  also implies a change in the aerodynamic center location.

The influence of speed derivatives is shown in Figure 44. Large errors in  $C_{x_u}$  and  $C_{L_u}$  will cause no problem. However,  $C_{m_u}$  should be accurately known, because large negative values of  $C_{m_u}$  cause the airplane to be statically unstable even though the c.g. is ahead of the aerodynamic center.  $C_{m_u}$  has only a small effect on the short period mode.

Powered lift airplanes are likely to have large values of  $C_{m_u}$ . In the trim condition a large aerodynamic pitching moment is required to balance the thrust moment. If a speed change occurs these two moments change at different rates causing a moment unbalance. There is another component, to  $C_{m_u}$ , due to thrust interference but this is generally small for a vectored thrust airplane.

Effects of aerodynamic lag or the  $\dot{\alpha}$  derivatives, on longitudinal dynamics are shown in Figure 45.  $C_{L\dot{\alpha}}$  has no noticeable effect. The real roots are not influenced by  $C_{m\dot{\alpha}}$  but the damping ratio of the short period mode appears to be sensitive to this term. As  $C_{m\dot{\alpha}}$  is increased the damping ratio increases and at two times the initial value the short period mode is critically damped. It would be desirable to know  $C_{m\dot{\alpha}}$  within 40% in order to know the damping ratio within about 10%.

Sensitivity to the pitch rate derivatives is shown in Figure 46. Varying  $C_{L_q}$  had no noticeable effect. A  $\pm 200\%$  error would be negligible. However, dynamic characteristics are sensitive to  $C_{m_q}$ . As  $C_{m_q}$  is increased from the initial value, the short period damping ratio is increased without much effect on undamped natural frequency. If  $C_{m_q}$  is reduced, undamped natural frequency and damping ratio both are reduced. The real roots are only slightly affected, but if  $C_{m_q}$  were increased still further than shown in Figure 46 a long period oscillatory mode would develop.

### 3.1.2 Lateral-Directional

The influence of sideslip, yaw rate, and roll rate derivatives on lateral-directional dynamics is shown in Figures 47 through 52. Derivatives that must be predicted with relative accuracy are:  $C_{n\beta}$ ,  $C_{l\beta}$ ,  $C_{n_p}$ ,  $C_{l_p}$ ,  $C_{n_r}$ , and  $C_{l_r}$ .

Sensitivity to variations in sideslip derivatives are shown in Figures 47 and 48.  $C_{Y\beta}$  has only a small influence on the Dutch roll mode and practically no effect on the spiral mode. Large errors in  $C_{Y\beta}$  would not seriously affect the Dutch roll characteristics. However,  $C_{l\beta}$  and  $C_{n\beta}$  strongly influence

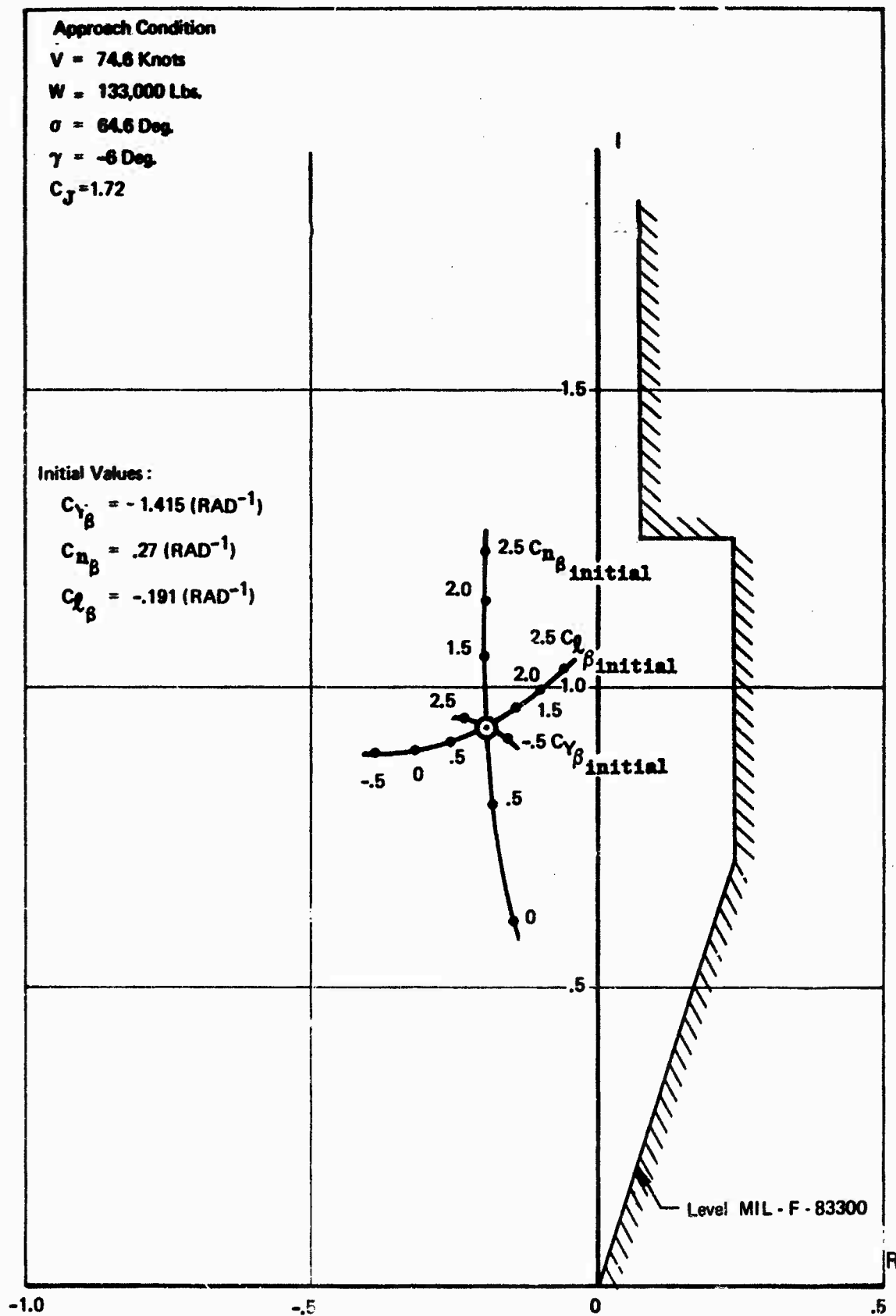


Figure 47 : Effect of Sideslip Derivatives on Dutch Roll Characteristics

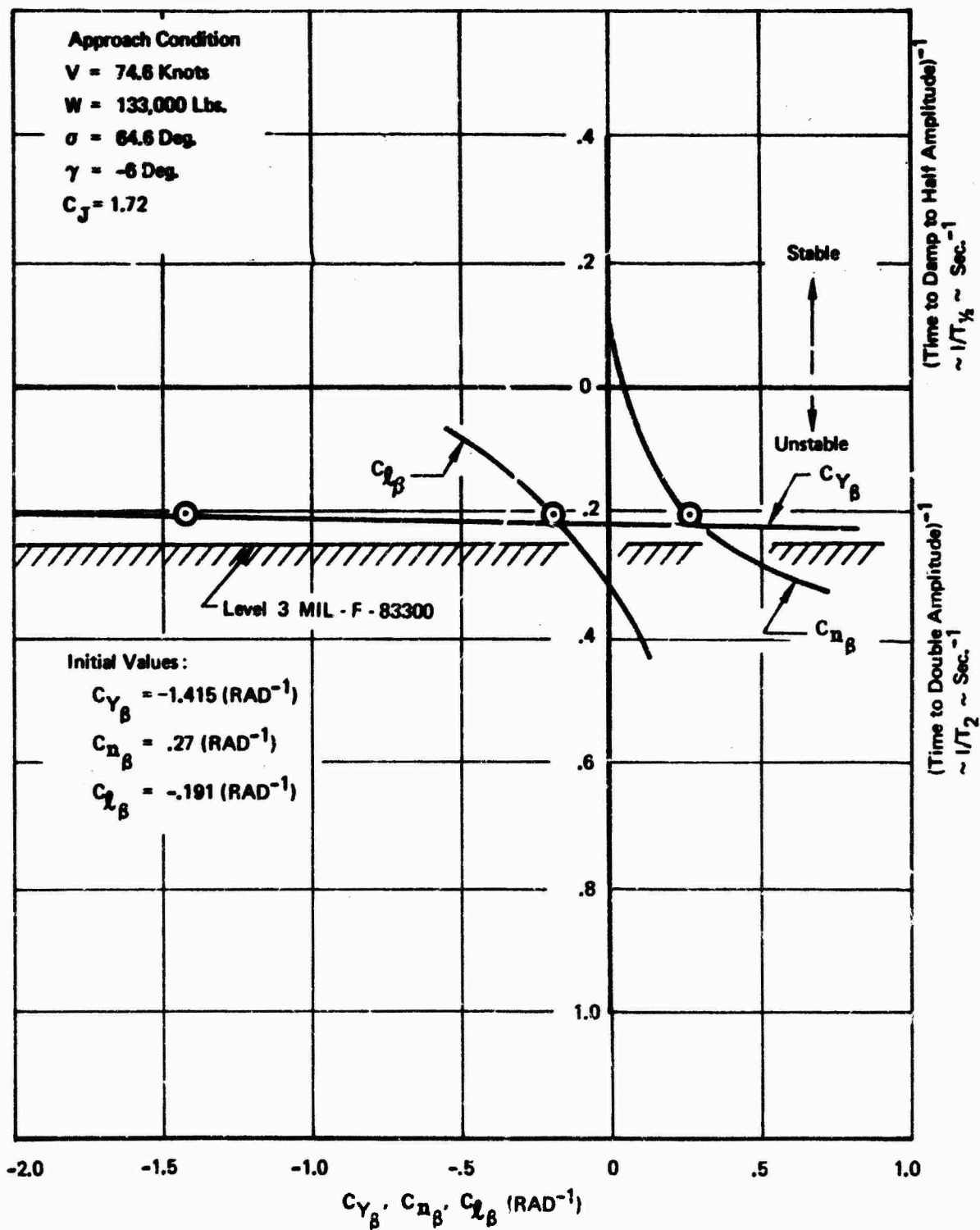


Figure 48 : Effect of Sideslip Derivatives on Spiral Mode Stability



both the Dutch roll and spiral modes. It is desirable to know both of these derivatives within an increment of  $\pm 0.03 \text{ rad}^{-1}$ , about 10 to 15 percent. It is interesting to note that variations in  $C_{n\delta}$  affect mainly the Dutch roll frequency while  $C_{l\delta}$  changes affect primarily the Dutch roll damping ratio. When  $C_{n\delta}$  is reduced to zero, the Dutch roll mode is still stable and the spiral mode becomes stable. If  $C_{l\delta}$  is reduced to zero the Dutch roll mode remains stable but the spiral mode gets more unstable.

Accuracy of calculations relating to cross wind landings and engine-out conditions is directly related to the quality of the side-slip derivatives. This should be taken into account when deciding on the required accuracy of the derivatives.

Figures 49 and 50 show the effect of roll rate derivatives.  $C_{Y\dot{p}}$  has no effect on any of the roots of the characteristic equation and for this purpose can be ignored.  $C_{np}$  and  $C_{lp}$  effect both the spiral and Dutch roll modes and should be known within an increment of  $\pm 0.1 \text{ rad}^{-1}$ , or about 20%. The cross derivative,  $C_{np}$ , affects mainly Dutch roll frequency and the roll damping derivative,  $C_{lp}$ , affects mainly the Dutch roll damping ratio. When  $C_{lp}$  went to zero, the Dutch roll damping did too, even though  $C_{n\delta}$  and  $C_{l\delta}$  both have stable values.

The effects of yaw rate derivatives are shown in Figures 51 and 52. Again the side force derivative has no effect. The cross derivative,  $C_{lr}$ , affects both Dutch roll damping ratio and frequency. The yaw damping derivative affects mainly Dutch roll damping.  $C_{nr}$  and  $C_{lr}$  both affect the spiral mode with  $C_{lr}$  having the greater influence. Reducing  $C_{lr}$  would stabilize the spiral mode while reducing the Dutch roll damping ratio.  $C_{nr}$  and  $C_{lr}$  should be determined within an increment of  $\pm 0.1 \text{ rad}^{-1}$ .

### 3.2 Stability and Control

This section presents a simple empirical method of predicting aerodynamic interference effects due to vectored thrust on stability and control derivatives. The method consists of applying a thrust correction factor to the tail-off derivative and taking into account the power effect on the downwash, sidewash, and dynamic pressure at the tail. It is assumed that the power-off characteristics are known, either estimated or from wind tunnel data. Correction factors are all based on wind tunnel data. The wind tunnel data are presented in Reference 5.

All derivatives and coefficients in this section are net values, that is; direct thrust forces are not included.

It is appropriate to state here some general observations and opinions regarding the wind tunnel yaw data.

- o Spanwise engine location has a negligible effect on lift curve slope.

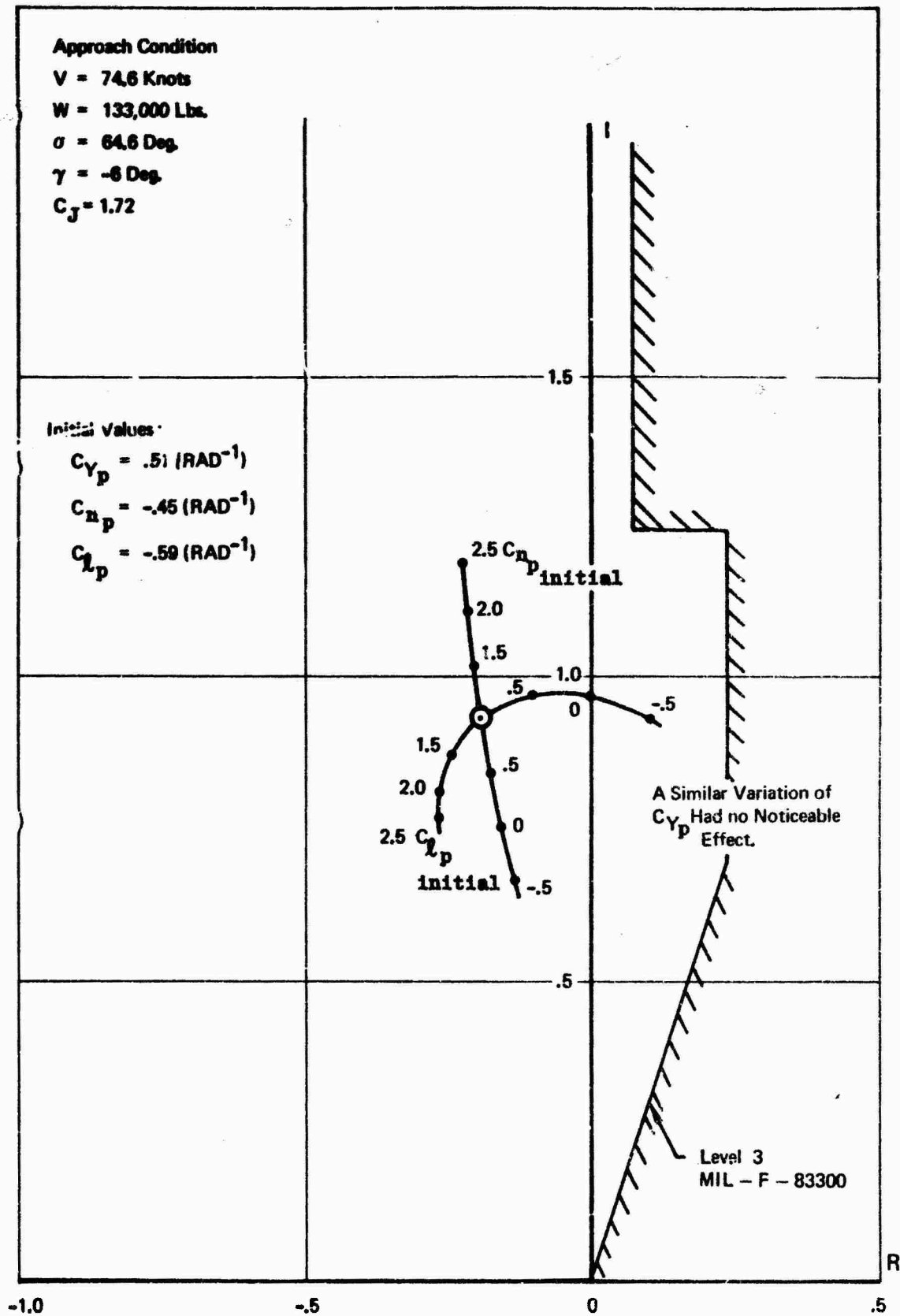


Figure 40 : Effect of Roll Rate Derivatives on Dutch Roll Characteristics

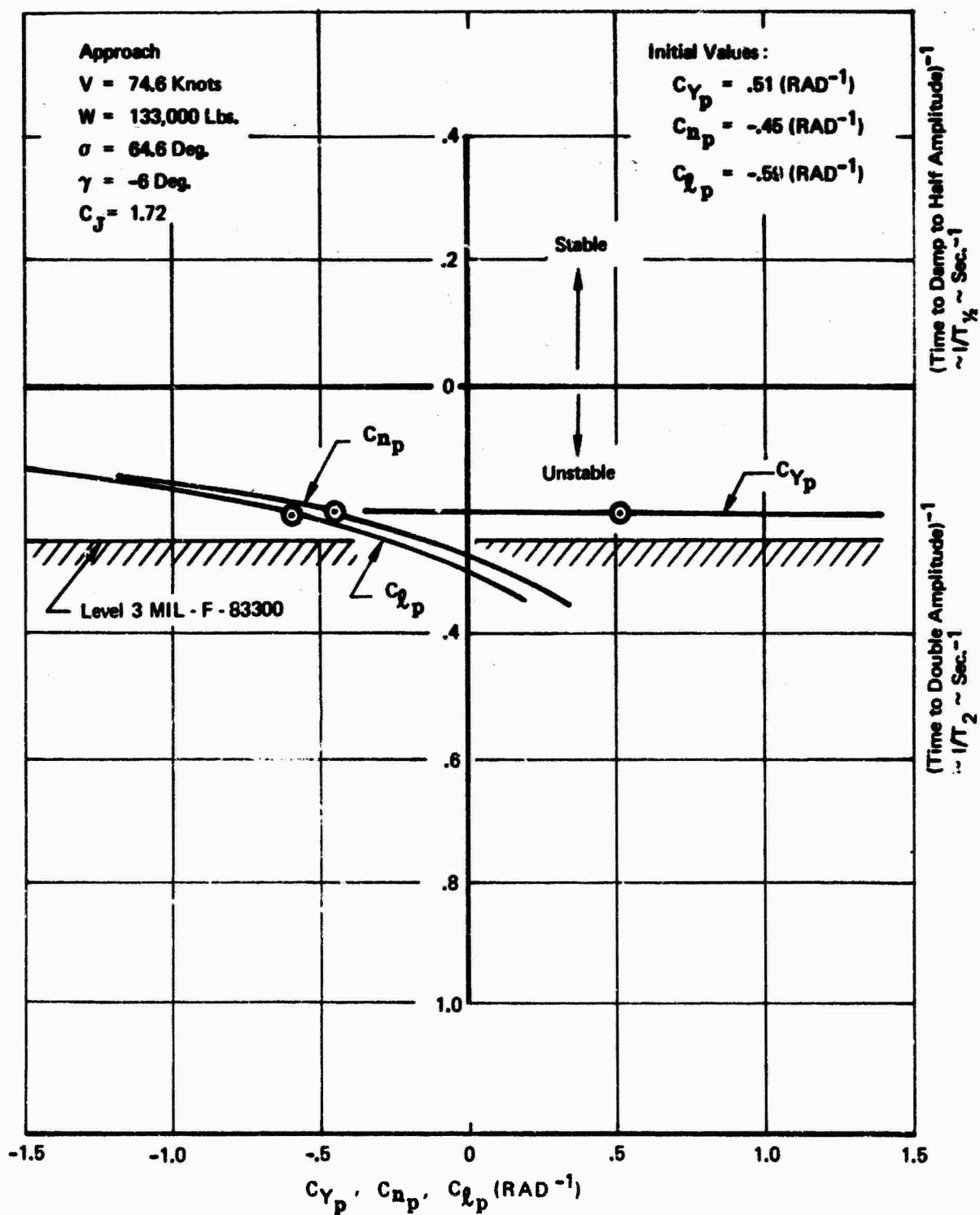


Figure 50 : Effect of Roll Rate Derivatives on Spiral Mode Stability

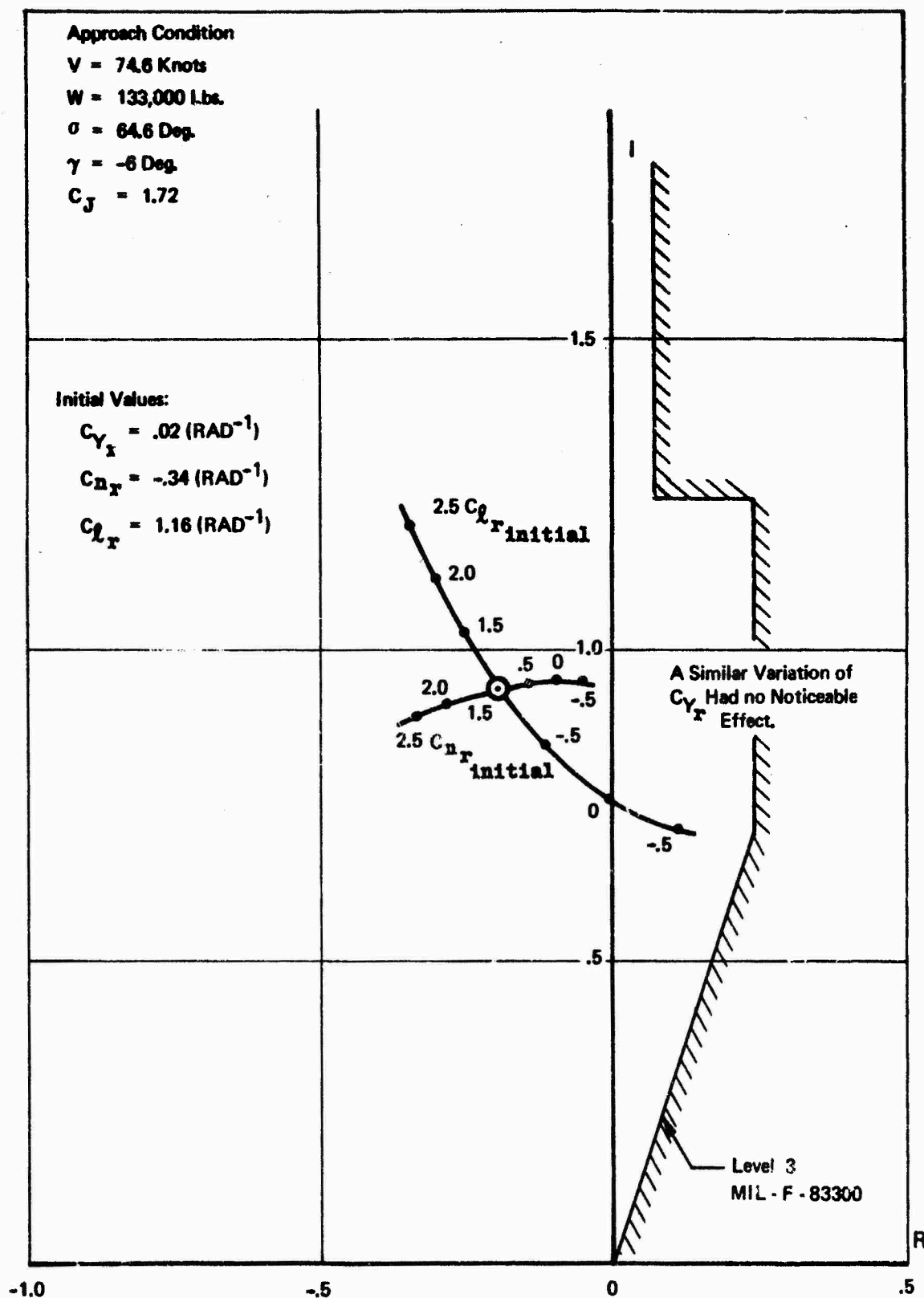


Figure 51 : Effect of Yaw Rate Derivatives on Dutch Roll Characteristics

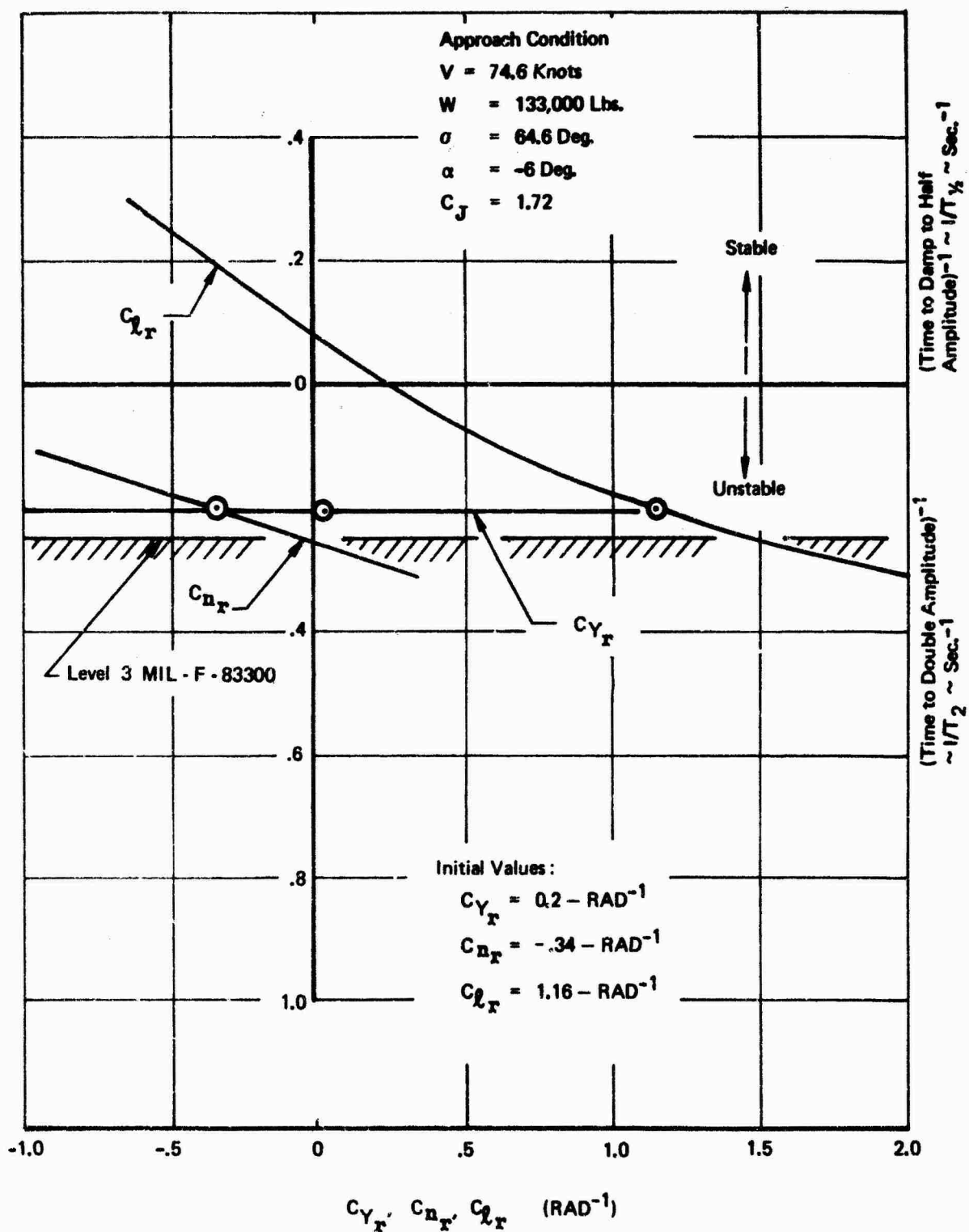


Figure 52 : Effect of Yaw Rate Derivatives on Spiral Mode Stability

- o Engine-out has little effect on sideslip derivatives.
- o Thrust has small effect on sideslip derivatives except at high thrust deflection or when the nacelles are double podded inboard.
- o Angle of attack effects on sideslip derivatives are small, although a little greater at the higher wing sweep and in-ground effect.
- o Chordwise nozzle position has a negligible effect on sideslip derivatives.
- o Ground effects, on sideslip derivatives, are small except at high thrust settings with 90 degree thrust vector angle. There is apparently a flow breakdown at this condition.
- o Thrust has negligible effect with flaps up.

Thrust effects may be magnified by having poor flow on the model at zero thrust. With the leading edge flap deflected 70 degrees, flow is stalled on the bottom of the wing, so the trailing edge flaps are "seeing" stalled air. Tuft studies, in the wind tunnel, show that the trailing edge flaps are in turbulent flow up to about 12 degrees angle of attack. Also, the lift curve slope is very high at low angle of attack, indicating something (probably the wing undersurface) is becoming unstalled as angle of attack increases. All of the yaw runs were done at angles of attack less than or equal to 12 degrees. Therefore, the flaps never had "clean" air in any yaw run. The engines are located in this stalled air. They are an energy source that probably tends to straighten the stalled flow. This might mean that the power effects, presented here, are merely increments tending to swing the data back to where the power-off data would have been if the bottom of the wing had not been stalled.

### 3.2.1 Longitudinal Stability and Control

This section presents a method for estimating the aerodynamic interference effect of engine thrust on longitudinal stability and control derivatives. This method has an empirical basis and has been derived from the vectored thrust blowing test (BVWT 099, Reference 5). Methods for predicting lift and pitching moment are also presented in Section 2. However, the methods presented here, although less precise, are more appropriate for preliminary design purposes because they are faster.

#### 3.2.1.1 Static Stability Derivatives

The test pitching moment and lift curves are quite nonlinear with respect to angle of attack. To obtain the results reported here, slopes were measured at 8° angle of attack, which is representative of takeoff and landing conditions. The method has been compared to test data at  $\alpha=4^\circ$  and  $8^\circ$  and agreement is quite good at both angles of attack.

Figures 53 through 55 show the effect of nozzle location, vector angle, and  $C_J$  on tail-off lift curve slope and aerodynamic center. These are corrections which should be applied to power off  $C_{L\alpha}$  and  $ac$  by equations 3.1 and 3.2.

$$C_{L\alpha} = C_{L\alpha_{C_J=0}} + \left( \frac{\Delta C_{L\alpha}}{C_J} \right) C_J \quad (3.1)$$

$$ac = ac_{C_J=0} + \left[ \left( \frac{\Delta ac}{C_J} \right)_a + \left( \frac{\Delta ac}{C_J} \right)_b \right] C_J \quad (3.2)$$

where:

$\Delta C_{L\alpha}$  - per degree

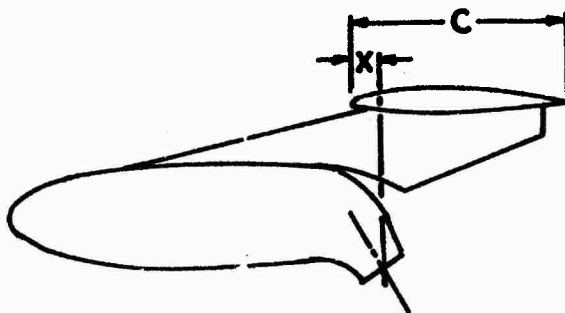
a.c. - aerodynamic center shift in fraction of MAC,  
positive aft

Subscripts:

a - means at constant spanwise nacelle location

b - means at varying spanwise nacelle location

The nozzle chordwise location is the position of the center of the nozzle exit plane in percent of the wing local chord, as shown in the sketch below.



For ease of application data are shown for wing sweeps of  $0^\circ$ ,  $15^\circ$ , and  $30^\circ$ . Power effects were measured in the wind tunnel at  $15^\circ$  and  $30^\circ$  only. the  $0^\circ$  sweep is an extrapolation of these data.

Figures 53 and 54 are for the engines at 27% and 43.5% semispan locations. To account for the effect of different spanwise positions Figure 55 has been developed. Figure 55 shows the effect of mean spanwise nacelle position (average between inboard and outboard) on a.c. The lift curve slope is not affected; however, inward movement of the nacelles has a stabilizing effect on a.c. shift due to interference.

The increments obtained from these figures are compared to the wind tunnel test results at  $\alpha = 4^\circ$  and  $8^\circ$  and for several nacelle positions, both with single and double pods, in Table III and Figures 56 and 57.

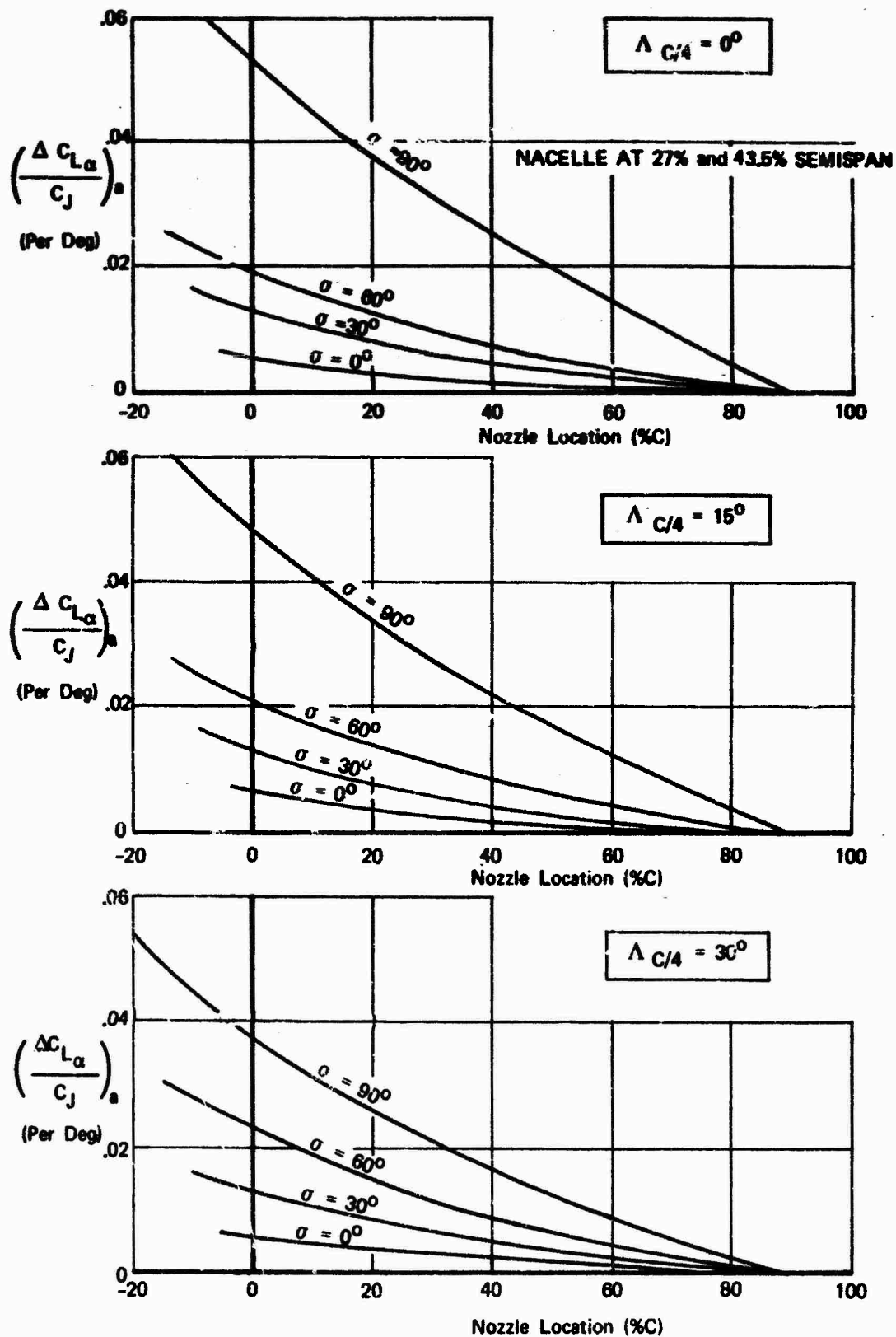


Figure 53 Effect of Vectored Thrust on Lift Curve Slope



# NACELLES AT 27% and 43.5% SEMISPAN

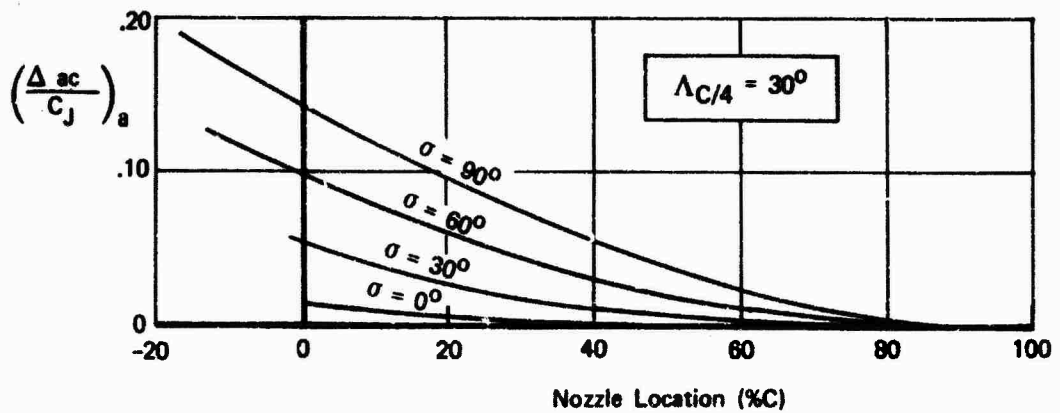
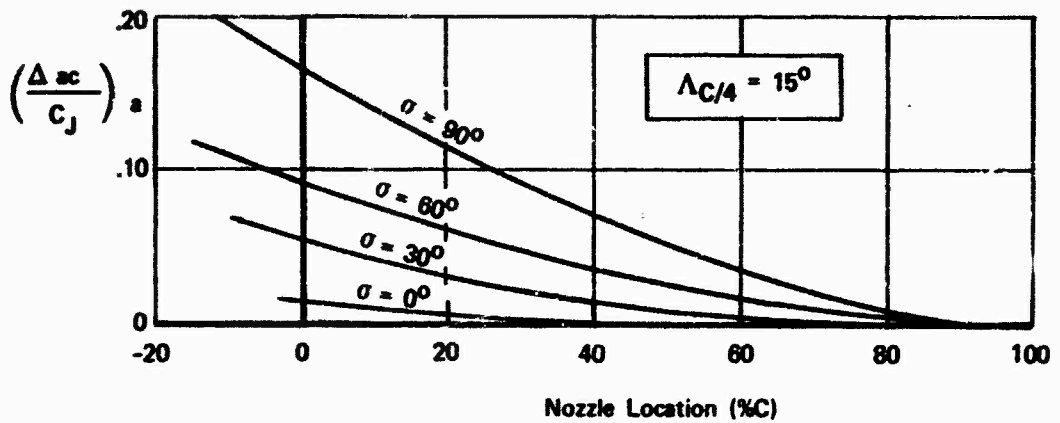
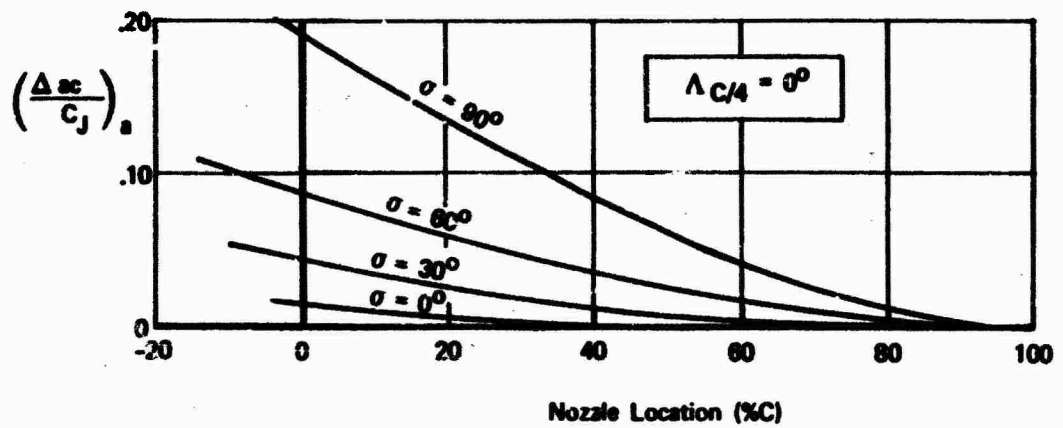


Figure 54 Effect of Vectored Thrust on Aerodynamic Center

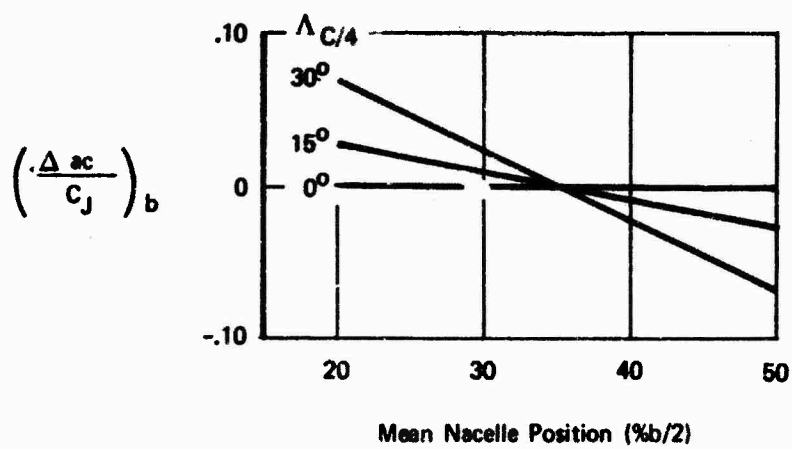


Figure 55 Effect of Nacelle Spanwise Location on Aerodynamic Center

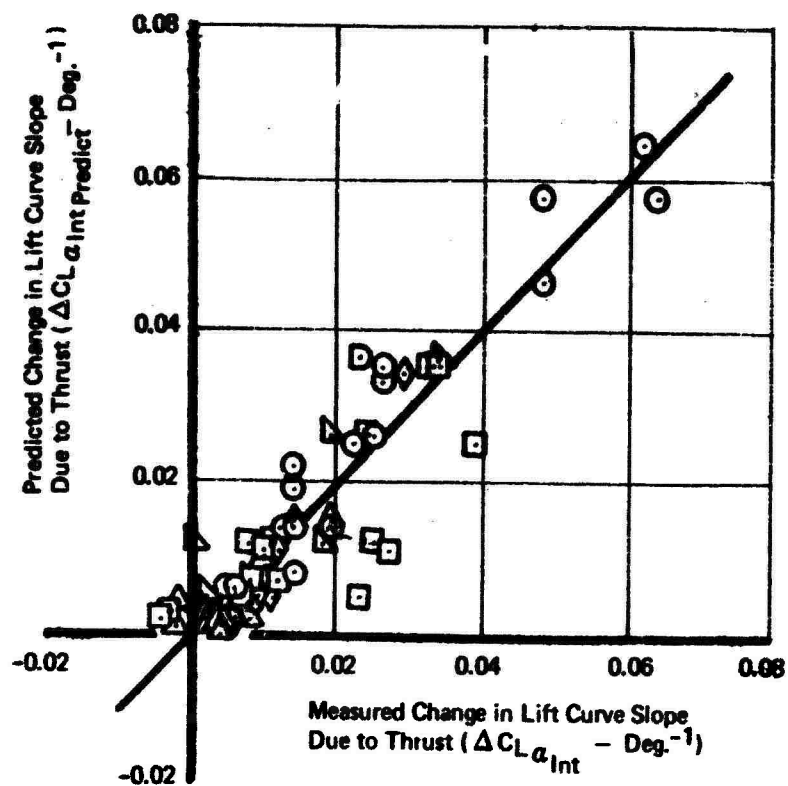
TABLE III

TEST - PREDICTION COMPARISON, ANGLE OF ATTACK DERIVATIVES

Nacelle Location	Angle of Attack	Wing Sweep	Flap / Nozzle	$\frac{\Delta C_{L\alpha}}{C_J}$			$\frac{\Delta a_c}{C_J}$		
				Predicted	Measured	Error	Predicted	Measured	Error
P1 P4 - Engines at 27 and 43.5% semispan. Nozzles at 0% chord (nominal).	8°	15°	0° / 0°	.006	.006	0	.012	.010	.002
			20°/30°	.014	.012	.002	.056	.023	.033
			35°/30°	.014	.019	-.005	.056	.071	-.015
			35°/60°	.025	.022	.002	.103	.097	.006
			35°/90°	.064	.062	.002	.213	.217	-.004
	4°	30°	0° / 0°	.006	.005	.001	.012	.012	0
			20°/30°	.014	.008	.006	.058	.038	.020
			35°/30°	.014	.014	0	.058	.088	-.030
			35°/60°	.026	.035	-.009	.112	.138	-.026
			35°/90°	.048	.046	.002	.180	.170	.010
	8°	15°	35°/30°	.014	.019	-.005	.056	.062	-.007
			35°/60°	.025	.026	-.001	.103	.132	-.029
			35°/90°	.064	.057	.007	.213	.123	.090
			35°/30°	.014	.022	-.008	.058	.058	0
			35°/60°	.026	.033	-.007	.112	.135	-.013
P2 P5 - Engines at 27 and 43.5% semispan. Nozzles at 35% chord (nominal)	8°	15°	35°/90°	.048	.057	-.009	.180	.115	.065
			0° / 0°	.002	-.004	.006	.002	-.005	.007
			20°/30°	.005	.007	-.002	.017	.013	.004
			35°/30°	.005	.006	-.001	.017	.005	.012
			35°/60°	.011	.010	.001	.052	.045	.007
	4°	30°	35°/90°	.035	.034	.001	.012	.011	.001
			0° / 0°	.003	-.003	.006	.002	.005	-.003
			20°/30°	.007	.008	-.001	.015	.011	.004
			35°/30°	.007	.008	-.001	.015	.013	.002
			35°/60°	.012	.008	.004	.048	.028	.020
	8°	15°	35°/90°	.025	.024	.001	.092	.086	.006
			48°/60°	.012	.008	.004	.048	.027	.021
			35°/30°	.005	.023	-.018	.017	.049	-.032
			35°/60°	.011	.027	-.016	.052	.081	-.029
			35°/90°	.035	.033	.002	.120	.070	.050
	4°	30°	35°/30°	.007	.012	-.005	.015	.021	-.006
			35°/60°	.012	.025	-.013	.048	.050	-.002
			35°/90°	.025	.039	-.014	.092	.100	-.008

TABLE III (Continued)  
TEST - PREDICTION COMPARISON, ANGLE OF ATTACK DERIVATIVES

Nacelle Location	Angle of Attack	Wing Sweep	Flap / Nozzle	$\frac{\Delta C_{L\alpha}}{C_J}$		$\frac{\Delta C_J}{C_J}$	
				Predicted	Measured	Predicted	Measured
P3 P6 - Engines at 27 and 43.5% semispan. Nozzles at 70% chord (nominal)	8°	15°	0° / 0°	0	.004	0	.028
			20° / 30°	.001	-.002	.001	.001
			35° / 30°	.001	-.003	.001	.034
		30°	35° / 60°	.004	-.004	.015	.022
			35° / 90°	.015	-.004	.047	.005
			0° / 0°	.001	-.001	0	.022
	4°	15°	20° / 30°	.002	-.004	.001	.001
			35° / 30°	.002	0	.001	.004
			35° / 60°	.004	-.001	.008	.015
		30°	35° / 90°	.010	0	.029	.025
			48° / 60°	.004	-.001	.008	.010
			35° / 30°	.001	.003	.001	-.002
P5 P8 - Engines at 43.5 and 60% semispan. Nozzles at 35% chord (nominal)	8°	15°	35° / 60°	.004	.006	.015	.009
			35° / 90°	.015	.001	.047	-.007
			35° / 30°	.002	-.006	.001	.009
		30°	35° / 60°	.004	-.003	.008	.026
			35° / 90°	.010	0	.029	.042
			0° / 0°	.002	-.001	-.025	.022
	8°	15°	20° / 30°	.005	.003	-.010	.005
			35° / 30°	.005	-.005	-.010	.010
			35° / 60°	.012	-.006	.025	.014
		30°	35° / 90°	.036	.002	.098	.094
			35° / 30°	.007	-.001	.058	.040
			35° / 60°	.012	.012	-.025	-.015
P12 - Double Podded Engines at 27% semispan. Nozzles at 35% chord (nominal)	8°	15°	35° / 90°	.026	.007	.021	.055
			0° / 0°	.002	-.004	.017	.010
			20° / 30°	.005	-.004	.034	.053
		30°	35° / 30°	.005	-.006	.034	.085
			35° / 60°	.011	-.001	.069	.062
			35° / 90°	.034	.005	.132	.124
	8°	15°	35° / 30°	.055	-.005	.003	.007
			35° / 60°	.012	.001	.040	.037
			35° / 90°	.036	.013	.108	.076
		30°	35° / 30°	.007	-.008	.007	.007
			35° / 60°	.011	-.003	.037	.003
			35° / 90°	.023	.013	.108	.032



- $P_1 P_4$  — Engines at 27 and 43.5% Semispan  
Nozzles at 0% Chord
- $P_2 P_5$  — Engines at 27 and 43.5% Semispan  
Nozzles at 35% Chord
- △  $P_3 P_6$  — Engines at 27 and 43.5% Semispan  
Nozzles at 70% Chord.
- ▷  $P_5 P_8$  — Engines at 43.5 and 60% Semispan  
Nozzles at 35% Chord
- ◇  $P_{12}$  — Double Podded Engines at 27%  
Semispan. Nozzles at 35% Chord.
- ▷  $P_{13}$  — Double Podded Engines at 43.5%  
Semispan. Nozzles at 35% Chord

Figure 56 : Lift Curve Slope Error

- P<sub>1</sub> P<sub>4</sub> — Engines at 27 and 43.5% Semispan  
Nozzles at 0% Chord
- P<sub>2</sub> P<sub>5</sub> — Engines at 27 and 43.5% Semispan  
Nozzles at 35% Chord
- △ P<sub>3</sub> P<sub>6</sub> — Engines at 27 and 43.5% Semispan  
Nozzles at 70% Chord
- ▷ P<sub>5</sub> P<sub>8</sub> — Engines at 43.5 and 60% Semispan  
Nozzles at 35% Chord
- ◇ P<sub>12</sub> — Double Podded Engines at 27%  
Semispan Nozzles at 35% Chord
- ▷ P<sub>13</sub> — Double Podded Engines at 43.5%  
Semispan Nozzles at 35% Chord

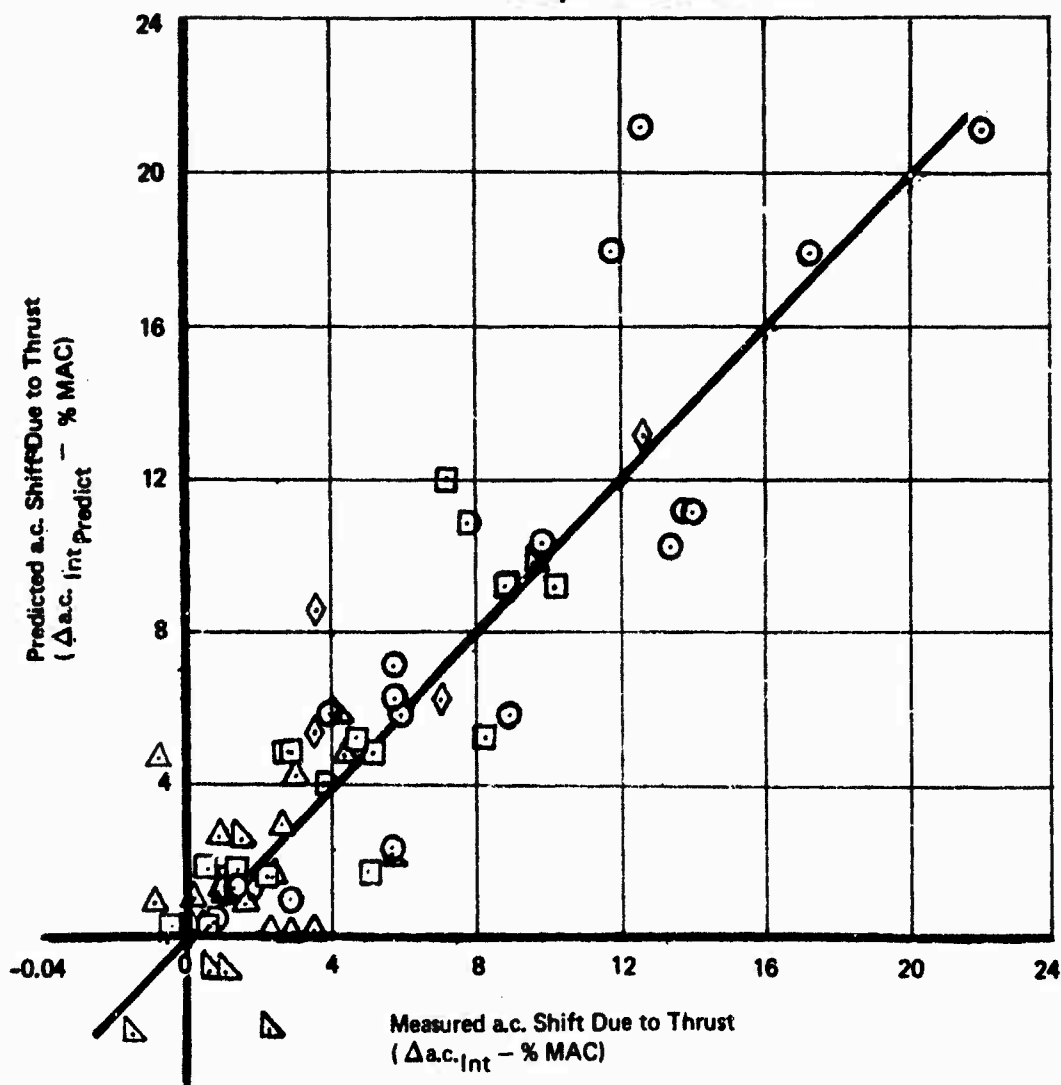


Figure 57 : Aerodynamic Center Error

The interference drag term  $\Delta C_{D_{\alpha}}$  has also been derived from BVWT 099 (Reference 5) test data. Interference drag is a function of lift interference, vector angle, and nacelle chordwise location and is presented in Figures 32 through 34. From these figures an average

slope of  $\frac{\partial C_{D_{\text{INT}}}}{\partial C_{L_{\text{INT}}}}$  is obtained. This term, when multiplied by  $\Delta C_{L_{\alpha \text{INT}}}$  from Figure 53 gives the  $\Delta C_{D_{\alpha \text{INT}}}$  term:  $\Delta C_{D_{\alpha \text{INT}}} = .3 \Delta C_{L_{\alpha \text{INT}}}$

The vectored thrust effect on horizontal tail input to lift curve slope and aerodynamic center is caused by a change in dynamic pressure and downwash at the tail. Power-off tail effectiveness should be corrected for thrust effects by Equations 3.3 and 3.4

$$\Delta C_{L_{\alpha_H}} = \left( \Delta C_{L_{\alpha_H}} \right)_{C_J=0} \left( \frac{q}{q_{C_J=0}} \right) \frac{\left( 1 - \frac{\partial \epsilon}{\partial \alpha} \right)}{\left( 1 - \frac{\partial \epsilon}{\partial \alpha} \right)_{C_J=0}} \quad (3.3)$$

$$\Delta a_{c_H} = \left( \Delta a_{c_H} \right)_{C_J=0} \left( \frac{q}{q_{C_J=0}} \right) \frac{\left( 1 - \frac{\partial \epsilon}{\partial \alpha} \right)}{\left( 1 - \frac{\partial \epsilon}{\partial \alpha} \right)_{C_J=0}} \quad (3.4)$$

$$\frac{\left( 1 - \frac{\partial \epsilon}{\partial \alpha} \right)_{C_J}}{\left( 1 - \frac{\partial \epsilon}{\partial \alpha} \right)_{C_J=0}} = 0$$

is given in Figure 58. Downwash is based on tail-

on, tail-off, and tail control power test data from BVWT 099 (Reference 5). The downwash shown is the averaged value based on wing sweeps of 15° and 30° and on vector angles of 30°, 60° and 90°. This shows good agreement with downwash from wake rake data obtained in BVWT 101 (Reference 5).

An attempt to measure power effects on dynamic pressure at the tail proved unsatisfactory because of wind tunnel instrumentation problems. Figure 59 is presented instead, as a representative example of the effect of vectored thrust. This data was extracted from horizontal tail effectiveness tests at 60° vector angle.

Vectored thrust has an effect on the horizontal tail drag. However, this is only a small increment and for preliminary design purposes may be neglected.

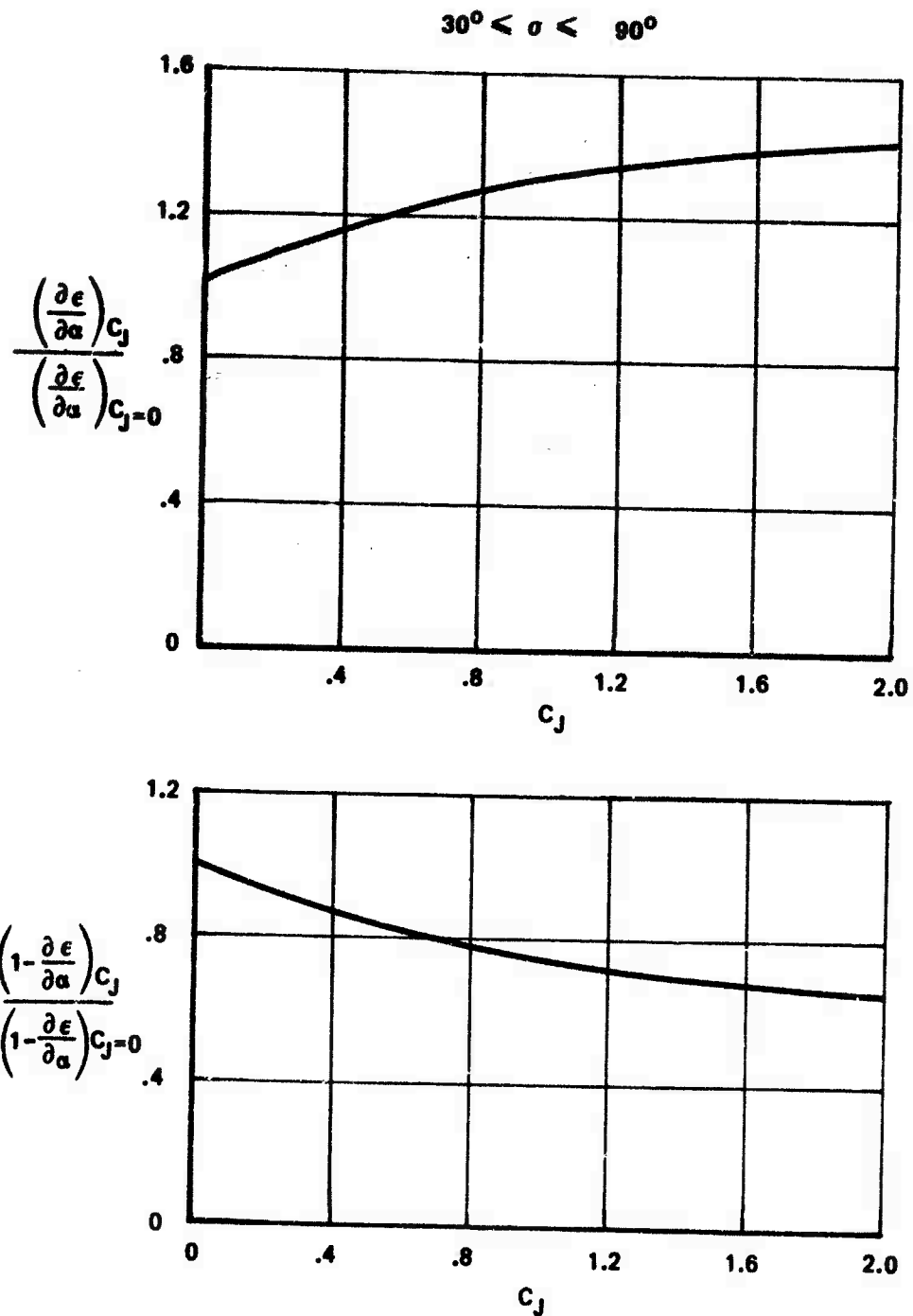


Figure 58 : Effect Of Vectored Thrust On Downwash



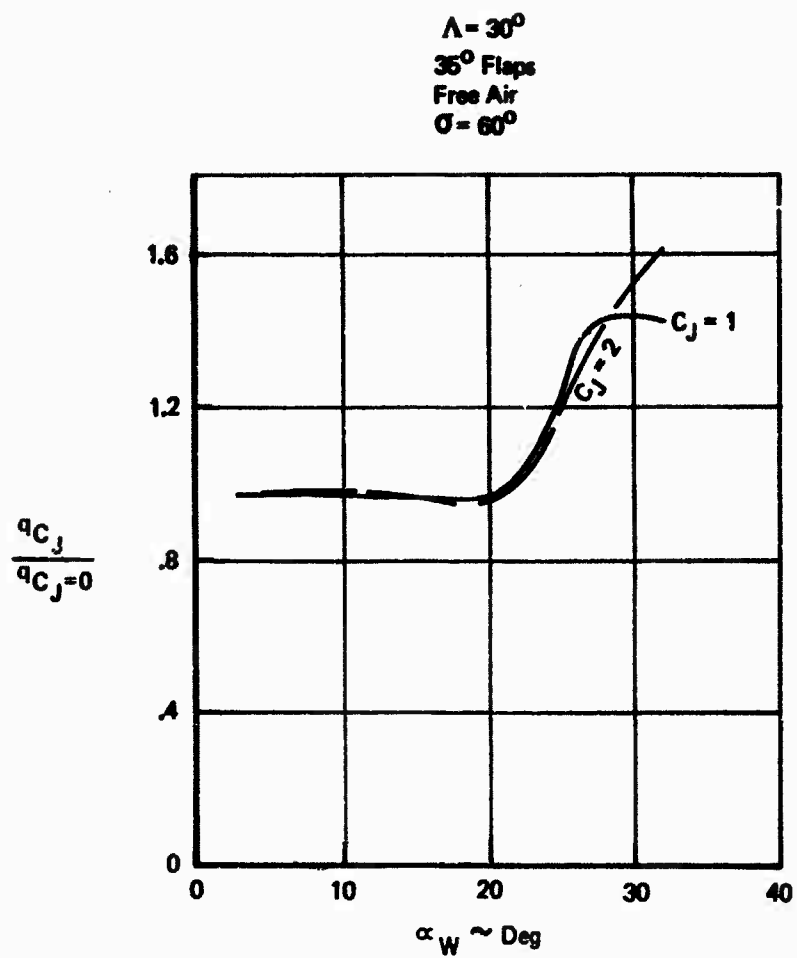


Figure 59 : Effect Of Vectored Thrust On Horizontal Tail Dynamic Pressure

## 3.2.1.2

## Derivatives with Respect to Forward Speed

The speed derivatives  $C_{Z_u}$ ,  $C_{X_u}$ , and  $C_{m_u}$  are a function of both direct thrust and thrust interference. The force and moment equations are:

$$C_Z = -C_{L_{C_J=0}} - \Delta C_{L_{INTERFERENCE}} - C_J \sin(\alpha + \sigma) \quad (3.5)$$

$$C_X = -C_{D_{C_J=0}} - \Delta C_{D_{INTERFERENCE}} + C_J \cos(\alpha + \sigma) \quad (3.6)$$

$$C_m = C_{m_{C_J=0}} + \Delta C_{m_{INTERFERENCE}} + C_J(Z_T \cos \sigma + X_T \sin \sigma) \quad (3.7)$$

Referenced to these equations the speed derivatives are:

$$C_{Z_u} = 2C_J \left[ \frac{\partial(\Delta C_L)}{\partial C_J} \right]_{\alpha=\text{CONST}} \quad (3.8)$$

$$C_{X_u} = -2C_D + 2C_J \left[ \frac{\partial(\Delta C_D)}{\partial C_J} \right]_{\alpha=\text{CONST}} \quad (3.9)$$

$$C_{m_u} = -2C_J(Z_T \cos \sigma + X_T \sin \sigma) - 2C_J \left[ \frac{\partial(\Delta C_m)}{\partial C_J} \right]_{\alpha=\text{CONST}} \quad (3.10)$$

where  $C_D = C_{D_{C_J=0}} + \Delta C_{D_{INTERFERENCE}}$

$X_T$  = distance from c.g. to thrust vector in fraction of MAC,  
positive fwd.

$Z_T$  = distance from c.g. to thrust vector in fraction of MAC,  
positive down.

From the above equations, the thrust interference terms are

$$\Delta C_{zu\_INTERFERENCE} = 2C_J \left[ \frac{\partial(\Delta C_L)}{\partial C_J} \right]_{\alpha=CONST} \quad (3.11)$$

$$\Delta C_{xu\_INTERFERENCE} = 2C_J \left[ \frac{\partial(\Delta C_D)}{\partial C_J} \right]_{\alpha=CONST} \quad (3.12)$$

$$\Delta C_{mu\_INTERFERENCE} = -2C_J \left[ \frac{\partial(\Delta C_m)}{\partial C_J} \right]_{\alpha=CONST} \quad (3.13)$$

The terms  $\left[ \frac{\partial(\Delta C_L)}{\partial C_J} \right]$ ,  $\left[ \frac{\partial(\Delta C_D)}{\partial C_J} \right]$ , and  $\left[ \frac{\partial(\Delta C_m)}{\partial C_J} \right]$

can be calculated from Equations 3.14 through 3.16.

$$\left[ \frac{\partial(\Delta C_L)}{\partial C_J} \right]_{\alpha=CONST} = \frac{.35(C_{L\_INT} + \Delta C_{L\_INT})_{C_J=2}}{\sqrt{C_J}} \quad (3.14)$$

$$\left[ \frac{\partial(\Delta C_D)}{\partial C_J} \right]_{\alpha=CONST} = \frac{.105(C_{L\_INT} + \Delta C_{L\_INT})_{C_J=2}}{\sqrt{C_J}} \quad (3.15)$$

$$\left[ \frac{\partial(\Delta C_m)}{\partial C_J} \right]_{\alpha=CONST} = \frac{-.119(C_{L\_INT} + \Delta C_{L\_INT})_{C_J=2}}{\sqrt{C_J}} \quad (3.16)$$

where  $[C_{L\_INT} + \Delta C_{L\_INT}]_{C_J=2}$  is obtained from Figures 29 and 30

Since this term varies with  $C_J$  by the equation:

$$\Delta C_L = [C_{L\_INT} + \Delta C_{L\_INT}] = [C_{L\_INT} + \Delta C_{L\_INT}]_{C_J=2} \sqrt{\frac{C_J}{2}} \quad (3.17)$$

The term  $\frac{\partial(\Delta C_L)}{\partial C_J}$  is obtained by differentiating with respect to  $C_J$   $\frac{\partial(\Delta C_D)}{\partial C_J}$

is obtained by multiplying  $\frac{\partial C_D}{\partial C_L}$ , based on Figures 30 through 32 by  $\frac{\partial(\Delta C_L)}{\partial C_L}$ .  $\frac{\partial(\Delta C_m)}{\partial C_J}$  is obtained by multiplying  $\frac{\partial C_m}{\partial C_L}$ , based on Figures 33 through 35, by  $\frac{\partial(\Delta C_L)}{\partial C_J}$

### 3.2.1.3 Pitch Rate and Angle of Attack Rate Derivatives

No testing was done to evaluate the effect of vectored thrust on the wing body contribution to the derivatives  $C_{m_q}$ ,  $C_{Z_q}$ ,  $C_{m_{\dot{\alpha}}}$ , and  $C_{Z_{\dot{\alpha}}}$ . However, this is expected to be small, and existing methods to predict the power off wing-body damping should provide sufficient accuracy. The horizontal tail contribution to pitch rate damping derivatives  $C_{m_q}$  and  $C_{Z_q}$  is influenced by engine thrust through the change in dynamic pressure at the tail. Power off  $C_{m_q}$  and  $C_{Z_q}$  should be obtained by existing methods and the tail contribution should be corrected for thrust effects by Equations 3.18 and 3.19.

$$C_{m_{q_H}} = (C_{m_{q_H}})_{C_J=0} \left( \frac{q}{q_{C_J=0}} \right) \quad (3.18)$$

$$C_{Z_{q_H}} = (C_{Z_{q_H}})_{C_J=0} \left( \frac{q}{q_{C_J=0}} \right) \quad (3.19)$$

The horizontal tail contribution to angle of attack rate damping derivatives  $C_{m_{\dot{\alpha}}}$  and  $C_{Z_{\dot{\alpha}}}$  is a function of both the dynamic pressure change and the downwash change due to vectored thrust. These derivatives should be predicted by existing methods, with the tail contribution corrected for thrust effects by:

$$C_{m_{\dot{\alpha}_H}} = (C_{m_{\dot{\alpha}_H}})_{C_J=0} \left( \frac{\frac{\partial \epsilon}{\partial \alpha}}{\left( \frac{\partial \epsilon}{\partial \alpha} \right)_{C_J=0}} \right) \left( \frac{q}{q_{C_J=0}} \right) \quad (3.20)$$

$$C_{Z_{\dot{\alpha}_H}} = (C_{Z_{\dot{\alpha}_H}})_{C_J=0} \left( \frac{\frac{\partial \epsilon}{\partial \alpha}}{\left( \frac{\partial \epsilon}{\partial \alpha} \right)_{C_J=0}} \right) \left( \frac{q}{q_{C_J=0}} \right) \quad (3.21)$$

### 3.2.1.4 Control Derivatives

The tail control derivatives  $C_{m\delta_E}$ ,  $C_{x\delta_E}$ , and  $C_{z\delta_E}$  are also a function of the dynamic pressure at the tail. Power off tail effectiveness should be predicted by existing methods such as DATCOM, and a power correction applied by Equations 3.22 through 3.24.

$$C_{m\delta_E} = (C_{m\delta_E})_{C_T=0} \left( \frac{q}{q_{C_T=0}} \right) \quad (3.22)$$

$$C_{x\delta_E} = (C_{x\delta_E})_{C_T=0} \left( \frac{q}{q_{C_T=0}} \right) \quad (3.23)$$

$$C_{z\delta_E} = (C_{z\delta_E})_{C_T=0} \left( \frac{q}{q_{C_T=0}} \right) \quad (3.24)$$

### 3.2.2 Lateral-Directional Stability Derivatives

This section presents a simple empirical method of predicting aerodynamic interference effects, due to vectored thrust, on lateral-directional stability derivatives. Correction factors are all based on wind tunnel data. The wind tunnel data are presented in Reference 5.

No large error would result in the tail-off sideslip derivatives if thrust effects were ignored. The data indicate that it is only in extreme conditions, like 90° thrust deflection in ground effect, that the thrust effects are large on the more important derivatives  $C_{n\beta}$  and  $C_{l\beta}$ . This would probably only be a transient condition and for preliminary design purposes might be ignored.

#### 3.2.2.1 Sideslip Derivatives

Thrust effect on sideslip derivatives can be accounted for by using the following five correction factors:

$$\left( \frac{C_Y}{C_Y} \right)_{C_T=0}^{C_T}, \left( \frac{C_{n\beta}}{C_{n\beta}} \right)_{C_T=0}^{C_T}, \left( \frac{C_{l\beta}}{C_{l\beta}} \right)_{C_T=0}^{C_T}, \frac{\partial \sigma}{\partial \beta} / \frac{\partial \sigma}{\partial \beta}_{C_T=0}, \frac{q_v}{q_{C_T=0}}$$

where

$\beta$  = sideslip angle

$C_Y$  = side force coefficient

$C_n$  = yawing moment coefficient

- $C_l$  = rolling moment coefficient  
 $q$  = dynamic pressure  
 $\sigma$  = sidewash angle

subscripts

TO vertical tail, denotes tail-off

$C_J=0$  denotes thrust is zero

Values for these terms are presented in Figures 60 and 61. Side-slip derivatives are then computed using Equations 3.25 through 3.27.

$$C_{Y\beta} = \left( \frac{C_{Y\beta}}{C_{Y\beta C_J=0}} \right) C_{Y\beta TO C_J=0} - a_v \frac{S_v}{S} \left( 1 - \frac{\frac{\partial \sigma}{\partial \beta}}{\frac{\partial \sigma}{\partial \beta C_J=0}} \frac{\frac{\partial \sigma}{\partial \beta C_J=0}}{\frac{\partial \sigma}{\partial \beta C_J=0}} \right) \eta_v \frac{z_v}{z_{v C_J=0}} \quad (3.25)$$

$$C_{n\beta} = C_{n\beta TO C_J=0} + a_v \frac{l_v S_v}{b S} \left( 1 - \frac{\frac{\partial \sigma}{\partial \beta}}{\frac{\partial \sigma}{\partial \beta C_J=0}} \frac{\frac{\partial \sigma}{\partial \beta C_J=0}}{\frac{\partial \sigma}{\partial \beta C_J=0}} \right) \eta_v \frac{z_v}{z_{v C_J=0}} \quad (3.26)$$

$$C_{l\beta} = \left( \frac{C_{l\beta}}{C_{l\beta C_J=0}} \right) C_{l\beta C_J=0} + a_v \frac{z_v S_v}{b S} \left( 1 - \frac{\frac{\partial \sigma}{\partial \beta}}{\frac{\partial \sigma}{\partial \beta C_J=0}} \frac{\frac{\partial \sigma}{\partial \beta C_J=0}}{\frac{\partial \sigma}{\partial \beta C_J=0}} \right) \eta_v \frac{z_v}{z_{v C_J=0}} \quad (3.27)$$

where

- $S$  = wing area  
 $b$  = wing span  
 $a$  = vertical tail lift curve slope  
 $S_v$  = vertical tail area  
 $l_v$  = distance from c.g. aft to vertical tail a.c.  
 $z_v$  = distance from c.g. down to vertical tail a.c.  
 $\eta_v$  = ratio of dynamic pressure at the tail to free stream dynamic pressure at  $C_J = 0$

Nacelles at 27%  
and 43.5% Semi-Span

FLAPS DOWN

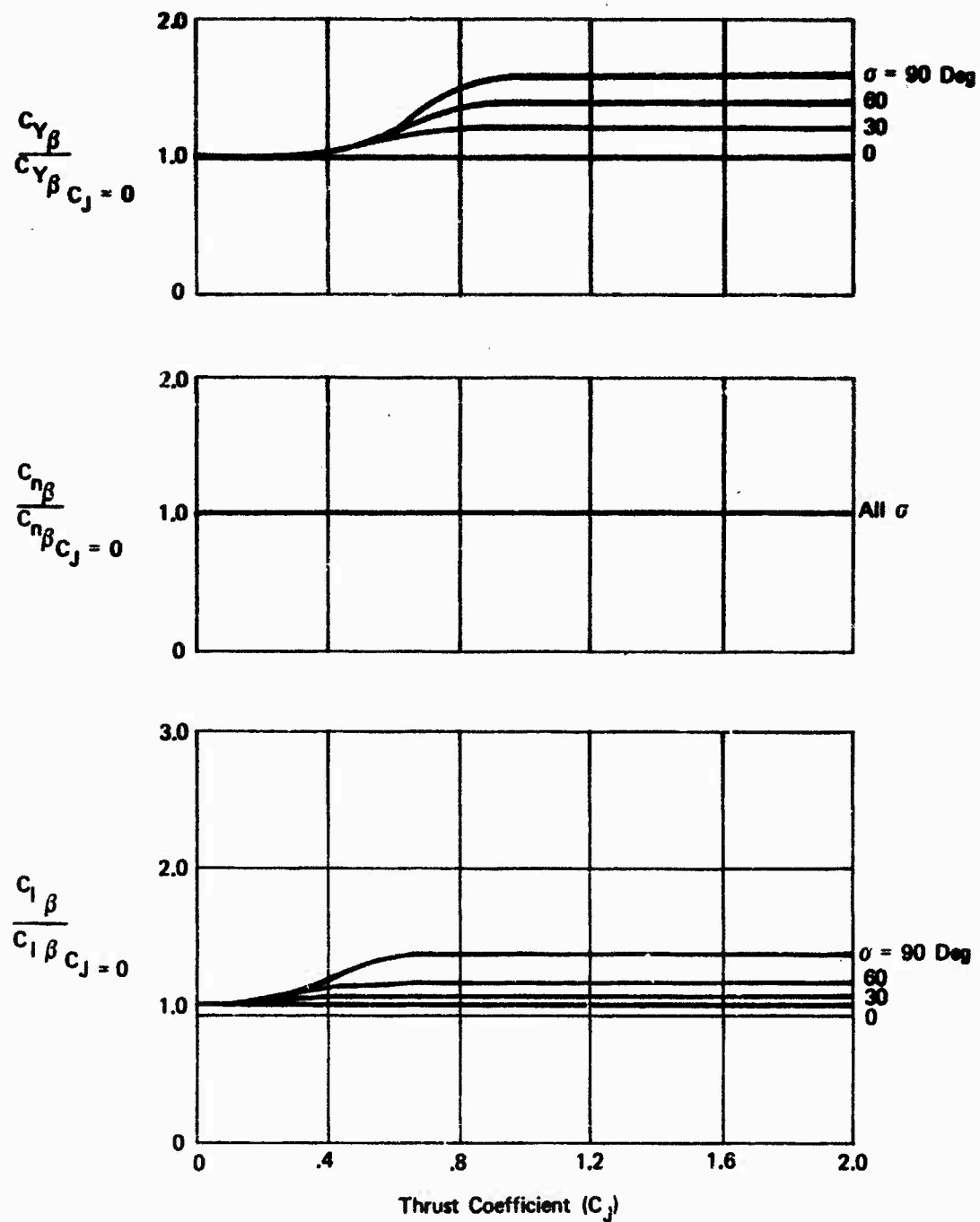


Figure 60 Vectored Thrust Effect Factors for Sideslip Derivatives Tail Off

# FLAPS DOWN

Nacelles at 27%  
and 43.5% Semi-Span

In Ground Effect,  $h/b = .21$

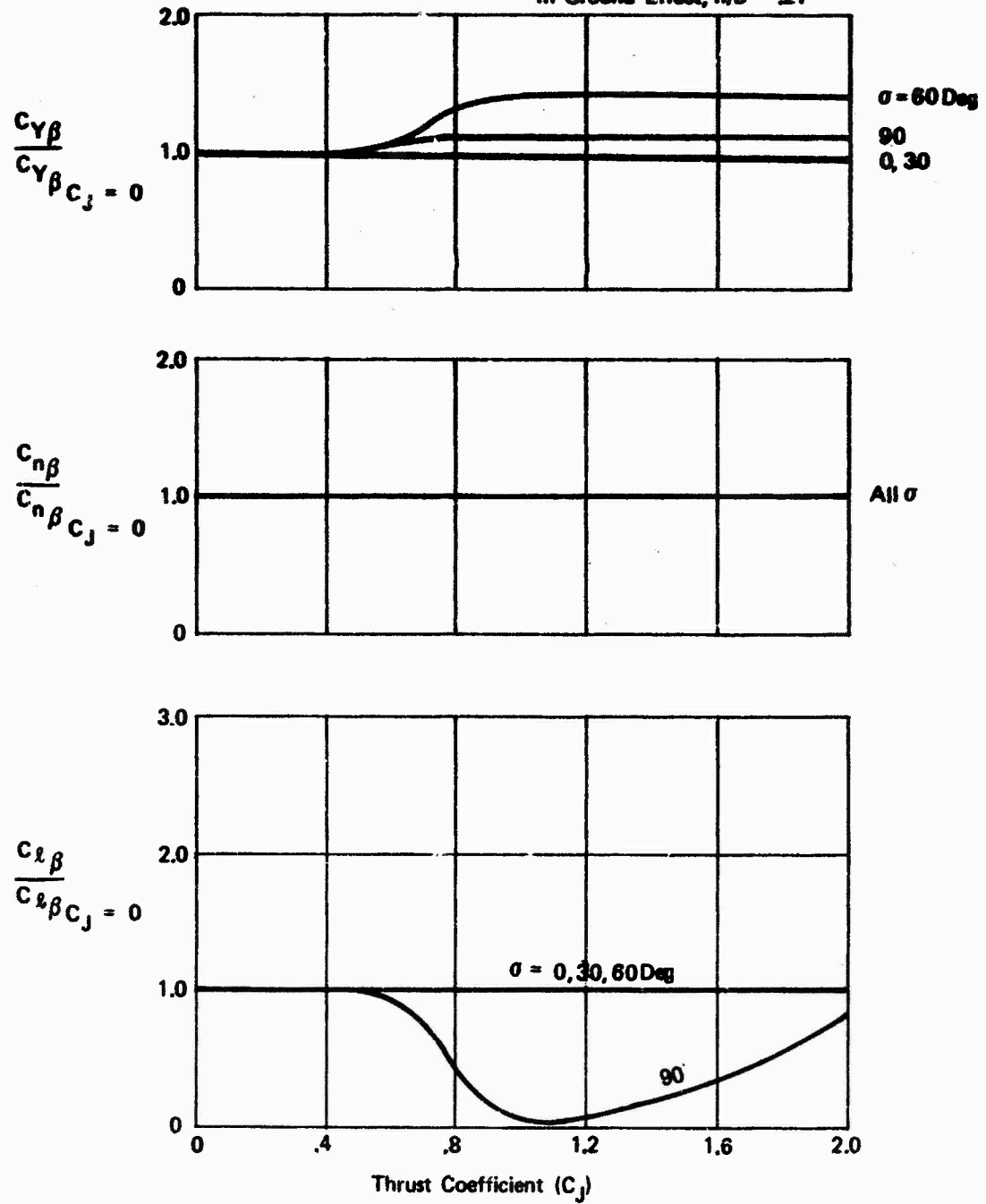


Figure 61 Vectored Thrust Factors for Sideslip Derivatives in Ground Effect, Tail Off



The biggest correction factor is for the sideforce derivative which is the least important of the three. See Section 3.1, Stability Derivative Sensitivity Study. The more important yawing moment derivative has no correction due to thrust. The other important derivative, rolling moment due to sideslip, has a correction factor of only 1.17 up to a thrust deflection of 60 degrees. It can be seen from the derivative sensitivity study, Section 3.1, that these corrections are not large.

Sidewash data are shown in Figure 62 . For this particular model, thrust had no influence so  $\frac{\partial \sigma}{\partial \beta} / \frac{\partial \sigma}{\partial \beta}_{C_T=0} = 1$ . However, it may be too much of a generalization to extrapolate this result to other configurations so the term is left in the equations. In the absence of additional data, assume no vectored thrust effect on sidewash.

An attempt to measure power affects on dynamic pressure at the vertical tail failed due to wind tunnel instrumentation problems. It is suggested that the values given in Figure 59 , for the horizontal tail, be used until more applicable data are available.

Table IV and Figure 63 show typical errors resulting from the application of the correction factors, presented in Figures 60 and 61 , to the power-off, tail-off data. While the percent error is sometimes large, the increment is usually small. These errors, when viewed in conjunction with the derivative sensitivity study presented in Section 3, are seen to be small.

#### 3.2.2.2 Roll Rate and Yaw Rate Derivatives

No dynamic testing was done in the wind tunnel upon which to base any corrections. Although the sideslip data obtained during the wind tunnel test program is not directly applicable to the yaw or roll rate case, it does provide a little insight upon which to base an opinion that the effect is small.

The quality of the roll damping derivative,  $C_{l_p}$ , can be improved by multiplying it by the lift curve slope correction factor, as given in Equation 3.28.

$$C_{l_p} = \left[ 1 + \left( \frac{\Delta C_{L_\alpha}}{C_T} \right) \frac{C_T}{C_{L_\alpha}_{C_T=0}} \right] C_{l_p}_{C_T=0} \quad (3.28)$$

This correction is applicable because the roll damping is proportional to the local lift curve slope which should be proportional to the 3-dimensional lift curve slope. The tail contribution should be ignored when computing  $C_{l_p}$  unless data on sidewash due to roll rate are available.

The vertical tail contribution to the damping derivatives can be improved by applying the dynamic pressure ratio factor, Equations 3.29 through 3.33.

Symbol	$\alpha$ (Deg)	$C_L$	$\sigma$ (Deg)	$h/b$	Run	Engine-Out
○	8.0	5/5/0/5	30	$\infty$	138	Right Inboard
△	8.0	5/5/5/0	30	$\infty$	139	Right Outboard
□	8.0	2.0	30	$\infty$	140	None
◇	8.0	2.0	30	.242	141	None
○	0	5/5/5/0	30	.242	142	Right Outboard
△	8.0	5/5/5/0	30	.242	142	Right Outboard
△	8.0	5/5/0/5	30	.242	143	Right Inboard
D	8.0	0	60	.242	144	—
△	8.0	2.0	60	.242	145	None
◇	6.0	2.0	30	.242	147	None

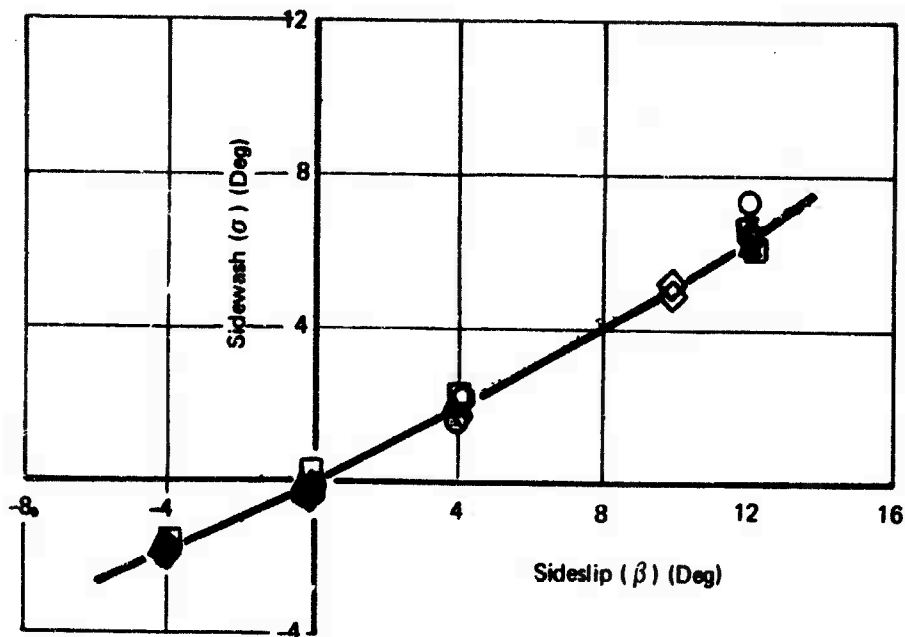


Figure 62: Sidewash at the Vertical Tail

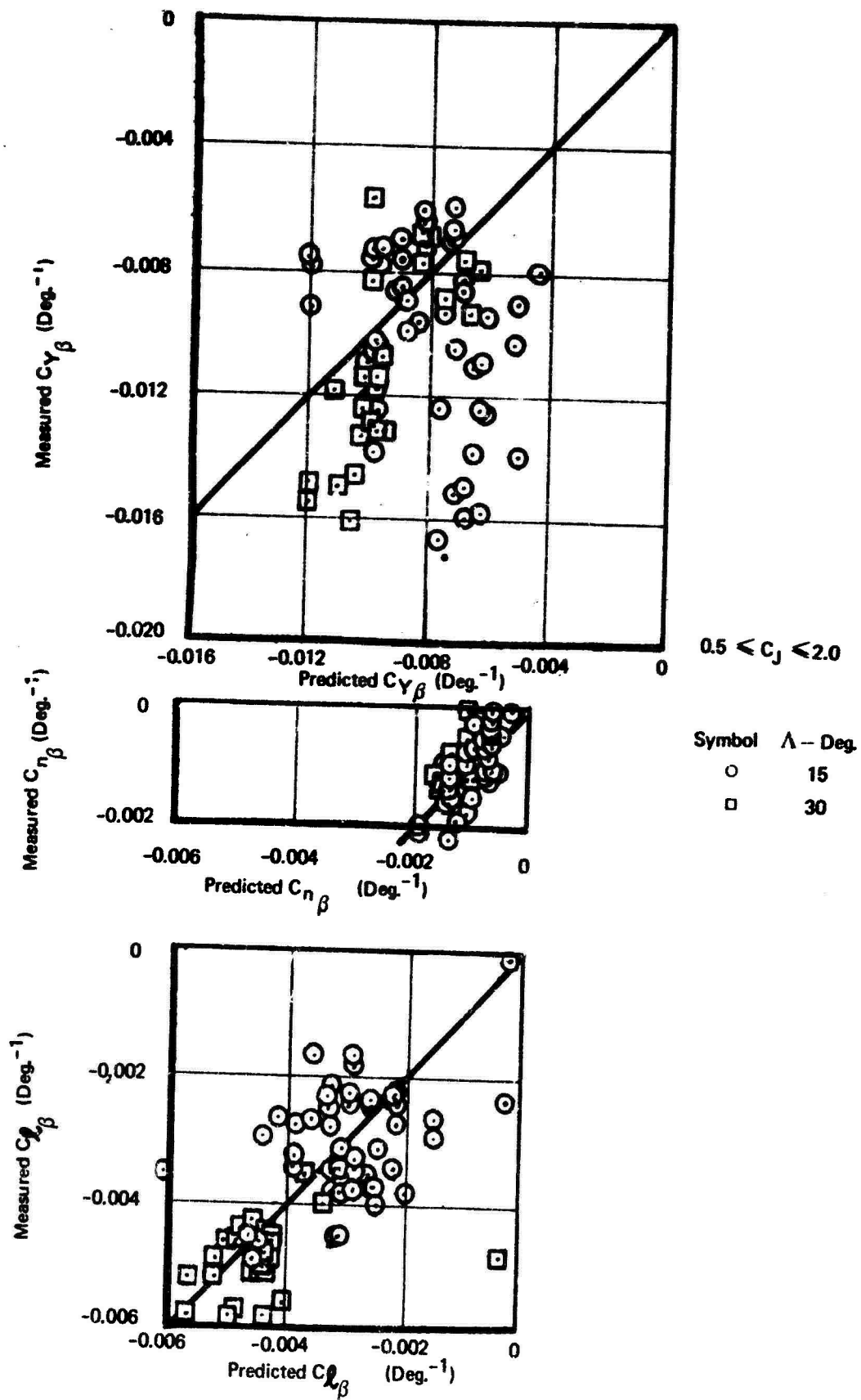


Figure 63 : Powered Sideslip Derivatives Error

TABLE IV

## TEST-PREDICTION COMPARISON, SIDESLIP DERIVATIVES

TAIL-OFF

 $\Lambda = 15 \text{ DEG}$ 

NACELLES: AT .35C

27 AND  $43.5\frac{b}{2}$ 

$\delta_f$ -DEG	$\sigma$ -DEG	h/b	$\alpha$ -DEG	$C_J$	TEST				PREDICT				ERROR $C_{N\beta}$	ERROR $C_{l\beta}$
					$C_{Y\beta}$ -DEG $^{-1}$	$C_{N\beta}$ -DEG $^{-1}$	$C_{l\beta}$ -DEG $^{-1}$	$C_{Y\beta}$ -DEG $^{-1}$	$C_{N\beta}$ -DEG $^{-1}$	$C_{l\beta}$ -DEG $^{-1}$	ERROR $C_{Y\beta}$	ERROR $C_{N\beta}$		
35	30	$\infty$	8	0	-.0075	-.0009	-.0029	-.0075	-.0009	-.0029	0	0	0	0
	↓			1.0	-.0077	-.0011	-.00275	-.0090	↓	-.0031	-.0013	.0002	-.00035	
	60			2.0	-.0070	-.0009	-.0021	-.0090	↓	-.0031	-.0020	0	-.0010	
				0	-.0070	-.00075	-.0021	-.0070	↓	-.0021	0	0	0	
				.5	-.0094	-.0008	-.0023	-.00749	↓	-.00244	.00191	-.00015	-.00014	
				1.0	-.0107	-.0008	-.0024	-.0098	↓	-.00244	.0009	-.00015	-.00004	
				2.0	-.0104	-.0009	-.0023	-.0098	↓	-.00244	.0006	-.00005	-.00014	
				0	-.0042	-.0010	-.0020	-.0042	↓	-.0020	0	0	0	
		.208		.5	-.0081	-.0010	-.0022	-.00437	↓	-.0020	.00373	0	.0002	
				1.0	-.0095	-.00095	-.0024	-.00609	↓	-.0020	.00341	-.00005	.0004	
				2.0	-.0127	-.00085	-.0027	-.00609	↓	-.0020	.00661	-.00015	.0007	
				0	-.0061	-.00075	-.0017	-.0061	↓	-.0017	0	0	0	
	90	$\infty$		1.0	-.0119	-.0007	-.0031	-.00976	↓	-.0023	.00214	-.00005	.0008	
				2.0	-.0126	-.00085	-.0040	-.00976	↓	-.0023	.00284	.0001	.0017	
		.21		0	-.0060	-.0010	-.0023	-.0060	↓	-.0023	0	0	0	
				1.0	-.0087	-.0011	0	-.0069	↓	-.0012	.0018	.0001	-.00012	
				2.0	-.0083	0	-.0038	-.0069	↓	-.00309	.0014	-.0010	-.00076	
	60	$\infty$	4	0	-.0072	-.00095	-.0017	-.0072	↓	-.0017	0	0	0	
				8	-.0070	-.0009	-.0020	-.0070	↓	-.0020	0	0	0	
			12	2.0	-.0071	-.0008	-.0020	-.0071	↓	-.0020	0	0	0	
				4	-.011	-.0005	-.0037	-.01008	↓	-.00238	.00092	-.00045	.00132	
			8	↓	-.0108	-.0009	-.0022	-.0098	↓	-.0028	.0010	0	-.0006	
			12	0	-.0123	-.0008	-.0024	-.00994	↓	-.0028	.00225	0	-.0004	
				8	-.0076	-.0014	-.0019	-.0076	↓	-.0019	0	0	0	
	30			2.0	-.0087	-.0012	-.0023	-.00912	↓	-.00203	-.00042	-.0002	.00027	
				0	-.0098	-.0015	-.0028	-.0098	↓	-.0028	0	0	0	
		.21		2.0	-.0079	-.0011	-.0033	-.0098	↓	-.0028	-.0019	-.0004	.0005	
			4	0	-.0061	-.0014	-.0017	-.0061	↓	-.0017	0	0	0	
		$\infty$		8	-.0075	-.0015	-.0019	-.0075	↓	-.0015	0	0	0	
				12	-.0070	-.00135	-.0023	-.0070	↓	-.0023	0	0	0	
				4	-.0071	-.0013	-.0028	-.00732	↓	-.0014	-.00022	-.0001	.00098	
			8	2.0	-.0086	-.0011	-.0024	-.0090	↓	-.0015	-.0004	-.0004	.00037	
				12	-.0097	-.0007	-.0025	-.0084	↓	-.00135	-.0013	-.00065	.00004	

TABLE IV

## TEST-PREDICTION COMPARISON, SIDESLIP DERIVATIVES (Continued)

TAIL-OFF  
 $\Lambda = 15 \text{ DEG.}$   
 NACELLES AT .35C

NACELLE LOC. $-y/\frac{b}{2}$	TEST				PREDICT				ERROR $C_N$	ERROR $C_{N\beta}$	ERROR $C_{N\beta}$
	$\delta_f$ -DEG	$\sigma$ -DEG	h/b	$\alpha$ -DEG	$C_j$	$C_{Y\beta}$ -DEG $^{-1}$	$C_{N\beta}$ -DEG $^{-1}$	$C_{L\beta}$ -DEG $^{-1}$	$C_{Y\beta}$ -DEG $^{-1}$	$C_{N\beta}$ -DEG $^{-1}$	$C_{L\beta}$ -DEG $^{-1}$
.27	20	30	$\infty$	8.0	0	-.0042	-.0013	-.0013	-.0042	-.0013	-.0013
					1.0	-.0091	-.0011	-.0013	-.00504	-.0013	-.00139
					2.0	-.0140	-.0009	-.0013	-.00504	-.0013	-.00139
			.21		0	-.0068	-.0010	-.0010	-.0068	-.0010	-.00295
					1.0	-.015	-.0009	-.0010	-.0068	-.0010	-.00295
					2.0	-.015	-.0007	-.0010	-.0068	-.0010	-.00295
.435/.60			$\infty$		0	-.0060	-.0018	-.0018	-.0060	-.0018	-.00295
					1.0	-.0067	-.0019	-.0018	-.0072	-.0018	-.00316
					2.0	-.0070	-.0020	-.0018	-.0072	-.0018	-.00316
.27	35		.219		0	-.0063	-.0006	-.0006	-.0063	-.0006	-.0029
					1.0	-.011	-.0004	-.0006	-.0063	-.0006	-.0029
					2.0	-.0158	-.0003	-.0006	-.0063	-.0006	-.0029
			$\infty$		0	-.006	-.0009	-.0009	-.0060	-.0009	-.0032
					1.0	-.016	-.0006	-.0009	-.0072	-.0009	-.00342
					2.0	-.0152	-.0002	-.0009	-.0072	-.0009	-.00342
					0	-.0047	-.0007	-.0007	-.0047	-.0007	-.0032
					1.0	-.0113	-.0005	-.0007	-.00658	-.0007	-.00374
					2.0	-.0139	-.0006	-.0007	-.00658	-.0007	-.00374
.435					0	-.0059	-.0007	-.0007	-.0059	-.0007	-.0023
					1.0	-.0061	-.0010	-.0007	-.00826	-.0007	-.00269
					2.0	-.0065	-.00095	-.0007	-.00826	-.0007	-.00269
.435/.60					0	-.0071	-.0013	-.0013	-.0094	-.0013	-.00175
					1.0	-.0077	-.00155	-.0013	-.0094	-.0013	-.00205
					2.0	-.0074	-.0022	-.0013	-.0094	-.0013	-.00205
.27			.219		0	-.0068	-.0003	-.0003	-.0068	-.0003	-.0037
					1.0	-.0103	-.0004	-.0003	-.00986	-.0003	-.0037
					2.0	-.0139	-.0006	-.0003	-.00986	-.0003	-.0037
			$\infty$		0	-.0048	-.0006	-.0006	-.0048	-.0006	-.0031
					.5	-.0104	-.0005	-.0006	-.00514	-.0006	-.00397
					1.0	-.0125	-.0006	-.0006	-.00768	-.0006	-.00425
					2.0	-.0167	-.0010	-.0006	-.00768	-.0006	-.00425
					0	-.0055	-.0006	-.0006	-.0055	-.0006	-.0022
					1.0	-.0090	-.0002	-.0006	-.0088	-.0006	-.00301
					2.0	-.0100	0	-.0006	-.0088	-.0006	-.00301
.435					0	-.0075	-.0013	-.0013	-.0075	-.0013	-.0020
					1.0	-.0092	-.0013	-.0013	-.0120	-.0013	-.00274
					2.0	-.0080	-.0014	-.0013	-.0120	-.0013	-.00274
			.21		0	-.0055	-.0003	-.0003	-.0055	-.0003	-.0037
					1.0	-.0125	0	-.0003	-.00633	-.0003	-.0019
					2.0	-.0080	-.0009	-.0009	-.00633	-.0009	-.00296
.435/.60			$\infty$		0	-.0060	-.0014	-.0012	-.0060	-.0012	-.00439
					2.0	-.0060	-.0014	-.0012	-.0072	-.0012	-.0038
					0	-.0069	-.0012	-.0012	-.0069	-.0012	-.0041
					2.0	-.0073	-.0018	-.0012	-.00966	-.0012	-.0041
					0	-.0076	-.0013	-.0013	-.0076	-.0013	-.0043
					2.0	-.0076	-.0013	-.0013	-.01216	-.0013	-.00590
					0	-.0046	-.0002	-.0002	-.0046	-.0002	-.0002
					1.0	-.0046	-.0002	-.0002	-.0046	-.0002	-.0002
					2.0	-.0046	-.0002	-.0002	-.0046	-.0002	-.0002
					0	-.0046	-.0002	-.0002	-.0046	-.0002	-.0002
					1.0	-.0046	-.0002	-.0002	-.0046	-.0002	-.0002
					2.0	-.0046	-.0002	-.0002	-.0046	-.0002	-.0002
					0	-.0046	-.0002	-.0002	-.0046	-.0002	-.0002
					1.0	-.0046	-.0002	-.0002	-.0046	-.0002	-.0002
					2.0	-.0046	-.0002	-.0002	-.0046	-.0002	-.0002
					0	-.0046	-.0002	-.0002	-.0046	-.0002	-.0002
					1.0	-.0046	-.0002	-.0002	-.0046	-.0002	-.0002
					2.0	-.0046	-.0002	-.0002	-.0046	-.0002	-.0002
					0	-.0046	-.0002	-.0002	-.0046	-.0002	-.0002
					1.0	-.0046	-.0002	-.0002	-.0046	-.0002	-.0002
					2.0	-.0046	-.0002	-.0002	-.0046	-.0002	-.0002
					0	-.0046	-.0002	-.0002	-.0046	-.0002	-.0002
					1.0	-.0046	-.0002	-.0002	-.0046	-.0002	-.0002
					2.0	-.0046	-.0002	-.0002	-.0046	-.0002	-.0002
					0	-.0046	-.0002	-.0002	-.0046	-.0002	-.0002
					1.0	-.0046	-.0002	-.0002	-.0046	-.0002	-.0002
					2.0	-.0046	-.0002	-.0002	-.0046	-.0002	-.0002
					0	-.0046	-.0002	-.0002	-.0046	-.0002	-.0002
					1.0	-.0046	-.0002	-.0002	-.0046	-.0002	-.0002
					2.0	-.0046	-.0002	-.0002	-.0046	-.0002	-.0002
					0	-.0046	-.0002	-.0002	-.0046	-.0002	-.0002
					1.0	-.0046	-.0002	-.0002	-.0046	-.0002	-.0002
					2.0	-.0046	-.0002	-.0002	-.0046	-.0002	-.0002
					0	-.0046	-.0002	-.0002	-.0046	-.0002	-.0002
					1.0	-.0046	-.0002	-.0002	-.0046	-.0002	-.0002
					2.0	-.0046	-.0002	-.0002	-.0046	-.0002	-.0002
					0	-.0046	-.0002	-.0002	-.0046	-.0002	-.0002
					1.0	-.0046	-.0002	-.0002	-.0046	-.0002	-.0002
					2.0	-.0046	-.0002	-.0002	-.0046	-.0002	-.0002
					0	-.0046	-.0002	-.0002	-.0046	-.0002	-.0002
					1.0	-.0046	-.0002	-.0002	-.0046	-.0002	-.0002
					2.0	-.0046	-.0002	-.0002	-.0046	-.0002	-.0002
					0	-.0046	-.0002	-.0002	-.0046	-.0002	-.0002
					1.0	-.0046	-.0002	-.0002	-.0046	-.0002	-.0002
					2.0	-.0046	-.0002	-.0002	-.0046	-.0002	-.0002
					0	-.0046	-.0002	-.0002	-.0046	-.0002	-.0002
					1.0	-.0046	-.0002	-.0002	-.0046	-.0002	-.0002
					2.0	-.0046	-.0002	-.0002	-.0046	-.0002	-.0002
					0	-.0046	-.0002	-.0002	-.0046	-.0002	-.0002
					1.0	-.0046	-.0002	-.0002	-.0046	-.0002	-.0002
					2.0	-.0046	-.0002	-.0002	-.0046	-.0002	-.0002
					0	-.0046	-.0002	-.0002	-.0046	-.0002	-.0002
					1.0	-.0046	-.0002	-.0002	-.0046	-.0002	-.0002
					2.0	-.0046	-.0002	-.0002	-.0046	-.0002	-.0002
					0	-.0046	-.0002	-.0002	-.0046	-.0002	-.0002
					1.0	-.0046	-.0002	-.0002	-.0046	-.0002	-.0002
					2.0	-.0046	-.0002	-.0002	-.0046	-.0002	-.0002
					0	-.0046	-.0002	-.0002	-.0046	-.0002	-.0002
					1.0	-.0046	-.0002	-.0002	-.0046	-.0002	-.0002
					2.0	-.0046	-.0002	-.0002	-.0046	-.0002	-.0002
					0	-.0046	-.0002	-.0002	-.0046	-.0002	-.0002
					1.0	-.0046	-.0002	-.0002	-.0046	-.0002	-.0002
					2.0	-.0046	-.0002	-.0002	-.0046	-.0002	-.0002
					0	-.0046	-.0002	-.0002	-.0046	-.0002	-.0002
					1.0	-.0046	-.0002	-.0002	-.0046	-.0002	-.0002
					2.0	-.0046	-.0002	-.0002	-.0046	-.0002	-.0002
					0	-.0046	-.0002	-.0002	-.0046	-.0002	-.0002
					1.0	-.0046	-.0002	-.0002	-.0046	-.0002	-.0002
					2.0	-.0046	-.0002	-.0002	-.0046	-.0002	-.0002
					0	-.0046	-.0002	-.0002	-.0046	-.0002	-.0002
					1.0	-.0046	-.0002	-.0002	-.0046	-.0002	-.0002
					2.0	-.0046	-.0002	-.0002	-.0046	-.0002	-.0002
					0	-.0046	-.0002	-.0002	-.0046	-.0002	-.0002
					1.0	-.0046	-.0002	-.0002	-.0046	-.0002	-.0002
					2.0	-.0046	-.0002	-.0002	-.0046	-.0002	-.0002
					0	-.0046	-.0002	-.0002	-.0046	-.0002	-.0002
					1.0	-.0046	-.0002	-.0002	-.0046	-.0002	-.0002
					2.0	-.0046	-.0002	-.0002	-.0046	-.0002	-.0002
					0	-.0046	-.0002	-.0002	-.0046	-.0002	-.0002
					1.0	-.0046	-.0002	-.0002	-.0046	-.0002	-.0002
					2.0	-.0046	-.0002	-.0002	-.0046	-.0002	-.0002
					0	-.0046	-.0002	-.0002	-.0046	-.0002	-.0002
					1.0	-.0046	-.0002	-.0002	-.0046	-.0002	-.0002
					2.0	-.0046	-.0002	-.0002	-.0046	-.0002	-.0002
					0	-.0046	-.0002	-.0002	-.0046	-.0002	-.0002
</											

TAIL-OFF

 $\Lambda = 30 \text{ DEG}$   
 NAGELLES AT:

 $.35C$   
 27 AND  $43.5\% \frac{b}{2}$ 

 TABLE IV  
 TEST-PREDICTION COMPARISON, SIDESLIP DERIVATIVES (Continued)

$\delta_f$ -DEG	$\sigma$ -DEG	h/b	$\alpha$ -DEG	$C_J$	TEST		PREDICT					ERROR $C_{N\beta}$	ERROR $C_{Y\beta}$	ERROR $C_{N\beta}$	ERROR $C_{Y\beta}$
					$C_Y$ -DEG $^{-1}$	$C_{N\beta}$ -DEG $^{-1}$	$C_{L\beta}$ -DEG $^{-1}$	$C_{Y\beta}$ -DEG $^{-1}$	$C_{N\beta}$ -DEG $^{-1}$	$C_{L\beta}$ -DEG $^{-1}$	$C_{Y\beta}$ -DEG $^{-1}$				
25	30	$\infty$	8	0	-.0083	-.00085	-.0038	-.0083	-.00085	-.0038	0	0	0	0	0
	60	$\infty$		1.0	-.0057	-.0010	-.0046	-.00995	$\downarrow$	-.00406	-.00425	.00015	.00015	.00015	.00054
		$\infty$		2.0	-.0084	-.0010	-.0045	-.00995	$\downarrow$	-.00406	-.00155	.00015	.00015	.00015	.00044
		.242		0	-.0070	-.0012	-.0036	-.0070	-.0012	-.0036	0	0	0	0	0
		$\infty$		.5	-.0089	-.0011	-.0050	-.0075	$\downarrow$	-.00417	.0014	-.0001	-.0001	-.0001	.00083
		$\infty$		1.0	-.0115	-.00085	-.0058	-.0098	$\downarrow$	-.00417	.0017	-.00035	-.00035	-.00035	.00163
		$\infty$		2.0	-.0132	-.00090	-.0048	-.0098	$\downarrow$	-.00417	.0034	-.00030	-.00030	-.00030	.00063
		.242		0	-.0066	-.0010	-.0041	-.0066	-.0010	-.0041	0	0	0	0	0
		$\infty$		.5	-.0077	-.0012	-.0049	-.00686	$\downarrow$	$\downarrow$	.00084	.0002	.0002	.0002	.0008
		$\infty$		1.0	-.010	-.0017	-.0045	-.00957	$\downarrow$	$\downarrow$	.00043	.0007	.0007	.0007	.0004
		$\infty$		2.0	-.0132	-.0011	-.0051	-.00957	$\downarrow$	$\downarrow$	.00363	.0001	.0001	.0001	.0010
		$\infty$		0	-.0060	-.0012	-.0040	-.0060	-.0012	-.0040	0	0	0	0	0
		.242		1.0	-.0132	-.0010	-.0052	-.0096	$\downarrow$	-.00544	.0036	-.0002	-.0002	-.0002	-.00024
		$\infty$		2.0	-.0108	-.0009	-.0058	-.0096	$\downarrow$	-.00544	.0012	-.0003	-.0003	-.0003	.00036
		$\infty$		0	-.0072	-.0007	-.0044	-.0072	-.0007	-.0044	0	0	0	0	0
		$\infty$		1.0	-.0078	-.0011	-.0048	-.00828	$\downarrow$	-.00022	-.00048	.0004	.0004	.0004	.00458
		$\infty$		2.0	-.0068	-.00115	-.0035	-.00828	$\downarrow$	-.00352	-.00148	.00045	.00045	.00045	-.00002
		$\infty$		0	-.0073	-.0012	-.0040	-.0073	-.0012	-.0040	0	0	0	0	0
		$\infty$		.5	-.0070	-.0013	-.0036	-.0070	-.0013	-.0036	0	0	0	0	0
		$\infty$		1.0	-.0086	-.0010	-.0042	-.0086	-.0010	-.0042	0	0	0	0	0
		$\infty$		2.0	-.0115	-.0008	-.0057	-.0102	-.0012	-.00464	.0013	-.0004	-.0004	-.0004	.00106
		$\infty$		0	-.0130	-.0008	-.0050	-.0098	-.0013	-.00418	.0032	-.0005	-.0005	-.0005	.00082
		$\infty$		.5	-.0148	-.0007	-.0046	-.01205	-.0010	-.00487	.00275	-.0003	-.0003	-.0003	-.00027
		$\infty$		1.0	-.0056	-.0013	-.0032	-.00663	-.0013	-.0032	0	0	0	0	0
		$\infty$		2.0	-.0094	-.0008	-.0040	-.00663	-.0013	-.00342	.00277	-.0005	-.0005	-.0005	.00058
		$\infty$		0	-.0063	-.0015	-.0042	-.0063	-.0015	-.0042	0	0	0	0	0
		$\infty$		2.0	-.0080	-.0012	-.0048	-.0063	-.0015	-.0042	.0017	-.0003	-.0003	-.0003	.0006
		$\infty$		0	-.0073	-.0014	-.0033	-.0073	-.0014	-.0033	0	0	0	0	0
		$\infty$		.5	-.0075	-.0012	-.0040	-.0075	-.0012	-.0040	0	0	0	0	0
		$\infty$		1.0	-.0076	-.0009	-.0043	-.0076	-.0009	-.0043	0	0	0	0	0
		$\infty$		2.0	-.0125	-.00085	-.0056	-.01022	-.0014	-.00383	.00228	-.00055	-.00055	-.00055	.00177
		.242		0	-.0146	-.0008	-.0046	-.0105	-.0012	-.00464	.0041	-.0004	-.0004	-.0004	-.00004
		$\infty$		.5	-.0161	-.0006	-.0049	-.01064	-.0009	-.00499	.00546	-.0003	-.0003	-.0003	-.00009
		$\infty$		1.0	-.0083	-.0010	-.0050	-.0083	-.0010	-.0050	0	0	0	0	0
		$\infty$		2.0	-.0115	-.0014	-.0052	-.01205	-.0010	-.0050	-.00055	.0004	.0004	.0004	.0002
		$\infty$		0	-.0068	-.0008	-.0041	-.0068	-.0008	-.0041	0	0	0	0	0
		$\infty$		1.0	-.0069	-.0009	-.00425	-.00817	$\downarrow$	-.00439	-.00127	.0001	.0001	.0001	-.00014
		$\infty$		2.0	-.0072	-.0011	-.0047	-.00817	$\downarrow$	-.00439	-.00097	.0003	.0003	.0003	.00031
		.242		0	-.0112	-.0008	-.0043	-.0112	$\downarrow$	-.0043	0	0	0	0	0
		$\infty$		1.0	-.0119	-.0012	-.0051	-.0112	$\downarrow$	-.0043	.00070	.0004	.0004	.0004	.0008
		$\infty$		2.0	-.0070	-.0011	-.0041	-.0070	-.0011	-.0041	0	0	0	0	0
		$\infty$		0	-.0074	-.0009	-.0036	-.0074	-.0009	-.0036	0	0	0	0	0
		$\infty$		.5	-.0079	-.0011	-.0039	-.0079	-.0011	-.0039	0	0	0	0	0
		$\infty$		1.0	-.0118	-.0009	-.0058	-.0098	-.0011	-.00475	.0020	-.0002	-.0002	-.0002	.00105
		$\infty$		2.0	-.0134	-.0009	-.0052	-.01038	-.0009	-.00418	.00302	0	0	0	.00102
		$\infty$		0	-.0150	-.0007	-.0044	-.01108	-.0011	-.00452	.00392	-.0004	-.0004	-.0004	-.00012

$$C_{YrV} = C_{YrV_{C_J=0}} \frac{q}{q_{C_J=0}} \quad (3.29) \quad C_{YpV} = C_{YpV_{C_J=0}} \frac{q}{q_{C_J=0}} \quad (3.32)$$

$$C_{nrV} = C_{nrV_{C_J=0}} \frac{q}{q_{C_J=0}} \quad (3.30) \quad C_{npV} = C_{npV_{C_J=0}} \frac{q}{q_{C_J=0}} \quad (3.33)$$

$$C_{irV} = C_{irV_{C_J=0}} \frac{q}{q_{C_J=0}} \quad (3.31)$$

where

$r$  is the yaw rate angle,  $\frac{Rb}{2V}$

$p$  is the wing tip helix angle,  $\frac{Pb}{2V}$

subscript V denotes vertical tail contribution.

The power effect on sidewash due to roll rate and yaw rate is not accounted for, since there are no data upon which to base a correction.

### 3.2.2.3 Control Derivatives

#### 3.2.2.3.1 Thrust Effect on Rudder Power

The effect of thrust on rudder power is shown in Figure 64. Side force, due to rudder deflection, goes down with thrust at 8 degrees angle of attack. At 20 degrees angle of attack, sideforce increases with thrust.

#### 3.2.2.3.2 Thrust Effect on Aileron Power

With no aileron BLC, thrust has little effect on aileron power, see Figures 65 and 66. However, Figure 67 shows that when the ailerons are blown, the presence of thrust ( $C_J=2.0$ ) increases the rolling moment coefficient by about .01. Figure 65 shows that side-slip can have a strong influence on the effect of thrust on aileron power.

#### 3.2.2.3.3 Thrust Effect on Spoiler Power

Thrust has a strong influence on spoiler effectiveness. This is shown in Figures 68 and 69. Thrust effect is low at zero angle of attack and increases with angle of attack. This is probably because thrust induces more lift for the spoilers to operate on. See  $C_{L\alpha}$  effects on Figure 53.

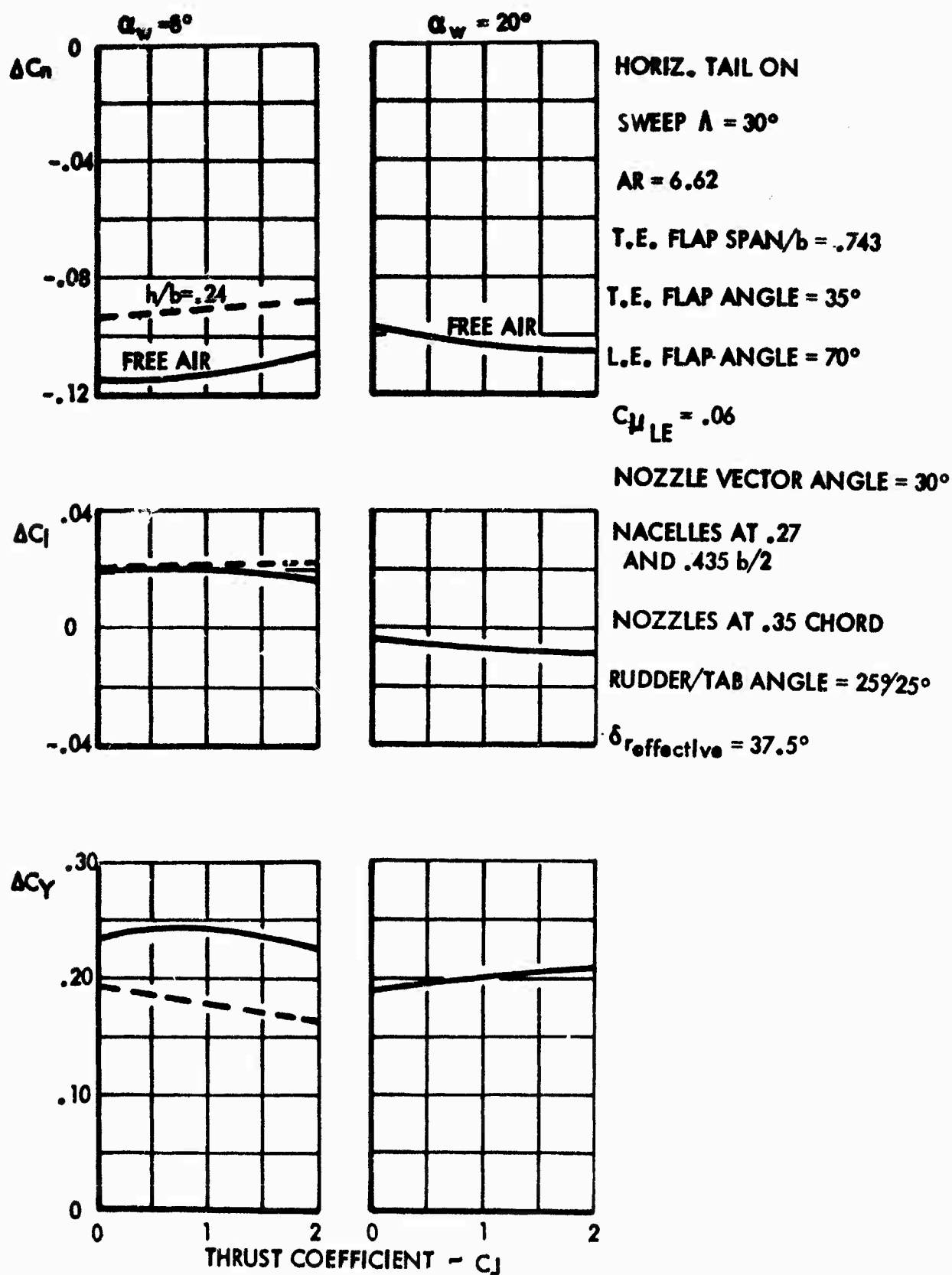
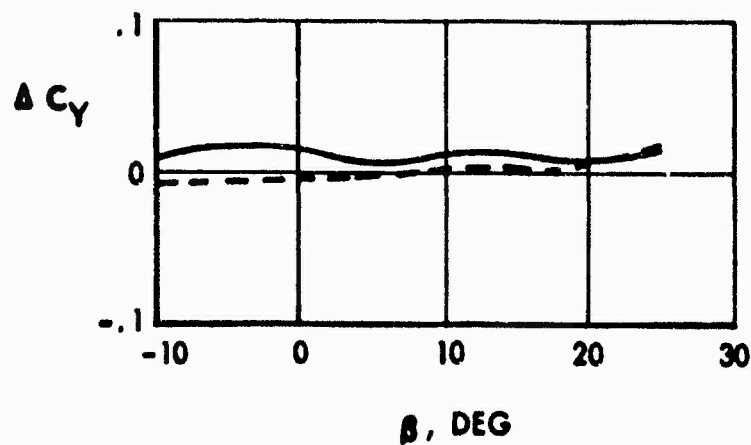
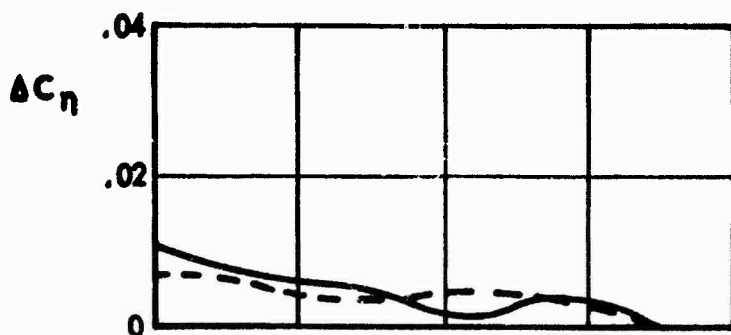
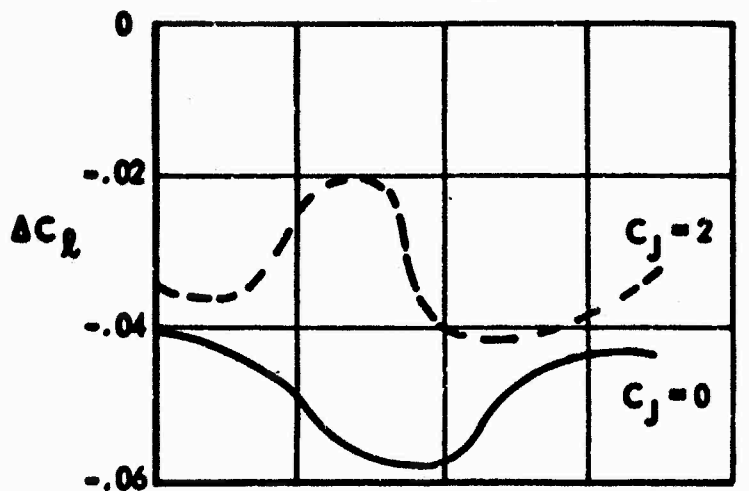


Figure 64 THRUST EFFECT ON RUDDER POWER

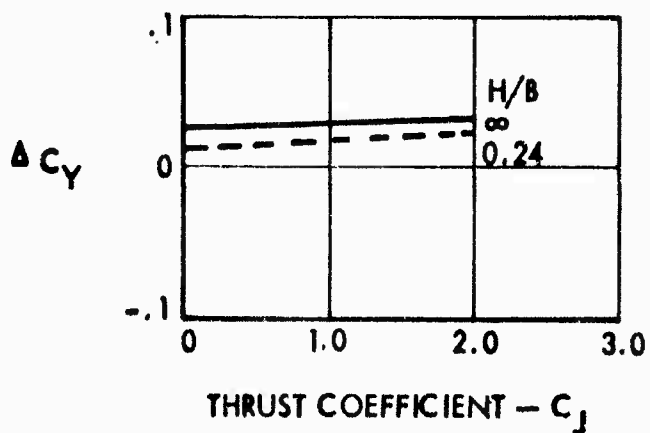
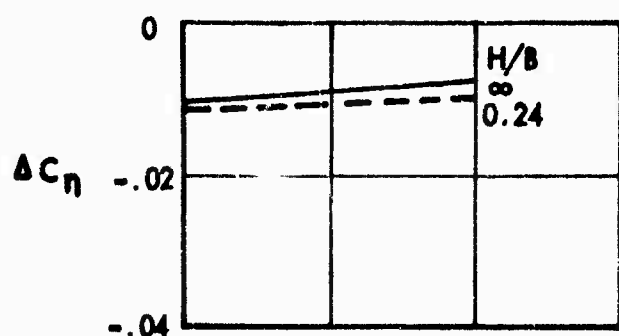
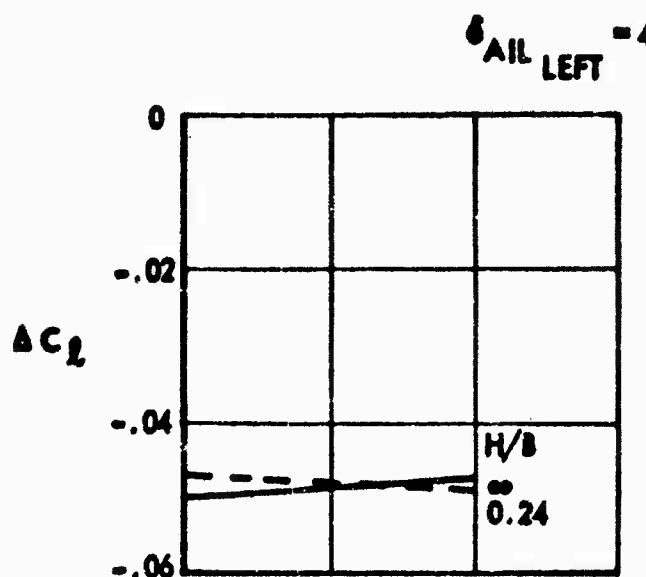


$\delta_{\text{AIL RIGHT}} = 40^\circ \text{ DOWN}, \alpha_W = 0 \text{ DEG.}$



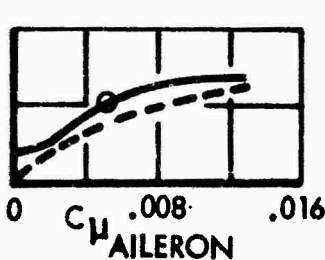
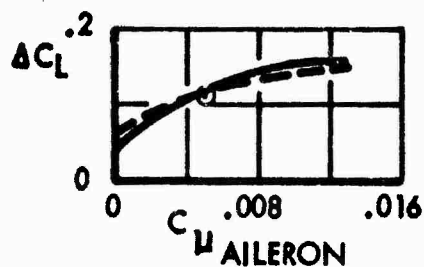
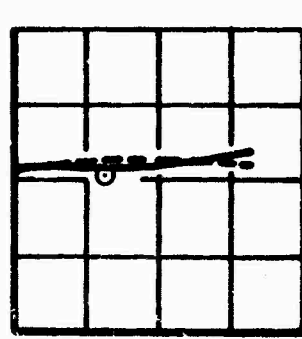
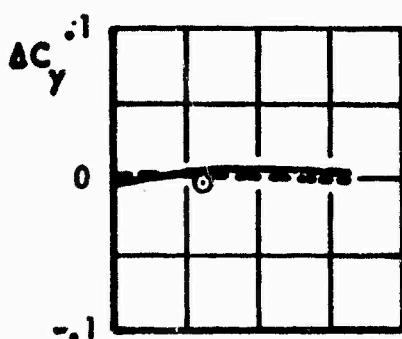
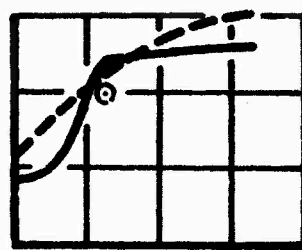
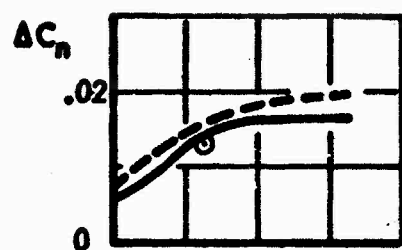
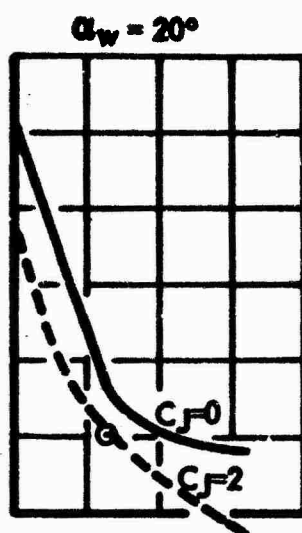
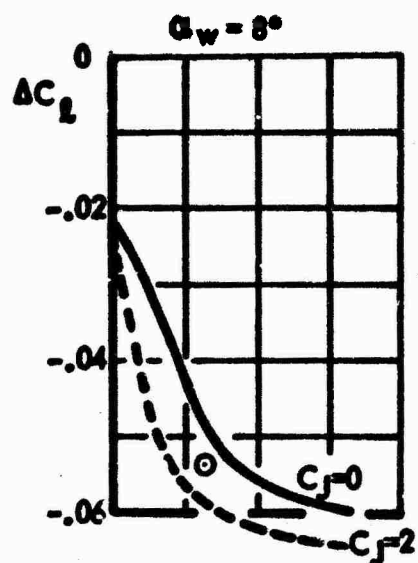
FREE AIR  
TAIL OFF  
NACELLES AT .27 AND  
.435  $b/2$   
NOZZLES AT .35 CHORD  
SWEEP =  $30^\circ$   
 $AR = 6.62$   
T.E. FLAP SPAN/ $b = .743$   
T.E. FLAP ANGLE =  $35^\circ$   
L.E. FLAP ANGLE =  $70^\circ$   
 $C_{\mu_{LE}} = .06$   
 $C_{\mu_{AIL}} = .005$   
NOZZLE VECTOR  
ANGLE =  $60^\circ$

Figure 65 EFFECT OF SIDESLIP ON AILERON POWER



TAIL OFF  
 NACELLES AT .27 AND  
 .435  $b/2$   
 NOZZLES AT .35 CHORD  
 SWEEP  $\Lambda = 30^\circ$   
 $AR = 6.62$   
 T. E. FLAP SPAN/ $b = .743$   
 T. E. FLAP ANGLE =  $35^\circ$   
 L. E. FLAP ANGLE =  $70^\circ$   
 $C_{\mu LE} = .06$   
 NACELLE VECTOR  
 ANGLE =  $30^\circ$   
 $C_{\mu AIL} = 0$

Figure 66 EFFECT OF THRUST ON AILERON EFFECTIVENESS  
 IN FREE AIR AND IN GROUND EFFECT



FREE AIR

TAIL OFF

NACELLES AT .27  
AND .435 b/2

NOZZLES AT .35 CHORD

SWEEP  $\Lambda = 30^\circ$

AR = 6.62

T.E. FLAP SPAN/b = .743

T.E. FLAP ANGLE =  $35^\circ$

L.E. FLAP ANGLE =  $70^\circ$

$C_{\mu LE} = .06$

NOZZLE VECTOR ANGLE

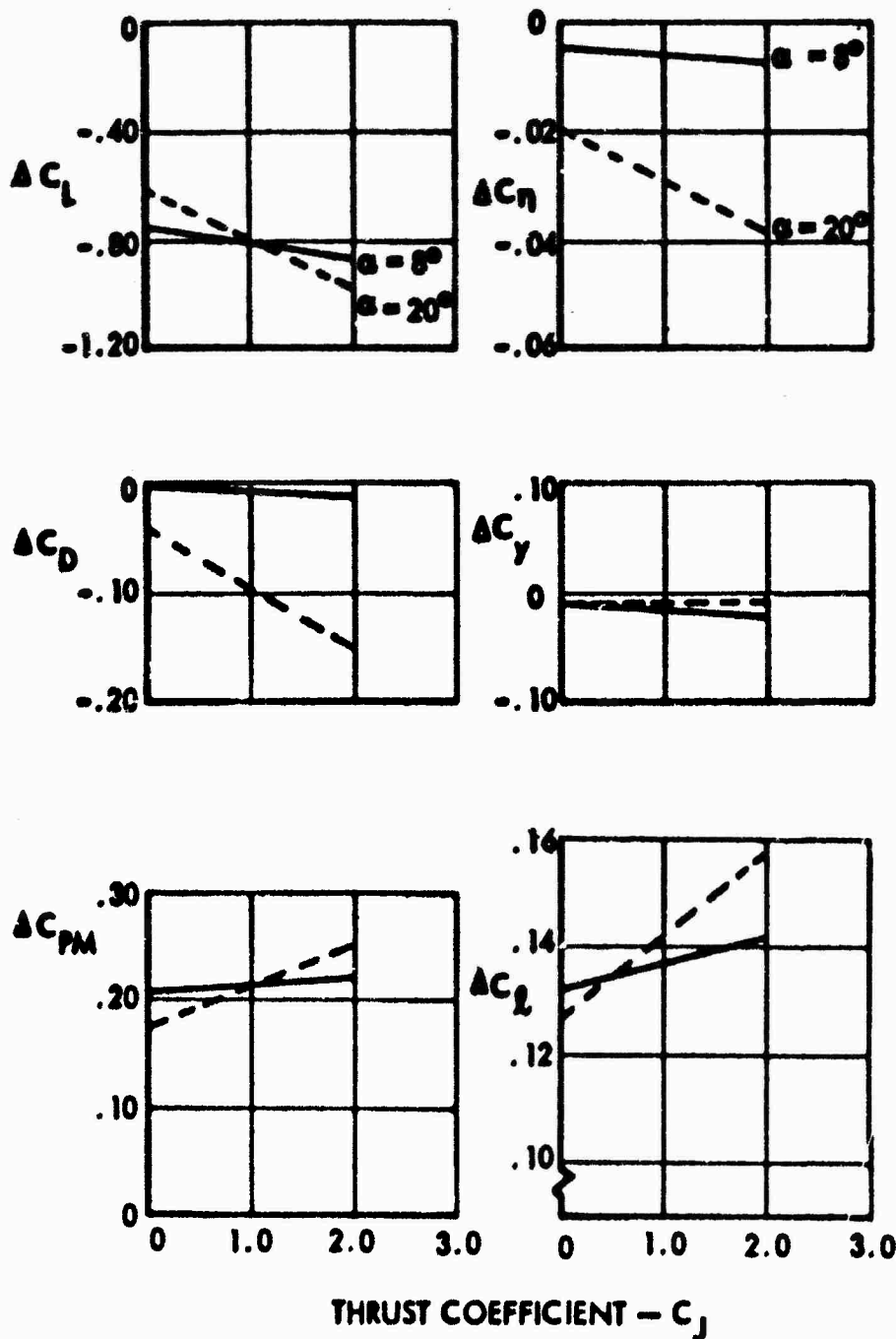
—  $\sigma = 0^\circ$   
○  $\sigma = 30^\circ$   
- - -  $\sigma = 60^\circ$

RIGHT HAND AILERON  
=  $40^\circ$  DN

EFFECT OF AILERON BLOWING AND ENGINE THRUST ON AILERON EFFECTIVENESS

Figure 67

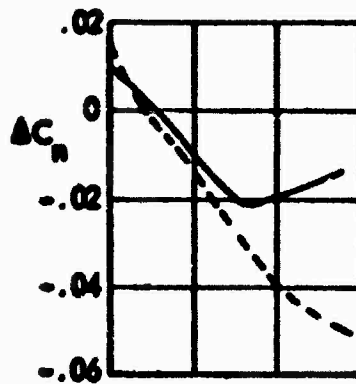
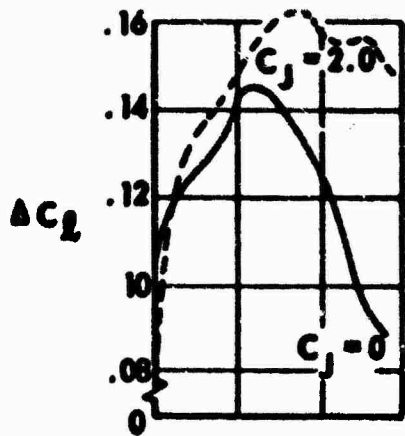
$\delta$  SPOILER =  $49^\circ$   
RIGHT



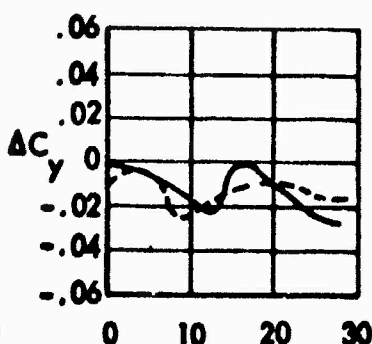
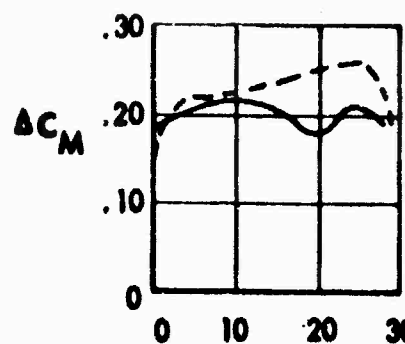
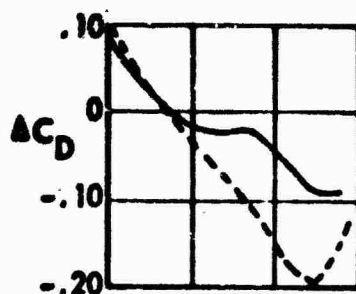
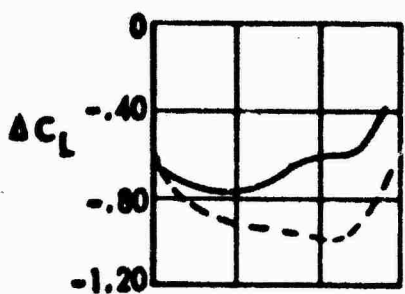
TAIL OFF  
NACELLES AT .27  
AND .435  $h/2$   
NOZZLES AT .35  
CHORD  
SWEEP =  $30^\circ$   
AR = 6.62  
T.E. FLAP  
SPAN/b = .743  
T.E. FLAP  
ANGLE =  $35^\circ$   
L.E. FLAP  
ANGLE =  $70^\circ$   
 $C_{H\text{ L.E.}} = .06$   
 $C_{H\text{ AIL}} = 0$   
NOZZLE VECTOR  
ANGLE =  $60^\circ$

Figure 68 EFFECT OF THRUST ON SPOILER EFFECTIVENESS

$\delta$  SPOILER =  $49^\circ$   
RIGHT



FREE AIR  
TAIL OFF  
NACELLES AT .27 AND  
.435  $b/2$   
NOZZLES AT .35 CHORD  
SWEEP =  $30^\circ$   
 $AR = 6.62$   
T.E. FLAP SPAN/ $b = .743$   
T.E. FLAP ANGLE =  $35^\circ$   
L.E. FLAP ANGLE =  $70^\circ$   
 $C_{\mu_{LE}} = .06$   
 $C_{\mu_{AIL}} = 0$   
NOZZLE VECTOR  
ANGLE =  $60^\circ$



$\alpha_W$  - DEG.

Figure 69 SPOILER EFFECTIVENESS

### 3.3 Engine Out

This section presents methods for calculating the pitching moment, rolling moment, and yawing moment due to engine failure for a vectored thrust airplane. These methods are based on test data from BVWT 099 (Reference 5).

In order to obtain the pitching moment on the airplane for engine out conditions, the pitching moment for the all engine case is calculated using methods previously outlined in Section 3.2.1.1. From this the direct thrust pitching moment is subtracted by the Equation:

$$\Delta C_{m_{\text{FAILED ENGINE}}} = \Delta C_{J_{\text{FAILED ENGINE}}} (X_T \sin \sigma + Z_T \cos \sigma) \quad (3.34)$$

where

$X_T$  = Distance from moment center to thrust vector in fraction of MAC, positive forward

$Z_T$  = Distance from moment center to thrust vector in fraction of MAC, positive down

Figures 70 and 71 show the effect of engine failure on rolling moment and yawing moment. These data are presented in the form

of  $\frac{\Delta C_l}{\Delta C_L}$  and  $\frac{\Delta C_n}{\Delta C_D}$  where  $\Delta C_L$  and  $\Delta C_D$  are the lift and drag

changes due to engine failure and include both direct thrust and interference effects. The rolling and yawing moments are calculated by Equations 3.35 and 3.36.

$$\Delta C_{l_{\text{FAILED ENGINE}}} = \frac{\Delta C_l}{\Delta C_L} \left[ \Delta C_{J_{\text{FAILED ENGINE}}} \sin(\alpha + \sigma) + C_{L_{\text{INT FAILED ENGINE}}} \right] \quad (3.35)$$

$$\Delta C_{n_{\text{FAILED ENGINE}}} = \frac{\Delta C_n}{\Delta C_D} \left[ \Delta C_{J_{\text{FAILED ENGINE}}} \cos(\alpha + \sigma) + C_{D_{\text{INT FAILED ENGINE}}} \right] \quad (3.36)$$

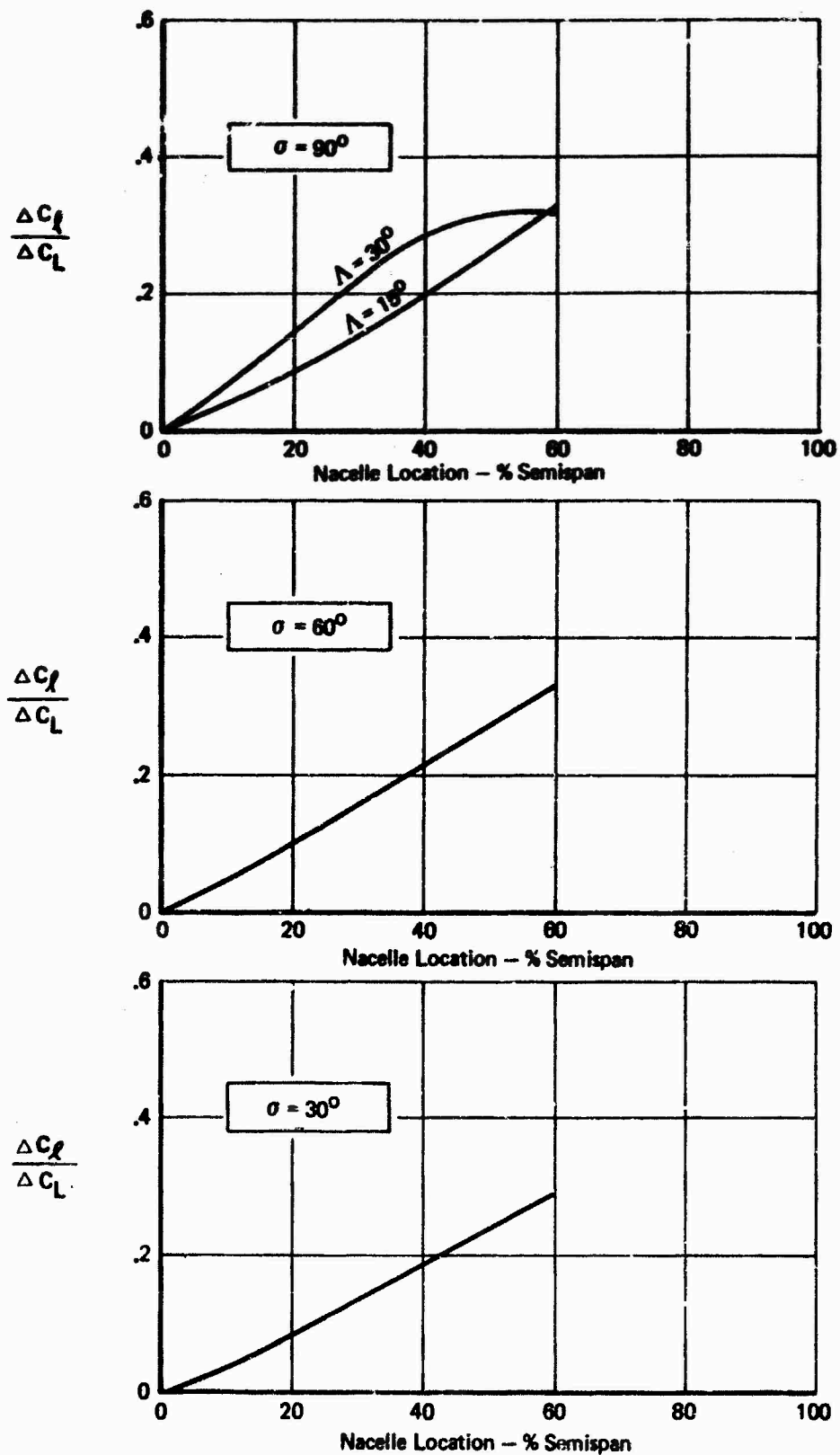


Figure 70 : ROLLING MOMENT DUE TO THRUST LOSS

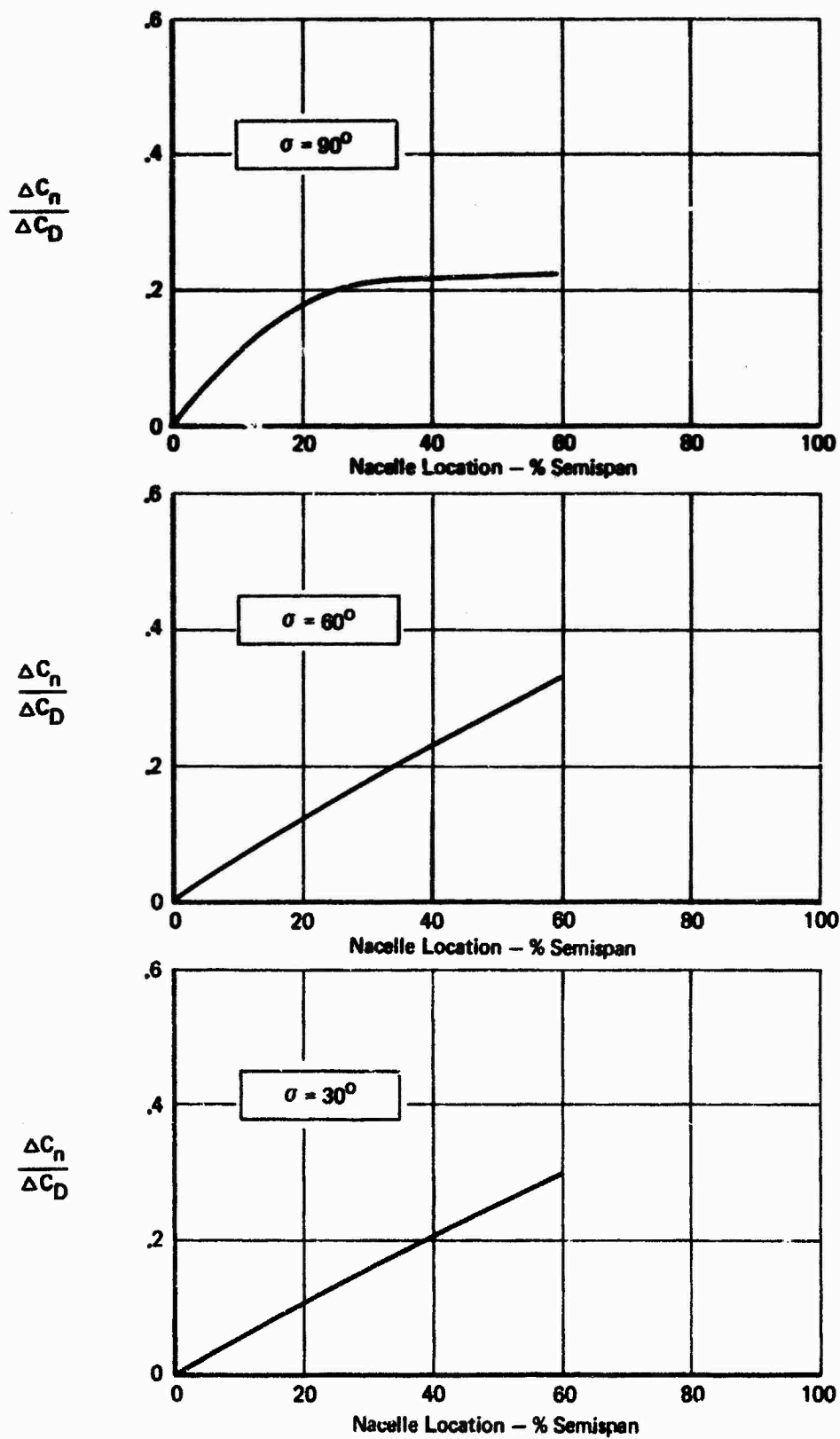


Figure 71: YAWING MOMENT DUE TO THRUST LOSS



## APPENDIX

### USERS' MANUAL FOR COMPUTER PROGRAM

#### 1. INTRODUCTION

##### 1.1 Program Description

The program calculates the aerodynamic characteristics of an airplane with various types and combinations of high lift devices. These characteristics include the additional lift, drag, and pitching moments of the high lift devices and the resultant trimmed totals. The high lift devices include leading edge flaps with and without boundary layer control (BLC), single slotted, double slotted, double slotted/double hinged, and triple slotted/double hinged trailing edge flaps.

The program is in FORTRAN IV source code compatible with the Control Data Corp. (CDC) FTN compiler on the SCOPE 3.3 operating system for the CDC 6000/7000 series computers. Eight general purpose mathematical routines from the BCS mathematical library used for interpolation (INTAB, OUTTAB, TBL, SEARCH, TBLU3, TERP1, TERP2, and TERP3) are included in FTN binary form only. The deck also includes the basic data tables developed in the main body of this document.

The program requires a number of tabular functions to be maintained on a permanent storage device file. The contents of this file, called the "permanent tables", actually form a substantial part of the data comprising the methodology defined in this report. The permanent tables may be permanently updated or temporarily modified if the user wishes to change the methodology. Input procedures for such changes are beyond the scope of this report, but are discussed in Reference 13.

##### 1.2 Input Sequence

Any number of cases may be done on a single computer run. Input data for the whole batch begins with a "starter" card. Next comes the first case's title card. Data cards for that case follow. Next comes the title card for the second case, and so forth.

##### 1.3 Output Summary

A printout of all permanent tables on the storage device is user selectable. When a table is modified, it is printed for verification, whether it is a temporary or permanent modification. The title for each case is printed, followed by all the input data for that case.

The coefficients of lift, drag, and pitching moment are printed following the input data for each case for free air, with ground effect, and vectored thrust. A single run may include several thrust coefficients, flap angles and wing/ground distances. The outputs for ground effect are repeated for each wing height. This output is repeated for each flap angle, and the entire output is repeated for each thrust coefficient.

## 2. INPUT CARD PUNCHING INSTRUCTIONS

The STARTER card must be punched with one-digit integers in specified columns. Title cards are punched as 72 columns of freely arranged alphameric data. With two exceptions noted in the discussion below, all other data are to be punched in 10-field seven digit format. This format requires all numbers to have a decimal point but permits arbitrary placement in the seven digit field.

### 2.1 Input Card Order

#### "STARTER" Card

1st Case	TITLE CARD	C01
	FLAP TYPE	C02
	Balance of Data	C04-C26
2nd Case	TITLE CARD	C01
	FLAP TYPE	C02
	Balance of Data	C04-C26

### 2.2 Input Card Formats

#### "STARTER" Card

<u>Column</u>	<u>Variable</u>	<u>Description</u>
7	IU	Input/output unit for permanent tabular data*
	= 2 - Permanent disk/scratch disk	
	= 4 - Magnetic tape/scratch disk	
14	NTBL	Number of permanent tables to be modified (Use 0)*
21	IP	Print option
	= 0 - Formal output printed	
	= 1 - Tables and formal output printed	
	= 2 - Tables, detailed intermediate computations, and formal output printed	
28	ICR	Permanent tables on card reader (Use 0)*
72-80	May be used for identification	

\*Modification or updation of tables requires nonzero inputs. This situation is discussed in Reference 13.

Card C01

<u>Column</u>	<u>Name</u>	<u>Description</u>
1-72		Title

Card C02

<u>Field</u>	<u>Name</u>	<u>Description</u>
1	AFLAP	Flap type identification. 1. Type 1 single slotted 2. Type 2 double slotted 3. Type 3 double slotted 4. Type 4 triple slotted (Refer to Figure 6 for description of the flap types.)
2	ATTBL	Number of temporary table updates. 0. To use existing tables in storage.

Card C03 - Temporary tables (Not normally used.)

Card C04

<u>Field</u>	<u>Name</u>	<u>Description</u>
1	WGROSS	Gross wing area, sq ft
2	WREF	Reference wing area, sq ft
3	SPAN	Wing span, ft
4	WPERMT	Wing semi-perimeter, ft (For example, refer to sample problem, Page 5.)

Card C05

<u>Field</u>	<u>Name</u>	<u>Description</u>
1	CPRIME	Extended wing chord length normal to extended wing half chord line, ft (Extended chord definition on Figure 6.)
2	CFLAP	Flap chord Types 1 and 2 flap normal to wing half chord line, ft
3	AQCORD	Sweep angle of wing quarter chord line, deg
4	AHCORD	Sweep angle of wing half chord line, deg

Card C05 (Continued)

<u>Field</u>	<u>Name</u>	<u>Description</u>
5	AHLAFT	Sweep angle of aft flap hinge line, deg. This is the hinge line for Types 1 and 2 flap or the aft hinge line for Types 3 and 4.

Card C06

<u>Field</u>	<u>Name</u>	<u>Description</u>
1	ADFLAP	Number of flap deflections, maximum of 4.

Card C07 (For Flap Type 1 or 2)

<u>Field</u>	<u>Name</u>	<u>Description</u>
1	DFLP <sub>1</sub>	First flap deflection, Type 1 or 2 flap, deg
2	DFLP <sub>2</sub>	Second flap deflection, deg
3	DFLP <sub>3</sub>	Third flap deflection, deg
4	DFLP <sub>4</sub>	Fourth flap deflection, deg

Card C07 (For Flap Type 3 or 4)

<u>Field</u>	<u>Name</u>	<u>Description</u>
1	DFFW <sub>1</sub> )	First flap deflection, Type 3 or 4 flap, deg
2	DFAF <sub>1</sub> )	
3	DFFW <sub>2</sub> )	Second flap deflection.
4	DFAF <sub>2</sub> )	
5	DFFW <sub>3</sub> )	Third flap deflection.
6	DFAF <sub>3</sub> )	
7	DFFW <sub>4</sub> )	Fourth flap deflection.
8	DFAF <sub>4</sub> )	

Card C08 (For Flap Type 3 or 4)

<u>Field</u>	<u>Name</u>	<u>Description</u>
1		Not used.

Card C08 (Continued)

<u>Field</u>	<u>Name</u>	<u>Description</u>
2	CPFLAP	Forward flap chord (includes aft flap rotated into forward flap chord plane) ft - see Figure 6 for definition.
3	CAFT	Aft flap chord measured normal to wing half chord line, ft
4	AHLFWD	Sweep angle of forward flap hinge line, deg

Card C09

<u>Field</u>	<u>Name</u>	<u>Description</u>
1	ETEIN	Distance from airplane centerline to inboard edge of trailing edge flap, semispans
2	ETEOUT	Distance from airplane centerline to outboard edge of trailing edge flap, semispans

Card C10

<u>Field</u>	<u>Name</u>	<u>Description</u>
1	CLEDGE	Leading edge flap chord measured normal to wing quarter chord line, ft
2	CHORD	Wing chord normal to wing quarter chord line, ft
3	DLEDGE	Leading edge flap deflection normal to flap hinge line, deg
4	ELEIN	Distance from airplane centerline to inboard edge of leading edge flap, semispans
5	ELEOUT	Distance from airplane centerline to outboard edge of leading edge flap, semispans

## Card C11

<u>Field</u>	<u>Name</u>	<u>Description</u>
1	CLAFU	Lift curve slope, flaps up, per degree
2	AOFLU	Angle of zero lift, flaps up, deg
3	CLMAXU	Maximum lift coefficient, flaps up
4	ALPHAI	Initial angle of attack for which data is desired, deg
5	DALPHA	Increment in angle of attack for which data is desired, deg
6	CHDLE	Extended wing chord length normal to wing leading edge with trailing edge flap extended, ft

## Card C12

<u>Field</u>	<u>Name</u>	<u>Description</u>
1	CLENLE	Chord length of leading edge device normal to wing leading edge, ft
2	CRDNLE	Wing chord length normal to wing leading edge, ft
3	DWTE	Increase in wing area due to trailing edge flap extension, sq ft
4	DWLE	Increase in wing area due to leading edge flap extension (including only the area forward of trailing edge flaps) sq ft
5	WPGROS	Basic wing area inboard of outboard edge of trailing edge flap, sq ft
6	CULE	Leading edge boundary layer control blowing momentum coefficient
7	AEDGE	Leading edge flap type. 1. Shaped leading edge devices. 2. Conventional slats.

## Card C13

<u>Field</u>	<u>Name</u>	<u>Description</u>
1	WGFLAP	Wing area including leading and trailing edge flap extension between the inboard and outboard edge of the trailing edge flap, sq ft
2	SPANLE	Planform area of leading edge device, sq ft
3	CRDDPM	Wing chord including leading and trailing edge extension normal to wing half chord line, ft
4	CDPMFU	Minimum drag flapsup

## Card C14

<u>Field</u>	<u>Name</u>	<u>Description</u>
1		Not used, leave blank
2	APQCHD	Sweep angle of quarter chord with leading edge extended, deg
3	XAC	Longitudinal location of aerodynamic center of basic trapezoidal wing, ft (Note, all longitudinal distances must be from a common reference point.)
4	S2	Wing area between the inboard and outboard edges of the leading edge flaps, sq ft
5	DSLE	Increase in wing area from extension of leading edge flaps, sq ft
6	S3	Wing area between the inboard and outboard edges of the trailing edge flaps, sq ft

## Card C15

<u>Field</u>	<u>Name</u>	<u>Description</u>
1	ALE	Location of inboard edge of leading edge flaps: 1. Start at side of body. 2. Start outboard of side of body.

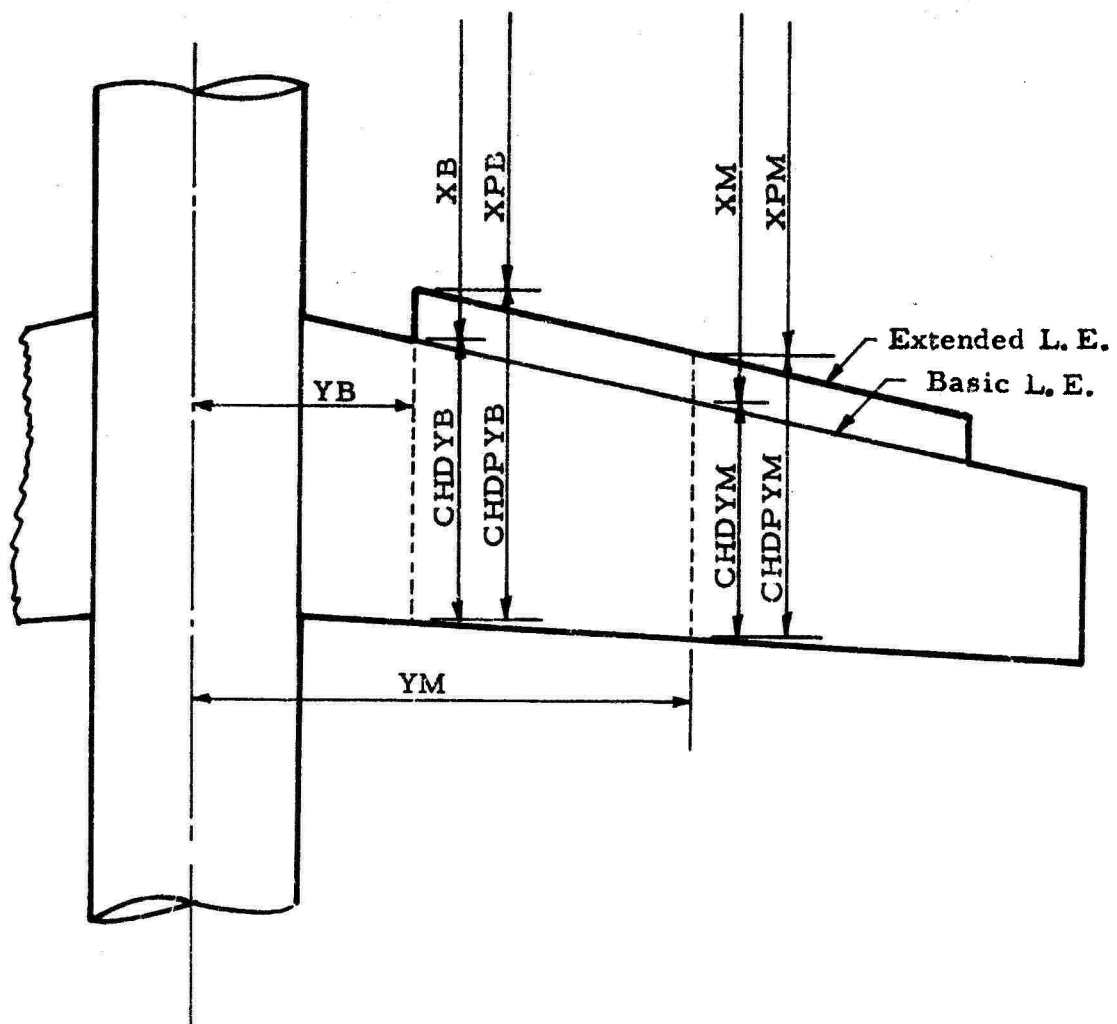


Figure 72: Nomenclature for Leading Edge Flap



Card C15 (Continued)

<u>Field</u>	<u>Name</u>	<u>Description</u>
2	ATE	Location of inboard edge of trailing edge flaps. 1. Start at side of body. 2. Start outboard of side of body.

Card C16 (For additional description of geometry on Cards C16 and C17 refer to Figure 72.)

<u>Field</u>	<u>Name</u>	<u>Description</u>
1	CHDYB	Streamwise wing chord length at inboard edge of leading edge flap, ft
2	XB	Longitudinal location of leading edge of streamwise wing chord (CHDYB) at inboard edge of leading edge flaps, ft Measured from the common reference point.
3	CHDPYB	Streamwise chord length at inboard edge of leading edge flaps with leading edge extended, ft
4	XPB	Longitudinal location of leading edge of streamwise chord (CHDPYB) with leading edge flaps extended, chord at inboard edge of leading edge flaps, ft
5	YB	Spanwise location of inboard edge of leading edge flaps, ft
6	YM	Spanwise location of leading edge flap semispan, ft

Card C17

<u>Field</u>	<u>Name</u>	<u>Description</u>
1	CHDYM	Streamwise chord at mid span of leading edge flap, ft
2	XM	Longitudinal location of leading edge of chord CHDYM, ft
3	CHDPYM	Extended streamwise chord at midspan of leading edge flap, ft
4	XPM	Longitudinal location of leading edge of chord CHDPYM, ft

Card C18 (For additional description of geometry on Cards C18 and C19, refer to Figure 73.)

<u>Field</u>	<u>Name</u>	<u>Description</u>
1	CHDYBT	Streamwise chord at inboard edge of trailing edge flap, ft
2	XBTE	Longitudinal location of leading edge of chord CHDYBT, ft
3	CDPYBT	Streamwise chord length at inboard edge of trailing edge flaps with trailing edge extended, ft
4	XPBTE	Longitudinal location of leading edge of chord CHPYBT, same as XBTE, ft
5	YBTE	Spanwise location of chord CHDYBT, ft
6	YMTE	Spanwise location of midspan of trailing edge flap, ft

Card C19

<u>Field</u>	<u>Name</u>	<u>Description</u>
1	CHDYMT	Streamwise chord at trailing edge flap semispan, ft
2	XMTE	Longitudinal location of leading edge of CHDYMT, ft
3	CPYMTE	Streamwise chord at trailing edge flap semispan, includes trailing edge flap extension, ft
4	XPMTE	Longitudinal location of leading edge of CPYMTE, same as XMTE, ft

Card C20

<u>Field</u>	<u>Name</u>	<u>Description</u>
1	CREF	Reference chord length for pitching moment, ft
2	CFLIB	Streamwise flap chord at inboard edge of trailing edge flap, flap type 1 or 2, ft
3	CFLOB	Streamwise flap chord at outboard edge of trailing edge flap, flap type 1 or 2, ft

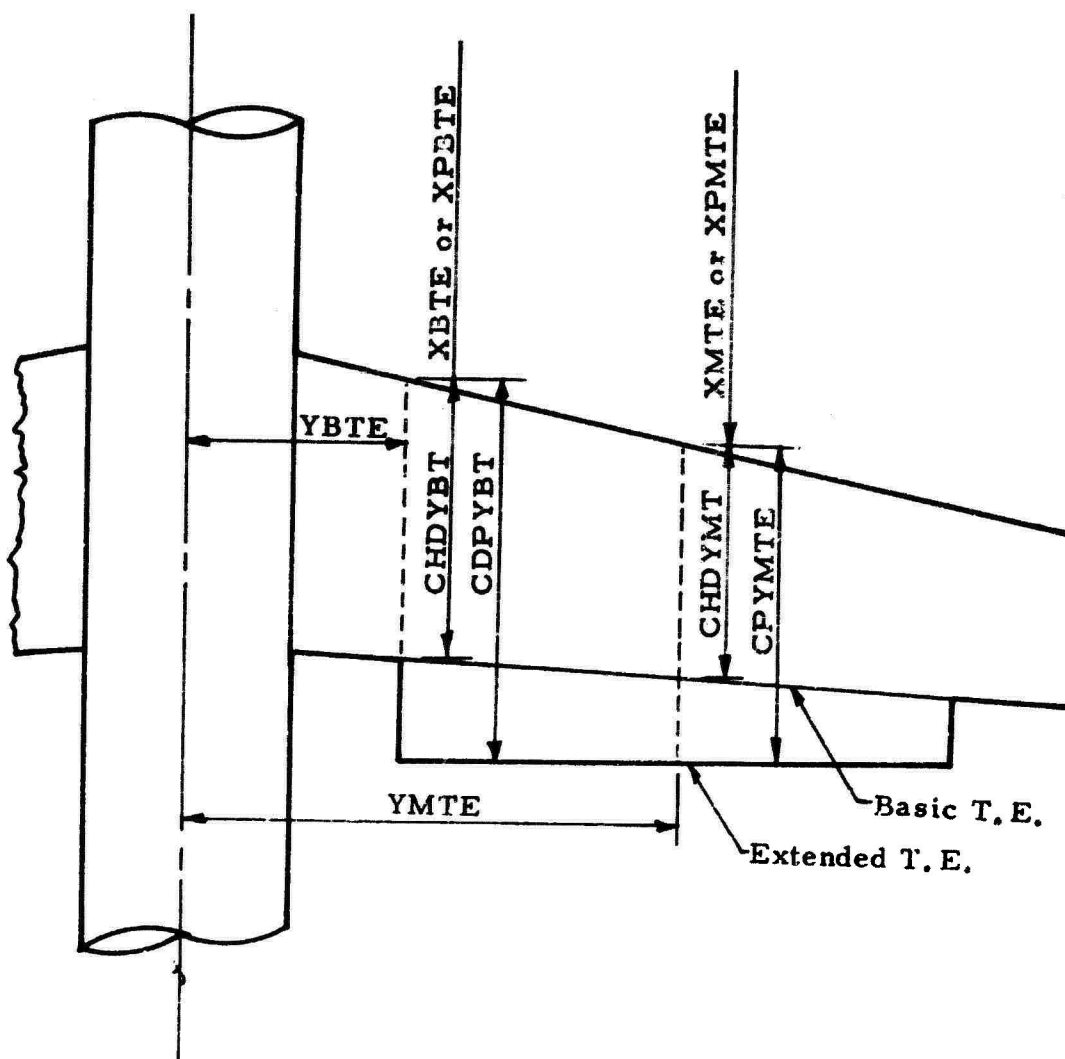


Figure 73: Nomenclature for Trailing Edge Flap

Card C20 (Continued)

<u>Field</u>	<u>Name</u>	<u>Description</u>
4	CPMIB	Streamwise wing chord at inboard edge of trailing edge flap (including trailing edge flap extension), ft
5	CPMOB	Streamwise wing chord at outboard edge of trailing edge flap (including trailing edge flap extension), ft

Card C21

<u>Field</u>	<u>Name</u>	<u>Description</u>
1	CPFLIB	Streamwise flap chord at inboard edge of trailing edge flap, includes aft flap rotated about hinge line into forward flap chord plane, flap type 3 or 4, ft
2	CPFLOB	Streamwise flap chord at outboard edge of trailing edge flap (includes aft flap rotated about hinge line into forward flap chord plane), flap type 3 or 4, ft
3	XIB	Longitudinal intersection of CPMIB and wing half chord line, ft
4	XOB	Longitudinal intersection of CPMOB and wing half chord line, ft
5	XPQCRD	Longitudinal location of wing quarter mac with the leading edge flap extended, ft
6	XCG	Longitudinal location of center of gravity, ft

Card C22

<u>Field</u>	<u>Name</u>	<u>Description</u>
1	CMOLFU	Pitching moment coefficient at zero lift, flaps up
2	EPTEIB	Distance from airplane centerline to intersection of CPMIB and wing half chord line, semispans

Card C22 (Continued)

<u>Field</u>	<u>Name</u>	<u>Description</u>
3	EPTEOB	Distance from airplane centerline to intersection of CPMOB and wing half chord line, semispans

Card C23

<u>Field</u>	<u>Name</u>	<u>Description</u>
1	THQM	Height of horizontal tail quarter mac above wing chord plane, ft
2	TLQM	Tail length, from wing quarter mac to tail quarter mac, ft
3	NWINGH	Number of ground heights to be considered, maximum of 4 (must be right adjusted integer in Column 21)
4	WHQM <sub>1</sub>	First ground height, ground to wing quarter mac, ft
5	WHQM <sub>2</sub>	Second ground height, ft
6	WHQM <sub>3</sub>	Third ground height, ft
7	WHQM <sub>4</sub>	Fourth ground height, ft

Card C24

<u>Field</u>	<u>Name</u>	<u>Description</u>
1	STAIL	Horizontal tail area, sq ft
2	EPSO	Downwash angle at horizontal tail, flaps up, zero angle of attack, deg
3	DEPDAL	Rate of change of downwash with angle of attack, flaps up, degrees/degree
4	DCPDM	Horizontal tail minimum drag coefficient, referred to horizontal tail area
5	DCDDCL	$(dC_D/dC_L^2)$ , tail induced drag factor referred to tail lift coefficient and tail area

# Card C25

<u>Field</u>	<u>Name</u>	<u>Description</u>
1	CDRAM	Ram drag coefficient
2	ENGVEC	Engine vector angle referred to wing chord plane, deg
3	XNACEL	Longitudinal distance from wing leading edge to nozzle exit divided by wing chord length at the same streamwise station
4	XNOZLE	Longitudinal distance from center of gravity to nozzle exit centerline, ft
5	ZNOZLE	Vertical distance from center of gravity to nozzle exit centerline, ft
6	ZINLET	Longitudinal distance from center of gravity to centerline of inlet face, ft
7	ZINLET	Vertical distance from center of gravity to centerline of inlet face, ft

Note: For multi-engine configurations use average values for nozzle and inlet locations.

# Card C26

<u>Column</u>	<u>Name</u>	<u>Description</u>
7	NCG	Number of engine thrust coefficients; (integer 5)

<u>Field</u>	<u>Name</u>	<u>Description</u>
2-NCJ+1	CJ <sub>1</sub>	Array of engine thrust coefficients; NCJ fields are used.

## 3.0 EXECUTING FROM CARDS

To execute the program from the FORTRAN source deck with the tables on cards, saving the tables on a magnetic tape file, TAPE4, and printing the tables, the deck setup required is shown on Figure 74.

### 3.1 Using the External Table File

The deck is stacked with the REQUEST control card as in Section 3.0 for magnetic tape. The tables are retrieved from the tape without

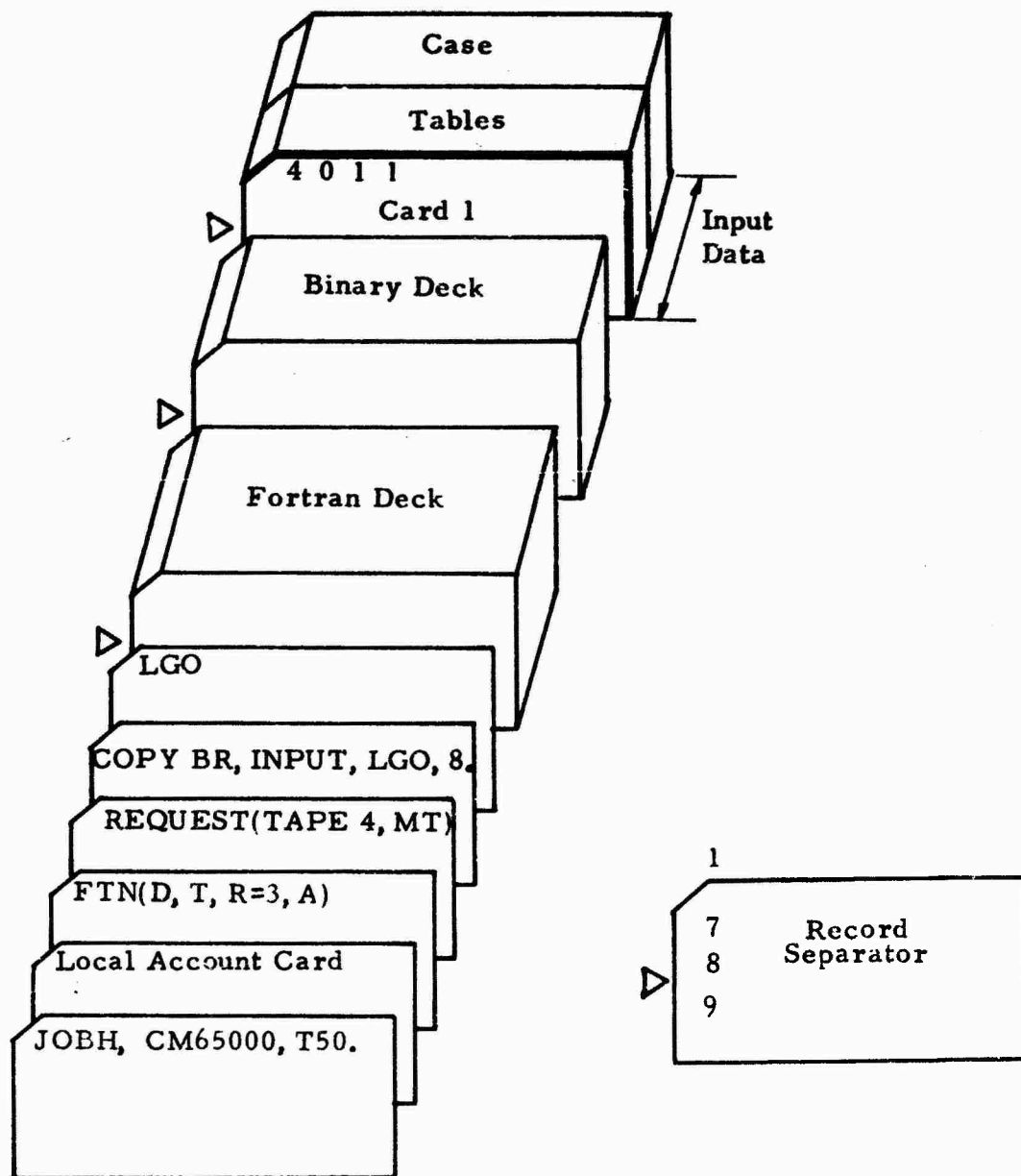


Figure 74: Program Deck Stacking

the full set of tables in the data. The installation convention for identification of the tape is required on the REQUEST card. A permanent disk file can be used instead of the magnetic tape file and permanent or temporary table updates may be supplied as discussed in Reference 13, Section 2. Column 28 of Card 1 is zero.

If execution without the FORTRAN source deck is desired, consult a programmer for the most desirable approach for your installation. This would be preferred in a production situation where no changes are being made to the program.

#### 4. SAMPLE INPUT AND OUTPUT

The sample problem used in this document is presented on an input data form in Table V, followed by the corresponding output.

The output data begins with a recapitulation of the input data. The constants defining the power off lift, moment and drag curves are then stated, followed by tabulated tail-off lift, moment and drag, and by tabulated trimmed lift and drag, for both power-off and power-on conditions. If ground effect data is called for, tabulated characteristics in ground effect come next.

#### 5. PROGRAM LISTING

A FORTRAN IV source code listing of the program begins on page 163.



TABLE V  
SAMPLE INPUT

TEN FIELD, SEVEN DIGIT CRD FORMAT

1	2	3	4	5	6	7	8	9	10	11	12	13	14	15	16	17	18	19	20	21	22	IDENT
4	0	2	1																			STARTER
SAMPLE	PROBLEM																					C01
4.0	0.																					C02
(NOT	USED	FUR	THIS	PROBLEM)																		C03
8.592	6.104	7.0284	8.41267																			C04
1.0722	.346	15	11.652	3.525																		C05
10																						C06
45.14	15.13																					C07
	3463	.0976	7.295																			C08
.145	.750																					C09
.13975	83567	70.	.145	1.																		C10
.076	0.	.90	0.	2.																		C11
.13889	83567	1.104	.624	5.199	.06	1.0																C12
5.577	.802	1.2119	.060																			C13
	15.0	3.165	4.945	.802	3.884																	C14
1.	1.																					C15
1.14508	2.61417	1.284	2.47325	.50835	2.01																	C16
.02333	3.097	.96225	2.950																			C17
1.14508	2.6142	1.4692	2.6417	.50835	1.57183																	C18
.91767	2.9558	1.77742	2.9558																			C19
.93158			1.46917	.88567																		C20
.4745	20608	.33480	2.7398	3.044	3.165																	C21
- .110	145	.75																				C22
1.46383	4.0476	1	1.46775																			C23
1.624	0.	.25	.0075	.0999																		C24
0.	30.	.02917	-.0055	.23225	1.007	.23225																C25
1	2.																					C26
TITLE SAMPLE PROBLEM																					DATE	PAGE 1 OF 1

AD 3776

6-7000

# TRIPLE SLOTTED FLAP TYPE 4

## SAMPLE PROBLEM

WING S WING REF SPAN PERIMETER  
8.59 6.16 7.02 8.41

CPRIME C FLAP SWEEP 1/4C SWEEP 1/2C SWEEP AFT  
1.07 .35 15.00 11.65 3.53

NO FLAP ANGLES OFFWD(1) DFAFT(1) OFFWD(1)  
1 45.14 15.13

C FWD C PRIME FWD C AFT SWEEP FWD  
-0.00 .35 .10 7.29

ETA IB TE ETA OB TE  
.145 .750

CHORD LE C CHORD DELTA LE ETA IB LE ETA OB  
.14 .84 70.00 .145 1.000

CL ALPHA FU ALPHA ZERO L CLMAX FU ALPHA DALPHA CPRIME NLE  
.076 0.0 0.980 0.00 2.00 1.07

C LE NLE CHORD NLE DELS TE CELS LE S PRM GROSS CU LE EDGE TYPE  
.14 .84 1.10 .62 5.20 .060 1.

S FLAPPED SPAN LE C DBL PM CDPHFU  
5.577 .882 1.212 .060

CMO SWEEP PM C/4 XAC TRAP S2 DSLE S3  
-0.00 15.00 3.17 4.94 .88 3.88

ARE THE FLAP EDGES ADJACENT TO THE BODY SIDE OR NOT.  
IF FLAG = 1, YES, = 2, NO. FLAG LE = 1 FLAG TE = 1

### LEADING EDGE

CHORD Y BODY X BODY C PRM BUY X PM BUY Y BODY Y MID SPAN  
1.15 2.61 1.28 2.48 .51 2.01

CHORD Y MID X MID C PRM MID X PM MID  
.82 3.13 .96 2.96

# SAMPLE PROBLEM

TRAILING EDGE									
CHORD Y BODY	X BODY	C PRM BUY	X PM BUY	Y BODY	Y MID SPAN				
1.15	2.61	1.47	2.61	.51	1.57				
CHORD Y MID	X MID	C PRM MID	X PM MID						
.92	2.36	1.18	2.96						
REF CHORD	C FLAP IB	C FLAP OB	C PRM IB	C PRM OB					
.93	-0.30	-0.00	1.47	.89					
CPRM FLAP IB	CPRM FLPOE	X IB	X OB	XPRM C/4	XCG				
.47	.29	3.35	3.74	3.07	3.17				
CM OLFU	ETAPRM TE IB	ETAPRM TE OB							
-.110	.145	.750							
TAIL H	TAIL LENGTH	NO. WING H/S	WING(1)	WING H(2)	WING H(3)	ALL MAC/4			
1.46	4.10	1	1.47						
S TAIL	EPSILON 0	D EPS/D ALP	DCPD M/LN	CU/CL TAIL					
1.624	0.300	.250	.008	.100					
RAM DRAG	SIGMA ENG	X NACELLE	X NOZZLE	Z NOZZLE	X INLET	Z INLET			
0.00	30.30	.03	-.61	.23	1.01	.23			
NO. OF CJ	CJ(1)	CJ(2)	CJ(3)	CJ(4)	CJ(5)				
1	2.30								

# SAMPLE PROBLEM

## ANGLES OF ATTACK - ZERO LIFT -----

FLAP UP	LE DOWN	TE DOWN	BOTH DOWN
0.00000	1.67830	-19.91228	-18.23398

## LIFT PARAMETERS -----

SLOPE	SLOPE	COEF	COEF	COEF
FLAPS UP	FLAPS DOWN	DEL CL FD	CLMAX FU	CLMAX FD
.07600	.09885	1.80249	.98000	4.37882

## DRAG COEFFICIENTS -----

MINIMUM FLAPS UP	DEL MIN TE	DEL MIN LE
.06000	.04380	.02204

## PITCHING MOMENT COEFFICIENTS -----

ZERO LIFT	DEL OL TE	DEL OL LE
-.11000	-.48886	.00266

# SAMPLE PROBLEM

## UNPOWERED CHARACTERISTICS \*\*\*\*\*

### F R E E   A I R

GROSS THRUST  
COEFFICIENT  
0.00

FLAP ANGLES  
45.14   15.13

WING  
HEIGHT (SPANS)  
0.00

### T A I L   O F F

### T R I M M E D

ALPHA  
0.00  
2.00  
4.00  
6.00  
8.00  
10.00  
12.00  
14.00  
16.00  
18.00  
20.00  
22.00  
24.00  
26.00

CL  
1.80249  
2.00019  
2.19790  
2.39560  
2.59331  
2.79102  
2.98872  
3.18643  
3.38413  
3.58184  
3.77955  
3.97725  
4.17496  
4.37266

CU  
.29141  
.31918  
.35005  
.38402  
.42113  
.46236  
.50691  
.55458  
.60657  
.66287  
.72227  
.78554  
.85531  
.92818

CM  
-.56894  
-.56595  
-.56296  
-.55996  
-.55697  
-.55398  
-.55099  
-.54800  
-.54501  
-.54202  
-.53903  
-.53604  
-.53305  
-.53006

CL  
1.67314  
1.87152  
2.06991  
2.26830  
2.46668  
2.66507  
2.86345  
3.06184  
3.26023  
3.45861  
3.65700  
3.85538  
4.05377  
4.25216

CD  
.28570  
.31345  
.34431  
.37828  
.41537  
.45659  
.50113  
.54879  
.60078  
.65706  
.71646  
.77973  
.84948  
.92235

# SAMPLE PROBLEM

## POWER-ON CHARACTERISTICS \*\*\*\*\*

F R E E   A I R

GROSS THRUST  
COEFFICIENT  
2.00

FLAP ANGLES  
45.14   15.13

WING  
HEIGHT (SPANS)  
0.00

T A I L   O F F

T R I M M E D

ALPHA	CL	CD	CM	CL	CD
0.00	2.37815	-1.49835	-.02305	2.37291	-1.49693
2.00	2.71206	-1.41312	-.04576	2.70166	-1.41226
4.00	3.03429	-1.32546	-.06487	3.01954	-1.32511
6.00	3.34316	-1.23544	-.07997	3.32498	-1.23555
8.00	3.64101	-1.14225	-.09185	3.62013	-1.14278
10.00	3.91463	-1.04979	-.09611	3.89278	-1.05060
12.00	4.19503	-.94944	-.10317	4.17157	-.95064
14.00	4.48215	-.84157	-.11303	4.45645	-.84330
16.00	4.76921	-.72730	-.12344	4.74115	-.72964
18.00	5.07039	-.60236	-.13917	5.03874	-.60557
20.00	5.38322	-.47019	-.15975	5.34690	-.47457
22.00	5.70765	-.32781	-.18491	5.66561	-.33353
24.00	6.04363	-.17162	-.21385	5.99500	-.17917
26.00	6.39110	-.00573	-.24656	6.33504	-.01570

# SAMPLE PROBLEM

## UNPOWERED CHARACTERISTICS

### GROUND EFFECT

GROSS THRUST  
COEFFICIENT  
0.00

FLAP ANGLES  
45.14 15.13

WING  
HEIGHT (SPANS)  
.21

T A I L O F F				T R A N M E D			
ALPHA	CL	CD	CM	CL	CD		
-1.26	1.74479	.24378	-.55073	1.61953	.23800		
.60	1.92934	.26087	-.54590	1.80523	.25508		
2.47	2.11257	.27991	-.54110	1.98955	.27410		
4.33	2.29450	.30088	-.53633	2.17257	.29506		
6.19	2.47514	.32376	-.53160	2.35428	.31793		
8.05	2.65450	.34951	-.52689	2.53472	.34367		
9.91	2.83259	.37732	-.52221	2.71387	.37148		
11.78	3.00942	.40698	-.51756	2.89176	.40113		
13.64	3.18530	.43960	-.51294	3.06838	.43375		
15.50	3.35934	.47514	-.50835	3.24377	.46928		
17.36	3.53245	.51244	-.50379	3.41791	.50658		
19.22	3.70433	.55220	-.49926	3.59083	.54633		
21.09	3.87501	.59681	-.49475	3.76253	.59095		
22.95	4.04448	.64312	-.49028	3.93302	.63725		

# SAMPLE PROBLEM

## POWER-ON CHARACTERISTICS \*\*\*\*\*

### G R O U N D   E F F E C T

CROSS THRUST  
COEFFICIENT  
2.00

FLAP ANGLES  
45.14   15.13

WING  
HEIGHT (SPANS)  
.21

#### T A I L   O F F

#### T R I M M E D

ALPHA	CL	CD	CM	CL	CD
-1.26	2.22885	-1.58380	.01505	2.23227	-1.58145
.60	2.54738	-1.51099	-.00647	2.54591	-1.50918
2.47	2.85451	-1.43915	-.02463	2.84891	-1.43778
4.33	3.15021	-1.36532	-.03979	3.14116	-1.36432
6.19	3.43260	-1.29043	-.05136	3.42092	-1.28970
8.05	3.70410	-1.21259	-.06016	3.69042	-1.21206
9.51	3.95281	-1.13712	-.06222	3.93867	-1.13664
11.78	4.20615	-1.05584	-.06673	4.19098	-1.05547
13.64	4.46436	-.96775	-.07369	4.44731	-.96754
15.50	4.72040	-.87503	-.08106	4.70197	-.87499
17.36	4.98674	-.77522	-.09272	4.96566	-.77545
19.22	5.26199	-.66922	-.10854	5.23731	-.66979
21.09	5.54609	-.55348	-.12845	5.51689	-.55448
22.95	5.83902	-.43038	-.15235	5.80439	-.43187



```

PROGRAM HILIFT(INPUT,OUTPUT,TAPE1=INPUT,TAPE2,TAPE3=OUTPUT,TAPE4,
1 TAPE7,TAPE5=INPUT)
TAPE7 BACKUP FILE FOR TABULAR FUNCTIONS
SW7 SENSE SWITCH IF ON BACKUP FILE IS TO BE SAVED.
CR PERMANENT TABLES ON CARD
CR NE O F.G. YES - PERMANENT TABLES ON CARD READER.=BLANK- ON PERM FILE
HIGHLIGHT PROGRAM WRITTEN IN SUPPORT OF D162-10050-1, PARAGRAPHS
2.2.2.1.3 AND 2.6. FOR THE AIRFORCE FLIGHT DYNAMICS LABORATORY
WRIGHT PATTERSON AIR FORCE BASE, OHIO.
THE PROGRAM CALCULATES THE AERODYNAMIC CHARACTERISTICS OF A WING
WITH VARIOUS TYPES AND COMBINATIONS OF HIGH LIFT DEVICES
LIFT AND DRAG COEFFICIENTS OF THE FLAPS AS WELL AS TOTAL WING
LIFT AND DRAG COEFFICIENTS
P.J. REIDIG AND R.A. PAJETTE SEPTEMBER, 1972

```

# NOMENCLATURE

```

IU INPUT UNIT FOR TABULAR DATA =1-CARD RDR, 2-PERM DISK, 4-MAG TAPE
NPTBL NUMBER OF PERMANENT TABLES TO BE MODIFIED
NTTBL NUMBER OF TEMPORARY TABLES TO BE MODIFIED
IP PRINT OPTION =0 BRIEF PRINT OPTION NF 0 FULL PRINT - TABLES
IN STANDARD INPUT STREAM
IO STANDARD OUTPUT STREAM

```

```

REAL KEAPT2,KEIFE0,LAMETA
COMMON
1 APLFCR (30),DCLACC(30),DCLACC(30),DCLACC(30),DCLACC(30),
2 DCDTFD(30),DCDTFT(30),DCKCR(30),KEAPT2(77),KEIFE0(77),DCDCLN(30),
3 AMSDR(30),XCPAR2(77),ECPCL2(77),DCAUT(30),AKRYCY(30),DKCLL2(77),
4 CLIAS2(77),DCLIB(182),CDIB(231),CMIB(231),DEPS(182),DCLIG2(77),
5 DCMIG2(77),DCDIG2(77)
TABLF LENGTH 2 INDFP VAR 6 POINTS =56 WORDS 7=11 8= 120
TABLF LENGTH 1 INDEPENDENT VAR 6PTS=18 WORDS, 7=20, 10 =26
DIMENSION TRLS(2000)
EQUIVALENCE (ACRFS2,TRLS)
COMMON /INTARC/IN,IN,IO,ICK,NPTBL,IP
COMMON /CJ/NCJ,ACJ(5)
COMMON /COMPUTER/ D(2),V(2)
COMMON /TROW/ ILOST
COMMON /OUTARG/ IOT
COMMON /CASEFIN/ TITLE(18),IFLAP,WGRVSS,WKFF,WPERMT,WDFLAP,

```



```

IF (ICR.NF.0) GO TO 16
IF (ICR.FQ.0) BUJFER IN(IU,1) (TALS(1),TALS(1000))
IF (UNIT(IU)) 16,15,15
15 WRITE(10,11)
16 CALL TRLEIN
18 IF (INPTRL.FQ.0) GO TO 20
PERMANENT TABLE MODS REQUIRED
CALL PTBUDT(NPTBL)
C IF ILOST = 1, PERMANENT TABLES NOT READ CORRECTLY. STOP 1
20 IF (ILOST.NE.0) 22,23
22 WRITE(10,3) ILOST
STOP 1
C READ IN THE NEXT CASE OF DATA
23 CALL CASINI
ICASE=ICASE+1
C *** ENGINE THRUST COEFFICIENT
DO 300 J=1,NCJ
CJ=ACJ(J)
C
DO 200 IF=1,NDFLAP
IF (IFLAP.GT.2) GO TO 50
C
C STUFF FLAP DEFLECTIONS TYPE 1 AND 2
DFLAP = DFLP(IF)/RAD
GO TO 60
C
50 CONTINUE
C STUFF FLAP DEFLECTIONS TYPE 3 AND 4
DFFWD = DFFW(IF)/RAD
DFAFT = DFAF(IF)/RAD
60 CONTINUE
C ** FREE AIR
CALL LIFT (IFR)
IF (IFR.NF.0) WRITE(10,5) IER
CALL MXLIFT(IFR)
IF (IFR.NF.0) WRITE(10,6) IER
CALL DRAG (IFR)
IF (IFR.NE.0) WRITE(10,7) IER
CALL PITCH (IFR)

```

```

IF (IFR.NE.0) WRITE(10,8) IER
CALL VTFREE(IFR)
IF (IFR.NE.0) WRITE(10,9) IER

C ** GROUND EFFECT
C
C DO 100 I=1,NWINGH
C
C *** WING HEIGHTS FOR GROUND EFFECT
C
CALL GRNDE(I)
CALL VTGF(I,IFR)
IF (IFR.NE.0) WRITE(10,10) IER
CALL CASOUT(I,WHQM(I))
100 CONTINUE
200 CONTINUE
300 CONTINUE
C NEXT CASE
GO TO 22
END

SUBROUTINE TPLFIN
TABLE PRINT OPTION. IF .NE. 0, PRINT TABLES.
C IP
C
C * * * TABULAR NOTATION * * * * *
C
NTXX TABLE NUMBER FROM NT1 - NTXX
C
C NUMBER OF POINTS ALLOWED IN TABLES9
C NT = 1 7 POINTS FOR A DIMENSION OF 20
C NT = 2 6 BY 5 FOR ARRAY OF 56
C NT = 3 7 BY 6 FOR ARRAY OF 63
C NT = 4 7 BY 7 FOR ARRAY OF 71
C
C ACRES2 ALPHA FLAP EFFECTIVENESS VS COND RATIO VS DELTA FLAP SINGLE SLOT TB 1
C1. 1. 57.2958 TB 1
C ACRES2 ALPHA FLAP EFFECTIVENESS VS COND RATIO VS DELTA FLAP DOUBLE SLOT TB13
C1. 1. 57.2958 TB 13
C ADCRA2 RATIO FLAP EFFECTIVENESS VS COND RATIO VS INVERSE A TB 2
C LAMETA SPAN LOADING FACTOR LAMBDA VS ETA TB 3
C ADLECR ALPHA DELTA LEADING EDGE VS COND RATIO TB 4
C RKCLE2 BODY LIFT CARRYOVER K VS CLTE VS ETAIB TB 21

```

C	DCLACC	DELTA CLMAX / COS50 ALPHA VS CORD RATIO CONVENTIONAL SLATS	1B 19
C	DCLACS	DELTA CLMAX / COS50 ALPHA VS CORD RATIO SHAPED LEADING EDG	1B 5
C	DCLRCR	DELTA CL RATIO VS CORD RATIO	1B 6
C	DCLACM	DEL CL MAX / COS50 ALPHA VS CORD RATIO BOUNDARY LAYER EFFICIENCY	1B 7
C	DCLTF	DEL CL TF VS FLAP ANGLE, DOUBLE SLOTTED	1B 8
C	DCLTF	DEL CL TF VS FLAP ANGLE, TRIPLS SLOTTED	1B 9
C	FLAPR	DEL FLAP DRAG RATIO VS CORD RATIO	1B 10
C	KFAP12	KA VS ETA 1B VS ALPHA / 2 PI	1B 11
C	KF1F02	KE VS ETA 1B VS ETA 1B	1B 12
C	KF1F02	KE VS ETA 1B VS ETA 1B	1B 14
C	KF1F02	KE VS ETA 1B VS ETA 1B	1B 15
C	KF1F02	KE VS ETA 1B VS ETA 1B	1B 16
C	KF1F02	KE VS ETA 1B VS ETA 1B	1B 17
C	KF1F02	KE VS ETA 1B VS ETA 1B	1B 18
C	KF1F02	KE VS ETA 1B VS ETA 1B	1B 19
C	KF1F02	KE VS ETA 1B VS ETA 1B	1B 20
C	KF1F02	KE VS ETA 1B VS ETA 1B	1B 21
C	KF1F02	KE VS ETA 1B VS ETA 1B	1B 22
C	KF1F02	KE VS ETA 1B VS ETA 1B	1B 23
C	KF1F02	KE VS ETA 1B VS ETA 1B	1B 24
C	KF1F02	KE VS ETA 1B VS ETA 1B	1B 25
C	KF1F02	KE VS ETA 1B VS ETA 1B	1B 26
C	KF1F02	KE VS ETA 1B VS ETA 1B	1B 27
C	KF1F02	KE VS ETA 1B VS ETA 1B	1B 28
C	KF1F02	KE VS ETA 1B VS ETA 1B	1B 29
C	KF1F02	KE VS ETA 1B VS ETA 1B	1B 30
C	KF1F02	KE VS ETA 1B VS ETA 1B	1B 31
C	KF1F02	KE VS ETA 1B VS ETA 1B	1B 32
C	KF1F02	KE VS ETA 1B VS ETA 1B	1B 33
C	KF1F02	KE VS ETA 1B VS ETA 1B	1B 34
C	KF1F02	KE VS ETA 1B VS ETA 1B	1B 35
C	KF1F02	KE VS ETA 1B VS ETA 1B	1B 36
C	KF1F02	KE VS ETA 1B VS ETA 1B	1B 37
C	KF1F02	KE VS ETA 1B VS ETA 1B	1B 38
C	KF1F02	KE VS ETA 1B VS ETA 1B	1B 39
C	KF1F02	KE VS ETA 1B VS ETA 1B	1B 40
C	KF1F02	KE VS ETA 1B VS ETA 1B	1B 41
C	KF1F02	KE VS ETA 1B VS ETA 1B	1B 42
C	KF1F02	KE VS ETA 1B VS ETA 1B	1B 43
C	KF1F02	KE VS ETA 1B VS ETA 1B	1B 44
C	KF1F02	KE VS ETA 1B VS ETA 1B	1B 45
C	KF1F02	KE VS ETA 1B VS ETA 1B	1B 46
C	KF1F02	KE VS ETA 1B VS ETA 1B	1B 47
C	KF1F02	KE VS ETA 1B VS ETA 1B	1B 48
C	KF1F02	KE VS ETA 1B VS ETA 1B	1B 49
C	KF1F02	KE VS ETA 1B VS ETA 1B	1B 50
C	KF1F02	KE VS ETA 1B VS ETA 1B	1B 51
C	KF1F02	KE VS ETA 1B VS ETA 1B	1B 52
C	KF1F02	KE VS ETA 1B VS ETA 1B	1B 53
C	KF1F02	KE VS ETA 1B VS ETA 1B	1B 54
C	KF1F02	KE VS ETA 1B VS ETA 1B	1B 55
C	KF1F02	KE VS ETA 1B VS ETA 1B	1B 56
C	KF1F02	KE VS ETA 1B VS ETA 1B	1B 57
C	KF1F02	KE VS ETA 1B VS ETA 1B	1B 58
C	KF1F02	KE VS ETA 1B VS ETA 1B	1B 59
C	KF1F02	KE VS ETA 1B VS ETA 1B	1B 60
C	KF1F02	KE VS ETA 1B VS ETA 1B	1B 61
C	KF1F02	KE VS ETA 1B VS ETA 1B	1B 62
C	KF1F02	KE VS ETA 1B VS ETA 1B	1B 63
C	KF1F02	KE VS ETA 1B VS ETA 1B	1B 64
C	KF1F02	KE VS ETA 1B VS ETA 1B	1B 65
C	KF1F02	KE VS ETA 1B VS ETA 1B	1B 66
C	KF1F02	KE VS ETA 1B VS ETA 1B	1B 67
C	KF1F02	KE VS ETA 1B VS ETA 1B	1B 68
C	KF1F02	KE VS ETA 1B VS ETA 1B	1B 69
C	KF1F02	KE VS ETA 1B VS ETA 1B	1B 70
C	KF1F02	KE VS ETA 1B VS ETA 1B	1B 71
C	KF1F02	KE VS ETA 1B VS ETA 1B	1B 72
C	KF1F02	KE VS ETA 1B VS ETA 1B	1B 73
C	KF1F02	KE VS ETA 1B VS ETA 1B	1B 74
C	KF1F02	KE VS ETA 1B VS ETA 1B	1B 75
C	KF1F02	KE VS ETA 1B VS ETA 1B	1B 76
C	KF1F02	KE VS ETA 1B VS ETA 1B	1B 77
C	KF1F02	KE VS ETA 1B VS ETA 1B	1B 78
C	KF1F02	KE VS ETA 1B VS ETA 1B	1B 79
C	KF1F02	KE VS ETA 1B VS ETA 1B	1B 80
C	KF1F02	KE VS ETA 1B VS ETA 1B	1B 81
C	KF1F02	KE VS ETA 1B VS ETA 1B	1B 82
C	KF1F02	KE VS ETA 1B VS ETA 1B	1B 83
C	KF1F02	KE VS ETA 1B VS ETA 1B	1B 84
C	KF1F02	KE VS ETA 1B VS ETA 1B	1B 85
C	KF1F02	KE VS ETA 1B VS ETA 1B	1B 86
C	KF1F02	KE VS ETA 1B VS ETA 1B	1B 87
C	KF1F02	KE VS ETA 1B VS ETA 1B	1B 88
C	KF1F02	KE VS ETA 1B VS ETA 1B	1B 89
C	KF1F02	KE VS ETA 1B VS ETA 1B	1B 90
C	KF1F02	KE VS ETA 1B VS ETA 1B	1B 91
C	KF1F02	KE VS ETA 1B VS ETA 1B	1B 92
C	KF1F02	KE VS ETA 1B VS ETA 1B	1B 93
C	KF1F02	KE VS ETA 1B VS ETA 1B	1B 94
C	KF1F02	KE VS ETA 1B VS ETA 1B	1B 95
C	KF1F02	KE VS ETA 1B VS ETA 1B	1B 96
C	KF1F02	KE VS ETA 1B VS ETA 1B	1B 97
C	KF1F02	KE VS ETA 1B VS ETA 1B	1B 98
C	KF1F02	KE VS ETA 1B VS ETA 1B	1B 99
C	KF1F02	KE VS ETA 1B VS ETA 1B	1B 100

2DCDCTED(30),DCDCTFT(30),FDRCR(30),KEAPI2(77),NEIEU2(77),DCDCLM(30),  
 3AMSBK(30),XCPAR2(77),ECPFI2(77),DCABT(30),ANKRYCY(30),RNCLE2(77),  
 4CLIAS2(77),DCLIA(182),CMI3(231),DEPS3(182),DCLIS2(77),  
 5DCMIG2(77),DCDIG2(77)

DIMENSION TPLS(3000)  
 EQUIVALENCE(ACRES2,TPLS)

1UTVP = 1U

1U = IN

CALL TLRP(NT1,1,ACRES2)  
 CALL TLRP(NT1,1,ACRFD2)  
 CALL TLRP(NT2,2,ACRA2)  
 CALL TLRP(NT3,3,LAMETA)  
 CALL TLRP(NT4,4,AULECR)  
 CALL TLRP(NT21,21,PKCLE2)  
 CALL TLRP(NT10,19,DCCLACC)  
 CALL TLRP(NT5,5,DCCLACS)  
 CALL TLRP(NT6,6,DCCLRCR)  
 CALL TLRP(NT7,7,DCCLACM)  
 CALL TLRP(NT8,8,DCCTFN)  
 CALL TLRP(NT9,9,DCCTFT)  
 CALL TLRP(NT10,10,FDRCR)  
 CALL TLRP(NT11,11,KEAPI2)  
 CALL TLRP(NT12,12,KEIEO2)

TABLE 13 FOLLOWS TABLE 1

CALL TLRP(NT14,14,DCDCLR)  
 CALL TLRP(NT15,15,AMSBK)  
 CALL TLRP(NT16,16,XCPAR2)  
 CALL TLRP(NT17,17,ECPFI2)  
 CALL TLRP(NT18,18,DCART)

TABLE 19 FOLLOWS TABLE 5

CALL TLRP(NT20,20,ANKRYCY)

TABLE 21 FOLLOWS TABLE 4

CALL TLRP(NT22,22,CLIAS2)  
 CALL TLRP(NT23,23,DCLIA)  
 CALL TLRP(NT24,24,CMI3)  
 CALL TLRP(NT25,25,CMI3)  
 CALL TLRP(NT26,26,DEPS3)  
 CALL TLRP(NT27,27,DCDIG2)  
 CALL TLRP(NT28,28,DCMIG2)  
 CALL TLRP(NT29,29,DCDIG2)

TABLES READ FROM PERM FILE. DO NOT RECREATE PERM FILE.

```

111 = IUTMP
IF(ICR.EQ. 0) RETURN
REWIND 11
BUFFER OUT (IU,1) (TRLS(1),TRLS(3000))
IF (UNIT(IU)) 50,60,60
50 REWIND IU
60 RETURN
END
SUBROUTINE TLRP(NTX,NTI,TARF)
C THIS ROUTINE CALLS ROUTINES INTAB AND OUTTAB TO READ AND PRINT TABLES
C NTX INTEGER VARIABLE WHERE X IS THE TABLE NUMERK -INPUT
C NTI INTEGER CONSTANT, TARF NUMBER -INPUT
C TARF ARRAY IN WHICH THE TABLE IS STORED -OUTPUT
C COMMON /INTARC/IU,IN,IU,ICR,NPTBL,IP
C IF TABLES ARE READ FROM TAPE OR DISK, PRINT THEM ONLY.
IF (ICR.EQ. 0) GO TO 10
NTX = INTAB(TARF)
IF(NTX.LE. 0) CALL TBOMB(NTX,TABLE,NTI)
IF(IP.NE. 0) IER = OUTTAB(0,TABLE)
IF(IP.NE. 0) AND. IER.NE. 0) WRITE(IU,1) NTI,IER
10 FORMAT(50HITROUBLE HAS BEEN ENCOUNTERED WITH PRINTING TABLE ,I3,
1/20HOUTAR ERROR FLAG = ,I2 )
RETURN
END
SUBROUTINE PTRINT(NT)
C THIS ROUTINE CREATES A BACKUP FILE FOR TABULAR FUNCTIONS, STORED IN
C COMMON. IT UPDATES THE PERMANENT FILE OF TABLES OR SAVES A BACKUP
C FILE, IF PROBLEMS OCCUR IN READING TABLE MOVS IN SUBROUTINE RDEPTB.
C
REAL KEAPI2,KEIEO2,LAMETA
COMMON
ACRFS2(77),ACRFD2(77),ADCR2(77),LAMEIA(30),
1ADLECR (30),DCLACC(30),DCLACK(30),DCLACM(30),
2DCDTFC(30),DCDTFT(30),FDRCK(30),KEAPI2(77),KEIEU2(77), DCDCLM(30),
3AMSBK(30),XCPAR2(77),FCPFI2(77),DCABT(30),AKRYCY(30),BKCLE2(77),
4CLIAS2(77),DCLI3(182),CDI3(231),CMI3(231),DEPS3(182),DCLIG2(77),
5DCMIG2(77),DCDTG2(77)
COMMON /INTARC/IU,IN,IU,ICR,NPTBL,IP
DIMENSION TRLS(3000)
EQUIVALENCE (ACRFS2,TRLS)
C TRLS IS USED TO TRANSFER ENTIRE BLOCK OF TABLES IN COMMON

```

```

1  FORMAT(61H)THE FOLLOWING PERMANENT TABLES ARE BEING REVISED AS FOL
1  LWS )
2  FORMAT(44H)PARITY OR FOF ON BUFFER STATEMENT IN PTRUDT // )
    REWIND IU
    REWIND 7
    IF(ICR.NF. 0) GO TO 10
    BUFFERIN(IU,1) (TBL(1),TBL(3000))
    IF(UNIT(IU))10,8,8
    WRITE(10,2)
10  BUFFER OUT (7,1)(TBL(1),TBL(3000))
    READ TABLES TO BE CHANGED
    WRITE(10,1)
    CALL RDEFTR(NT,IEF)
    IF(IEF.EQ. 1) GO TO 20
    WRITE MODIFIED PERMANENT TABLES TO IU
    REWIND IU
    BUFFER OUT (IU,1)(TBL(1),TBL(3000))
    IF(UNIT(IU)) 15,14,14
14  WRITE(10,2)
15  RETURN
20  CALL ONSW(7)
    SWITCH TO BACKUP FILE 7 FOR TABLES
    IU = 7
    RETURN
    END
    SURROUTINE TRUMR(NPTS,ARY,NT)
    THIS ROUTINE SETS A FLAG, ILOST, TO 1, IF AN ERROR OCCURRED WHILE
    READING A TABLE FROM CARDS.
    NPTS  ERRONEOUS NUMBER OF POINTS, RETURNED BY INTAB.
    ARY   ARRAY CONTAINING TABLE (INCORRECT)
    NT    TABLE NUMBER
    ILOST FLAG IN COMMON. = 0, NO PROBLEM. = 1 - JOB MUST BE ABORTED.
    REAL KFAP12,KFTFO2,LAMETA
    COMMON      ACRES2(77),ACRF2(77),ADCR2(77),LAMETA(30),
1ADLECR (30),DCLACC(30),DCLACR(30),DCLACM(30),
20CDTFT(30),DCDTFT(30),FDRCR(30),KEAP12(77),KEIEJ2(77), DCDCLN(30),
3AMSPR(30),XCPAR2(77),FCPF12(77),DCABT(30),AKRYCY(30),AKCLF2(77),
4CLIAS2(77),DCLI3(182),CMI3(231),DEPS3(182),DCLIG2(77),
5DCMIG2(77),DCDIG2(77)

```



```

COMMON /TROWH/ ILOST
COMMON /INTARC/IO,IN,IO,ICR,NPBL,IN
COMMON /OUTARC / IOT
ILOST = 1
WRITE(IO,1) NT,NPTS
ER = OUTARC(50,ARY)
RETURN
FORMAT(15HIERRO IN INPUT DATA, TABLE NUMBER ,13,16H)AS POINT COUN
IT , 15,120H TABLE FOLLOWS (10 LOCATIONS) )
END
SUBROUTINE CASINI

```

HILIFT INPUT ROUTINE P.O.J. REIG 12/72

CARD	C01	TITLE
------	-----	-------

TITLE 72 CHARACTER TITLE FOR EACH CASE

PART I - FREE AIR SECTION 1, COEFFICIENT OF LIFT

CARD	C02	FLAP TYPE
------	-----	-----------

FLAP FLAP TYPE 1-SINGLE SLOT, 2-DOUBLE SLOT, 3-DOUBLE SLOT, DBLE HINGE  
4-TRIPLE SLOTTED

ATTBL = NTTBL - NUMBER OF TEMPORARY TABLE UPDATES

CARDS	C03	TEMP TABLES
-------	-----	-------------

\*\* SEE SECTION 2 FOR FORMAT OF TABULAR DATA

CARD	C04	GEOM CL
------	-----	---------

WGROSS GROSS WING AREA  
WREF REFERENCE WING AREA  
WSPAN WING SPAN  
WPERMT SEMI PERIMETER OF WING GROSS AREA

CARD	C05	TYP 1 - 4
------	-----	-----------

C CPRISE WING CHORD NORMAL TO 1/2 CHORD LINE WITH FLAPS  
 C CFLAP FLAP CHORD NORMAL TO 1/2 CHORD LINE SINGLE SLOT  
 C ACCORD ALPHA SWEEP ANGLE OF WING 1/4 CHORD LINE.  
 C AHCORD ALPHA SWEEP ANGLE OF WING 1/2 CHORD LINE.  
 C AHLEFT ALPHA SWEEP ANGLE OF AFT HINGE LINE.  
 C CARD COA NO. FLAP ANGLES  
 C ADELAP = NOFLAP - NUMBER OF FLAP DEFLECTIONS - MAXIMUM OF 4.  
 C \*\* CARD COT TYPE 1+2  
 C DELAP FLAP DEFLECTION, TYPE 1 AND 2. ARRAY  
 C CARD COT TYPE 3+4  
 C DEFWD FWD FLAP DEFLECTION, TYPE 3 AND 4. ARRAY  
 C DELEFT AFT FLAP DEFLECTION, TYPE 3 AND 4. ARRAY  
 C \*\* CARD COT TYPE 3+4  
 C CARD R NUMBER FOR FLAP TYPES 3 AND 4  
 C CFWD FORWARD FLAP CHORD MEASURED STREAMWISE.  
 C CPELAP FORWARD FLAP CHORD MEASURED NORMAL TO 1/2 CHORD LINE.  
 C CAFT AFT FLAP CHORD MEASURED NORMAL TO 1/2 CHORD LINE.  
 C AHLEWD ALPHA SWEEP ANGLE OF FORWARD HINGE LINE.  
 C CARD COO TYPE 1 - 4  
 C FLEIN NON DIMENSIONAL WING SEMI SPAN TO INBOARD FLAP EDGE (ETA) T.O.F.  
 C FLEOUT NON DIMENSIONAL WING SEMI SPAN TO OUTBOARD FLAP EDGE (ETA) T.O.E.  
 C CARD C10 1 CL 1  
 C CLEDGE LEADING EDGE FLAP CHORD NORMAL TO 1/4 CHORD LINE  
 C CHORD WING CHORD NORMAL TO 1/4 CHORD LINE  
 C CLEDGE LEADING EDGE FLAP DEFLECTION, NORMAL TO HINGE LINE (DELTA)  
 C FLEIN NON DIMENSIONAL WING SEMI SPAN TO INBOARD EDGE OF LEADING E+J FLAPS  
 C FLEOUT NON DIMENSIONAL WING SEMI SPAN TO OUTBOARD EDGE OF LEADING E+J FLAPS  
 C CARD C11 1 CL 2  
 C CLAFU COEF OF LIFT FLAPS UP

C ACLEU ANGLE OF ZERO LIFT FLAPS UP  
 C CLMAXU MAX LIFT FLAPS UP  
 C ALPHAI INITIAL ANGLE OF ATTACK  
 C DALPHA INCREMENT TO ALPHA TO CLMAX  
 C CHROFL WING CHORD INCL FOWLER ACTION OF TE NORMAL TO LE

CARD C12 2 CLMAX

PART 1 FREE AIR, SECTION 2 CLMAX

C CLENLE CHORD LENGTH OF LEADING EDGE DEVICE, NORMAL TO L.O.E.  
 C CRONLE TOTAL WING CHORD LENGTH, NORMAL TO L.O.E.  
 C DWTE DELTA (INCREASE) IN WING AREA T.O.E. FLAP  
 C DWLE DELTA (INCREASE) IN WING AREA L.O.E. FLAP  
 C WPGROS BASIC WING AREA INBOARD OF OUTBOARD EDGE OF T.O.E. FLAP  
 C CULE LEADING EDGE FLC MOMENTUM COEFFICIENT  
 C AEDGE = LEADING EDGE TYPE = 1 CONVENTIONAL = 2 SHAPED

CARD C13 3 CDRA

PART 1 FREE AIR, SECTION 3 DRAG

C WGFLEP FLAPPED WING AREA  
 C SPANLE AREA OF L.O.E. DEVICE  
 C CROOPM CHORD, C DOUBLF PRIME, INCLUDING LEADING EDGE EXT, NORMAL TO LE  
 C CDPWFU MINIMUM DRAG, FLAPS UP

CARD C14 4 CM 1

PART 1 FREE AIR SECTION 4 PITCHING MOMENT

C CMQ PITCHING MOMENT FOR ZERO LIFT  
 C APQCHN SWEEP ANGLE, PRIME OF QUARTER CHORD  
 C XAC AERODYNAMIC CENTER OF BASIC WING TRAPEZOID  
 C S2 AREA OF TRAPEZOID BETWEEN IB AND OB FLAP EDGES OF LEADING EDGE FLAPS  
 C DSLE DELTA S, CHANGE IN AREA LE  
 C S2 AREA OF TRAPEZOID BETWEEN IB AND OB FLAP EDGES OF TRAILING EDGE FLAPS

CARD C15 4 CM 2

ALE FLAPS ADJACENT TO BODY SIDE OR NOT. =1, YES, =2, NO LE  
 ATE FLAPS ADJACENT TO BODY SIDE OR NOT. =1, YES, =2, NO TE

CARD C16 4 CM 3

\* \* LEADING EDGE DEVICE DATA FOR AERODYNAMIC CENTERS OF PRESSURE

CHDYB STREAMWISE CHORD AT THE BODY SIDE  
 XB LOCATION OF LEADING EDGE OF CHDYB FROM THE STANDARD ORIGIN  
 CHDPYB STREAMWISE CHORD AT THE BODY SIDE WITH THE LE FLAP EXTENDED

XPR XPRIME BODY SIDE - LOCATION OF THE LEADING EDGE OF CHDPYB WITH LE EXT  
 YR Y BODY SIDE - SPANWISE LOCATION OF THE LEADING EDGE AT THE BODY SIDE  
 YM Y MID SPAN SPANWISE LOCATION OF THE LEADING EDGE AT MIDSPAN LE FLAP

CARD C17 4 CM 4

CH' M STREAMWISE CHORD THROUGH YM AT MIDSPAN  
 XM X MID SPAN - LOCATION OF LEADING EDGE OF CHDYM  
 CHDPYM STREAMWISE CHORD PRIME AT MID SPAN WITH LE EXTENDED  
 XPM X PRIME MID SPAN - LOCATION OF LEADING EDGE OF CHDPYM

\* \* TRAILING EDGE DEVICE DATA FOR AERODYNAMIC CENTERS OF PRESSURE

CARD C18 4 CM 5

CHDYRT STREAMWISE CHORD AT BODY SIDE = CHDYR  
 XRT XR - LOCATION OF THE LEADING EDGE OF CHDYRT  
 CDPYRT STREAMWISE CHORD PRIME BODY SIDE WITH TE EXTENDED  
 XPRTE X PRIME BODY SIDE - LOCATION OF LEADING EDGE OF CDPYRT = XBTE  
 YBTE Y BODY SIDE - SPANWISE LOCATION OF THE STREAMWISE BODYSIDE CHORD, CHDYRT  
 YMTF Y MID SPAN - SPANWISE LOCATION OF THE STREAMWISE MIDSPAN CHORD, CHDYMT

CARD C19 4 CM 6

CHDYMT STREAMWISE CHORD MID SPAN OF TE FLAP  
 XMTF X MID SPAN - LOCATION OF LEADING EDGE OF CHDYMT  
 CPMTE CHORD PRIME AT MID SPAN WITH TE EXTENDED  
 XPMTE X PRIME MID SPAN - LOCATION OF LE OF CPMTE = XMTE

CARD C20 4 CM 7

CRFF REFERENCE CHORD LENGTH  
 CFLIR FLAP CHORD NORMAL TO HALF CHORD LINE AT INBOARD EDGE OF TE FLAP  
 CFLOIR FLAP CHORD NORMAL TO HALF CHORD LINE AT OUTBOARD EDGE OF TE FLAP  
 CPXOR C PRIME - CHORD NORMAL TO 1/2 CHORD LINE OUT BOARD EDGE OF TE FLAP. I  
 CPMIR C PRIME - CHORD NORMAL TO 1/2 CHORD LINE IN BOARD EDGE OF TE FLAP. INCL

CARD C21 4 CM 8

CPFLIR FLAP CHORD I.B. NORMAL TO 1/2 CHORD LINE  
 CPLOIR FLAP CHORD O.B. NORMAL TO 1/2 CHORD LINE  
 XIB LONGITUDINAL INTERSECTION CPMIR AND WING 1/2 CHORD LINE I.B.  
 XOB LONGITUDINAL INTERSECTION CPMOR AND WING 1/2 CHORD LINE O.B.  
 XPOCRD X PRIME - LOCATION OF 1/4 AERODYNAMIC CHORD. INCL LEADING EDGE  
 XCG LONGITUDINAL LOCATION OF CENTER OF GRAVITY

CARD C22 4 CM 9

CMOLEU PITCHING MOMENT ZERO LIFT, FLAPS UP.  
 EPTEOR ETA PRIME TE OR, WING SEMISPAN, LONGITUDINAL LOCATION OF CPMOB  
 AND HALF CHORD LINE  
 EPTEIR ETA PRIME TE IR, WING SEMISPAN, LONGITUDINAL LOCATION OF CPMIB  
 AND HALF CHORD LINE

CARD C23 5 6 7 GE

THGM HEIGHT OF TAIL 1/4 MAC ABOVE OR BELOW WING CHORD PLANE

PART II GROUND EFFECT SECTION 6 LIFT  
 PART II GROUND EFFECT SECTION 7 MAX LIFT

TLGM TAIL LENGTH WING 1/4 MAC TO TAIL 1/4 MAC

NWINGH NUMBER OF WING HEIGHTS TO BE CONSIDERED. MAXIMUM OF FOUR.  
 WHQM ARRAY OF WING HEIGHTS 1/4 MAC

CARD C24 8 TRIMGE

PART II GROUND EFFECT SECTION 8 DRAG

STAIL HORIZONTAL TAIL AREA  
 EPSG DOWNWASH ANGLE AT TAIL AT ZERO ALPHA.  
 DEPDAL RATE OF CHANGE OF DOWN WASH ANGLE AT TAIL. FLAPS UP VS DAPHA.  
 DCPDMM TAIL MINIMUM DRAG COEFF  
 DCDODCL CHANGE IN TAIL DRAG DUE TO TAIL LIFT

CARD C25 0 POWER 1

CDRAW PAV DRAG  
 ENGVEF SIGMA,ENGINE VECTOR ANGLE FROM THE HORIZONTAL IN DEG  
 XNACFL X COORDINATE OF NACELLE FROM AN ARBITRARY ORIGIN  
 XNOZLF X COORDINATE OF NOZZLE FROM AN ARBITRARY ORIGIN  
 ZNOZLF Z COORDINATE OF NOZZLE FROM AN ARBITRARY ORIGIN  
 XINLET X COORDINATE OF INLET FROM AN ARBITRARY ORIGIN  
 ZINLET Z COORDINATE OF INLET FROM AN ARBITRARY ORIGIN

CARD C26 0 POWER 2

NCJ NUMBER OF ENGINE THRUST COEFFICIENTS ON INPUT CARD (MAX 5)  
 ACJ ARRAY OF VALUES OF ENGINE THRUST COEFFICIENTS

COMMON /CASEFIN/ TITLE(18),IFLAP,WGRUSS,WKEF,WPERNT,INDFLAP,  
 ACPRIME,CFLAP,DFLP(4),CFWD,CPFLAP,CAFT,UPFWD,UPART,AVLORD,ANLCRU,  
 1AHLFW,AHLAFT,ETFIN,ETFOU,CLEDGE,CHOKD,DLEDGE,ELEIN,ELEVOUT,CLAFU,  
 2AOLEF,CLFNL,CROWNLE,WGRUS,DVTE,OWLE,CLMAXU,ALPHAI,CULE,DALPHA,  
 3WGLFAP,SPANLE,CHROLF,XCPI,XCPLE,XCP2,XCP2TE,XAC,S2,USLE,S3,CPMUB  
 4,XCG,CREF,CFLIN,CFLON,CPMIB,CPFLIB,CPFLUB,XIB,XUB,FPTETIN,XPWCKD,  
 5XMOLEF,WQW(3),NWINGH,THWM,WCPAN,TLWM,STAIL,EPSFU,DCPDMM,DCDDCL  
 6,CHDYP,CHDYPY,CMD,APUCHD,XPB,XB,YB,YM,CHDYM,XM,CHDPYM,XPM,IEDGE  
 7,CHDYPT,XBTE,COPYRT,XPBT,YRTE,YMTF,CHDYMT,XMTF,CHYTE,XPMTF,  
 8,DFLAP,DEFW(4),DEAF(4),CRDDPM,CDPMFU,EPTEOB,EPSO,DFPDAL  
 9,CJ,ENGVEF,XNACEL,XNOZLE,ZNOZLE,XINLET,ZINLET,CDRAM,ILE,ITE  
 COMMON /INTARC/IN,IN,IC,ICR,NPTBL,TP  
 COMMON /IPAGE/ IPAGE,ICASE  
 COMMON/CJ/NCJ,ACJ(5)  
 COMMON TRLS(1000)

COMMON/BASIC/ARATIO,PI,RAD,AREF

DATA IPAGE/1/

FORMAT( 10F7.0)

FORMAT( 10I7)

FORMAT( 18A4)

FORMAT(1H1,/,115X,4HPAGE,13)

5 FORMAT(1H7,50X,18A4////)

FORMAT(43H0 WING S WING REF

SPAN

PERIMETER )

FORMAT(1X, 10(F7.2,4X) )

FORMAT(1X,10(F8.2,2X) )

FORMAT(1X,10(F8.2,2X) )

FORMAT(1X, 2(F7.2,4X), 7(F7.2,4X) )

FORMAT(1X, F9.2, F14.1,6X,F7.3,4F10.2 )

1

2

3

4

5

6

7

8

9

10

11

CARD COUNT

587

```

FORMAT(56HOUNRECOGNIZED FLAP TYPE PROHIBITS EXECUTION OF THIS CASE
1 // 24H * * * * * / 10H0 * * * * * /
2 17H0 IFLAP = 15 / )
FORMAT(25H0SINGLE SLOTTED FLAP TYPE, 12 / )
FORMAT(25H0DOUBLE SLOTTED FLAP TYPE, 12 / )
FORMAT(29H0DOUBLE SLOTTED DOUBLE HINGED FLAP TYPE, 12 / )
FORMAT(25H0TRIPLE SLOTTED FLAP TYPE, 12 / )
FORMAT(57H0 CPRIME C FLAP SWEEP 1/4C SWEEP 1/2C SWEEP AF
1T)
FORMAT(26H0 ETA 18 TE ETA OR TE )
FORMAT(54H0 CHORD LF C CHORD DELTA LE ETA 18 LE ETA 18 )
FORMAT(69H0CL ALPHA FU ALPHA ZERO L CLMAX FU ALPHA DALPHA
1 CPRIME NLE )
FORMAT(77H0CL NLE CHORD NLE DELS TE DELS LE S PRM GROSS
1 CU LF EDGE TYPE )
FORMAT(29H0S FLAPPED SPAN LE C DBL PM CDPMFU )
FORMAT(44H0CHORDY MID X MID C PRM MID X PM MID )
FORMAT(55H0REF CHORD C FLAP 18 C FLAP OB C PRM 18 C PRM OB )
FORMAT(52H0CPRM FLAP 18 CPRM FLAP 18 X 18 X OB XPRM C/4
1 XCG )
FORMAT(27H0 CM OLFU ETAPRM TE 18 ETAPRM TE OB )
FORMAT(77H0TAIL H TAIL LENGTH NO. WING H.S WING(1) WING H(2)
1 WING H(3) 9ALL MAC/4 )
FORMAT(60H0THE FOLLOWING TABLES ARE BEING MODIFIED FOR THIS CASE U
1NLY. )
FORMAT(57H0 S TAIL EPSILON 0 D EPS/D ALP DCPD MIN CU/CL TAI
1L )
FORMAT(55H0 C FWD C PRIME FWD C AFT SWEEP FWD )
FORMAT(11X, 2(F7.2,4X), 3(F8.2,3X), 1(F8.3,3X), F7.0 )
FORMAT(66H CHORD Y BODY C PRM BODY X PM RDY Y BODY
1Y MID SPAN )
FORMAT(2F7.0,17,7F7.0)
FORMAT(1X, 2(F7.2,4X), 17,4X, 7(F7.2,4X) )
FORMAT(17H0NO FLAP ANGLES , 4( 6HDFWD(,11, 9H) DFAFT(,11, 4H)
1 ) )
FORMAT(17H0NO FLAP ANGLES , 4(6HDFLAP(,11,4H) ) )
FORMAT(18,7X, 9(F8.2,3X) )
FORMAT(29H0 CMO SWEEP PM C/4 XAC IRAP 32,8X,13H0JLE
1 52 )
FORMAT(17H0 LEADING EDGE )
FORMAT(18H0 TRAILING EDGE )

```



```

41  FORMAT(54H0 ARE THE FLAP EDGES ADJACENT TO THE BODY SIDE ON NOT. /
    123H IF FLAG =1,YES. =2,NO., 12H FLAG LE = ,12, 11H FLAG TR = ,12)
42  FORMAT(/32H0FLAP FLAG SET. BEGIN NEXT CASE )
C   43 IS LAST AVAILABLE FORMAT STATEMENT NUMBER.
C   INITIALIZE TABLES IF NECESSARY.
    IF (ICASE.GT.1.AND.NITBL.NE.0) 45,46
45  REWIND IU
    BUFFER IN (IU,1) (TPLE(1),TPLS(3000))
    IF (UNIT(IU))46,150,150
150  WRITE(IO,151)
151  FORMAT(44H1PARITY OF FOR ON BUFFER STATEMENT IN CASINI //)
46  READ(IN,3) TTITLE
C   *   FORTRAN EXTENDED FOR 1FST
    IF(FOF(IN)) 47,57
    IF(FOF,IN ) 47,57
47  STOP 2
57  WRITE(IO,4) IPAGE
    WRITE(IO,5) TTITLE
    READ(IN,1) AFLAP,ATTBL
    NTBL = ATTBL
    IF(NTBL.EQ.0) GO TO 48
    WRITE(IO,27)
    IPAGE = IPAGE + 1
    CALL RDEFT8(NTTRL,IFR)
    WRITE(IO,4) IPAGE
48  CONTINUE
    IFLAP = AFLAP
    IFLAG = 0
    IF(IFLAP.LE.0.OR. IFLAP.GT.4) 49,50
    WRITE(IO,12) IFLAP
C   PROBLEM WITH FLAP TYPE - MUST STOP THIS CASE - SET IFLAG = 1
    IFLAG = 1
    GO TO 60
50  GO TO(51,52,53,54 ), IFLAP
51  WRITE(IO,13) IFLAP
    GO TO 60
52  WRITE(IO,14) IFLAP
    GO TO 60
53  WRITE(IO,15) IFLAP
    GO TO 60
54  WRITE(IO,16) IFLAP

```

\*\*\*  
FTN\*\*  
RUN

```

60 READ(IN,1) WGRSS,WREF,WSPAN,WPERMT
   WRITE(IO,6)
   WRITE(IO,8)WGRSS,WREF,WSPAN,WPERMT
   WRITE(IO,17)
   READ(IN,1) CPRIME,CFLAP,ACCORD,AHCUKD,AHLAFT
   WRITE(IO,7) CPRIME,CFLAP,ACCORD,AHCUKD,AHLAFT
   READ(IN,1) ADELAP
   NDELAP= ADELAP
   IF (IFLAP.GT.2) GO TO 70
   WRITE(IO,36) (I,I=1,NDELAP)
   READ(IN,1) (DELPI,I=1,NDELAP)
   WRITE(IO,37) NDELAP, (DELPI,I=1,NDELAP)
   GO TO 80

70 WRITE(IO,35) (I,I=1,NDELAP)
   READ(IN,1) (DEFW(I),DEFAF(I),I=1,NDELAP)
   WRITE(IO,37) NDELAP, (DEFW(I),DEFAF(I),I=1,NDELAP)
   WRITE(IO,29)
   READ(IN,1) CFW,CDELAP,CAFT,AHLEWD
   WRITE(IO,7) CFW,CDELAP,CAFT,AHLEWD
   CONTINUE

   WRITE(IO,18)
   READ(IN,1)
   WRITE(IO,9)
   WRITE(IO,19)
   READ(IN,1)
   WRITE(IO,10)
   WRITE(IO,31)
   READ(IN,1)
   WRITE(IO,11)
   WRITE(IO,20)
   READ(IN,1)
   WRITE(IO,30)
   IFGE=AFDGE
   WRITE(IO,21)
   READ(IN,1)
   WRITE(IO,9)
   WRITE(IO,38)
   READ(IN,1)
   WRITE(IO,8)
   READ(IN,1) ALE,ATF
   ILE=ALF

   CLFDGE,CHORD,ULEDGE,ELLIN,ELEOUT
   CLEDGE,CHORD,ULEDGE,ELLIN,ELEOUT
   CLAFI,AULFU,CLMAXU,ALPHA1,DALPHA,CHRDLE
   CLAFU,AOLFU,CLMAXU,ALPHA1,DALPHA,CHRDLE
   CLENLE,CRONLE,DWLE,DWLE,WPKUS,CULE,AFDGE
   CLENLE,CRONLE,DWLE,DWLE,WPKUS,CULE,AFDGE
   WGFLAP,SPANLE,CRDDPM,CDPMFU
   WGFLAP,SPANLE,CRDDPM,CDPMFU
   CMO,APQCHD,XAC,S2,DSLF,S3
   CMO,APQCHD,XAC,S2,DSLF,S3
   ALE,ATF
   ILE=ALF

```

```

ITF=ATF
WRITE(10,41) ILF,ITF
WRITE(10,39)
WRITE(10,32)
READ(IN,1) CHDYB,XH,CHDPYB,XPB,YB,YM
WRITE(10,7) CHDYB,XH,CHDPYB,XPB,YB,YM
WRITE(10,22)
READ(IN,1) CHDYM,XM,CHDPYM,XPM
WRITE(10,7) CHDYM,XM,CHDPYM,XPM
IPAGE=IPAGE+1
WRITE(10,4) IPAGE
WRITE(10,5) TITLE
WRITE(10,40)
WRITE(10,32)
READ(IN,1)
WRITE(10,7) CHDYRT,XRTF,CDPYBT,XPRTF,YBTF,YMTE
WRITE(10,22)
READ(IN,1) CHDYMT,XMTF,CPYMTF,XPMTE
WRITE(10,7) CHDYMT,XMTF,CPYMTF,XPMTE
WRITE(10,23)
READ(IN,1) CREF,CFLIB,CFLOR,CPMIB,CPMOB
WRITE(10,8) CREF,CFLIB,CFLOR,CPMIB,CPMOB
WRITE(10,24)
READ(IN,1) CPFLIR,CPFLOB,XIB,XOR,XPGCRD,XCG
WRITE(10,7) CPFLIR,CPFLOB,XIB,XOR,XPGCRD,XCG
WRITE(10,25)
READ(IN,1) CMOLFU,EPTIN,EPTIOB
WRITE(10,9) CMOLFU,EPTIN,EPTIOB
WRITE(10,26)
READ(IN,33) THQM,TLQM,NWINGH,(WHQM(I),I=1,NWINGH)
WRITE(10,34) THQM,TLQM,NWINGH,(WHQM(I),I=1,NWINGH)
WRITE(10,28)
READ(IN,1) STAIL,EPSO,DEPDAL,DCPDWN,DCDDCL
WRITE(10,9) STAIL,EPSO,DEPDAL,DCPDWN,DCDDCL
WRITE(10,43)
43 FORMAT( 77H0 RAM DRAG SIGMA ENG X NACELLE X NUZZLE Z NUZ
1ZLF X INLET 2 INLET )
READ(IN,1) CDRAM,ENGVEC,XNACEL,XNOZLE,ZNOZZLE,XINLET,ZINLET
WRITE(10,8) CDRAM,ENGVEC,XNACEL,XNOZLE,ZNOZZLE,XINLET,ZINLET
WRITE(10,101)
101 FORMAT( 63H0NO. OF CJ CJ(1) CJ(2) CJ(3) CJ(4)

```

```

1      CJ(5) )
100  READ(IN,160)NCJ,(ACJ(I),I=1,NCJ)
101  FORMAT(17,5F7.0)
102  WRITE (10,102)NCJ,(ACJ(I),I=1,NCJ)
103  FORMAT(5X,11,5X,5(F7.2,4X))
104  SET  CARD READER FLAG TO RESTORE TABLES
105  ICR = 0
106  * *
107  * CONVERT ALL ANGLES TO RADIANS AND STORE IN SAME LOCATIONS
108  * CONVERT FEET TO INCHES (AS READ) AND STORE IN SAME LOCs.
109  *
110  * ACCORD = ACCORD/RAD
111  * AHCORD = AHCORD/RAD
112  * AOLFU = AOLFU /RAD
113  * ALPHAI = ALPHAI/RAD
114  * DALPHA = DALPHA/RAD
115  * APOCHD = APOCHD/RAD
116  * EPSO = EPSO /RAD
117  * DEPDAL = DEPDAL/RAD
118  * AHLAFT=AHLAFT/RAD
119  IF (IFLAP.GT.2) AHLFWD=AHLFWD/RAD
120  DLEDGF=DLFDGF/RAD
121  ENGVEC=ENGVEC/RAD
122  WSPAN = 12.*WSPAN
123  WPERMT = 12.*WPERMT
124  CPRIME = 12.*CPRIME
125  CFLAP = 12.*CFLAP
126  CPFLAP = 12.*CPFLAP
127  CAFT = 12.*CAFT
128  CLEDGF = 12.*CLEDGF
129  CHORD = 12.*CHORD
130  CHRDLE = 12.*CHRDLE
131  CLNLF = 12.*CLNLF
132  CRDNLF = 12.*CRDNLF
133  CRDDPM = 12.*CRDDPM
134  XAC = 12.*XAC
135  CHDYR = 12.*CHDYR
136  YR = 12.*YR
137  CHDPYR = 12.*CHDPYR
138  XPR = 12.*XPR
139  YR = 12.*YR

```

```

200
YM =12.*YM
CHDYA =12.*CHDYA
XM =12.*XM
CHDPY =12.*CHDPY
XPM =12.*XPM
CHDYRT =12.*CHDYRT
XRT =12.*XRT
CPDYRT =12.*CPDYRT
XPRT =12.*XPRT
YRT =12.*YRT
YMT =12.*YMT
CHDYMT =12.*CHDYMT
XMT =12.*XMT
CPYMT =12.*CPYMT
XPMT =12.*XPMT
CRFF =12.*CRFF
CFLR =12.*CFLR
CFLO =12.*CFLO
CPMR =12.*CPMR
CPMR =12.*CPMR
CPFLR =12.*CPFLR
CPFLR =12.*CPFLR
YR =12.*YR
XOR =12.*XOR
YPCRD =12.*YPCRD
XCG =12.*XCG
THQM=12.*THQM
TLQM =12.*TLQM
DO 200 II=1, NWINGH
WHQM(II)= 12.*WHQM(II)
XNOZLE =12.*XNOZLE
7NOZLE =12.*7NOZLE
XINLET =12.*XINLET
7INLET =12.*7INLET
IF(IFLAG .EQ.0 ) RETURN
WRITE(10,42)
IPAGE=IPAGE+1
GO TO 45
END

```

C SURROUTINE RDEFTR(NT,IFF)  
C RDEFTR REDEFINES NT TABLES IN THE COMMON BLOCK.

```

THE REPLACED TABLES ARE READ FROM THE CARD READER.
IFF - ERROR FLAG = 0 SUCCESSFUL READ. = 1 UNSUCCESSFUL, SO DO NOT
UPDATE THE PERMANENT FILE TABLE.

REAL KEAPI2,KE1FO2,LAMETA
COMMON
  ACRES2(77),ACKED2(77),ADCKA2(77),LAMETA(30),
  1ADLECR(30),DCLACC(30),DCLACR(30),DCLACM(30),
  2DCOTFD(30),DCOTFT(30),FORCK(30),KEAPI2(77),KE1FO2(77),DCDCLK(30),
  3AMSR(30),XCPAR2(77),ECPFI2(77),DCABT(30),ANKVY(30),RNCLE2(77),
  4CLIAS2(77),DCLIA(182),CUI3(231),CMI3(231),DEPS3(182),DCLIG2(77),
  5DCMIG2(77),DCDIG2(77)
INTEGER TNAME

FOR ADDITION OF NEW TABLES, UPDATE LENGTH OF TNAME, DATA ENTRIES AND DO 10
3 LATER - CHANGE FIRST DIMENSION OF TNAME AS TABLES ARE ADDED. ***
DIMENSION DUM(128),IRLS(3000),TNAME(29,2)
EQUIVALENCE (ACRES2,IRLS)
COMMON /INTARC/II,IN,IO,ICR,NPTRL,IP
DATA TNAME
  1ADCLACC,6HDCCLACS,6HDCCLCR,6HDCCLACM,6HDCCLTF,6HDCCLTFI,6HDCCLCR,
  26HKEAPI2,6HKE1FO2,6HDCCLCR,6HDCCLCR,6HDCCLCR,6HDCCLCR,6HDCCLCR,
  36HAKRYCY,6HKBKCLE2,6HKBKCLAS2,6HKBKCLAS,6HKBKCLAS,6HKBKCLAS,6HKBKCLAS,
  44HDCMIG2,6HDCDIG2,
  51,78,155,232,262,322,352,382,412,442,472,502,579,656,686,716,
  6793,870,900,930,1307,1354,1256,1497,1728,1910,1937,2037,2141
  ITVP = IP
  IU = IN
  FORMAT(10A7)
  1 FORMAT(41HNO MATCH FOUND FOR PERMANENT TABLE NAME , A12,
  2 1 55HNO THE TABLE FOLLOWS, BUT IS NOT BEING USED FOR THIS RUN. )
  3 FORMAT(34H1TABULAR DATA FOR PERMANENT TABLE , A12/,71H IS IN ERRO
  4R. OLD BACKUP FILE OF TABLES WILL BE USED. CORRECT INPUT. /
  529H FIRST CARD OF TABLE FOLLOWS )
  DO 100 K = 1,N
  READ(IN,1) NAME
  DO 10 I=1,29
  II=I
  IF(NAME.EQ.TNAME(I,1))GO TO 20
  10 CONTINUE
  2 NO MATCH FOUND.
  WRITE(10,2)NAME
  N=INTAR(DUM)
  ***

```

```

      ER = OUTTAB(0,NIV)
      GO TO 100
C   TABLE NAME FOUND
      20 INAM = TNAME(II,2)
      N = INTAB(TPLS(INAM))
      IF(N.GT.0)GO TO 30
C   ERROR ON PERMANENT UPDATE READ. PLRM FILE CANNOT BE UPDATED. SET FLAG
      IFF = 1
      WRITE(10,3) NAME, N
      ER = OUTTAB(0,TPLS(INAM))
      GO TO 100
      30 ER = OUTTAB(0,TPLS(INAM))
      100 CONTINUE
      IIV = ITMP
      RETURN
      END
C   SUBROUTINE CASOUT(IMODE,WINGH)
C   THIS ROUTINE PRINTS OUT THE RESULTS FOR EACH CASE AFTER IT IS
C   COMPUTED.
      IMODE 1 - FIRST ENTRY BASIC DATA, FREE AIR, GROUND EFFECT WINGH(1)
           = 2 - GROUND EFFECT WINGH(2), ETC.
      WINGH WHQM(1), I=1 FOR IMODE(1), ETC.
C   CLAFU LIFT CURVE SLOPE FLAPS UP
C   CLAFD LIFT CURVE SLOPE FLAPS DOWN
C   CLTO COEF LIFT TAIL OFF FREE AIR
C   AOLFU ANGLE OF ATTACK FOR ZERO LIFT - FLAPS UP
C   LFD ANGLE OF ATTACK FOR ZERO LIFT - LE DOWN
C   TFD ANGLE OF ATTACK FOR ZERO LIFT - TE DOWN
C   FD ANGLE OF ATTACK FOR ZERO LIFT - BOTH DOWN
C   DCLBFD FLAP LIFT INCREMENT BOTH FLAPS DOWN
C   CLMAXU MAX LIFT FLAPS UP
C   CLMAXD MAX LIFT FLAPS DOWN
C   CDRMFU MINIMUM DRAG FLAPS UP
C   DCDTE MINIMUM DRAG INCREMENT TE FLAPS
C   DCDLE MINIMUM DRAG INCREMENT LE FLAPS
C   CMOLEFU ZERO LIFT PITCHING MOMENT
C   DCMOTE ZERO LIFT PITCHING MOMENT INCREMENT TE
C   DCMOTE ZERO LIFT PITCHING MOMENT INCREMENT LE
C   CMOBFD ZERO LIFT PITCHING MOMENT BOTH FLAPS DOWN

```

```

C CLMAXG MAX LIFT IN GROUND EFFECT - ARRAY FOR SEVERAL WING HEIGHTS
C ALPHA INITIAL ANGLE OF ATTACK FOR LIFT, DRAG, MOMENT COEFFICIENTS
C DALPHA INCRMENT TO ALPHA
C NALPHA NUMBER OF INCRMENTS TO ALPHA
C
C CLTOG COEF LIFT TAIL OFF GROUND EFFECT
C CLTRG COEF LIFT TRIMMED GROUND EFFECT
C CLTRG COEF LIFT TAIL OFF FREE AIR
C CDTO COEF DRAG TAIL OFF FREE AIR
C CDTOG COEF DRAG TAIL OFF GROUND EFFECT
C CDTRG COEF DRAG TRIMMED GROUND EFFECT
C CDTR COEF DRAG TRIMMED FREE AIR
C
C CMTO COEF PITCHING MOMENT TAIL OFF FREE AIR
C CMTOG COEF PITCHING MOMENT TAIL OFF GROUND EFFECT
C CMTRG COEF PITCHING MOMENT TRIMMED GROUND EFFECT
C CMTR COEF PITCHING MOMENT TRIMMED FREE AIR
C
C COMMON /INTARC/IU,IN,IO,ICK,NPTBL,IP
C COMMON /IPAGE/ IPAGE,ICASE
C COMMON/CJ/NCJ,ACJ(5)
C COMMON /CASEIN/ TITLE(18),IFLAP,WGROSS,WKEF,WPERMT,NDFLAP,
ACPRIME,CFLAP,DFLAP(4),CFWD,CPFLAP,CAFT,UFFWD,UFAT,ACCURD,ACCURD,
1AHLFWD,AHLAFT,FTEIN,ETEOUT,CLEGE,CHUNK,DLEDGE,ELEIN,ELEOUT,CLAFU,
2AOLFU,CLENLE,CRDNLE,WPGROSS,DWTE,DWLE,CLMAXU,ALPHA1,CULE,DALPHA,
3WGFAP,SPANLF,CHRDLE,XCPI,XCPLE,XCP2,XCP2TE,XAC,S2,DSLE,S3,CPMVB
4,XCG,CREF,CFLIR,CFLUB,CPMIB,CPFLIR,CPFLUB,XIB,XUB,EPTIN,XPMCKD,
5CMOLFU,WHQM(3),NWINGH,THUM,WSPAN,TLM,STAIL,EPSFU,DCPDMM,DCDDCL
6,CHDYR,CHDPYR,CMU,APUCHD,XPB,XB,YR,YM,CHDYM,XM,CHDPYM,XPM,IEDGE
7,CHDYRT,XBTE,COPYRT,XPBTE,YBTE,YMTE,CHDYMT,XMTE,CPYMT,XPMTE
8,DFLAP,OFFW(4),DEAF(4),CRDDPM,CDPMFU,EPTIOB,EP50,DFPDAL
9,CJ,ENGVEF,XNACFL,XNOZLE,ZNOZLE,XINLET,ZINLET,CDKAM,ILE,ITE
C COMMON /OUTPUT/ NALPHA,CLAFU,CLAFD,AULLFD,AULTFD,AULBFD
1,DCLBFD,CLMAXD,DCOTE,DCULE,DCMOTE,DCMOLE,CDFATR(20),
2CMOBFD,CLMAXG(1)
C COMMON /OUTPUT/ ALPHA(20),CLTU(20),CDTU(20),CMTU(20),CLTR(20),
1CDTR(20),ALPHAG(20),CLTOG(20),CDTOG(20),CMTUG(20),CLTRG(20)
1,CDTRG(20),CLPOFA(20),CLINT(20),CDPOFA(20),CDPOFA(20),DEPOFA(20),
5CLPOGE(20),CDPOGE(20),CMPOGE(20),CLUEIR(20),CDGETR(20),CLFATR(20)
DATA DEG /57.295779/
FORMAT(1H1, 115X, 5HPAGE, 12)
2 FORMAT(/// 49X, 28HANGLES OF ATTACK - ZERO LIFT / 49X, 28(1H-))//

```





PRINT BASIC DATA WHICH REMAINS CONSTANT FOR THIS CASE.

```

IPAGE = IPAGE+1
WRITE (IO,1) IPAGE
WRITE (IO,15) TITLE
WRITE (IO,2)
WRITE (IO,3) AOLEP,AOLLEP,AULTED,AULDED
WRITE (IO,7)
ZZ=CLAFD/DEG
WRITE (IO,4) CLAFU,ZZ ,DCLBED,CLMAXU,CLMAXD
WRITE (IO,8)
WRITE (IO,5) CDPMEU,DCDTE,DCDLE
WRITE (IO,9)
WRITE (IO,14) CMOLEU,DCMOTE,DCMOLE

```

FREE AIR TABLE ALPHA VS COEFFICIENTS

```

IPAGE=IPAGE+1
WRITE (IO,1) IPAGE
WRITE (IO,15) TITLE
WRITE (IO,101)
WRITE (IO,10)
WRITE (IO,11)
IF (IFLAP.LE.2) WRITE (IO,16) ZERO, DS, ZERO
IF (IFLAP.GT.2) WRITE (IO,17) ZERO, DF, DA, ZERO
WRITE (IO,13)
DO 50 I=1,NALPHA
50 WRITE (IO,104) ALPHA(I),CLTU(I),CDTU(I),CLTR(I),CDTR(I)

```

```

IPAGE=IPAGE+1
WRITE (IO,1) IPAGE
WRITE (IO,15) TITLE
WRITE (IO,102)
WRITE (IO,10)
WRITE (IO,11)
IF (IFLAP.LE.2) WRITE (IO,16) CJ,DS,ZERO
IF (IFLAP.GT.2) WRITE (IO,17) CJ,DF,DA,ZERO
WRITE (IO,12)
DO 51 I=1,NALPHA
51 WRITE (IO,104) ALPHA(I),CLPOFA(I),CDPOFA(I),CLPATR(I),
1 CPATR(I)
51 CONTINUE

```

```

C GROUND EFFECT TABLE ALPHA VS COEFFICIENTS
C I MODE - SUBSCRIPT OF WING HEIGHT
C
200 IPAGE = IPAGE + 1
   WRITE (IO,1) IPAGE
   WRITE (IO,15) TITLE
   WRITE (IO,101)
   WRITE (IO,12)
   WRITE (IO,11)
   IF (IFLAP.LE.2) WRITE (IO,16) ZFKO, DS, WUB
   IF (IFLAP.GT.2) WRITE (IO,17) ZFKO, DF, DA, WUB
   WRITE (IO,12)
C
DO 210 I=1,NALPHA
210 WRITE (IO,104) ALPHAG(I), CLTUG(I), CDTUG(I), CMTUG(I), CLING(I),
      1 CDTRG(I)
C
   IPAGE=IPAGE+1
   WRITE (IO,1) IPAGE
   WRITE (IO,15) TITLE
   WRITE (IO,102)
   WRITE (IO,12)
   WRITE (IO,11)
   IF (IFLAP.LE.2) WRITE (IO,16) CJ,DS,WUB
   IF (IFLAP.GT.2) WRITE (IO,17) CJ,DF,DA,WUB
   WRITE (IO,13)
DO 300 I=1,NALPHA
300 WRITE (IO,104) ALPHAG(I), CLPUGE(I), CDPUGE(I), CMPUGE(I), CLGETR(I),
      1 CDGETR(I)
200 CONTINUE
C
C CONVERT DEGREES BACK TO RADIANS FOR NEXT GROUND HEIGHT.
DO 220 I=1,NALPHA
220 ALPHA(I) = ALPHA(I)/DEG
   ALPHAG(I) = ALPHAG(I)/DEG
   AOLFI = AOLFI /DEG
   RETURN
END
SUBROUTINE LIFT(IFERROR)
COMMON /INTABC/II,IN,IO,ICK,NPTBL,IP

```

```

REAL KEAPI2,KEFIFO2,LAMETA
COMMON
  ACRFS2(77),ACRFD2(77),ADCKA2(77),LAMETA(30),
  1ADLCR(30),DCLACC(30),DCLCKC(30),DCLACM(30),
  2DCLTFD(30),DCLTFT(30),DCKCK(30),KEAPI2(77),KEFIFO2(77),DCKCLN(30),
  3AMSBR(30),XCPAR2(77),ECPE12(77),DCAHT(30),AKKYCY(30),DCKLE2(77),
  4CLIAS2(77),DCLI3(182),CMI3(231),DEPSJ(182),DCLIG2(77),
  5CMIG2(77),DCLIG2(77)
COMMON/BASIC/ARATIO,PI,RAD,AREF
COMMON/INTER/DCLTF,ETATE,DCLLE,DEPST,DCLB
COMMON /CASEIN/ TITLE(18),IFLAP,WGRUSS,WREF,WPERMT,NDFLAP,
ACPRIME,CFLAP,DFLP(4),CFWD,CPLAP,CAFT,DFFWD,DFAFT,AWCCKU,AMCURU,
1AHLFWD,AHLAFT,ETEIN,ETFOUT,CLEDGE,CHUKD,DLEDGE,ELEIN,ELEOUT,CLAFU,
2AULFU,CLENLE,CRONLF,WGRUSS,DWTE,DWLE,CLMAXU,ALPHA1,CULE,DALPHA,
3WGLAP,SPANLE,CHROLE,XCPI,XCPLE,XCP2,XCP2TE,XAC,52,DSLE,53,CPMUB
4,XCG,CREF,CFLIR,CFLOR,CPMIR,CPFLIR,CPFLUB,XIB,XUR,FPIEIN,XPWCKD,
5CMOLFU,WHQM(3),NWINGH,THUM,WSPAN,TLM,STAIL,EPSTU,DCPDMM,DCDDCL
6,CHDYB,CHDPYB,CMO,APUCHD,XPB,XB,YB,YM,CHDYM,XM,CHDPYM,XPM,IEDGF
7,CHDYBT,XBTE,COPYRT,XPRT,YBTE,YMTE,CHDYMT,XMTE,CPYMT,XPMTE
8,DFLAP,DEFW(4),DEFAF(4),CRDUPM,COPMFU,EPTEOB,EPSTU,DEPDAL
9,CJ,FNGVFC,XNACEL,XNUZLE,XNUZLE,XINLET,ZINLET,CUKAM,ILE,ITE
COMMON /OUTPUT/ NALPHA,CLAFD,AULLEF,AULTFD,AULBFD
1,DCLBFD,CLMAXU, DUTE,DCULE,DCMUTE,DCMULE,CJFATR(20),
2CMORFD,CLMAXG(3),ALPHA(20),CLTU(20),CDTU(20),CMTU(20),CLTK(20),
1CDTR(20),ALPHA(20),CLTUG(20),CDTUG(20),CMTUG(20),CLTRG(20)
1,CDTRG(20),CLPOFA(20),CLINT(20),CDPUFA(20),CMTUFA(20),DEPUFA(20),
5CLPOGF(20),CDPOGF(20),CMPUGF(20),CLGETR(20),CDGETR(20),CLFATR(20)
DIMENSION V(3), OI(3)
DATA OI/3*1./
**
*****
**
IFERROR=0
ARATIO=WSPAN**2/(144.*WGRUSS)
AREF=WSPAN**2/(WREF*144.)
**
** FLAP DOWN LIFT CURVE SLOPE
**
**
X=2.*PI*ARATIO/((WPERMT/WSPAN)*ARATIO+2.)
CLAFD=X*(WGRUSS/WREF)

```

```

*****
**
** SHIFT IN ANGLE OF ATTACK FOR ZERO LIFT WITH 10% FLAP, CORR.
**
*****
IF (IFLAP.LE.0.0R.IFLAP.GT.4) GO TO 9100
V(1)=ETFIN
ZIN=TRL(LAVETA,V.01,IF)
V(1)=FTFOUT
ZOUT=TRL(LANETA,V.01,IF)
IF (IF.NE.0) GO TO 9100

STATE=ZOUT-ZIN
IF (IFLAP.GT.2) GO TO 10

**
** SINGLE AND DOUBLE SLOTTED-SINGLE HINGED FLAPS (TYPES 1-2)
**
ZZA=TAN(DFLAP)*COS(AHCOR0-AHLAFT)
DE1=ATAN(ZZA)
V(1)=CFLAP/CPRIME
V(2)=DFLAP
IF (IFLAP.EQ.1) X=TRL(ACRFS2,V.01,IF)
IF (IFLAP.EQ.2) X=TRL(ACRFD2,V.01,IF)
IF (IF.NE.0) GO TO 9100

V(1)=CFLAP/CPRIME
V(2)=1./ARATIO
V=TRL(ACRA2,V.01,IF)
IF (IF.NE.0) GO TO 9100

DAOL=X*DE1*Y*ETATE*((COS(AHCOR0))*2/COS(AHCOR0))
GO TO 200

100 CONTINUE
**
** DOUBLE AND TRIPLE SLOTTED-DOUBLE HINGED FLAPS (TYPES 3-4)
**
ZZA=TAN(DFLAP)*COS(AHCOR0-AHLAFT)
DE1=ATAN(ZZA)
ZZA=TAN(DFLAP)*COS(AHCOR0-AHLAFT)

```

```

DE2=ATAN(ZZA)
V(1)=CPFLAP/CPRIME
V(2)=CFEWD
IF (IFLAP.NE.4) X1=TRL(ACR+D2,V,D1,1E)
IF (IFLAP.EQ.4) X1=TRL(ACR+D2,V,D1,1E)
IF (IF.NE.0) GO TO 9100

V(1)=CAFT/CPRIME
V(2)=CFEFT
X2=TRL(ACRES2,V,D1,1E)
IF (IF.NE.0) GO TO 9100

V(1)=CPFLAP/CPRIME
V(2)=1./ARATIO
Y=TRL(ACRA2,V,D1,1E)
IF (IF.NE.0) GO TO 9100

DAOL=(X1*DE1+X2*DE2)*Y*ETATE*((COS(AMOUN2))*R2/COS(AMOUN1))

200 CONTINUE
IF (IP.NE.2) GO TO 7000
WRITE (10,8000)DE1,DE2,ZIN,ZOUT,DAOL,X1,X2
8000 FORMAT(1H1,27HDE1,DE2,ZIN,ZOUT,DAOL,X1,X2/ 7(1X,F10.4))
7000 CONTINUE
**
** T.O.F. FLAP INCREMENT AT THE ANGLE FOR ZERO LIFT WITH
** FLAPS RETRACTED
**
DCLTF=CLAFD*(-DAOL)
**
** BODY CARRY OVER LIFT INCREMENT
**
V(1)=DCLTF
V(2)=FTEIN
X=TRL(BKCLE2,V,D1,1E)
IF (IF.NE.0) GO TO 9100

DCLP=DCLTF*X*(ZIN/ETATE)
**

```

```

**  SHIFT IN ANGLE OF ATTACK FOR ZERO LIFT WITH L.O.F. FLAPS DOWN **
**
V(1)=CLEDEGE/CHORD
X=TRL(ADLECR,V,DI,IF)
IF (IF.NE.0) GO TO 9100

V(1)=ELEIN
ZIN=TRL(LAMETA,V,DI,IF)
V(1)=ELFOUT
ZOUT=TRL(LAMETA,V,DI,IF)
IF (IF.NE.0) GO TO 9100

ETALE=ZOUT-ZIN
DAOLLE=X*DLFDFG*(COS(ACCORD)*ETALE

**
**  L.O.F. LIFT INCREMENT AT ANGLE FOR ZERO LIFT FLAPS RETRACTED
**
DCLLF=CLAFD*(-DAOLLE)

**
**  L.O.F. AND T.O.F. FLAP LIFT INCREMENT AT ANGLE FOR ZERO LIFT
**  WITH FLAPS DOWN
**
DCLBFD=DCLLF+DCLTF+DCLH

**
**  ANGLE OF ATTACK FOR ZERO LIFT L.O.F. FLAPS DOWN
**
AOLEFD=AOLEFD+DAOLLE

**

```

CARD COUNT 647







```

IF (IP.NF.0) GO TO 9100
SLOPE=Y1/X1
IF (IP.NF.2) GO TO 7001
WRITE (IO.8001)X,Y,DCLCAM,X1,Y1,SLOPE
FORMAT(IH0.284X,Y,DCLCAM,X1,Y1,SLOPE / (10(1X.F10.4)))
7001 CONTINUE
X=(CLMAXU+DCLMLF)*(DATE/(WPGROS+DWLE))
Y=SLOPE*(COS(ACCORD))**2
Z=(CLEGE/CHORD-CLEHKE/CHKOLE)*(WPGROS+DWLE)/WKEE
DCLFOW=(X-Y*Z)*ETATE
DCLMTE=DCLCAM+DCLFOW
IF (IP.NF.2) GO TO 7002
WRITE (IO.8002)X,Y,Z,DCLFOW,ETATE,DCLMTE
FORMAT(IH0.254X,Y,Z,DCLFOW,ETATE,DCLMTE / (10(1X.F10.4)))
7002 CONTINUE
**
** LIFT INCREMENT FROM LEADING EDGE RLC
**
V1)=CULE
X=TRL(DCLACM,V,01,IF)
DCLBLC=X*(COS(ACCORD))**2
**
** MAX LIFT FLAPS DOWN
**
CLMAXD=CLMAXU+DCLMLF+DCLMTE+DCLBLC
**
** GENERATE ANGLES OF ATTACK AND CORRESPONDING LIFT COEFF.
**
XEWANG=ALPHA1
DO 300 I=1,20
IF ((CLAFD*(XEWANG-AOLBPD))>.GT.CLMAXD) GO TO 920
NALPHA=I
ALPHA(I)=XEWANG
CLTO(I)=CLAFD*(XEWANG-AOLBPD)
XEWANG=XEWANG+DALPHA
300 CONTINUE
GO TO 9200

```

```

0100 CONTINUE
1 ERROR=1

0200 CONTINUE
RETURN
END

SUBROUTINE DRAG( IERROR)
REAL KEAPI2,KEIF02,LAMETA
COMMON
1 ADELFR (30),DCLACC(20),DCLACK(30),DCLACK(30),DCLACK(30),
2 DCLTFC(30),DCLTFT(30),DCLTFR(30),KEAPI2(77),KEIF02(77),DCLACK(30),
3 AMSRR(30),XCPAR2(77),ECPET2(77),DCAET(30),AKRYCY(30),DCLC2(77),
4 CLIAS2(77),DCLT3(182),CPI3(231),DEPS3(132),DCLIG2(77),
5 DCMIG2(77),DCLIG2(77)
COMMON/INTER/DCLT,FIATE,DCLIE,DEPSF,DCLB
COMMON/RASIC/ARATIO,PI,RAD,AREF
COMMON /CASEFIN/ TITLE(18),IFLAP,WGROSS,WKEF,XPERNT,NOELAP,
ACPRIME,CFLAP,DFLP(4),CFWD,CPFLAP,CAFI,DFEWD,LFAPT,AGCWD,AICWD,
1 AHEWD,AHLAFT,ETEIN,TEOUT,CLEDDGE,CUORD,CLEDDGE,ELEIN,ELEOUT,CLAFU,
2 AOLEF,CLENLE,CRONLF,PPGRUS,QWTF,DWLE,CLMAXU,ALPHA1,CULF,DALPHA,
3 WGFELAP,SPANLE,CHROLF,XCP1,XCPLE,XCP2,XCP2FE,XAC,22,DULE,S3,CPMUD
4,XCG,CREF,CFLIP,CFLOR,CPMIP,CPFLIR,CPFLUD,XIR,XOR,EPTIEN,XPMUCND,
5 CROLEF,WHW(13),NVAINGH,THUM,WCPAN,TLAM,STAL,EPSFU,DCPDMM,DCDDCL
6,CHDYP,CHDPYP,CMO,APACHD,XPR,XH,YR,YM,CHDYM,XM,CHDPYM,XPM,IEDGE
7,CHDYAT,XRTE,COPYRT,YPRT,YRTE,YMTE,CHDYMT,XMTE,CPYMT,XPMTE
8,DELAP,DEFW(4),DEAF(4),CRDDPM,CDPMFU,EPTESB,EPSO,DEPDAL
9,CJ,ENGVEF,XNACFL,XNUZLE,ZNUZLE,XINLET,ZINLET,CDNAM,ILE,ITE
COMMON /OUTPUT/ NALPHA,CLAFD,AULFED,AULFID,AULBFD
1 DCLBFD,CLMAXD,
2 CMORFD,CLMAXG(3),ALPHA(20),CLT(20),CHT(20),CHT(20),CLIN(20),
3 CTR(20),ALPHAG(20),CLTUG(20),CDTUG(20),CHTUG(20),CLING(20)
4,CDTRG(20),CLPOFA(20),CLINI(20),CDPOFA(20),CMPOFA(20),CLPOFA(20),
5 CLPOGE(20),CDPOGE(20),CMPOGE(20),CLSEFR(20),CDSEFR(20),CLFAIR(20)
DIMENSION VIC(1),OIC(1)
DATA OI/3*1./
**
*****
**
IERROR=0

```

\*\*\*

```

** ** TRAILING EDGE FLAPS PARASITE DRAG
** **
** IF (IFLAP.LT.3) GO TO 1
V(1)=CPFLAP/CPRIME
V(2)=OFFWD
IF (IFLAP.EQ.3) ALF1=TRL(ACRFS2,V,DI,IE)
IF (IFLAP.EQ.4) ALF1=TBL(ACRFD2,V,DI,IE)
IF (IF.NE.0) GO TO 9100

V(1)=CAFT/CPRIME
V(2)=DEAFT
ALF2=TRL(ACRFS2,V,DI,IE)
IF (IF.NE.0) GO TO 9100

10 CONTINUE
IF (IFLAP.LE.2) FFQ=DEFLAP
IF (IFLAP.GE.3) FFQ=OFFWD+(ALF2/ALF1)*DEAFT
V(1)=FFQ
IF (IFLAP.EQ.4) X=TRL(DCDTFT,V,DI,IE)
IF (IFLAP.NE.4) X=TRL(DCDTFD,V,DI,IE)
IF (IF.NE.0) GO TO 9100

```

\*\*\*

```

** ** LEADING EDGE FLAP PARASITE DRAG
** **
** DCDLF=.154*(SPANLF/WREF)

```

\*\*\*

```

** ** FLAP INDUCED DRAG
** **
V(1)=ETFIN
V(2)=.5*ARATIO/PI
CA=TBL(KEAPI2,V,DI,IE)

```

```

      IF (IF.NF.0) GO TO 9100
      V(1)=FTFOUT
      V(2)=FTFIN
      CF=TRL(KEIEO2,V,DI,IE)
      IF (IF.NF.0) GO TO 9100

      C=CA*CF
      DCNI=C*(DCLTE)**2/(PI*AREF)

      **
      ** RLC DRAG DELTA
      **
      DCDBLC=-.5*CULE

      **
      ** CALCULATE DRAG VALUES FOR OUTPUT
      **
      DO 300 I=1,NALPHA
      V(1)=CLTO(I)/CLMAXD
      DCDP=TRL(DCDCLR,V,DI,IE)
      IF (IF.NE.0) GO TO 9100

      CNI=CLTO(I)**2/(PI*AREF)
      CDTO(I)=CDPMFU+DCULE+DCDTL+DCDI+DCDP+CNI+DCDBLC
300 CONTINUE
      GO TO 9200

9100 CONTINUE
      IERROR=1

9200 CONTINUE
      RETURN
      END
      SUBROUTINE PITCH(IERROR)
      REAL KEAPI2,KEIEO2,LAMETA
      COMMON
      ACRES2(77),ACREF2(77),ADCKA2(77),LAMETA(30),
      1ADLECR (30),DCLACC(30),DCLACK(30),DCLACM(30),
      2DCDTED(30),DCDTFT(30),FDRCR(30),KEAPI2(77),KEIEO2(77),DCDCLR(30),
      3AMSPR(30),XCPAR2(77),FCPEI2(77),DCABT(30),AKKYCY(30),BKCLF2(77),
      4CLIAS2(77),DCLIA2(182),CMI3(231),DEPS3(182),DCLIG2(77),

```

\*\*\*

\*\*\*



```

V(1)=YM/CHDYM
XK=TRL(AKRYCY,V,D2,IF)
IF (V(1).GT.1.) XK=0.
Y2=XM+CHDYM*(.25+AQCORD*XK)
IF (IF.NE.0) GO TO 9100

V(1)=YM/CHDYM
XK=TRL(AKRYCY,V,D2,IF)
IF (V(1).GT.1.) XK=0.
X2P=XPM+CHDPM*(.25+APUCHD*XK)
IF (IF.NE.0) GO TO 9100

V(1)=ELEFOUT-ELEFIN
XMU=TRL(AMSPR,V,D2,IF)
IF (IF.NE.0) GO TO 9100

V(1)=ELEFIN
XIN=TRL(LAMETA,V,D1,IF)
IF (IF.NE.0) GO TO 9100

V(1)=ELEFOUT
XAT=TRL(LAMETA,V,D1,IF)
IF (IF.NE.0) GO TO 9100
XOT=XAT-XIN

A=(1.+XMU*DSE/S2)*X2P-X2
R=1.+(XMU*DSE/S2)*XOT
DXLFSD=((XIN*(XIP-XI)+XOT*A+XAC)/R)-XAC
DXLFOR=((A*XOT+XAC)/R)-YAC
IF (IP.NE.2) GO TO 7000
WRITE (IO,8000)X1,XIP,X2,X2P,XMU,XIN,XOT,A,B,DXLFSD,DXLFOR
8000 FORMAT(1H0, 43HX1,XIP,X2,X2P,XMU,XIN,XOT,A,B,DXLFSD,DXLFOR
, (1X,F10.4))
7000 CONTINUE

**
** AFRO CENTER SHIFT DUE TO T.E. FLAPS (FOWLER ACTION)
**
V(1)=YRTF/CHDYRT
XK=TRL(AKRYCY,V,D2,IF)
X1=XRTF+CHDYRT*(.25+AQCORD*XK)

```

\*\*  
\*\*  
\*\*

```

IF (IF.NE.O) GO TO 9100
V(1)=YBTE/CDPYRT
XK=TRL(AKRYCY,V,D2,IE)
X1P=XPBTE+CDPYRT*(.25+APQCHD*XK)
IF (IF.NE.O) GO TO 9100

V(1)=YMTF/CHDYMT
XK=TRL(AKRYCY,V,D2,IE)
IF (V(1).GT.1.) XK=0.
X2=XMTF+CHDYMT*(.25+AQCORD*XK)
IF (IF.NE.O) GO TO 9100

V(1)=YMTF/CPYMTF
XK=TRL(AKRYCY,V,D2,IE)
IF (V(1).GT.1.) XK=0.
X2P=XPMTF+CPYMTF*(.25+APQCHD*XK)
IF (IF.NE.O) GO TO 9100

V(1)=FTFIN
XIN=TRL(LAMETA,V,D1,IE)
IF (IF.NE.O) GO TO 9100

V(1)=FTFOUT
XAT=TRL(LAMETA,V,D1,IE)
IF (IF.NE.O) GO TO 9100
XOT=XAT-XIN

V(1)=FTFOUT-ETFIN
XMU=TRL(AMSR,V,D2,IE)
IF (IF.NE.O) GO TO 9100

C=(1.+XMU*QWTF/S3)*X2P-X2
R=1.+(XMU*DWTF/S3)*XOT
DYTFCD=((XIN*(V1P-Y1)+XOT*A+XAC)/9)-XAC
DXTEOB=((A*XOT+XAC)/B)-XAC

**
** PITCHING MOMENT AT ZERO LIFT DUE TO I.E. FLAPS
**
YCON=ARATIO/((WPERMT/WSPAN)*ARATIO+2.)

```

\*\*  
\*\*  
\*\*



```

IF (IP.NF.2) GO TO 7001
WRITE (IO,8001)X1,X2,X1P,X2P,XIN,XOI,XMU,A,B,DXTESD,DXTEUB,YCUN
8001 FORMAT(IH0, 48HX1,X2,X1P,X2P,XIN,XOI,XMU,A,B,DXTESD,DXTEUB,YCUN /
1 (10(1X,F10.4)))
7001 CONTINUE
XACFX=XAC+DXTEFD
IF (ITE.FG.2) XACF=XAC+DXTEFB
V(1)=FTFIN
V(2)=FTFOUT-FTFIN
ETACP=TRL(ETPH12,V,D2,IE)
IF (IE.NE.0) GO TO 9100

V(1)=YCON
V(2)=CFLIB/CPMIR
IF (IFLAP.GT.2) V(2)=CPFLIB/CPMIB
CCPIP=TRL(XCPAR2,V,D3,IE)*CPMIB
IF (IE.NE.0) GO TO 9100

V(1)=YCON
V(2)=CFLOR/CPMOR
IF (IFLAP.GT.2) V(2)=CPFLOS/CPMUB
CCPOR=TRL(XCPAR2,V,D3,IE)*CPMOR
IF (IE.NE.0) GO TO 9100

**
** DETERMINE INBOARD FLAP LOAD POINT
**
DCP=CCPIR-.5*CPMIR
XIRLD=DCP*COS(AHCORR)+XIB
IF (IP.NF.2) GO TO 7002
WRITE (IO,8002)XACFX,ETACP,CCPIB,CCPOB,DCP,XIRLD
8002 FORMAT(IH0, 39HXACFX,ETACP,CCPIB,CCPOB,DCP,XIRLD
1 (10(1X,F10.4)))
7002 CONTINUE

**
** DETERMINE OUTBOARD FLAP LOAD POINT
**
DCP=CCPOB-.5*CPMOR
XORLD=DCP*COS(AHCORR)+XOB
XX=XORLD-XIRLD

```

\*\*\*

\*\*\*

```

      YY=1/(FIFOUT-FTEIN)
      Z7=FTACP-FTEIN
      XCPTF=XX*YY*Z2+X1RLD
      DCMOTE=-(DCLB+DCLTF)*(XCPTF-XACEX)/CREF
      **
      ** PITCHING MOMENT AT ZERO DUE TO L.E. DEVICES
      **
      XACLF=XAC+DXLESN
      IF (IP.NE.2) GO TO 7003
      WRITE (IO,8003)DCP,XOBLD,
8003  FORMAT(1H3, 2BHDCP,XOBLD,
1      (10(1X,F10.4)))
7003  CONTINUE
      IF (ILF.EQ.2) XACLF=XAC+DXLFOR
      DCMOLF=DCLLF*(XPDCRU-XACLE)/CREF
      **
      ** CALCULATE PITCHING MOMENT FOR OUTPUT
      **
      XX=DXTECN
      IF (ITE.EQ.2) XX=DXTEFOR
      YY=DXLESN
      IF (ILF.EQ.2) YY=DXIFOR
      TXAC=XAC+XX+YY
      CON=XCG/CREF-(TXAC/CREF)
      DO 300 I=1,NALPHA
      CMT0(I)=CMOLFU+DCMOTE+DCMOLE+CON*DCLT0(I)
300  CONTINUE
      **
      ** CHANGE IN DOWNWASH AT THE TAIL DUE TO L.E. AND T.F. FLAPS
      **
      **
      CALL DELTAE(IE)
      IF (IP.NE.2) GO TO 7004
      WRITE (IO,8004)DCMOLE,XX,YY,TXAC,CON,DEP5F
8004  FORMAT(1H3, 2BHDCMOLE,XX,YY,TXAC,CON,DEP5F /
1      (10(1X,F10.4)))
7004  CONTINUE
      IF (IE.NE.0) GO TO 9100

```





```

20COTED(30),COTET(20),CORCK(30),KFAPI2(77),KEIEU2(77),DCDCLK(30),
30XSR(30),XCPAR2(77),ECPFI2(77),DCART(30),AKKYCY(30),RNCLE2(77),
40CLIAS2(77),DCLIA(182),CNI3(231),CMI3(231),DEPS3(182),DCLIG2(77),
50CMIG2(77),DCNIG2(77)
COMMON /CASEIN/ TITLE(18),IFLAP,WGRUSS,WKEF,PERMT,NDFLAP,
ACPRIME,CFLAP,DFLP(4),CPWU,CPLAP,CAFT,URFWU,UFART,WGLOK,ANLCUR,
1AHLFW,AHLAT,ETEIN,ETEUT,CLEDGE,CHORD,ULEDGE,ELEIN,ELEUT,CLAFU,
2AULFU,CLENLF,CRONLF,WPGKUS,OWTE,DVLE,CLMAXU,ALPHA1,CULE,DALPHA,
3WGLAP,SPANLE,CHRDLE,XCPI,XCPLE,XCP2,XCP2TE,XAC,52,USLL,53,CPMUB
4,XCG,CREF,CFLIR,CFLOR,CPMIB,CPLIR,CPFLUB,XIR,XCH,EPTETN,XPUCKD,
5CMOLEU,VHQM(3),NWMNGH,THMG,PCPAN,TLWM,STAIL,EPSFU,DCPDMA,DCDDCL
6,CHDYC,CHDPYB,CNU,APUCHO,XPB,XB,YR,YM,CHDYM,XM,CHDPYM,XPM,IEDGE
7,CHDYB,XRTE,COPYET,YRTE,YMTE,CHDYMT,XMTE,CYMT,XPMTE
8,DFLAP,DEFW(4),DEFA(4),CRDDPM,COPMEU,EPTUB,EPSO,DEPDAL
9,CJ,ENGVC,XNACEL,XNUZLE,ZNUZLE,XINLET,ZINLET,CNAM,ILE,ITE
COMMON /OUTPUT/ NALPHA,CLAFU,ACULE,AULTF,AULTF,AVLBFD
1,DCLREF,CLMAXO,DCDTL,DCULE,DCMUTE,DCMULE,CDEFATR(20),
2CWREF,CLMAXG(2)
COMMON /OUTPUT/ ALPHA(20),CLTO(20),CDIU(20),CMIU(20),CLIR(20),
1CDTR(20),ALPHA(20),CLTUG(20),CDTUG(20),CMUG(20),CLING(20)
1,CDTRG(20),CLPOEA(20),CLINT(20),CDPUFA(20),CDPUFA(20),CDPUFA(20),
5CLPUGF(20),CDPUGF(20),CMPUGF(20),CLGETR(20),CGETR(20),CLPATK(20)
COMMON/BASIC/RATIO,PI,RAD,AREF
DATA PI/3.1415926535897932384626433832795
CALCULATE CONSTANTS FOR FORMULAR OUTSIDE LOOP
GEHIGH=WHOM(TWING)
C1=(PI*WSPAN/(R.*GEHIGH))**2+1.-1.)/(PI*CURF*AREF)
C2=ALOG(1.+(WSPAN*PI/(R.*GEHIGH))**2)/ (PI*CURF*AREF)
C3=2./(PI*CURF*AREF)*ALOG(1.+(WSPAN*PI/(R.*GEHIGH))**2)
DO 50 I=1,NALPHA
CLTO(I)=(CLTO(I)*C1)/(1.+2.*CLTO(I)*C1)**2
ALPHA(I)=ALPHA(I)-(2.*CLTO(I)*C2)
IF (CLTO(I).EQ.0.) GO TO 100
CMTUG(I)=CMUG(I)/CLTO(I)*CLTOG(I)
COTUG(I)=COTUG(I)*(1.-CLTO(I)**2/CDTUG(I)*C3)*CLTO(I)/CLTO(I)
CLMAXG(TWING)=CLTUG(I)
GO TO 50
100 CONTINUE
CMTUG(I)=CMTUG(I)
COTUG(I)=COTUG(I)
50 CONTINUE

```

```

**
**      CALCULATE TRIM CL AND CO FOR POWER OFF IN GROUND EFFECT
**
**
MODE=2
CALL TRIM(MODE,GEMHIGH)
RETURN
END
SUBROUTINE TRIM(MODE,GEMHIGH,K)
*****
**
**      CALCULATE TRIM CL AND CO FOR VARIOUS CONDITIONS
**
**
**      MODE = 1  POWER OFF IN FREE AIR
**      = 2  POWER OFF IN GROUND EFFECT
**      = 3  POWER ON IN FREE AIR
**      = 4  POWER ON IN GROUND EFFECT
**
*****
COMMON/BASIC/ARATIO,PI,RAD,AREF
COMMON /INTARC/IO,IN,IO,ICR,RP1BL,IP
COMMON/INTER/DCLTE,LTATE,DCLLE,DCLLE,DEPST,DCLH
COMMON /CASEIN/ TITLE(18),ISLAP,WGROSS,ARFF,INPLN41,NDFLAP,
ACPPIME,CFLAP,DILP(4),CEND,CPLAP,CALF,DFFAD,UFAPT,AVCLOC,ALCLOC,
1AHLFND,AHLAFT,CTFIN,CTEOUT,CLEPGE,CHORD,DLEDOE,ELEIN,ELEOUT,CLAPD,
2AOLFU,CLENLE,CRDNLE,RPGRUS,DTE,DWLL,CLMAXU,ALPHA1,CULLE,DALPHA,
3WGFELAP,SPANLE,CHKOLF,XCP1,XCPLE,XCP2,XCP2TE,XAC,52,D5LE,53,CPRND
4,XCG,CREF,CFLIS,CFLOH,CPIB,CPLIB,CPLFLO,XIO,XDD,EPTIN,XPCKU,
5CVOLFU,WJHM(3),WJNGH,THUM,WSPAN,TLUM,STAIL,EPSFO,DCPDW,DCCDCL
6,CHDYR,CHDPYR,CAC,AP,CHD,XPR,XR,YR,YM,CHDYM,XIO,CHDYM,XPM,LEDGE
7,CHDYRT,XPT,COPYRT,XPRTE,YATE,YATE,CHDYM,XIO,CHDYM,XPM,LEDGE
8,DELAP,DEEN(4),DEAF(4),CRDPR,COPRSD,EPTES,EP50,DEPDAL
9,CJ,ENGVEF,XNACEL,XNACZLE,ZMZLE,XINLET,ZINLET,CDNAM
COMMON /OUTPUT/ NALPHA,CLAPD,AULLE,AULTED,AULTEF
1,DCLRED,CLMAXD,
2,CREF,CLMAXG(3)
COMMON /OUTPUT/ ALPHA(20),CLIO(20),CPIO(20),CMIO(20),CLIK(20),
1COTR(20),ALPHA(20),CLTUS(20),COTUG(20),CMUG(20),CLIG(20)
1,COTRG(20),CLPOFA(20),CLINT(20),COPUFA(20),CMPOFA(20),DEPOFA(20),
5CLPOGE(20),CPOGE(20),CLOGE(20),CLOIR(20),CULIR(20),CLFAIR(20)
**

```

```

*****
**
PISQ=PI*PI
IF (MODE.LI.1.OR.MODE.GT.4) GO TO 910
GO TO (100,200,300,400),MODE

100 CONTINUE
**
** CALCULATE TRIM CL AND CD FOR POWER OFF IN FREE AIR
**
DO 110 I=1,NALPHA
ERASIC=EPS0+DEPDAL*ALPHA(I)
ETAIL=ERASIC+DEPSE
DCLTR=CMTO(I)/TLQM*CREF
CLPTO=WREF/STAIL*DCLTR
DCPTR=DCLTR*ETAIL+(DCPMMIN+DCDDCL*CLPTO**2)*STAIL/WREF
CLTR(I)=CLTO(I)+DCLTR
CDTR(I)=CDTO(I)+DCPTR
110 CONTINUE
GO TO 9100

200 CONTINUE
**
** CALCULATE TRIM CL AND CD FOR POWER OFF IN GROUND EFFECT
**
C1 = TLQM*TLQM +(2.*GEHIGH-THQM)*(2.*GEHIGH-THQM)
C2 =(2.*GEHIGH-THQM)*(2.*GEHIGH-THQM) + PISQ*WSPAN*WSPAN/64.
C2 = THQM*THQM + C2
SORC2= SORT(C2)

```

CARD COUNT 644

EGENT=WRFF/(8.\*PI)\*(TLG/(1/SURC2+(1.+TLG)/SURC2)/C3)

```

210 I=1,NALPHA
  FBASIC=EPSO+DEPDAI*ALPHA(I)
  CGE=CLTO(I)*EGENT
  CTAIL=EBASIC+DEPSF+EGE
  DCLTRG=CMTOG(I)/TLG*CKEF
  CLPTOG=WRFF/STAIL*DCLTRG
  DCOTRG=DCLTRG*FTAIL+(DCPDMM+DCDDCL*CLPTOG**2)*STAIL/WRFF
  CLTRG(I)=CLTOG(I)+DCLTRG
  COTRG(I)=COTOG(I)+DCOTRG
210 CONTINUE
GO TO 9100

```

```

200 CONTINUE
**
** CALCULATE TRIM CL AND CD WITH POWER ON IN FREE AIR
**
DEVT=GEHIGH
FBASIC=EPSO+DEPDAI*ALPHA(K)
FTAIL=EBASIC+DEPSF+DEVT
DCLTR=CMPOFA(K)/TLG*CKEF
CLPTO=WRFF/STAIL*DCLTR
DCOTR=DCLTR*FTAIL+(DCPDMM+DCDDCL*CLPTO**2)*STAIL/WRFF
CLEATR(K)=CLPOFA(K)+DCLTR
CEATR(K)=CEPOFA(K)+CLEATR
GO TO 9100

```

```

400 CONTINUE
**
** CALCULATE TRIM CL AND CD WITH POWER ON IN CONDUIT EFFECT
**
C1=TLG**2+(2.*GEHIGH-TLGM)*C2*(GEHIGH-TLGM)
C2=(2.*GEHIGH-TLGM)*C2*(GEHIGH-TLGM)+PI*DEW*DEAI**2/64.
C2=THG**2+C2
C4=SQRT(C2)
EGENT=WRFF/(8.*PI)*(TLG/(1/C4+(1.+TLG)/C4)/C2)
EGE=CLPOG(K)*EGENT
FBASIC=EPSO+DEPDAI*ALPHA(K)
FTAIL=EBASIC+DEPSF+EGE
DCLTRG=CMPOG(K)/TLG*CKEF

```



```

CLPTOG=WRFF/STAIL*DCLTRG
DCNTRG=DCLTRG*STAIL+(DCPDMM+DCDDCL*CLPTOG**2)*STAIL/WRFF
CLGETR(K)=CLPOGE(K)+DCLTRG
CGETR(K)=CDPOGE(K)+DCNTRG

0100 CONTINUE
RETURN
END
SUBROUTINE VTRFF(IFRROR)
REAL KEAPI2,KEFEO2,LAMETA
COMMON
  1ACRS2(77),ACRF2(77),ACRA2(77),LAMEFA(30),
  2DCLACC(30),DCLACC(30),DCLRCR(30),DCLACM(30),
  3DCCTE(30),DCCTE(30),EDRCR(30),KEAPI2(77),KEFEO2(77),DCDCLN(30),
  4AVSBR(30),XCPAR2(77),ECPEL2(77),DCABT(30),AKRYCY(30),BACLE2(77),
  5CLIAS2(77),DCL13(182),CMI3(231),CMY3(231),DEPS3(182),DCLIG2(77),
  6DCMIG2(77),DCLIG2(77)
COMMON /INTABC/IO,IN,IO,ICR,NPTBL,IP
COMMON /INTER/DCLTE,ETATE,DCLLE,DEPSF,DCLD
COMMON /BASIC/ARATIO,PI,RAD,AREF
COMMON /CASFIN/ TITLE(18),IFLAP,WGRUSS,WKEF,WPERMT,INDFLAP,
  1ACPRIME,CFLAP,DELP(4),CFWD,CPFLAP,CAFT,DFFWD,CAFT,ACCURD,AHCCURD,
  2AHLEWD,AHLAFT,ETEIN,ETEOUT,CLEGE,COKO,DLEGE,ELEIN,ELLEUT,CLAFJ,
  3AOLFU,CLENLE,CRDNLE,APGROS,D,ILE,DWLL,CLMAXJ,ALPHA1,CULE,DALPHA,
  4WCELAP,SPANLE,CHROLE,XCP1,XCPLE,XCP2,XCP2TF,XAC,S2,DSLE,S3,CPMUB
  5XCG,CREF,CFLR,CFLW,CPM1B,CPFLR,CPFLW,XIB,XUB,EPTIN,VFJCRD,
  6CMOLFU,WHOM(2),N,INGH,THQM,WCPAN,TLM,STAIL,EPSJ,DCPDMM,DCDCL
  7CHDYB,CHDPYR,CMD,AP,CHD,XPB,XB,YR,YM,CHDYM,XM,CHDPYM,XPM,IEDGE
  8CHDYRT,XBTE,COPYRT,XPBTE,YRTE,YMTE,CHDYM1,XMT,CPYMIE,XPMTE
  9CJ,ENGVEC,XNACFL,XNOZLE,ZINOZLE,XINLET,ZINLET,CORAM,ILE,ITE
COMMON /OUTPUT/ NALPHA,CLAFD,AULLFD,AULTFD,AULBFD
  1DCLBFD,CLMAXD,DCOTE,DCOLE,DCMUTE,DCMLE,CDFAIR(20),
  2CMORFD,CLMAXG(2),ALPHA(20),CLTU(20),CDTU(20),CMTU(20),CLTR(20),
  3CCTR(20),ALPHAG(20),CLTOG(20),CDTOG(20),CMTOG(20),CLTRG(20)
  4COTRG(20),CLPOFA(20),CLINT(20),CDPOFA(20),CMPOFA(20),DEPUFA(20),
  5CLPOGE(20),CDPOGE(20),CMPOGE(20),CLGETR(20),CNGETR(20),CLFAIR(20)
  6DIMENSION V(3), D1(2), D2(2)
DATA D1/2*1./
DATA D2/2*2./
**
*****

```

```

**
ERROR=0
IF (NALPHA.LF.O) GO TO 9100
DXC=XNACEL-.25
YTERM=CJ*(XNOZLF/CREF*SIN(ENGVEC)+ZNOZLE/CREF*COS(ENGVEC))
DO 100 I=1,NALPHA
XTERM=CGRAM*(XINLET/CREF*SIN(ALPHA(I))-ZINLET/CREF*COS(ALPHA(I)))
**
** CALCULATE LIFT FOR POWER ON - FREE AIR
**
V(1)=ALPHA(I)
V(2)=ENGVEC
CLTRL=TRL(CLIAS2,V,D2,IF)
IF (IF.NE.O) GO TO 9100
V(1)=ALPHA(I)
V(2)=ENGVEC
V(3)=DXC
DCLINT=TRL(DCLI3,V,D2,IE)
IF (IF.NE.O) GO TO 9100
CLINT(I)=(CLTRL+DCLINT)*SQRT(.5*CJ)
IF (IP.NE.2) GO TO 7000
WRITE (IO,8000)CLTRL,DXC,ALPHA(I),ENGVEC,DCLINT,CLINT(I)
FORMAT(1H0, 41HCLTRL,DXC,ALPHA(I),ENGVEC,DCLINT,CLINT(I) /
1 10IX,F10.4)
7000 CONTINUE
CLPOFA(I)=CLTO(I)+CLINT(I)+CJ*SIN(ALPHA(I)+ENGVEC)
**
** CALCULATE FOR POWER ON - FREE AIR
**
V(1)=XNACEL
V(2)=ENGVEC
V(3)=CLINT(I)
CPINT=TRL(CPIA,V,D2,IE)
IF (IE.NE.O) GO TO 9100
CPPOFA(I)=CPIC(I)+CPINT-CJ*COS(ALPHA(I)+ENGVEC)+CGRAM

```

\*\*  
\*\*  
\*\*

\*\* CALCULATE PITCHING MOMENT FOR POWER ON - FREE AIR

\*\*  
\*\*  
\*\*

V(1)=XNOZLE/CRFF

V(2)=ENGVEF

V(3)=CLINT(1)

CMINT=TRL(CM13,V,D1,IE)

IF (IF.NE.0) GO TO 9100

CMPOFA(1)=CMTO(1)+CMINT+YTERM+XTERM

IF (IP.NE.2) GO TO 7001

WRITE (10,8001)CLPOFA(1),CDINT,CDPOFA(1),XTERM,YTERM,CMPOFA(1)

8001 FORMAT(1H0, 47HCLPOFA(1),CDINT,CDPOFA(1),XTERM,YTERM,CMPOFA(1) /

1 10(1X,F10.4))

7001 CONTINUE

\*\*  
\*\*  
\*\*

\*\* CALCULATE POWER ON INTERFERENCE EFFECTS ON DOWNWASH

\*\*  
\*\*  
\*\*

V(1)=ALPHA(1)

V(2)=ENGVEF

V(3)=CJ

DEVT=TRL(DEPS3,V,D2,IF)

IF (IF.NE.0) GO TO 9100

\*\*  
\*\*  
\*\*

\*\* CALCULATE TRIM CL AND CD FOR POWER ON IN FREE AIR

\*\*  
\*\*  
\*\*

MODE=3

CALL TRIM(MODE,DEVT,1)

CONTINUE

GO TO 9200

9100 CONTINUE

IFPROP=1

9200 CONTINUE

RETURN

END

SUBROUTINE VTGF(IWING,IEROR)

Reproduced from  
best available copy.

```

REAL KLAIP2,KLEI22,LAMETA
COMMON
  ACRS2(77),ACRFD2(77),ADCKA2(77),LAMEIA(30),
  1ADLECR(30),DCLACC(30),DCLCKN(30),DCLACM(30),
  2DCATEQ(30),DCATFT(30),EDRCK(30),KEAPI2(77),KEIEU2(77),DCDCLN(30),
  3AMSPR(30),XCPAR2(77),ECPFI2(77),DCABT(30),ANKYCY(30),RKCLE2(77),
  4CLIAS2(77),DCLV3(182),CMI3(231),DEPS3(182),DCLIG2(77),
  5DCMIG2(77),DCDIG2(77)
COMMON /INTARC/IU,IN,IO,ICR,NPIRL,IP
COMMON /INTER/DCLIF,ETATE,DCLLE,DEPCF,DCLB
COMMON /BASIC/ARATIO,PI,RAD,AREF
COMMON /CASEIN/ TITLE(18),IFLAP,WGRUSS,WKEF,XPERMI,WDFLAP,
ACPRIME,CFLAP,DFLP(4),CFWD,CHEFLAP,CAET,DEFFWD, DFAFT,AWCKRU,AMCKRU,
1AHLEWD,AHLEFT,FTLIN,LEOUT,CLEUGE,CHOKU,DLEUGE,ELLEIN,ELEOUT,CLAFU,
2AOLFU,CLENF,CROWLF,MPGRUS,DWTE,DWLE,CLMAXU,ALPHA1,CULE,DALPHA,
3WGFAP,SPANLE,CHRDLE,XCPI,XCPLE,XCP2,XCP2IE,XAC,32,D3LE,S3,CPMOD
4,XCG,CREF,CFLIR,CFLOR,CPMIB,CPFLIR,CPFLUB,XIR,XJR,EPIFIN,XPWCKD,
5CMOLEU,WHUM(2),JWINGH,THUM,SPAN,TLV,STAIL,EPSFU,DCPD,IN,DCDDCL
6,CHDYR,CHDPYR,CWO,AD,CHD,XPR,XB,YR,YM,CHDYM,XH,CHDPYM,XPM,IEDGE
7,CHDYRT,XBIE,COPYRT,XPPIE,YSTE,IMTE,CHDYMT,XMTE,CPYMTIE,XPMTE
8,DELAP,DEFFW(4),DEAF(4),CRDDPA,CDPVEU,EPIEUB,EPSO,DEPDAL
9,CJ,ENGVEC,XNACEL,XNOZLE,ZNOZLE,XINLET,ZINLET,CURV,ILE,ITE
COMMON /OUTPUT/ NALPHA,CLAPD,AOLFD,AULTFD,AOLBFD
1,DCLBED,CLMAXD,DCBFI,DCOLE,DCMUTE,DCMOLE,COFATN(20),
2CMOBFD,CLMAXG(2),ALPHA(20),CLIU(20),CLIU(20),CMIO(20),CLIR(20),
1CDTR(20),ALPHA2(20),CLTUG(20),COTUG(20),CHUG(20),CLIRG(20),
1,CDIRG(20),CLPOFA(20),CLINT(20),CDPOFA(20),CMPOFA(20),DEPOFA(20),
5CLPOGE(20),CDPOGE(20),CDPOGE(20),CLGIR(20),CDUEIR(20),CLFAIR(20),
DIMENSION V(2),D1(2),D2(2)
DATA D1/D1,1./
DATA D2/D2,2./
**
*****
**
IFERROR=0
IF (NALPHA.LE.0) GO TO 9100
WINGHT=WHQW(INING)
DXC=XNACFL-.35
XANG=ENGVEF
XX=30./RAD
IF (ENGVEF.LE.XX) XANG=XX
YY=60./RAD

```

```
IF (ENGVEF*GF.VY) XANG=YY
YTRY=CJ*(XNOZLF/CREFF*SIN(ENGVEC)+ZNOZLE/CREFF*COS(ENGVEC))
```

```
DO 100 I=1,NALPHA
XTERM=CDRAX*(XINLET/CREFF*SIN(ALPHA(I))-ZINLET/CRNF*
1COS(ALPHA(I)))
```

```
**
** CALCULATE LIFT IN GROUND EFFECT FOR POWER ON
**
```

```
V(1)=XANG
V(2)=WINGHT/WSPAN
DCLTGE=TBL(DCLIG2,V,D1,IE)
IF (IF.NE.0) GO TO 9100
```

```
V(1)=ALPHA(I)
V(2)=ENGVEC
XCL=TBL(CLIAS2,V,D2,IE)
IF (IE.NE.0) GO TO 9100
```

```
V(1)=ALPHA(I)
V(2)=ENGVEC
V(3)=DXC
XDCL=TBL(DCLI3,V,D2,IE)
IF (IF.NE.0) GO TO 9100
```

```
CLPAGE=(XCL+XDCL)*SORT(.5*CJ)
IF (IP.NE.2) GO TO 7000
WRITE (10,8000)XANG,WINGHT,WSPAN,DCLTGE,XCL,DXC,XDCL,CLPAGE
8000 FORMAT(1H0, 44HXANG,WINGHT,WSPAN,DCLTGE,XCL,DXC,XDCL,CLPAGE
1 10(1X,F10.4))
7000 CONTINUE
```

```
CLPAGE(I)=CLTOS(I)+CLPAGE+DCLTGE+CJ*SIN(ALPHA(I))+ENGVEC
```

```
**
** CALCULATE DRAG IN GROUND EFFECT FOR POWER ON
**
```

```
V(1)=XNACFL
V(2)=ENGVEC
V(3)=CLPAGE
CDPAGE=TBL(CDI3,V,D2,IE)
```

```

IF (IF.NE.0) GO TO 9100
V(1)=XANG
V(2)=WINGHT/MSPAN
DCMGF=TRL(DCMIG2,V,PI,IF)
IF (IF.NE.0) GO TO 9100

CDPOGE(1)=CDTUG(1)+CDPAGE+DCDGE-CJ*COS(ALPHAH(1)+ENUGEC)+CDRAM
**
**
** CALCULATE PITCHING MOMENT IN GROUND EFFECT FOR POWER ON
**
IF (IP.NE.2) GO TO 7001
WRITE (10,8001)CLPOGE(1),CDPAGE,DCDGE,CDPOGE(1),YTERM,XTERM
8001 FORMAT(1H0, 44HCLPOGE(1),CDPAGE,DCDGE,CDPOGE(1),YTERM,XTERM /
1 10(1X,F10.4))
7001 CONTINUE
V(1)=XNACFL
V(2)=ENUGVFC
V(3)=CLPAGE
CMPAGE=LBL(CM12,V,PI,IF)
IF (IF.NE.0) GO TO 9100

V(1)=XANG
V(2)=WINGHT/MSPAN
DCMGF=TRL(DCMIG2,V,PI,IF)
IF (IF.NE.0) GO TO 9100

CMPDGE(1)=CDTUG(1)+CDPAGE+DCDGE+YTERM+XTERM
IF (IP.NE.2) GO TO 7002
WRITE (10,8002)CMPAGE,DCMGF,CMPDGE(1),CJ,ALPHAH(1)
8002 FORMAT(1H0, 45HCLPAGE,DCMGF,CMPDGE(1),CJ,ALPHAH(1)
1 10(1X,F10.4))
7002 CONTINUE

**
**
** CALCULATE TRIP PL AND CD FOR POWER ON IN GROUND EFFECT
**
MODE=4
CALL TRIP(MODE,WINGHT,1)
100 CONTINUE

```

GO TO 9200

9100 CONTINUE  
IF ERROR=1

9200 CONTINUE  
RETURN  
END

CARD COUNT 295

## REFERENCES

1. Ellison, D. E. and Malthan, L. V., USAF Stability and Control Datcom, Revised July 1963.
2. Royal Aeronautical Society Aerodynamics Data Sheets.
3. Polhamus, E. C., A Simple Method of Estimating the Subsonic Lift and Damping in Roll of Sweptback Wings, NACA TN 1862, April 1949
4. Jones, R. T. and Cohen, D., High Speed Wing Theory, Princeton University Press, Princeton, N. J., 1960 (Unclassified).
5. Monk, J. R., et al, STOL Tactical Aircraft Investigation, Volume IV, Technical Report AFFDL-TR-73-19 Vol. IV.
6. Eldridge, A. H., Informal Communication (Unclassified).
7. Eldridge, A. H., Approximate Calculation Procedures for Aeroplane Aerodynamic Characteristics, D6A12022-p, The Boeing Company, July 1970.
8. Campbell, I. J., Aerodynamic Characteristics of Rectangular Wings of Small Aspect Ratio, Aeronautical Research Council R&M 3142, December 1956
9. Herbert, J., et al, Effects of High Lift Devices on V/STOL Aircraft Performance, USAAVLABS TR 70-33A, Vol. 1, June 1969
10. Young, A. D., Aerodynamic Characteristics of Flaps, Aeronautical Research Council R&M 2622, February 1947.
11. Neely, R. H., et al, Summary and Analysis of Horizontal Tail Contributions to Longitudinal Stability of Swept Wing Airplanes at Low Speeds, NACA TP R-49, 1959.
12. Carroll, R., et al, STOL Tactical Aircraft Investigation Configuration Definition: Medium STOL Transport with Vectored Thrust/Mechanical Flaps, AFFDL-TR-73-19, Vol. 1, May 1973.
13. Redig, P. J., STOL Tactical Aircraft Investigation, High Lift Programmers Manual, D180-14409-3, The Boeing Company, February 1973.